

**ANALYTICAL CHARACTERIZATION OF
TECHNOLOGICALLY IMPORTANT MATERIALS
USING TXRF AND EDXRF**

by
SANGITA DHARA LENKA
Bhabha Atomic Research Centre, Mumbai, INDIA

*A thesis submitted to the
Board of Studies in Chemical Sciences*

*In partial fulfillment of requirements
For the degree of*

DOCTOR OF PHILOSOPHY
of
HOMI BHABHA NATIONAL INSTITUTE

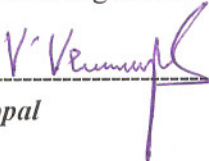


February 2012

HOMI BHABHA NATIONAL INSTITUTE

Recommendations of the Viva Voce Board

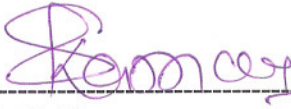
As members of the Viva Voce Board, we certify that we have read the dissertation prepared by Mrs. Sangita Dhara Lenka entitled "*Analytical characterization of technologically important materials using TXRF and EDXRF*" and recommend that it may be accepted as fulfilling the dissertation requirement for the degree of doctor of philosophy.

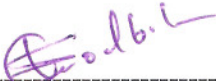

-----Date: 4/5/12
Chairman – Prof. V. Venugopal


-----Date: 4/6/12
Guide/ Convener – Prof. S. K. Aggarwal


-----Date: 4/6/12
Co-Guide – Dr. N.L. Misra


-----Date: 4/6/2012
External Examiner – Dr. M. Sudarshan


-----Date: 4/6/12
Doctoral Committee Member – Dr. S. Kannan


-----Date: 4/6/2012
Doctoral Committee Member – Dr. S. V. Godbole

The modifications as per the examiners' comments have been incorporated in the respective portions of the thesis. Final approval and acceptance of this dissertation is contingent upon the candidate's submission of the final copies of the dissertation to HBNI.

I hereby certify that I have read this dissertation prepared under my direction and recommend that it may be accepted as fulfilling the dissertation requirement.

Date: 4.6.12

Place: RLG, BARC, Mumbai

STATEMENT BY AUTHOR

This dissertation has been submitted in partial fulfillment of requirements for an advanced degree at Homi Bhabha National Institute (HBNI) and is deposited in the Library to be made available to borrowers under rules of the HBNI.

Brief quotations from this dissertation are allowable without special permission, provided that accurate acknowledgement of source is made. Requests for permission for extended quotation from or reproduction of this manuscript in whole or in part may be granted by the Competent Authority of HBNI when in his or her judgment the proposed use of the material is in the interests of scholarship. In all other instances, however, permission must be obtained from the author.


(Sangita Dhara Lenka)

DECLARATION

I hereby declare that the work reported in the thesis titled “**Analytical characterization of technologically important materials using TXRF and EDXRF**” is my own contribution to the research work carried out under the guidance of Dr. N.L. Misra (Co-Guide) and Dr. S.K. Aggarwal (Guide). This work has not been submitted previously to any other institution for the award of any degree.



Signature of the Student

(Sangita Dhara Lenka)

We certify that the above declaration is correct.



(N.L Misra)

Co- Guide



(S. K. Aggarwal)

Guide

DEDICATED
TO
MY BELOVED PARENTS

Smt. Rekha Dhara
&
Late. Shri. Prasanta Kumar Dhara

ACKNOWLEDGEMENTS

I express my sincere gratitude to my research guide **Prof. S. K. Aggarwal**, Associate Director, RC&I (R) Group & Head, Fuel Chemistry Division, for his constant source of inspiration throughout my work. I am deeply indebted to him for his encouragement, valuable guidance and keen interest at each and every stage of this work. I am also deeply indebted and express my sincere gratitude to my co-guide and mentor **Dr. N. L. Misra**, FCD, for introducing me to the field of X-ray spectroscopy. I owe completely to him for his keen interest, extended co-operation, suggestions and enormous support during the entire course of my work.

I am grateful to **Prof. V. Venugopal**, Chairman, Doctoral Committee, for his continuous encouragement. Thanks are due to **Dr. S. Kannan**, Head, X-ray Structural Studies Section, FCD for his helpful suggestion and support as a Doctoral Committee Member and **Dr. S. V. Godbole**, Head, Actinide Spectroscopy Section, RCD and Doctoral Committee Member, for his constructive suggestions during my Ph.D presentations.

I am extremely thankful to **Dr. Imre Varga**, Eötvös Loránd University, Hungary, for his guidance and allowing me to work in his laboratory during the course of my Ph.D. I am also thankful to **Prof. Peter Wobrauschek** and **Prof. Christina Strelj**, Atominstitut, Vienna, for their useful suggestions.

Also, it is my utmost pleasure to express my sincere thanks to my colleagues in X-ray Structural Studies Section, **Mr. S. Sanjay Kumar** for his support and extended co-operation and **Dr. K. Krishnan**, for helping me with XRD measurements. I also take this opportunity to thank **Dr. S.K. Sali**, **Dr. N.D. Dahale**, **Dr. N.K. Kulkarni**, **Dr. Meera Keskar**, **Mr. Rohan Phatak** and **Mr. Bal Govind Vats**, who have helped me willingly at different stages of my work.

I also thank my co-authors their help during various experimental works.

Last but not least, I thank my husband **Mr. Raja Kishora Lenka**, for his wholehearted support, care and co-operation during the entire course of my Ph.D work.

TABLE OF CONTENTS

Title	Page No.
SYNOPSIS	i
LIST OF FIGURES	xx
LIST OF TABLES	xxiv
CHAPTER-1	1
INTRODUCTION	
1.1. Technologically Important Materials	2
1.2. Nuclear Energy	3
1.3. Technologically Important Materials in Nuclear Industry	6
1.3.1. Nuclear fuel	6
1.3.2. Other technologically important materials	8
1.4. Analytical Characterization of Nuclear Fuel	12
1.4.1. Trace metal assay	13
1.4.2. Trace non-metal assay	15
1.4.3. Bulk element assay	16
1.5. Analytical Characterization of Other Nuclear Materials	17
1.6. Non-conventional Sources of Uranium	19
1.7. Techniques Used for the Characterization of Nuclear Materials	19
1.7.1. Role of X-ray fluorescence for characterization of nuclear materials	20
1.8. Objective of the Thesis	23
1.9. References	26
CHAPTER-2	31
INSTRUMENTAL TECHNIQUES AND EXPERIMENTAL METHODS	
2.1. Introduction	32
2.2. X-Ray Fluorescence Spectrometry	37

2.3.	Interaction of X-rays with Matter	40
2.3.1.	Photoelectric absorption	41
2.3.2.	Scattering	43
2.3.3.	Pair production	44
2.4.	X-Ray Production	44
2.4.1.	X-ray tube sources	45
2.4.2.	Radioisotopic sources	48
2.4.3.	Synchrotron sources	50
2.5.	X-Ray Spectrum	51
2.5.1.	Continuum spectrum	51
2.5.2.	Characteristic line spectrum	52
2.6.	X-Ray Detectors	55
2.7.	Total Reflection X-Ray Fluorescence (TXRF)	58
2.7.1.	Fundamentals of total reflection of X-rays	61
2.7.2.	Sample carriers	67
2.7.3.	Instrumental parameters	69
2.7.4.	Calibration and quantification	71
2.8.	Energy Dispersive X-Ray Fluorescence (EDXRF)	80
2.9.	Spectrometers Used in the Present Work	85
2.9.1.	ITAL STRUCTURES TX-2000	85
2.9.2.	WOBISTRAX	86
2.9.3.	Jordan Valley EX-3600 TEC	88
2.10.	References	90
CHAPTER-3		
ANALYTICAL CHARACTERIZATION OF NUCLEAR MATERIALS BY TXRF: TRACE METALLIC DETERMINATIONS		94
3.1.	Introduction	95

3.2.	Determination of Trace Element in Thorium Oxide Using TXRF	97
3.2.1.	Experimental	98
3.2.1a.	Sample preparation	98
3.2.1b.	Instrumentation	99
3.2.2.	Results and discussion	100
3.3.	Determination of Low Atomic Number Elements at Trace Levels in Uranium Matrix Using Vacuum Chamber TXRF	106
3.2.1.	Experimental	108
3.2.1a.	Sample preparation	108
3.2.1b.	Instrumentation	109
3.2.2.	Results and discussion	110
3.4.	Conclusions	115
3.5.	References	116

CHAPTER-4

ANALYTICAL CHARACTERIZATION OF NUCLEAR MATERIALS BY TXRF: TRACE NON METALLIC DETERMINATIONS **120**

4.1.	Introduction	121
4.2.	Determination of Sulphur in Uranium Matrix by TXRF	122
4.2.1.	Experimental	123
4.2.1a.	Sample preparation	123
4.2.1b.	Instrumentation	126
4.2.2.	Results and discussion	127
4.3.	Chlorine Determination in Nuclear Fuel Samples by TXRF Without Dissolution	133
4.3.1.	Experimental	134
4.3.1a.	Sample preparation	134
4.3.1b.	Instrumentation	136
4.3.2.	Results and discussion	136

4.4.	A Novel Approach for Chlorine Determination in Acidic Medium by TXRF	142
4.4.1.	Experimental	143
4.4.1a.	Sample preparation	143
4.4.1b.	Instrumentation	144
4.4.2.	Results and discussion	145
4.5.	Conclusions	148
4.6.	References	148

CHAPTER-5

ANALYTICAL CHARACTERIZATION OF NUCLEAR MATERIALS BY TXRF: BULK DETERMINATIONS **151**

5.1.	Introduction	152
5.2.	Bulk Determination of Uranium and Thorium in Presence of Each Other by TXRF	153
5.2.1.	Experimental	154
5.2.1a.	Sample preparation	154
5.2.1b.	Instrumentation	155
5.2.2.	Results and discussion	155
5.2.2a.	Analytical strategy	155
5.2.2b.	Effect of sample amount	158
5.2.2c.	Effect of using different internal standards	159
5.3.	Characterization of (U,Th)O₂ Solid Samples by TXRF Without Dissolution	162
5.3.1.	Experimental	163
5.3.1a.	Sample preparation	163
5.3.1b.	Instrumentation	163
5.3.2.	Results and discussion	164
5.4.	Conclusions	171
5.5.	References	171

CHAPTER-6	
DETERMINATION OF URANIUM BY TXRF IN NON-CONVENTIONAL RESOURCES: SEAWATER AND FERTILIZERS	173
6.1. Introduction	174
6.2. Uranium Determination in Seawater by TXRF	175
6.2.1. Experimental	176
6.2.1a. Sample preparation	176
6.2.1b. Instrumentation	177
6.2.2. Results and discussion	178
6.2.2a. Selective extraction of uranium by diethyl ether	178
6.2.2b. Uranium determination in seawater	181
6.3. Determination of Uranium in Fertilizer Samples by TXRF	183
6.3.1. Experimental	184
6.3.1a. Sample preparation	184
6.3.1b. Instrumentation	185
6.3.2. Results and discussion	186
6.4. Conclusions	188
6.5. References	188
CHAPTER-7	
ANALYTICAL CHARACTERIZATION OF NUCLEAR MATERIALS USING EDXRF :BULK AND TRACE DETERMINATION	191
7.1. Introduction	192
7.2. An EDXRF Method for Determination of Uranium and Thorium in AHWR Fuel After Dissolution	193
7.2.1. Experimental	193
7.2.1a. Sample preparation	193
7.2.1b. Instrumentation	194

7.2.2.	Result and discussion	197
7.2.2a.	Uranium determinations	200
7.2.2b.	Thorium determinations	200
7.3.	EDXRF Determination of Cadmium in Uranium Matrix Using Cd $K\alpha$ Line Excited by Continuum	206
7.3.1.	Experimental	207
7.3.1a.	Sample preparation	207
7.3.1b.	Instrumentation	211
7.3.2.	Results and discussion	211
7.3.2a.	Cadmium determination in absence of uranium	213
7.3.2b.	Cadmium determination in presence of uranium	214
7.4.	Conclusions	219
7.4.1.	Bulk determination of uranium and thorium	219
7.4.2.	Trace determination of cadmium in uranium matrix	219
7.5.	References	220
	SUMMARY	222
	LIST OF PUBLICATIONS	226

Synopsis of the thesis submitted to the
Homi Bhabha National Institute
for Ph.D. Degree in Chemical Sciences



Name of the Student : *SANGITA DHARA LENKA*

Name of the Guide : *Prof. Suresh Kumar Aggarwal*
Associate Director, RC&I (R) Group,
Bhabha Atomic Research Centre,
Trombay, Mumbai- 400 085.

Name of the Co-Guide : *Dr. Nand Lal Misra*
Fuel Chemistry Division,
Bhabha Atomic Research Centre,
Trombay, Mumbai- 400 085.

Place of Work : Fuel Chemistry Division
Bhabha Atomic Research Centre,
Trombay, Mumbai- 400 085.

Enrolment No. & Date : CHEM01200604029

Title of the Thesis : Analytical characterization of
technologically important materials using
TXRF and EDXRF

S.K. Aggarwal

Signature of
the Guide

Nand Lal Misra

Signature of the
Co- Guide

Sangita Dhara Lenka

Signature of the
Student

SYNOPSIS

Technologically important materials play a significant role in various fields of science for the betterment of human life. Any material which has a significant contribution in the scientific, industrial and economic progress of mankind can be considered as technologically important. In this era of fast technological advancements, there is a great demand to improve the quality of various materials for their better performance and thereby develop methodologies to ensure the same. The quality of such materials is greatly influenced by the trace and major elements present in them. In order to assess their quality for subsequent applications, these materials need to be analysed for various elements at bulk, minor, trace and ultra-trace concentrations. This makes analytical characterization of technologically important materials a step of immense importance for their quality control and development.

Nuclear Energy is one of the prominent sources for electricity generation all over the world. In nuclear technology, fuel, coolant, moderator and structural components are technologically important materials. Among the above materials, uranium, thorium and plutonium bearing nuclear fuels are the basic elements for the production of nuclear energy and, therefore, have special importance. For the efficient as well as safe operation of the reactors, chemical quality control and characterization of starting materials, process intermediates and final products w.r.t. their trace impurities content and bulk composition is mandatory [1,2]. Moreover in order to meet the stringent specifications, it is essential that the analytical method used should deliver results with high accuracy and reliability. X-Ray Fluorescence (XRF) is one such well established non-destructive analytical technique for qualitative as well as quantitative determination of elemental composition in samples independent of their chemical and physical forms [3]. In XRF, either electrons or photons (X-rays/ gamma rays) used as excitation source, are incident on the sample thereby exciting the atoms of the elements present in the sample. The incident beam falls on the sample at an angle of about 45° and the detector is placed at 45° angle w.r.t. the sample surface to reduce the background (angle between the incident and detected beam is 90°). This geometry is known as 45° - 45° geometry.

XRF is normally operated in one of its two modes i.e. Energy Dispersive X-Ray Fluorescence (EDXRF) or Wavelength Dispersive X-Ray Fluorescence (WDXRF). In WDXRF,

the characteristic X-ray radiations of different energies obtained after excitation of specimen are dispersed spatially according to their wavelengths using a dispersion crystal and are detected sequentially by rotating the detector on the goniometer. In EDXRF, the characteristic X-rays are not dispersed spatially but are detected by a detector and multichannel analyser. These classical XRF spectrometers have their own advantages and disadvantages. Because of the relatively poor detection limits, they cannot compete with the well established methods for trace and ultra- trace element determinations such as Inductively Coupled Plasma- Mass Spectrometry (ICP-MS), Inductively Coupled Plasma- Atomic Emission Spectrometry (ICP-AES), Atomic Absorption Spectrometry (AAS), Neutron Activation Analysis (NAA), etc. Moreover, in classical XRF, X-rays penetrate the surface layer of about 100 micron thickness inside the specimen and therefore have severe matrix effects which lead to errors during quantitative analysis if matrix correction is not applied properly. Thus matrix effect and poor detection limits are the two major drawbacks of conventional XRF which limit its application for ultra- trace element analysis [3, 4].

Yoenda and Horiuchi in the year 1971 put forwarded the possible application of total reflection of X-rays for trace elemental analysis [5]. Total Reflection X-ray Fluorescence (TXRF) is an advanced variant of EDXRF which utilizes the property of total external reflection of X-rays. In TXRF,

(i) The X-ray beam falls on a flat polished smooth surface, containing the sample in the form of a thin film of a few nm thickness, at a grazing angle less than the critical angle of the surface ($\sim 0^\circ$) and gets totally reflected. Due to this condition, the penetration of the beam inside the sample support is negligible. This leads to less scattering and the background is drastically reduced.

(ii) The sample is excited by both the incident and the totally reflected beam which results in doubling of the fluorescent intensity.

(iii) It is possible to position the detector very close to the sample surface which results in a large solid angle for the detection of the fluorescent signal.

These features together improve the detection limits of TXRF by several orders of magnitude compared to those achievable in the conventional XRF instruments. This geometry where the exciting beam falls at a grazing angle and detector is placed at 90° is known as 0° - 90° geometry. TXRF is a micro analytical technique and requires only a few microgram or

microliters of the sample for analysis. Apart from lower background, presentation of sample specimen in the form of a thin film leads to negligible matrix effects in TXRF compared to the conventional XRF. These features of TXRF make this technique competitive and in certain cases better than the well established trace determination methods. Since most of the technologically important nuclear materials are radioactive, it is imperative that the characterization techniques produce less analytical waste and consume less sample so that the radioactive dose involved and consumption of precious nuclear materials are minimum. As TXRF satisfies both these requirements, it is very promising for nuclear materials analysis. Due to the non-availability of matrix matched standards for quantification, analysis of nuclear materials by standard based techniques becomes difficult. In TXRF, since the matrix effects are negligible, matrix matched standards are not required for quantification. Calibration of the spectrometer can be done with any certified standard material and that calibration holds for all samples with varied matrices. The only criterion is that the sample should be in the form of uniform thin film. Hence neither matrix matched standards nor cumbersome calibration plots are required [6]. Despite these superior features, not much literature data on applicability of TXRF methods in the field of nuclear technology are reported. Keeping these points in view, studies on the development of TXRF for the determination of metallic and non-metallic trace impurities in various nuclear material matrices and bulk characterization of uranium and thorium in nuclear fuel were initiated. In addition to this, trace and bulk characterization of nuclear materials by EDXRF are reported in this thesis. The thesis is divided into seven chapters as described below:

CHAPTER ONE

Introduction

This Chapter gives an introduction to the technological importance of various materials used in nuclear reactors and the significance of analytical characterization of these materials. The Chapter introduces the features of the Indian Nuclear Energy Program and the role of chemical quality assurance during the fabrication of high quality nuclear materials. Uranium, thorium and plutonium being the most important components of any nuclear reactor, it is mandatory to follow the chemical specifications stringently. This Chapter also includes the discussion on the effects

of various trace elements on the performance of the nuclear materials and their specifications. The knowledge of major elements content in the nuclear fuel is also equally essential, to ensure the fissile content. The importance of major, minor, trace and ultra-trace elemental determinations in the development of technologically important materials has been described in this Chapter. A brief discussion on the various analytical techniques used for such characterization of nuclear materials and the advantages of TXRF and EDXRF over these techniques are also given. Finally, the main objective of this thesis i.e. development of TXRF and EDXRF analytical methods for the trace and bulk characterization of nuclear materials is presented in this Chapter.

CHAPTER TWO

Instrumental Techniques and Experimental Methods

Since their discovery in the year 1895, X-rays have played a very crucial role in the field of analytical sciences for material characterization. Most of the X-ray methods are based on the scattering, emission and absorption properties of X-rays. The most common of them are X-Ray Diffraction (XRD), X-Ray Absorption Spectroscopy (XAS) and X-Ray Fluorescence (XRF). This Chapter gives the theory, principle and instrumentation involved in XRF spectrometry [3, 4]. The basis of XRF analysis was established by Moseley in terms of Moseley's Law and since then, XRF has become one of the well known methods of spectrochemical analysis. In XRF, X-rays of sufficient energy produced from an X-ray source are incident on the sample and excite the atoms of various elements present in it by removing the electrons from the inner levels and thus making the atom unstable. Electrons from outer levels fall into the vacancies created by the incident X-ray beam to stabilize the atom. The energy difference of the initial and final electronic energy levels of such transitions appears as X-rays which are characteristic of the atom and are used as the signatures of the elements involved in this process. Using various advances in the instrumentation, XRF can be used for the analysis of almost all the elements except H and He which cannot undergo such transitions [7]. The intensity of the characteristic X-rays produced, as described above, is related to their concentrations. The various sources of X-rays such as X-ray tube, radioisotopes and synchrotron as well as their detection using various detectors are discussed in this Chapter along with the advances in the modification of the tube spectrum with

the use of filters and secondary targets. Because of its versatility and advanced features, XRF is being used widely for chemical characterization of materials of different origin e.g. industrial, environmental and biological. In nuclear industry, XRF is being routinely used for the elemental characterization of nuclear materials for its minor and major constituent determinations [8].

An important advancement in the field of XRF is the discovery of TXRF which is based on the principle of total reflection of X-rays, the phenomenon discovered by Compton in 1923. The basic difference between EDXRF and TXRF is in the geometry of excitation and detection with consequent improvement in detection limits of TXRF. TXRF is mainly used for trace, micro analysis and depth profiling. The process of total reflection is characterized by three parameters i.e. critical angle, reflectivity and penetration depth [6]. In this thesis, TXRF was primarily used for micro, trace and ultra trace analysis. For this purpose, a very small quantity of the sample, mostly in solution form, is placed on a highly polished flat sample support, dried and its TXRF spectrum is measured. In TXRF, sample preparation is very critical and its role in quantification is discussed in the Chapter. Apart from sample preparation, the support on which the sample is deposited also should have some unique properties. The critical angle, reflectivity and penetration depth depend on the nature of the sample support. A survey of various types of sample supports and their advantages and disadvantages are also given in this Chapter.

Details of the instruments employed: ITAL STRUCTURES TXRF spectrometer TX-2000, Vacuum Chamber TXRF spectrometer WOBISTRAX from Atominstut, Vienna and Jordan Valley EDXRF Spectrometer EX-3600TEC, in the present work are reported in this Chapter.

CHAPTER THREE

Analytical Characterization of Nuclear Materials by TXRF: Trace Metallic Determinations

In this Chapter, applicability of TXRF spectrometry for the determination of trace metallic impurities at ppm and sub ppm concentration level in thorium and uranium oxides are described. Trace metallic impurities, which get incorporated into the fuel material during various fuel fabrication operations viz. milling, crushing, grinding, dissolution, pelletization, etc., not only affect their properties and performance but also lead to decrease in the total fissile content

of the fuel. Therefore, stringent specifications are given w.r.t. trace metallic impurities for various types of fuel materials [9].

Studies were, therefore, taken up to determine trace metallic impurities in thorium oxide using an Ital Structures TX-2000 TXRF spectrometer and Mo K α excitation source. Before the development of the TXRF methodology for trace metallic determinations, the spectrometer was calibrated and validated using multielement working standard solutions. The TXRF determined values deviated from the certified concentration by 8% and the precision observed was 5% (1s, n=4) at $\mu\text{g/mL}$ level of concentrations. Another important step in TXRF analysis is the sample preparation. For TXRF determination of trace impurities in nuclear fuels, separation of the bulk matrix i.e. thorium or uranium is essential for two reasons: i) One of the requirements of TXRF analysis is that the thickness of sample deposited should be a few nm with total matrix less than 10-50 μg (depending on the nature of matrix). In such low amount of matrix, the analyte transferred on the sample support is sometimes below the detection limits of TXRF. Due to this constrain, the major matrix is selectively separated from a concentrated solution. ii) The separation of major matrix (uranium/thorium) helps in avoiding the absorption of the characteristic X-ray lines of trace analyte by the heavy elements and also decreases the background caused by scattering of the X-rays by the matrix during TXRF measurements. A convenient separation technique for TXRF analysis of actinide oxides is solvent extraction. Hence, a solvent extraction process, using tri-n-butyl phosphate (TBP) in 30% dodecane as extractant, was employed for this purpose. This separation also acts as a preconcentration step. After separation, the major matrix which comes into the organic phase was discarded and the aqueous phase containing the trace elements was analysed.

Trace elements present in thorium oxide samples, which were later developed as standard by the Department of Atomic Energy, Government of India, were analysed after dissolution of the samples and separation of major matrix as described above. The concentrations of trace elements were in the range of 1 to 500 $\mu\text{g/g}$ in thorium. A comparison of TXRF determined concentrations of trace elements in thorium oxide samples with the certified values was made. The TXRF determined concentrations have an RSD of 20% (1 s for n=4) and are within an agreement of 20% of the certified values in most of the cases. The TXRF determined analytical results obtained in the above studies helped in the certification of Ca, V, Cr, Mn, Fe, Ni and Cu

trace metals in thorium oxide samples. Four such standards (ThO₂-B, ThO₂-D, ThO₂-S, and ThO₂-MOX) were developed and TXRF played a significant role in their development.

Low *Z* elements especially Na, Mg and Al, if present in uranium oxide fuel in amounts higher than the specified levels, apart from affecting the fuel performance and fissile content, may form appreciable amounts of uranates of these elements having uranium in lower and higher oxidation states in reactor operating and transient conditions. These uranate compounds have very low density and if formed in appreciable amounts, may cause expansion of fuel volume leading to rupture of fuel cladding. Also in accidents involving minor cracking of the clad, uranates with higher valency of uranium may be formed which may lead to fuel expansion and may propagate further cracking of the clad. Hence, quantification of these elements in nuclear fuel is very important. Unfortunately, not many techniques are available for the determination of low *Z* elements. In XRF, determination of low *Z* elements is difficult due to the low fluorescence yield of the characteristic X-rays, higher background in that energy region and high absorption of these X-rays by the spectrometer components and the matrix. With efficient excitation sources for these low *Z* elements (low *Z* target X-ray tubes like Cr and synchrotron radiation), modified geometry of the TXRF spectrometer and use of vacuum chamber, these losses can be minimized. Since the spectrometer used for the above studies (ITAL Structures TX 2000) is not sensitive for low *Z* elements (below Al), for the determination of low *Z* trace metallic impurities such as Na, Mg and Al in uranium matrix a special geometry TXRF spectrometer having vacuum chamber developed by Atominstitut, Vienna WOBISTRAX [10] and low energy excitation source (Cr K α radiation) was used. This spectrometer was calibrated using single element calibration solutions of Na, Mg, Al and Sc (Internal Standard). The concentrations of Na, Mg and Al were in the range of 100–300 $\mu\text{g/g}$ w.r.t. uranium and 10–20 $\mu\text{g/mL}$ in the solutions. A similar solvent extraction procedure as described above was employed for the separation of major matrix. A comparison of the TXRF determined concentrations of low *Z* elements with the expected values based on the preparation of the synthetic solution showed an average deviation of 14 %.

The applicability of TXRF for the determination of low *Z* elements in uranium matrix was demonstrated for the first time and the above studies showed the potential of TXRF for the determination of trace metallic impurities in thorium and uranium oxides.

CHAPTER FOUR

Analytical Characterization of Nuclear Materials by TXRF: Trace Non-Metallic Determinations

This Chapter deals with the TXRF methodologies developed for the determination of trace non-metallic impurities in nuclear materials. Sulphur and chlorine are two non-metals which, if present, at trace levels in nuclear fuel materials cause detrimental effect on the performance of nuclear fuel. During the fabrication of ThO₂, UO₂ and PuO₂ based fuels, the fuel is taken in the form of pellets and sintered at high temperatures (≈ 2000 K) in Ar–H₂ atmosphere to get high density pellets. Sulphur, as an impurity, when present in these fuel materials forms corresponding actinide oxo sulphides and H₂S leading to shattering of the fuel pellets in powder form during the sintering. Hence, it is essential to control the trace amounts of sulphur in fuel materials below the specification limits before the fuel is sintered and subsequently put into the nuclear reactors [11]. Also, different actinide sulphates are reported in literature for different applications as well as for academic research [12]. Thus, determination of sulphur at trace as well as major concentration levels is essential for the characterization of nuclear and other materials of technological importance. For the development of TXRF method for analysis of such samples, calibration solutions and samples of sulphur in uranium matrix were prepared by mixing uranium in the form of a standard uranyl nitrate solution and sulphur in the form of Na₂SO₄ standard solution. For trace level determination of sulphur in uranium matrix, the major matrix was first separated by solvent extraction using 30% TBP in dodecane whereas for major element analysis of sulphur, separation of uranium was not required. The TXRF determination for sulphur at trace levels was followed after separation of major matrix and analysis of the aqueous phase containing sulphur. In order to countercheck the TXRF results, Rb₂U(SO₄)₃, a chemical assay standard for uranium, was diluted to different dilutions and sulphur content in these solutions was determined. The TXRF determined results for trace amounts of sulphur in these diluted solutions were counterchecked after addition of another uranium solution, so that sulphur is at trace level compared to uranium. For such TXRF determinations, cobalt was used as an internal standard and W L α was used as the excitation source. The precision and accuracy of the method was assessed for trace and major amount determinations and was found to be better

than 8% (1σ RSD) and 15% at a concentration level of 1 $\mu\text{g/mL}$ of sulphur whereas for $\text{Rb}_2\text{U}(\text{SO}_4)_3$, these values were found to be better than 4 and 13%, respectively.

Similarly, chlorine because of its corrosive nature has strict specifications in fuel and coolant tubes. Presence of high concentrations of chlorine affects the mechanical properties of the structural materials [13]. In nuclear industry, there are strict specification limits for chlorine in fuels, clad and coolant tubes depending upon the type of the material and the reactor. These specifications range from 5 to 50 ppmw. For such trace determination of chlorine in nuclear materials, it is mandatory to remove the major matrix elements by suitable procedure. Solid samples are generally dissolved in acid and the major matrix elements are removed by solvent extraction process. During this process the resultant solution in which trace impurities have to be determined becomes acidic in nature. When such samples, which are slightly acidic, are taken for analysis by TXRF, chlorine is lost as HCl , during the sample preparation which requires heating of the sample on quartz sample supports. Hence a TXRF methodology was developed for chlorine determination in acidic solution samples. Moreover, TXRF determination requires addition of a suitable internal standard to the sample solution. The internal standard solution is generally slightly acidic and when added to the aqueous solution of the sample for trace element determinations, acidifies the sample solution. Also, when the water samples are preserved for analysis, a small amount of suprapure nitric acid is added to avoid possible hydrolysis of the trace elements in the solution and this leads to chlorine loss during TXRF sample preparation. To counter such problem, a novel methodology was developed to determine chlorine in acidic solutions. It is based on the addition of a known excess amount of AgNO_3 solution to the sample containing chlorine in acidic medium for precipitating silver chloride. This is followed by TXRF determination of silver in supernatant solution after filtering. A known amount of cadmium was added as an internal standard. As $\text{Ag } K_{\text{abs}}$ and $\text{Cd } K_{\text{abs}}$ have higher energy than the $\text{Mo } K\alpha$, continuum was used for sample excitation. To countercheck this method, samples of NaCl prepared in HNO_3 medium of different molarities to obtain the chlorine concentrations ranging from 1 to 60 $\mu\text{g/ml}$ were analysed with the developed methodology. The precision of such TXRF determinations of chlorine in nitric acid medium samples was found to be better than 10% (1σ) and the results deviated from the expected chlorine concentrations by less than 15%. Though this method has direct application for determination of chlorine in water and acid samples, it can be extended to other materials also after suitable modifications.

Another novel methodology for trace determination of chlorine in solid nuclear samples using TXRF and without dissolving the samples was developed. For such studies the TXRF spectrometer was first calibrated and the results counterchecked using calibration/sample solutions of chlorine prepared by dissolving NaCl in NaOH (5 mM) solution, having chlorine concentrations from 125 to 4000 ng/mL. Merck single element certiPUR ICP standard of cobalt diluted in NaOH solution was used as an internal standard. All samples and standards were prepared in NaOH medium to avoid the loss of chlorine as HCl when heated on TXRF sample supports. 30 μ L of the sample was deposited on cleaned quartz sample supports in duplicate and presented for TXRF measurements. W L α source was used for excitation of the sample. The chlorine present in trace quantities in nuclear fuel materials such as U₃O₈, (U, Pu)C, PuO₂ and Pu alloys was first separated from the solid matrix by pyrohydrolysis. This involves heating of the samples to a high temperature (900-1000 °C), followed by collection of the evolved chlorine, due to the breaking of the matrix, in the form of HCl by the moist Ar carrier gas in a buffer solution of NaOH. This solution was analyzed for chlorine by TXRF spectrometry using the instrumental parameters used for calibration. The precision for such determination was found to be within 25% (n=4) when the analysis was carried out in air atmosphere. Using of helium gas purging into the sample chamber, the precision improved to 15% (n=4). Using this approach, chlorine could be determined in (U,Pu)C, PuO₂ powder and Pu alloys and the most significant advantage of this methodology is that plutonium bearing radioactive samples can be analysed without putting the spectrometer inside the radioactive glove box and no sample dissolution is required.

CHAPTER FIVE

Analytical Characterization of Nuclear Materials by TXRF: Bulk Determinations

Apart from the determination of trace and ultra trace elements in nuclear materials, determination of the major/ bulk components is also equally important for the chemical quality assurance of such materials [14]. Studies to assess the applicability of TXRF, as a microanalytical technique for the determination of uranium and thorium as major elements in presence of each other are reported in this Chapter. Calibration and sample solutions with uranium and thorium contents in the range of 16 to 84% were prepared by mixing the standard

solutions of uranyl nitrate and thorium nitrate in different proportions. Mo K α X-rays were used to excite the samples. With a sample size of 10 μ L, the concentrations of the analytes in the range of 1–50 μ g/mL and total matrix concentration less than 200 μ g/mL, the precision and accuracy of the method were found to be better than 3% (1 s) and 4%, respectively. For higher concentration ranges of the analytes (up to 700 μ g/mL), the precision and accuracy values were slightly poor, 6% (1 s) and 5%, respectively. This may be because of the formation of thick film on the quartz sample support at such a higher concentration which results in appreciable matrix effects and comparatively poor results. In conventional XRF like EDXRF and WDXRF, the internal standard is chosen in such a way that the analytes and standards have similar matrix effect. Since the matrix effects are negligible in TXRF, any element which is not present in the sample can be used as an internal standard irrespective of the matrix. In order to support this, three single element standards of cobalt, gallium and yttrium, were added in the uranium-thorium solution and analysed. The analytical results of uranium and thorium showed that use of different internal standards did not affect the final results significantly. The microanalytical capability of TXRF has an advantage for radioactive samples, as it requires very less sample amount for analysis thereby producing very small radioactive waste and imparting minimum dose on the instrument and analyst. However, the method requires sample dissolution.

Dissolution of ceramic nuclear fuels, especially ThO₂ and PuO₂, is a cumbersome process. A fast non-destructive technique giving the elemental composition of the fuel is strongly desirable. In order to avoid sample dissolution, a TXRF method was developed for characterization of sintered and green (U, Th)O₂ samples in different forms like pellets, powder and microspheres, without dissolution. This method involves rubbing the pellet on TXRF quartz sample support very gently so that a few nanogram of the sample is transferred on the support and then TXRF measurement is made. In case of powder samples, the sample is mixed with collodion in a pestle mortar to make a paste and the pestle is just touched on the sample support with the tip of pestle, in such a manner that not more than a few nanogram of the material is transferred. After leaving this for a few minutes, a thin film of the sample is formed on the support. Uranium determinations from TXRF spectra of such specimens were made with respect to thorium and the uranium percent in (U+Th) was calculated. Samples having uranium atom percent from 0-100 % were analyzed for uranium by TXRF and the results showed a precision and accuracy better than 6% in most of the cases. The TXRF method thus developed was

compared with the Vegards Law method of uranium percent determination in (U,Th)O₂ solid solutions using XRD.

CHAPTER SIX

Determination of Uranium by TXRF in Non-conventional Resources: Seawater and Fertilizers

As stated earlier uranium is one of the most technologically important elements for nuclear technology. It is the only fissionable actinide, available naturally, for carrying out the nuclear fission. Due to the limited reserves of uranium in the form of ores, different scientific groups all over the world are in search of new sources of uranium. Seawater is a treasure of many salts and elements — precious and strategic in nature. Uranium is also present in seawater, though in very small concentrations of about 3.3 ng/mL [15] distributed uniformly all over the world. Other relatively rich resources of uranium are the phosphate rocks, phosphoric acid and phosphate fertilizers. It is estimated that in phosphate fertilizers, the uranium content ranges from 3 ppm to 220 ppm [16]. Considering the huge amount of seawater in the world, the total amount of uranium in seawater works out to be approximately 1000 times of the uranium in earth crust. Due to such importance and limited resources of uranium, studies are being pursued by different research groups all over the world, on the methodology to recover uranium from non-conventional sources. Separation of uranium from seawater and phosphate fertilizers is very important from recovery point of view of such technologically important material. In order to assess the efficiency of such recovery technologies, a suitable method for accurate determination of uranium in these samples is required. In view of these points, development of TXRF methods of trace determination of uranium in seawater and fertilizer samples was taken up and is reported in this Chapter. In both methodologies, separation and preconcentration of uranium was carried out by solvent extraction process. Uranium from seawater was selectively extracted using diethyl ether and determined by TXRF after its preconcentration by natural evaporation and subsequent dissolution in a small volume of 1.5% suprapure HNO₃. A known volume of yttrium was added to these samples as an internal standard. Before using diethyl ether for selective extraction of uranium from seawater, its extraction behavior for different elements was studied using a multielement standard solution having elemental concentrations at 5 ng/mL levels. It was

observed that the extraction efficiency of diethyl ether for uranium was about 100% whereas for other elements, it was negligible. The concentrations of uranium in seawater samples determined by TXRF are in good agreement with the values reported in the literature. The method shows a precision within 5% (1σ). For TXRF determinations of uranium in phosphate fertilizers, four fertilizer samples of Hungarian origin were processed with nitric acid and the uranium present was selectively removed by solvent extraction using tri-n-butyl phosphate as the extractant. The organic phase containing uranium was equilibrated with 1.5% suprapure nitric acid to bring out uranium in aqueous phase. This aqueous phase was mixed with internal standard Y and the TXRF spectra were measured by depositing samples on float glass supports. The amount of uranium in the fertilizer samples was determined by processing these TXRF spectra. Uranium concentrations in the two fertilizer samples were found to be in the range of 4–6 $\mu\text{g/g}$, whereas two fertilizer samples did not show any uranium. The precision of the TXRF determination of uranium was found to be better than 8% (1σ).

CHAPTER SEVEN

Analytical Characterization of Nuclear Materials by EDXRF: Bulk and Trace Determinations

In order to safeguard the analyst, analysis of radioactive elements is carried out inside the glove boxes. But putting the instruments inside the glove box makes the maintenance process very difficult and working in a glove box is sometimes tedious and time consuming process. Therefore, a need to develop an EDXRF methodology for analysis of radioactive samples without putting the instrument inside the glove box was felt. If the sample requirement for analysis is very less and it can be sealed properly, radioactive samples can be analysed without putting the instrument inside the glove box. Hence, studies were initiated to exploit the different features of EDXRF and are described in this Chapter. The severe matrix effects in XRF, which cause errors in analytical determinations, are almost negligible in specimens behaving like thin film which were used in the present work. The remaining matrix effect was taken care by the addition of a suitable internal standard having similar matrix effect as that of the analyte. Calibration solutions and samples covering the AHWR fuel composition range (0–5% of uranium in U+Th), were prepared by mixing uranium and thorium nitrate solutions. Natural U

was used as a surrogate for ^{233}U . A known fixed amount of internal standard yttrium (Y) was added to these solutions. EDXRF spectra of calibration solutions and samples were measured by taking 20 μL aliquots, containing $< 50 \mu\text{g}$ of U, on filter papers and drying them. Since a very small amount of the analyte is dispersed on the filter paper, the specimens behave as thin film. A Jordan Valley EX-3600 TEC EDXRF spectrometer having Rh target and operated at 40 kV and 500 μA was used for sample excitation. An Rh filter was used to increase the peak to background ratio. Calibration plots were made by plotting U/Y, U/Th and Th/Y amount ratios against the respective intensity ratios of Th $L\alpha$, U $L\alpha$ and Y $K\alpha$. Using the respective calibration plots the amounts of the analytes were determined. The uranium and thorium determinations showed a precision of about 3% (1s) and the results deviated from the expected values by $<3\%$ in most of the cases. The advantages of this approach is that it requires only microgram amounts of sample, thus mitigating radiation hazards associated with radioactive samples as well as the amount of radioactive analytical waste generated is quite less. Though the specimens in the present study were analysed directly, these can be sealed using thin PVC bags which will allow the X-rays to pass through in such a way that there is no loose contamination and analysed as described earlier. The application of filters and short distance between the source - sample, sample-detector was helpful in such approach.

Apart from major element analysis, EDXRF can be used for the trace element determination as well by using appropriate filters and excitation parameters. Among the trace impurities present in nuclear fuel, determination of neutron poisons are very significant for thermal reactors for neutron economy as well as for certifying the total impurities as a part of the chemical quality assurance of fuels [17]. Cadmium has a very high neutron absorption cross-section for thermal neutrons. Hence its presence at a concentration level >1 ppm is not acceptable in nuclear materials. Further, Cd being one of the heavy toxic elements present in our environment in minute quantities, its presence at trace level has to be monitored in water, food and environment periodically to avoid its adverse health effects on human and animals. Because of the above reasons, determination of Cd at trace and major levels, in presence and absence of uranium is important. In absence of high energy sources required for excitation of Cd $K\alpha$ lines, generally cadmium determination by XRF is made using Cd $L\alpha$ line, though it has certain disadvantages e.g. low fluorescence yield, lines lying in low energy region having high background and spectral interference. In the presence of uranium, the situation is very

complicated as there is strong interference of U M α line (3.171 keV) with Cd L α line (3.133 keV). It is very difficult to resolve Cd L α line from U M α using EDXRF because of its comparatively poor resolution than WDXRF. If cadmium is determined by XRF using Cd K α (23.172 keV) as analytical line these problems can be circumvented to a large extent provided a suitable excitation source is available for Cd K α excitation. The commonly available X-ray tubes have Mo, Ag or Rh targets and use mainly Mo K α , Ag K α and Rh K α lines for sample excitation. None of these lines can excite Cd K α . The continuum part of X-ray tube spectra can be optimized for exciting Cd K α analytical line for the determination of cadmium for routine sample analysis. However in such determinations of cadmium in uranium matrix Cd K α line will be strongly absorbed by uranium, since U L1 and U L2 absorption edges at 21.757 and 20.948 keV, respectively are just below Cd K α . In order to overcome this problem uranium must be separated from the samples before XRF determinations. In the present work, the possibility of determination of cadmium in uranium using the continuum produced by the Rh target to excite the Cd K α lines was explored. In order to improve the detection limits as well as to minimize the matrix effect, uranium was separated by solvent extraction from the calibration and sample solutions. Though continuum sources are of lesser intensity compared to characteristic X-rays, these can be suitably tuned for experimental requirements by suitable choice of instrumental parameters. Use of Mo filter in between the excitation source and the sample reduced the spectral background in the range of 20-26 keV where Cd K α line lies thereby improving the detection limits. Calibration and sample solutions of cadmium, with and without uranium, were prepared by mixing different volumes of standard solutions of cadmium and uranyl nitrate, both prepared in suprapure nitric acid. The concentration of cadmium in calibration solutions and samples was in the range of 6 to 90 $\mu\text{g/mL}$ whereas its concentration w.r.t. uranium ranged from 90 to 700 $\mu\text{g/g}$ of uranium. From the calibration solutions and samples containing uranium, the major matrix uranium was selectively extracted using 30% tri-n-butyl phosphate in dodecane. Fixed volumes (1.5 mL) of aqueous phases thus obtained were taken directly in specially designed in-house fabricated leak proof perspex sample cells for the EDXRF measurements and calibration plots were made by plotting Cd K α intensity against respective cadmium concentration. For the calibration solutions free from uranium, the EDXRF spectra were measured without any extraction and cadmium calibration plots were made accordingly. The results obtained showed a precision of 2% (1σ) and the results deviated from the expected values by 4% on average.

The important highlights of the thesis are:

- [1] Development of a TXRF method for the determination of trace metallic impurities at a concentration of a few $\mu\text{g/g}$ in ThO_2 .
- [2] Methodology was developed for determination of low atomic number impurities (Na, Mg & Al) at trace levels in uranium matrix by TXRF.
- [3] TXRF methodology was developed for the determination of non-metallic impurities (sulphur & chlorine) in uranium matrix.
- [4] Successful application of TXRF as a microanalytical technique for the bulk determination of uranium and thorium in solution and solid samples.
- [5] Trace determination of uranium in seawater and fertilizer samples by TXRF.
- [6] A novel EDXRF methodology was developed for the fast and accurate determination of uranium and thorium. The developed method requires very less sample amount such that enclosing the instrument in the glove box can be avoided.
- [7] An EDXRF methodology was developed for the determination cadmium at trace levels in uranium using continuum excitation and Mo filter.

The above developments are reported for the first time in the literature and have resulted in 9 (nine) peer reviewed journal publications, 6 (six) international symposia and 4 (four) national symposia. Following are the list of journal publications:

1. Trace Determination of Uranium in Fertilizer Samples by TXRF, N.L. Misra, ***Sangita Dhara***, Arijeet Das, G.S. Lodha, S.K. Aggarwal, and I. Varga, PRAMANA- journal of physics, 76 (2011) 357-360.
2. Energy dispersive X-ray fluorescence determination of cadmium in uranium matrix using Cd $K\alpha$ line excited by continuum, ***Sangita Dhara***, N.L. Misra, S.K. Aggarwal, V.Venugopal, Spectrochimica Acta Part B: Atomic Spectroscopy, 65 (2010) 461-465.
3. Determination of low atomic number elements at trace levels in uranium matrix using vacuum chamber total reflection X-ray fluorescence, N.L. Misra, ***Sangita Dhara***, M. Óvári, Gy. Zárny, S.K. Aggarwal, Imre Varga, Spectrochimica Acta Part B 65 (2010) 457–460.

4. A novel approach for chlorine determination in acidic medium by total reflection X-ray fluorescence, N.L. Misra, Imre Varga, *Sangita Dhara* and S.K. Aggarwal, X-ray Spectrometry 38 (2009) 182-185.
5. An EDXRF method for determination of uranium and thorium in AHWR fuel after dissolution, *Sangita Dhara*, S. Sanjay Kumar, N.L. Misra and Suresh K. Aggarwal, X-ray Spectrometry 38 (2009) 112-116.
6. Trace element determination in thorium oxide using total reflection X-ray fluorescence spectrometry, N.L. Misra, *Sangita Dhara*, V.C. Adya, S.V. Godbole, K.D. Singh Mudher, S.K. Aggarwal, Spectrochimica Acta Part B 63 (2008) 81–85.
7. Determination of sulphur in uranium matrix by total reflection X-ray fluorescence spectrometry, *Sangita Dhara*, N.L. Misra and S.K. Aggarwal, Spectrochimica Acta Part B 63 (2008) 1395-1398.
8. Bulk determination of uranium and thorium in presence of each other by Total Reflection X-ray Fluorescence spectrometry, *Sangita Dhara*, Nand Lal Misra, Khush Dev Singh Mudher, Suresh Kumar Aggarwal, Spectrochimica Acta Part B 62 (2007) 82–85.
9. Uranium determination in seawater by total reflection X-ray, fluorescence spectrometry, N.L. Misra, *S. Dhara*, K.D. Singh Mudher, Spectrochimica Acta Part B 61 (2006) 1166–1169.

References:

1. M.V. Ramaniah, Analytical chemistry of fast reactor fuels- A review, Pure and Appl. Chem., 54 (1982) 889.
2. C. Ganguly, R.N. Jayaraj, Characterization and quality control of nuclear fuels, Allied publishers: New Delhi (2002).
3. E.A. Bertin, Principle and Practice of X-ray Spectrometric Analysis, 2nd Edition, Plenum Press, New York (1984).
4. R. E. Van Grieken, A. Markowicz, Handbook of X-Ray Spectrometry (2nd edn), Marcel Dekker Inc., New York (1993).
5. H. Yoneda, T. Huriuchi, Opticle flats for use in X-ray spectrochemical microanalysis, Rev. Sci. Instrum., 42 (1971) 1069.

6. R. Klockenkaemper, Total Reflection X-ray Fluorescence Analysis, Chemical Analysis, vol. 140, John Wiley & Sons, New York (1996).
7. C. Strelı, H. Aiginger, P. Wobrauschek, Light element analysis with a new spectrometer for total reflection X-ray fluorescence, Spectrochim. Acta, Part B, 48 (1993) 163.
8. G. Pepponi, P. Wobrauschek, F. Hegedüs, C. Strelı, N. Zöger, C. Jokubonis, G. Falkenberg, H. Grimmer, Synchrotron radiation total reflection X-ray fluorescence and energy dispersive X-ray fluorescence analysis on AP1™ films applied to the analysis of trace elements in metal alloys for the construction of nuclear reactor core components: a comparison, Spectrochim. Acta, Part B, 56 (2001) 2063.
9. N.L.Misra, K. D. Singh Mudher, V.C. Adya, B. Rajeswari, V. Venugopal, Determination of trace elements in uranium oxide using Total reflection X –ray Fluorescence spectrometry, Spectrochimica Acta, Part B, 60 (2005) 834.
10. C. Strelı, P. Wobrauschek, G. Pepponi, N. Zoeger, A new total reflection X-ray fluorescence vacuum chamber with sample changer analysis using a silicon drift detector for chemical analysis, Spectrochim. Acta, Part B, 59 (2004) 1199.
11. U. Basak, M.R. Nair, R. Ramachandran, S. Majumdar, Fabrication of high density ThO₂, ThO₂–UO₂ and ThO₂–PuO₂ fuel pellets for heavy water reactors, BARC Newsletter, Founder's day special issue October (2001)
(<http://www.barc.ernet.in/publications/nl/>).
12. Valérie Vallet, Ingmar Grenthe, On the structure and relative stability of uranyl (VI) sulphate complexes in solution, C.R. Chimie, 10 (2007) 905.
13. R. Shekhar, J. Arunachalam, H. R. Ravindra, B. Gopalan, Quantitative determination of chlorine by glow discharge quadrupole mass spectrometry in Zr–2.5Nb alloys J. Anal. At. Spectrom., 18 (2003) 381.
14. Keshav Chander, S. P. Hasilkar, A. V. Jadhav, H.C. Jain, A titrimetric method for the sequential determination of thorium and uranium, J. Radioanal. Nucl. Chem., 174 (1993) 127.
15. <http://en.wikipedia.org/wiki/uranium.mining>
16. Ione Makiko Yamazakia, Luiz Paulo Geraldob, Uranium content in phosphate fertilizers commercially produced in Brazil, Appl. Radiat. and Isot., 59 (2003) 133.

17. B. Li, M. Luo, J. Li, W. Liu, Y. Sun, G. Guo, Determination of cadmium and lead in high purity uranium compounds by flame atomic absorption spectrometry with on-line micro-column preconcentration by CL-7301 resin, *J. Radioanal. Nucl. Chem.*, 278 (2008) 3.

LIST OF FIGURES

S. No.	Title	Page No.
1.1	Typical schematic diagram of nuclear fuel cycle	5
1.2	Various parts of AHWR fuel pin assembly	9
1.3	Relative detection limits of INAA, TXRF, ET-AAS and ICP-MS	24
2.1	X-Ray absorption curve of platinum	35
2.2	XAFS spectra showing Fe K- absorption edge	36
2.3	Moseley's Law plot of energy versus the atomic number	38
2.4	Schematic diagram of basic difference between WDXRF and EDXRF	40
2.5	Interaction of X-ray photons with matter	41
2.6	Photoelectric effect resulting in (a) Characteristic X-ray emission and (b) Auger electron production	42
2.7	Schematic diagram of an X-ray tube of Coolidge type	46
2.8	Effect of X-ray tube current, potential and target element on the intensity of continuum radiation	47
2.9	Spectrum generated from rhodium target X-ray tube	47
2.10	Schematic representation of a synchrotron source facility	51
2.11	Schematic picture of continuum production	52
2.12	Electron transition producing characteristic X-ray spectrum	53
2.13	Plot of X-ray fluorescence yield versus Auger electron yield	55
2.14	Cross sectional view of a Si(Li) detector crystal	57
2.15	Comparison of the geometrical difference between (a) conventional EDXRF and (b) TXRF	59
2.16	Schematic view of the total reflection geometry	61
2.17	The incident, reflected and refracted beam at the interface of two media with refractive indices n_1 and n_2 in (a) $n_1 < n_2$ and (b) $n_2 < n_1$	62
2.18	Dependence of beam path on the glancing angle α_1	64

2.19	Reflectivity versus the glancing angle for quartz, copper and platinum	65
2.20	Penetration of X-rays depending on the grazing angle for 17.5 keV radiation in silicon	66
2.21	Liquid sample pipetted on a clean quartz sample support which leaves a dry residue after evaporation	68
2.22	TXRF spectrum of a quartz sample carrier after cleaning	69
2.23	Efficiency for the excitation of elements with respect to the excitation source and photon energies	71
2.24	A typical TXRF spectrum of multi-element standard solution having a concentration of 5µg/mL	72
2.25	Plot of relative sensitivity of different elements versus their atomic number for (a): K lines and (b): L lines	76
2.26	The different steps of quantification applied for TXRF analysis	77
2.27	Variation of TXRF detection limits with atomic number	79
2.28	Basic layout of EDXRF spectrometers	81
2.29	EDXRF spectra of Cu and Ga (a) without Fe filter and (b) with Fe filter	82
2.30	Absorption-enhancement effect of aluminum and silicon on each other	84
2.31	a) ITAL STRUCTURES TX-2000 TXRF spectrometer and b) the inside view of the spectrometer	86
2.32	a) View of WOBISTRAX TXRF spectrometer and b) sample chamber with 12 position sample holder	88
2.33	(a) Jordan Valley Ex-3600 TEC EDXRF spectrometer (b) sample chamber	89
3.1	A typical TXRF spectrum of a processed thorium oxide (ThO ₂ -MOS) with gallium internal standard	100
3.2	A comparison of analytical results of different laboratories with certified and TXRF determined calcium concentration in ThO ₂ -S	104
3.3	A comparison of analytical results of different laboratories with certified and TXRF determined manganese concentration in ThO ₂ -B	105
3.4	Plot of efficiency of a Si(Li) detector versus the X-ray energies of elements	107
3.5	Flow chart showing the processing of the sample solutions for the TXRF analysis	110
3.6	Relative sensitivities of sodium, magnesium, aluminum with respect to gallium	111

3.7	TXRF spectrum after selective extraction of uranium and addition of scandium internal standard	112
3.8	Expanded TXRF spectrum after selective extraction of uranium	113
3.9	Comparison of calculated and TXRF determined concentrations of low Z elements Na, Mg and Al in sample -1, sample-2 and sample-3	115
4.1	The TXRF spectrum of aqueous phase of sample (SU-2) after preconcentration and addition of cobalt internal standard	128
4.2	A comparison of TXRF spectra of aqueous phase of a standard solution of sulphur obtained after different number of equilibrations with TBP	129
4.3	Plot between expected and TXRF determined sulphur concentrations in samples	131
4.4	Pyrohydrolysis set up for separation of chlorine from nuclear materials	135
4.5	Comparison of TXRF determined and expected chlorine concentration in sample solutions	137
4.6	TXRF spectrum of pyrohydrolysed (U, Pu)C-3 sample	138
4.7	Effect of helium gas purging on TXRF spectrum	140
4.8	A typical TXRF spectrum of the filtrate obtained after addition of cadmium internal standard	146
4.9	A comparison of expected and TXRF determined concentrations of chlorine in samples	147
5. 1	TXRF spectrum of a uranium-thorium synthetic sample (U-Th-4) mixed with internal standard	156
5.2	Calibration plot of TXRF determined and expected concentration of (a) uranium and (b) thorium in U-Th samples	160
5.3	TXRF spectrum of $(U_{0.04}Th_{0.96})O_2$ sample measured after rubbing the pellet on sample support	165
5.4	Expected and TXRF determined uranium percent in $(U,Th)O_2$ solid solution samples	167
5.5	XRD patterns of $(U,Th)O_2$ solid solutions	168
5.6	Cell parameter versus TXRF determined uranium atom percent	170
5.7	Cell parameter versus expected uranium atom percent	170
6. 1	A comparison of concentrations of different elements present in standard before and after extraction	180
6.2	TXRF spectrum of organic phase obtained after selective extraction of uranium in diethyl ether	181

6.3	Comparison of TXRF determined concentration of uranium in four seawater samples and literature reported concentration	183
6.4	Flow chart showing steps involved in the sample preparation methodology for TXRF analysis of uranium in fertilizer samples	185
6.5	Profile fitted TXRF spectrum of a processed fertilizer sample (Sample Code :1845)	187
7.1	An EDXRF spectrum of calibration solution	198
7.2	Calibration curve for uranium determination of Set –I	201
7.3	Calibration curve for uranium determination of Set –II	201
7.4	Calibration curve for thorium determination of Set -I	203
7.5	Calibration curve for thorium determination of Set -II	203
7.6	Flow chart used for processing of calibration solutions of Set-I and II, the samples of both the sets were processed using the procedure of Set-II	210
7.7	Effect of Mo and Rh filters on the tube spectrum in Cd $K\alpha$ energy region	212
7.8	Calibration plot for cadmium determination in samples without uranium	213
7.9	Effect of extraction of uranium on the intensity of Cd $K\alpha$	215
7.10	Calibration plot for cadmium determination in samples of Set-I	216

LIST OF TABLES

S. No.	Title	Page No.
1.1	Composition of Zr alloys used in various nuclear reactors	10
1.2	Specifications of metallic impurities in nuclear fuels (in ppmw)	14
1.3	Specifications for non metals in nuclear fuels (in ppmw)	16
1.4	Specifications of trace element impurities in Zirconium and zircaloy (in ppmw)	18
1.5	Comparison of important analytical features of various techniques in the field of determination of trace elements	21
2.1	X-ray techniques and their applications	33
2.2	List of commonly used radioisotope sources for X-ray radiation	49
2.3	Selection rules for characteristic X-ray production	54
2.4	Critical angle of total reflection for various media and different incident radiation energy	64
2.5	Important characteristics of different sample support materials	68
2.6	Concentration and the calculated relative sensitivity values of various elements along with their X-ray energies	75
2.7	TXRF analysis results of multi-element standard	78
2.8	A few primary beam filters and the elements that can be analysed using those filters	82
2.9	Characteristic X-ray energy and the fluorescence yield of low Z elements	87
3.1	Comparison of TXRF determined elemental concentrations of different elements with the corresponding certified values in thorium oxides ThO ₂ -B and ThO ₂ -D	102
3.2	Comparison of TXRF determined elemental concentrations of different elements with the corresponding certified values in thorium oxides ThO ₂ -S and ThO ₂ -MOS	103
3.3	Details of preparation of sample solutions for low Z elements	109
3.4	Results of TXRF determinations of low Z elements in sample solutions	114
4.1	Details of sample solutions of sulphur in uranium matrix	124
4.2	Details of the standard solutions prepared with Rb ₂ U(SO ₄) ₃	126
4.3	Elemental characteristic X-ray lines used for TXRF measurements and corresponding absorption edges	128

4.4	Comparison of TXRF determined and expected sulphur concentrations in standard solutions	130
4.5	TXRF determined and expected of sulphur concentrations in certified reference material $Rb_2U(SO_4)_3$	132
4.6	Typical specification limits for chlorine in nuclear materials	133
4.7	Comparison of TXRF(in air atmosphere) and Ion Chromatography determination of chlorine in (U,Pu)C samples	139
4.8	Comparison of TXRF (in helium purge) and Ion Chromatography determined chlorine in nuclear material samples	141
4.9	Details of preparation of sample solutions of chlorine	144
4.10	Comparison of TXRF determined and expected chlorine concentrations	147
5.1	Composition of sample solutions of uranium-thorium mixtures	154
5.2	Composition of calibration standard solution used for relative sensitivity determinations of uranium and thorium with respect to yttrium	155
5.3	Comparison of TXRF determined and expected uranium concentrations in sample solutions	157
5.4	Comparison of TXRF determined and expected thorium concentrations in sample solutions	158
5.5	TXRF determination of uranium and thorium using Co, Ga and Y as internal standards	161
5.6	Results of TXRF determined composition of solid solutions and their expected values	166
5.7	Results of TXRF determined composition of solid solutions and their cell parameters	169
6.1	TXRF analysis results of elements present in multi-element standard	179
6.2	Results of TXRF determined uranium in seawater samples	182
6.3	TXRF determined values of uranium in fertilizer samples	187
7.1	Details of Set-I calibration and sample solutions	195
7.2	Details of Set-II calibration and sample solutions	196
7.3	Amounts of analyte and internal standard transferred on filter paper when 20 μ L solution was taken for EDXRF analysis	197
7.4	Intensities of U $L\alpha$, Th $L\alpha$ and Y $K\alpha$ and the intensity ratios of U $L\alpha$ / Y $K\alpha$ and Th $L\alpha$ / Y $K\alpha$ in AH-2-9 sample from Set-II	199

7.5	Analytical results of uranium determinations in sample solutions of Set-I and II	202
7.6	Analytical results of thorium determinations in sample solutions of Set-I and II	204
7.7	Comparison of EDXRF determined percent uranium and thorium with the expected values in samples of Set –I and II	205
7.8	Details of calibration and sample solutions of cadmium without uranium	208
7.9	Details of calibration solutions of cadmium in presence uranium in Set-I and II	209
7.10	Analytical results of EDXRF determination of cadmium in samples without uranium	214
7.11	Analytical results of EDXRF determination of cadmium in samples of Set-I	217
7.12	Analytical results of EDXRF determination of cadmium in samples of Set-II	218

Chapter-1

INTRODUCTION

- 1.1. Technologically Important Materials
- 1.2. Nuclear Energy
- 1.3. Technologically Important Materials in Nuclear Industry
 - 1.3.1. Nuclear fuel
 - 1.3.2. Other technologically important materials
- 1.4. Analytical Characterization of Nuclear Fuel
 - 1.4.1. Trace metal assay
 - 1.4.2. Trace non-metal assay
 - 1.4.3. Bulk element assay
- 1.5. Analytical Characterization of Other Nuclear Materials
- 1.6. Non-conventional Sources of Uranium
- 1.7. Techniques Used for the Characterization of Nuclear Materials
 - 1.7.1. Role of X-ray fluorescence for characterization of nuclear materials
- 1.8. Objective of the Thesis
- 1.9. References

1.1. Technologically Important Materials

Technology is the application of science to achieve the industrial and commercial objectives, especially for the progress of the society, safety, comfort, communication, etc., required to improve the quality of life of mankind. It has become a need of day to day activities and human life is greatly dependent on it in the present civilization. The most important focus nowadays is on the activities that improve the utility of the existing technology for the betterment, in terms of set goal. Technologically important materials are those materials which play a significant role in implementation of the technology for human development because of their scientific, industrial, forensic and environmental applications. These materials find applications in almost every field of industry e.g. aeronautics, power production, electronics, agriculture, medical, environmental, etc. Some of the materials of technological importance are the high purity alloys and metals used in semiconductors and electronics industries. In the field of scientific research, high purity reagents and chemicals are required. Moreover, oil and petroleum products are an important part of many industries. The composition and purity of such materials is very important factor which controls their performance. In order to use these materials efficiently for the human benefit in any of the above mentioned area, it becomes mandatory to characterize them w.r.t their trace impurities content and bulk composition along with their physical characteristics [1-8]. In nuclear industry, some of the materials which have technological significance are those used as nuclear fuel, structural materials, coolant, control rods, reflectors, etc. [9-10]. Trace and major elements analyses of these materials is one of the important steps in the quality control program.

In recent years, tremendous developments have taken place for the advancement of physical methods of analysis resulting in increased sensitivity, reliability and thereby larger applications. The desired fundamental analytical requirements for any analysis are the best achievable accuracy, precision, selectivity and sensitivity. But it is seldom possible that a single technique can fulfill all these requirements for all types of materials. Hence selection of the most appropriate methodology is very important.

Many techniques such as Ultra Violet-Visible Spectrophotometry (UV-Vis), Atomic Absorption Spectrometry (AAS), Atomic Emission Spectrometry (AES), Mass Spectrometry (MS), Neutron Activation Analysis (NAA), Particle Induced X-ray Emission (PIXE), Laser Induced Breakdown Spectroscopy (LIBS) and X-Ray Fluorescence (XRF), have played

important roles in trace and micro-analysis of materials of importance [11-15]. Some of these techniques are completely destructive, some are partially destructive and a few are completely non-destructive. These techniques are also classified according to the sample amount required for the analysis, limitations of elemental analysis, detection limits and capital and maintenance cost.

XRF is a well established analytical technique for qualitative as well as quantitative determination of elemental composition of materials and is independent of their chemical and physical form in most of the cases. It is widely used in different areas of industry, archaeology, medical and environmental science for research as well as for different applications. The two main modes of operations of XRF spectrometry are: Energy Dispersive X-ray fluorescence (EDXRF) and Wavelength Dispersive X-ray fluorescence (WDXRF) [16-18]. However both these modes of XRF could never compete with the other well established trace element analysis techniques such as AAS, ICP-AES, ICP-MS, NAA, etc. For the last three decades, a comparatively new variant of XRF known as Total Reflection X-ray Fluorescence (TXRF) is gaining a significant importance as a trace and micro analytical technique [19, 20].

1.2. Nuclear Energy

In India, coal is the main source of electricity generation. But the reserves of coal are getting depleted day by day and with the present estimated industrial and economic growth of India, the country shall soon run out of its coal reserves. At present, nuclear energy of approximately 4500 MWe produced from 20 reactors in operation is about 2.9 % of the total electricity generation capacity of the country. India plans to supply 25% of the electricity by this route by the year 2050 and thus nuclear energy is set to play an important role in India's growing economy as a source of energy.

Uranium and plutonium are the main fissile actinides used for the production of electricity by fission. ^{238}U and ^{232}Th , though not fissile, can be converted to fissile materials ^{239}Pu and ^{233}U , respectively. Thus these materials are technologically very important. Uranium reserve in earth's crust is estimated to be about one fourth of that of thorium and there are no natural resources of plutonium. About 4 ppm (parts per million) of uranium is reported to be present in granite which makes 60% of the earth's crust. In phosphate fertilizers, it is found to be as high as 400 ppm and coal deposits contain about 100 ppm of uranium. Seawater is reported to

contain approximately 3ppb (parts per billion) of uranium. Though this concentration is very low, but in view of the amount of seawater available, this amount can be quite appreciable. Hence, considering the limited amount of uranium available in earth's crust, researchers and scientists all over the world are in search of non-conventional sources of uranium. Work is in progress towards the possibility of recovering uranium from seawater and phosphate fertilizer [21-23]. India has a very moderate reserve of uranium and one of the largest resources of thorium. Hence, the strategy of the Indian nuclear program, designed by its founder Dr. J. Homi Bhabha, is to optimize the utilization of the resources for power generation in a systematic way. For optimum utilization of uranium and thorium in the nuclear energy program, India has envisaged a three stage nuclear power program. The first stage of the nuclear power program is based on the utilization of natural uranium as a fuel for the Pressurized Heavy Water Reactors (PHWRs). These reactors produce ^{239}Pu by neutron absorption by ^{238}U . The Fast Breeder Reactors (FBRs) form the second stage of the nuclear program and will use plutonium as a fuel, extracted from the spent fuel reprocessing of the first stage. In these reactors, thorium oxide blanket will be used to produce ^{233}U by the neutron capture in ^{232}Th . In the third stage, ^{233}U -Th and ^{239}Pu -Th based reactors namely Advanced Heavy Water Reactors (AHWRs) are proposed to be setup [24-27]. The first stage of nuclear program is already well established and is in the industrial domain. Now the current trend is to develop advanced fuels and also advance the existing technology to achieve the desired objective of increasing the nuclear electricity generation. A lot of man power and technology input is required to develop such indigenous projects starting from mining and milling of ores, fuel and structural materials fabrication and processing, chemical and physical quality control and quality assurance, spent fuel reprocessing, radioactive waste management, including designing, manufacturing, construction of infrastructure and instruments. A schematic diagram of the processes involved in a nuclear fuel cycle program is given in Figure 1.1.

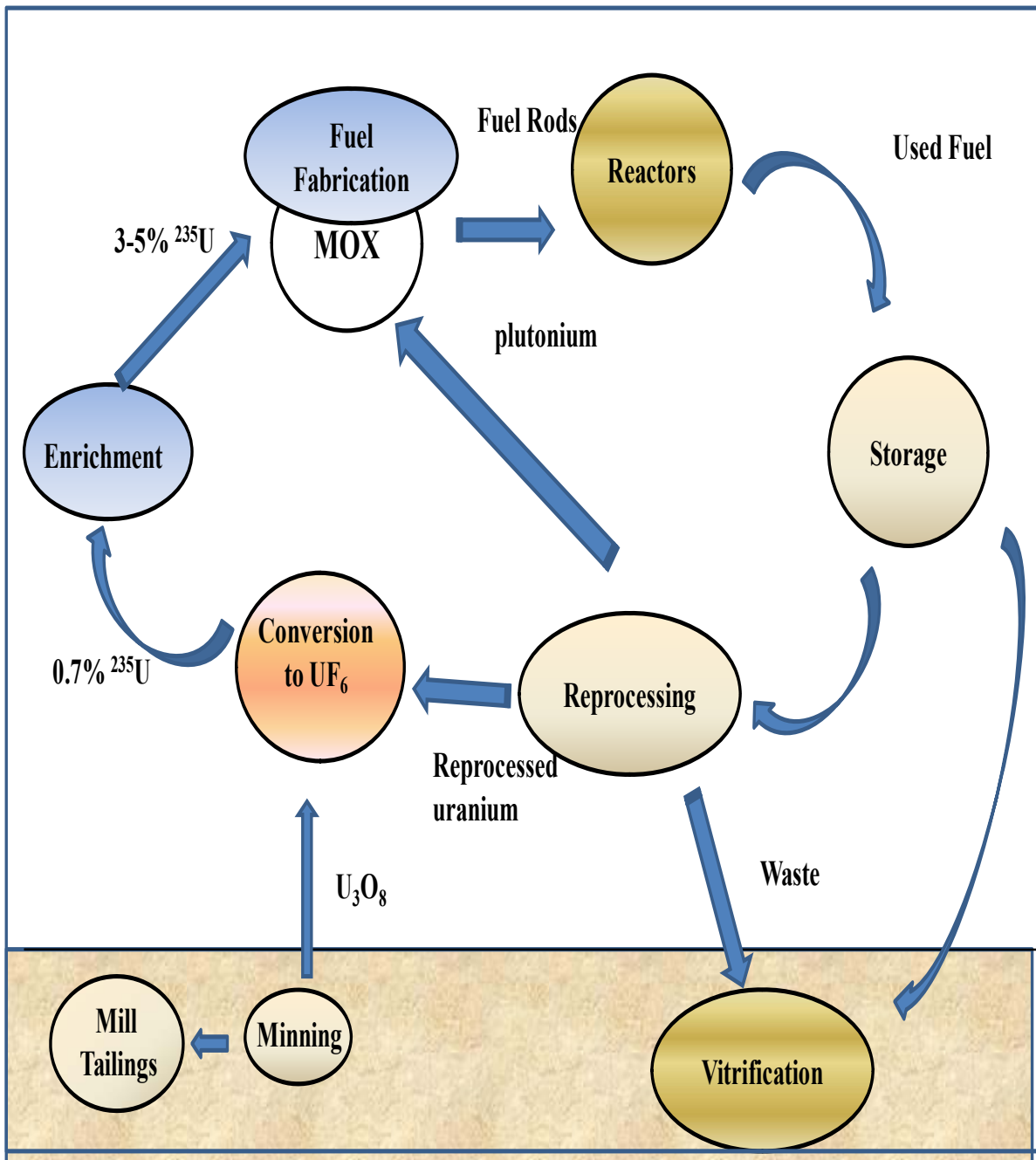


Figure 1.1: Typical schematic diagram of nuclear fuel cycle

1.3. Technologically Important Materials in Nuclear Industry

1.3.1. Nuclear fuel

The most important component of a nuclear reactor is its fuel. The fuel undergoes fission and the heat generated during this process is extracted to generate electricity. Uranium, plutonium and thorium are the actinides used as nuclear fuel in the reactors. The isotopes of these heavy fissile elements e.g. ^{233}U , ^{235}U and ^{239}Pu undergo fission to generate energy. It is this material which faces the most severe environment inside the reactor. The fuel sees very high temperature (the centerline temperature of the fuel pellets goes upto 2000°C), pressure and radiation field. Moreover, the fuel has to accommodate the radioactive fission products formed during the nuclear fission. With use the central part of fuel pellets gets overheated and many fission products and interaction products, some of which are low density compounds, gets accommodated into the fuel pellet. This leads to swelling of the fuel pellets. These conditions are remarkably dependent on the type of fuel, fuel composition and trace impurities present in these fuels. In view of this, the nuclear fuel has to be extremely well designed product with specific composition and trace impurity tolerance limits.

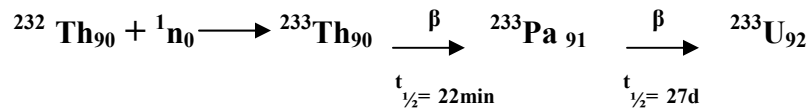
Uranium was the first element that was found to be fissile. Natural uranium has three isotopes ^{238}U (99.275%), ^{235}U (0.72 %) and ^{234}U (0.0054%). But only ^{235}U undergoes fission with neutrons of all energy thereby producing energy of about 200 MeV per fission. One of the possible reactions that takes place during fission is as follows:



Some of the released neutrons cause fission of another ^{235}U nucleus, thus sustaining the fission chain reaction. Uranium metal, alloy and oxide are the main forms of uranium used as fuel in research and power reactors. Metallic uranium has higher fissile element density than any of its compounds and therefore is considered to be an ideal fuel material in terms of power production. But metallic uranium and its alloy fuels are generally used in small research reactors and their use in large power reactors is limited. This is because of low melting point and high chemical reactivity at high temperatures and pressure with water, which is used as a coolant in the power reactors. Because of the fuel-coolant incompatibility of uranium metal, inert ceramic

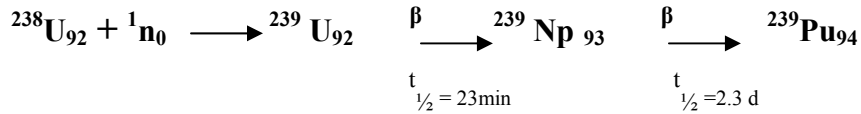
oxide fuel is more suitable for power reactors. Light Water Reactors (LWRs) and PHWRs use uranium dioxide as fuel due to its high melting point, adequate resistance to radiation and high chemical and thermal stability. Mixed Oxide (MOX- (U, Pu)O₂, (U, Th)O₂, (Th, Pu)O₂), Mixed Carbide ((U, Pu)C) and Mixed nitride ((U, Pu)N) fuels are considered as advanced alternative fuels for power reactors.

Because of the limited reserves of uranium, high priority is accorded to the development of thorium based nuclear fuel cycle in Indian nuclear energy program as thorium is present in large amounts in India. AHWRs are designed to make use of thorium fuel [28]. Thorium which is an alternate fuel is not a fissile material, but fertile. The melting point of ThO₂ (3300°C) is higher than that of UO₂ (2800 °C) and this higher melting point of ThO₂ ensures high burn-up and high temperature in the reactor core. Thorium does not undergo fission and gets converted into fissile material through neutron capture process described below.



This conversion is accomplished mainly in fast breeder reactors and to a limited extent in PHWRs. AHWR envisages the recycling of ²³³U produced by the above neutron capture reaction in thorium. Three types of mixed oxide (MOX) fuel assemblies having the composition: (Th_{0.97}-²³³U_{0.03})O₂, (Th_{0.9625}-²³³U_{0.0375})O₂ and (Th_{0.9675}-²³⁹Pu_{0.0325}) O₂ have been proposed for the AHWR fuel [26]. Thorium based fuels appear to be more promising than UO₂ for several reasons. A comparison of thermo-physical properties like thermal conductivity, specific heat capacity, thermal expansion coefficient and grain growth indicates ThO₂ to be superior than UO₂ from fuel performance point of view. Compared to uranium based fuels, thorium based fuels offer superior stability under irradiation. However, an important isotope of U i.e. ²³²U is of great concern in the thorium fuel cycle. Use of ²³³U as a fuel will lead to the introduction of ²³²U present in 100 to 500 ppmw in ²³³U. Two daughter products of ²³²U are ²⁰⁸Tl (61s, 0.78 MeV) and ²¹²Bi (3m, 2.6 MeV) and these are hard gamma emitters with short half lives and hence require remote handling during fuel fabrication.

Plutonium is another very important artificially produced fissile element used for the production of nuclear power. It is produced in reactors by conversion of ^{238}U into fissionable plutonium through the following reaction:



It is most beneficially used in fast breeder reactors as nuclear properties of plutonium permit higher breeding when the neutron spectrum is hard. Plutonium based fuels used in fast breeder reactors are PuO_2 , $(\text{U}, \text{Pu})\text{O}_2$ and $(\text{U}, \text{Pu})\text{C}$. Being highly radiotoxic element, plutonium has to be handled in specially designed facilities.

The nuclear fuel, which is technologically the most important component of a nuclear reactor, has to undergo very stringent quality control before being loading into the fuel pin shown in Figure 1.2.

1.3.2. Other technologically important materials

Apart from nuclear fuel, the other technologically important materials in a nuclear reactor are clad materials made of aluminum, stainless steel or zircalloy; coolant materials like liquid sodium (FBTR) and light water (PHWRs and BWRs); moderators (Heavy water in PHWR and light water in BWRs), reflector, control rods and structural materials. The clad is the material which encloses the fuel, thereby separating it from the other components of the reactor. The cladding tubes are exposed to the impact of nuclear fuel, fission products, radiation, corrosive coolant environment, high temperature and pressure. Therefore, they have to comply with very high quality of chemical composition, resistance to corrosion and stress, high strength, low radiation damage and the most importantly low neutron absorption cross-sections. Aluminum and its alloys are often used as clad in research reactors. Due to its physical and mechanical characteristics, compatibility, resistance against radiation damage and corrosion and favorable nuclear properties (low neutron absorption cross-section and rapid decay of neutron induced ^{28}Al radioactivity; $t_{1/2} = 3.2\text{ m}$). Presence of different impurities in aluminum can cause losses of neutrons during irradiation or radiation hazards when, after longer irradiation, the material is

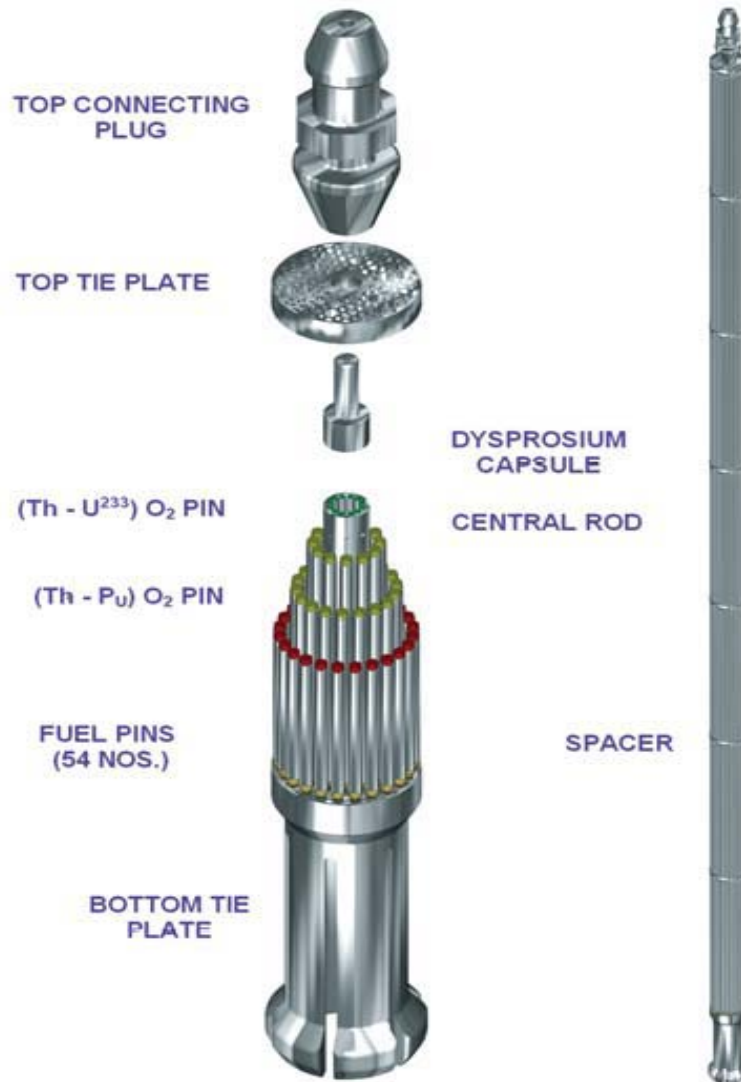


Figure 1.2: Various parts of AHWR fuel pin assembly

taken out for further handling [29]. Zirconium is another such material having excellent mechanical properties. In addition, it has corrosion resistance property, good radiation stability and very low thermal neutron cross-section (0.18 barns). Zirconium alloys (Zircalloys) are one of the principle cladding materials used in light water and heavy water reactors. Zircaloy-2 clad is used in Boiling Water Reactor (BWR) and Zircaloy-4 which has no nickel content (for less hydrogen uptake) is used in Pressurized Water Reactors (PWRs) and PHWRs. Zr-2.5% Nb is a binary alloy with Nb added to increase the mechanical strength. This alloy is utilized for pressure tubes in PHWRs. The composition of various Zr alloys used in nuclear industry is given in Table 1.1. For Fast Breeder Test Reactor (FBTR) and Prototype Fast Breeder Reactor (PFBR), stainless steel claddings are used.

The coolant and the moderators are another class of technologically important materials. The coolant acts as a heat transfer fluid to transfer heat generated during the fission to the steam generator and also to cool the condenser. The moderator slows down the fission neutrons. The requirements of coolant material are i) Good thermal conductivity, ii) Chemical compatibility with fuel, clad and structural materials and most importantly iii) Low neutron absorption cross section. In PHWR, heavy water (D_2O) is used as moderator as well as primary coolant. In BWR, light water is used as coolant and moderator. In FBTR and PFBR, which operate at a very high

Table 1.1: Composition of Zr alloys used in various nuclear reactors

Elements	Zircaloy-2 (in %)	Zircaloy-4 (in %)	Zr-2.5%Nb (in %)
Sn	1.20-1.70	1.20-1.70	--
Fe	0.07-0.20	0.18-0.24	--
Cr	0.05-0.15	0.07-0.13	--
Ni	0.03-0.08	--	--
Nb	--	--	2.40-2.80

temperature and does not require moderator, liquid sodium metal is used as coolant which is very reactive with air and moisture.

In order to reduce the neutron losses, the inner surface of the reactor core is surrounded by a material which helps to reflect these escaping neutrons back towards the core of the reactor. These materials are known as reflecting materials. The use of a proper reflector helps to reduce the size of the reactor core for a given power output since the number of neutrons leaking are minimised and they help to propagate the fission process. The essential requirements of reflector materials are i) Low neutron absorption (or capture) cross-section to minimize their losses, ii) High macroscopic scattering cross-section, iii) Temperature and Radiation stability. The commonly used reflector materials include pure water, heavy water (deuterium oxide), beryllium (as metal or oxide), carbon (graphite), and zirconium hydride. Most power reactors use water as the moderator and reflector, as well as the coolant. Graphite has been used extensively as moderator and reflector for thermal reactors. Beryllium is superior to graphite as a moderator and reflector material, but because of its high cost and poor mechanical properties, it has little prospect of being used to any extent. A control rod is made of chemical elements capable of absorbing many neutrons without undergoing fission. They are used in nuclear reactors to control the rate of fission. A variety of elements having high neutron absorption cross-section are used as control rods. These include silver, indium, cadmium, boron and rare earth elements or their alloys and compounds. The choice of materials for control rod is influenced by the energy of neutrons in the reactor, their resistance to neutron-induced swelling and the required mechanical and lifetime properties. The rods have the form of stainless steel tubes filled with neutron absorbing pellets or powder.

All these above described materials have high technological significance in the nuclear industry [3]. Maintaining the nuclear grade purity of all these materials is very important because the presence of trace impurities can lead to drastic changes in their thermal conductivity, formation of radioactive isotopes giving high radiation dose harmful to reactor operators and neutron losses. In addition to this, the characterization of the irradiated fuel obtained from the reactor is important for its reprocessing and waste immobilization.

1.4. Analytical Characterization of Nuclear Fuel

The nuclear fuel cycle consists of a series of industrial processes (Figure 1.1). For fabricating high quality nuclear fuels, chemical and physical quality control of the starting, intermediate and final product of this fuel cycle is essential. Chemical quality control ensures that the fuel material conforms to the chemical specifications for the fuel laid down by the fuel designer. These specifications are very stringent and include the major, the minor and trace constituents which cause detrimental effect on the fuel properties and performance under the reactor operating conditions. Therefore, trace and major element determinations in nuclear materials are of utmost importance.

The process of chemical quality assurance for trace elements includes pre-concentration and separation of the impurities from the sample matrix, followed by their quantification. There are various ways by which these impurities get incorporated into the fuel. Starting from mining, till its fabrication, the fuel material goes through a series of wet chemical processes which include dissolution (in nitric acid), purification by solvent extraction and precipitation. During all these processes, the impurities from the various reagents used in the above processes get added to the nuclear fuel material. Also during the nuclear fission, a number of fission products are produced which make the fuel matrix highly heterogeneous. A gamut of analytical methodologies is required for the chemical quality assurance of nuclear materials [30]. Analytical methodology for characterization involves the following steps:

- i) Sample dissolution
- ii) Trace metal determination
- iii) Trace non-metal determination
- iv) Isotopic composition determination
- v) Major content (Th, U, Pu) determination
- vi) Oxygen/ metal ratio determination
- vii) Americium determination

1.4.1. Trace metal assay

Among the trace impurities present in nuclear fuel, the trace metallic elements need to be determined because they affect the neutron economy as well as the physical properties of these materials adversely. As neutrons are the primary particles causing nuclear fission, their economy is of utmost importance. This can be adversely affected by the presence of neutron absorbing impurities in the fuel. Determination of these neutron poisons, viz. Boron (B), Cadmium (Cd) and some rare-earths e.g. Samarium (Sm), Europium (Eu), Gadolinium (Gd), Dysprosium (Dy), etc., [31] which have large neutron absorption cross-sections, is very significant in thermal reactors for assessing neutron economy as well as for certifying the total impurities as a part of the chemical quality assurance of fuels. Sodium, magnesium and aluminium, if present in uranium oxide fuel in amounts higher than the specified levels, may reduce the relative amount of fissile materials and form appreciable amounts of uranates of these elements with uranium in lower and higher oxidation states in reactor operating and transient conditions, respectively. If formation of these uranates is appreciable, it may cause expansion of fuel volume leading to rupture of fuel cladding. Also in minor accidents involving crack of cladding, uranates with higher valency of uranium may be formed which may lead to fuel expansion due to their low density and propagate further cracking of the clad. Hence quantifying these elements helps in deciding whether the prepared material can be taken for further use or has to be discarded. Zinc is another metal whose quantification is important. It has very low melting point and if present in larger amounts will cause liquid metal embrittlement thereby altering the fuel structure. Refractory elements like tungsten, molybdenum and tantalum, if present in large amounts, may cause creep resistance resulting in clad damage. Elements like iron, chromium, nickel are monitored to check for the process pick-up and condition of process equipment. Presence of iron and nickel in high concentration leads to problem in sintering of the fuel, which is required to increase the fuel density for higher power production. In particular, the trace metallic impurities affect the integrity of the fuel material and the neutron economy significantly [7]. Table 1.2 gives the specifications of some of the metallic trace elements in thermal and fast reactor fuels [32, 33]. Apart from nuclear fuel, various other materials such as moderator, coolant, structural materials need to conform to stringent specifications w.r.t. presence of trace and ultra trace metallic impurities in similar way.

Table 1.2: Specifications of metallic impurities in nuclear fuels * (in ppmw)

Elements	Thermal Reactors UO ₂		Fast Reactors (Ceramic Grade)			ThO ₂
	Natural	Enriched	UO ₂	PuO ₂	(U,Pu)O ₂	
Ag	1	25	1	10	20	-
Al	50	400	500	250	500	50
B	0.3	1	10	10	20	0.3
Be	-	-	20	20	20	1
Ca	50	250	100	500	250	200
Cd	0.2	1	20	20	20	0.2
Ce	-	-	-	-	-	4
Co	-	75	10	20	20	1
Cr	25	400	200	200	250	25
Cu	20	400	10	50	100	50
Dy	0.15	-	-	-	-	0.2
Eu	-	-	-	-	-	0.08
Fe	100	400	400	350	500	100
Gd	0.1	1	0.1	1	-	0.2
Mg	50	200	25	100	25	50
Mn	10	200	-	-	-	10
Mo	4	400	-	-	-	20
Na	-	400	-	-	100	-
Ni	30	400	400	300	500	30
Pb	-	400	-	-	-	20
Si	60	200	-	-	-	60
Sm	-	-	-	-	-	0.4
Sn	-	400	-	-	-	1
V	-	400	-	-	100	5
W	-	100	-	200	200	-
Zn	-	400	-	200	100	-

* Ref [32, 33]

1.4.2. Trace non-metal assay

The trace non-metallic impurities also affect the integrity of the fuel and structural materials. Some of the non-metals are present in gaseous form in reactor operating conditions. Apart from neutron economy, if gaseous impurities are present, they may cause swelling of the fuel which may result in rupturing of cladding. Hence the knowledge of non-metallics present in fuels is very important. Fluorine and chlorine get incorporated into the nuclear fuel during the mining and reprocessing processes. These two elements being very corrosive cause local depassivation of the oxide film on the internal surface of the clad tube leading to detrimental effect in the operating reactor environment. The effect of these halides is more prominent in the presence of moisture as they form their respective acids, on reacting with moisture, which leads to corrosion of the clad [34, 35]. During fabrication of fuel pellets, sintering is carried out in inert hydrogen atmosphere. If sulphur is present above certain specified limits in fuel pellets, it results in the formation of corresponding actinide oxo sulphides and H₂S during sintering and this causes shattering of the pellets especially, ThO₂ pellets in powder form [36]. Presence of carbon in excess amounts than the specified limits will cause carburization of structural materials by reacting with zirconium alloys in thermal reactors and stainless steel in fast breeder reactors, thereby making them fragile [37]. The hydrogen content of the sintered and dried nuclear fuel is an important quality feature. Higher hydrogen contents may lead to damages (“sunbursts”) of the Zircaloy cladding tube. Moisture content above the specified limits also causes corrosion of clad, modifies the O/M ratio of the fuel and releases hydrogen which can cause pressure build-up. In nuclear fuels, nitrogen gets incorporated as trace impurity during the dissolution and purification steps. Nitric acid is invariably added during all these steps. The main problem with nitrogen is formation of ¹⁴C by the ¹⁴N (n, p) ¹⁴C reaction and its release as CO, which leads to carburization and influences the operation of reprocessing process for spent nuclear fuel [38, 39]. Nitrogen also reacts with clad materials to form oxynitrides and these nitrides lead ultimately to poor corrosion resistance. Table 1.3 gives the specification of non-metallic impurities for various nuclear fuel materials [32, 40].

1.4.3. Bulk element assay

Apart from the determination of trace elements, it is also essential to determine the major composition of elements in nuclear materials. In the reactor core, pellets of different fuel composition are placed at different positions for the safe and efficient operation of the reactors. Determination of uranium, thorium and plutonium which are the major constituents of the fuel is necessary for elemental characterization in order to ensure the required fissile content [41].

Determination of carbon and nitrogen as major constituent is important for characterization of advanced Carbide and Nitride fuels, respectively. C/M and N/M (M is uranium, thorium or plutonium content) are important parameters to be controlled and determined precisely. If this ratio is not maintained as per the specifications, it will lead to phase segregation along with the formation of metal or free carbon or nitrogen. Excess of these elements (C & N) leads to clad carburization and nitriding. Lower carbon amounts may result in precipitation of plutonium metal in carbide fuel resulting in hot spots.

Table 1.3: Specifications for non-metals in nuclear fuels* (in ppmw)

Element	Natural UO ₂	Enriched UO ₂	Ceramic grade PuO ₂	ThO ₂
C	200	100	200	100
H	1	-	-	1
N	-	100	200	75
F	10	25	25	10
Cl	-	15	50	25
S	-	-	300	50

*Ref [32, 40]

Oxygen amounts other than the specified values may change the oxygen to metal ratio (O/M) of the oxide fuel resulting in changes in the physical and chemical properties of the fuel [42, 43]. O/M ratio affects the thermal conductivity, melting point, diffusion coefficients and vapour pressure. Apart from this, the O/M controls the chemical state of the fission product and their interaction with fuel.

1.5. Analytical Characterization of Other Nuclear Materials

Performance of a reactor is as much dependent on the purity of the structural materials as the fuel itself. Zirconium and its alloys have high strength and high corrosion resistance. But for their use in nuclear reactors, the materials should have to ensure their conformity to specifications. The elements like Fe, Cr and Ni which forms the solid solution with Zr at high temperature lead to the formation of intermetallic compounds during cooling. These compounds are brittle and have the ability to absorb hydrogen. Hydrogen forms zirconium hydride, which precipitates causing hydrogen embrittlement, thereby reducing fracture toughness and ductility. Chlorine also enhances the rate of hydrogen ingress during the operation of reactor resulting in loss of integrity and strength of the tube. Reactions of fluoride on constituent elements of various clad materials in the reactor environmental conditions are very complex. Presence of B, Cd and rare earths cannot be tolerated even in sub ppm levels for reactor grade zircaloy. Table 1.4 gives the specifications of various elements in zirconium and zircaloy [32].

Impurities present in the coolant lead to radiation field due to the neutron activation of these elements. Among the radioactive contaminants present, $^{60,58}\text{Co}$, ^{59}Fe , ^{54}Mn , ^{51}Cr , ^{124}Sb and ^{110}Ag are important as they have relatively longer half-lives and emit very high energy gamma radiations. Liquid sodium used as a coolant in fast reactors has to be of nuclear grade and the quality control of sodium at several stages of procurement and purification is quite a challenging task. The specification of nuclear grade sodium requires about 30 elemental impurities to be below 10 ppm. Because of high reactivity of sodium with oxygen and moisture, high purity inert atmosphere glove boxes, with oxygen and moisture levels less than 1ppm, are required for handling and analysis of sodium.

Table 1.4: Specifications of trace element impurities in Zirconium and Zircaloy* (in ppmw)

Elements	Zircaloy-2	Zircaloy-4	Zr-Nb 2.5%	Zr- Sponge
Al	75	75	75	75
B	0.5	0.5	0.5	0.5
C	270	270	125	250
Ca	30	30	25	30
Cd	0.5	0.5	0.5	0.5
Cl	20	20	0.5	1300
Co	20	20	20	20
Cr	500-1500	700-1300	200	200
Cu	50	50	50	50
F	< 2	< 2	0.5	-
H	25	25	5	25
Hf	200	200	50	100
Mg	20	50	50	600
Mn	50	50	50	50
Nb	100	100	2.4-2.8 %	-
Ni	300-800	70	70	70
O	1000-1400	1000-1400	900-1300	1400
Pb	130	130	130	100
Si	20	120	120	120
Sn	1.2-1.7%	1.2 – 1.7%	50	-
RE	-	-	-	15
Fe+ Cr+ Ni	0.18-0.38	0.28-0.37%	-	-

*Ref[32]

1.6. Non-conventional Sources of Uranium

The technological importance of uranium is vast. It is the only actinide element available in the nature which is fissionable. Apart from its applications in nuclear industries, uranium compounds are used as catalysts [44]. Uranium oxide is a semiconductor material having a band gap of about 1.3 eV, suggesting its possible use for efficient solar cells. Investigations are also going on the possible applications of uranium as material for rechargeable batteries and photo-electrochemical cells. Uranium dioxide, like U_3O_8 , is a ceramic material capable of withstanding high temperatures (about 2300°C), making it suitable for high-temperature applications like thermo-photovoltaic devices. Unfortunately, the resources of uranium are limited. The amount of economically mineable uranium in the earth is estimated to be around $5-6 \times 10^6$ tones. As the need for uranium is increasing, researchers all over the world are in search of new as well as non-conventional sources of uranium. Seawater and phosphate rocks are two promising non-conventional sources of uranium from which uranium can be recovered in an economical way. In seawater, uranium is present as dissolved salt having a concentration of 3.3 ppb. When we consider the total amount of uranium present in seawater, it is about 4×10^9 tones which are 1000 times more than the mine uranium [45]. An important step in these recovery studies is the determination of uranium in seawater. A few techniques are available for the uranium determination at such a low level and high salt matrix like that of seawater. Phosphate rocks have attracted more attention from the recovery point of view for uranium as these contain high uranium ranging from 0.01 to 0.02% [46]. Literature reports have showed that fertilizers containing phosphate also contain high concentration of uranium ranging from 3-200 ppm [23].

1.7. Techniques Used for the Characterization of Nuclear Materials

There has been a remarkable advancement in the technology for the development of nuclear fuels and other materials in the last few years. To keep pace with such development, a similar development in the advancement of quality control related programs is desirable. A vast number of instrumental techniques are used for the chemical characterization of nuclear materials. Each technique has its own advantages and disadvantages. Therefore, for the best utilization of these techniques, proper selection depending on the need is essential. In order to develop a methodology for analytical characterization of materials, various steps have to be

followed, which comprise of sampling of the material, preparation of suitable standards, calibration and validation of the spectrometer, sample preparation for measurement, data handling and processing along with the investigations of the associated problems and improve the analysis results. A comprehensive use of various analytical techniques is required for the chemical characterization of technologically important materials in nuclear industry. These include determination of metallic and non-metallic impurities, total gas content as well as the nuclear fuel elements i.e. uranium, thorium and plutonium in UO_2 , PuO_2 , $(\text{U}, \text{Pu})\text{O}_2$, UC, $(\text{U}, \text{Pu})\text{C}$, ThO_2 , $(\text{U}, \text{Th})\text{O}_2$, $(\text{Pu}, \text{Th})\text{O}_2$, alloy fuels and other reactor components.

Trace element analysis is routinely carried out using techniques like AAS, AES, ICP-MS, NAA, and electro-analytical techniques. TXRF is another upcoming technique competing with the above mentioned methods of trace analysis. Each of these techniques uses different physico-chemical properties for trace determination. No single technique can satisfy all the requirements of sample analysis. Hence depending on the nature of the sample, range of detection, spectral interference, speed of analysis and cost of equipment, the techniques used can be varied or modified. Table 1.5 gives a comparison of important analytical features of various techniques used for trace elements determination [33]. For the determination of major constituents, such as uranium, thorium and plutonium, complexometric titrations, electroanalytical methods and XRF are widely used in nuclear industry [41, 47-48]. Two important features of a technique to be suitable for the characterization of nuclear materials are:

- i) Consumption of minimum amount of sample and
- ii) Production of minimum analytical waste.

This saves the instrument and operator from the risk of radiation hazard and also minimizes the radioactive analytical waste disposal amount.

1.7.1. Role of X-ray fluorescence for characterization of nuclear materials

The importance of analytical characterization of nuclear materials has already been dealt in detail in the earlier part of this Chapter. Such characterization is required during various stages

Table 1.5: Comparison of important analytical features of various techniques in the field of determination of trace elements*

Features	TXRF	ICP-MS	INAA	ICP-AES	ET-AES	Electro analytical
Samples						
Volume	2-100 μ L	2-5 mL	10-200 mg	2-5 mL	5 μ L	2-5 mL
Analysis of solids	Digestion or suspension	Digestion or suspension	None	Digestion or suspension	Digestion or suspension	Digestion or suspension
Dissolution portion	<1%	<0.4%	any	<0.4%	-	-
Consumption	No	Yes	No	Yes	Yes	No
Detection						
Detection Limits	1 ppb	<0.01 ppb	<1 ppb	<1ppm	<0.1 ppb	ppb
Spectral interference	Very Few	Severe	A Few	Moderate	None	None
Elemental limitations	Z<5	H, C, N, O, F, P, S	Z<9, Tl, Pb, Bi	Non-metals	Refractory elements	-
Isotope detection	No	Yes	No	No	No	No
Quantification						
Calibration	One internal standard	Several standards	Pure element foils	Several standards	Standard for each element	-
Matrix effects	Negligible	Severe	Negligible	Moderate	Moderate	Moderate
Measurement time	100-1000s	~ 200s	30 min- few days	~300 s	~300s	~1000s
Expenditure						
Capital cost	Medium	High	Very high	High	Low	Low
Maintenance and running cost	Seldom low	High	Seldom high	High	Seldom low	Low

*Ref [33]

of the nuclear fuel cycle. A variety of techniques are used for this purpose as discussed above. Among all these methods, XRF, because of its simplicity, non-destructive nature and multi-analytical capability has attracted the attention of analytical scientists the most. XRF can be classified as energy dispersive and wavelength dispersive mode. Both are used for trace as well as bulk analysis of samples. In comparison to other analytical techniques, XRF has quite a few advantages. Unlike optical emission spectra, XRF spectra are simple, vary with atomic number in a systematic way and generally do not depend on the chemical state. It requires less effort for sample preparation and has precision and accuracy comparable with other techniques. There is almost no analytical method like XRF, which can deal with such a wide variety of samples forms (solid, liquid, paste, powder and even gas).

Theoretically, XRF can be used for the analysis of all elements except hydrogen and helium, but, because of low fluorescence yield and less energy, the low Z elements are difficult to analyse by XRF. Introduction of synthetic multilayer crystals, which became commercially available in the early eighties, to X-ray spectrometers has made possible the determination of very light elements with atomic numbers in the range from 4 (beryllium) to 9 (fluorine) [49]. XRF is applicable over an extremely wide concentration range starting from a few ppm to 100 percent. The two major limitations of the conventional XRF methods are high background and secondly severe matrix effects also known as absorption-enhancement effects. Various methods like standard addition method, thin-film method, matrix dilution method, internal standardization and mathematical corrections are used to account for the matrix effects. In nuclear industry, a fast analytical method like EDXRF is required to verify the composition of nuclear fuel during fabrication and processing, whereas an accurate and precise method is needed for its chemical quality assurance. WDXRF is also a well established technique in nuclear industry, but it is comparatively more time consuming because of its sequential multianalytical capability.

Total reflection X-ray fluorescence (TXRF), an improved variant of EDXRF, is comparatively a new technique which has better detection limits and negligible matrix effects. TXRF is primarily used for chemical micro- and trace analysis. With respect to the capabilities in terms of analytical features, cost and maintenance, TXRF has far surpassed the conventional XRF and is in competition with INAA, ICP-MS and AAS. For several features TXRF has advantage over these trace analysis methods. Its features such as (i) analysis of elements starting from boron to aluminum (in vacuum chamber), silicon to plutonium (air atmosphere)

(ii) analysis of metal and non-metals alike (iii) easy quantification requiring addition of a single internal standard (iv) negligible matrix eliminating the need of matrix matched standards and cumbersome calibration plots and (v) requiring very less sample amounts, has made this technique highly suitable for the analysis of nuclear samples. Therefore, TXRF has a vast potential for nuclear material characterization. The only limitations are impossibility of totally non-destructive analysis, limitations for volatile liquids and high matrix content and restriction to flat, smooth and highly polished surface. The relative detection limits of INAA, ET-AAS, ICP-MS and TXRF for trace elements in aqueous solution in a sample amount of 3mL needed for INAA and ICP-MS and 50 μ L specimen evaporated for TXRF and ET-AAS are shown in Figure 1.3. Hence, w.r.t the capabilities in terms of analytical features, cost and maintenance, TXRF has surpassed the conventional XRF and is in competition with INAA, ICP-MS and AAS.

1.8. Objective of the Thesis

Analytical characterization plays a vital role for quality control/assurance during the processing and fabrication of nuclear materials. Such characterization includes determination of ultra trace, trace, minor and the bulk composition of these materials. Moreover, since matrix matched standards for nuclear materials are not easily available, it is essential to use different analytical techniques having different physico-chemical properties. Hence it is necessary to develop suitable analytical methodologies for characterization of nuclear materials.

XRF is one of the well established techniques for elemental determination of materials from sodium to plutonium in solids as well as liquids. TXRF is comparatively a new technique having a vast area of application. It is used for trace and micro analysis. The two characteristic features of TXRF (i) requirement of very small sample amount and (ii) no matrix matched standards required for calibration makes this technique ideal and attractive for nuclear materials. But its utilization in the field of nuclear technology is quite limited.

The main motive of this thesis was to assess the applicability of TXRF and advanced features of EDXRF for elemental characterization of trace and bulk elements in nuclear materials. In this thesis, various TXRF and EDXRF methods developed for the characterization

Detection Limits (ppb)	1.000	Ni Mg, F Cr, Y			
	100	K, Zn, Ge Pt, Ta, Mo, Zn Cl Pd, Sn, Nd			
	10	Rb, Ba Co, Se Al Hg Ca Sb, Gd As, Cd, Rh, Sr, La Si Se, Ti Ag, na, W, Al K			
	1	Hg, U P Li Fe V, Cu, Ga S As, Pt, Sn, V P Sm Cl, Ag, In, U Sb Br Au, Hf Pd, Cd, Sn, Sb, Yb Bi, Au, Ni, Si, Ta Mo, K, Hf, Ta Ca, Pb, Tl Ir Lu W, Ba, Ca, La Ba B			
	0.1	Mn, Eu Pt, Au, Hg, Pb, Bi Rb, Sr, Y Co, Cu, Fe, Mo Na Ni, Ti, Cu, Se, As Al, Cr, Mn Be, Li In V, Co, Zn, Ga, Ge Cr Dy Cr, Mn, Fe Cd			
	0.01	INAA Mg Mg, I Cd Al, As, Ni Hg Zn Ag, Cu, Ge, Mo, Pd, Rb Ba, Gd, Mn, Nd, Pt ET-AAS Au, Dy, Ga, Pb			
	0.001	Co, Er, Nb Eu Bi, Cs, La, Hf, Ir, Re Co, Ho, In, Lu, Pr ICP-MS			
	0.0001				

Figure 1.3: Relative detection limits of INAA, TXRF, ET-AAS and ICP-MS

of nuclear fuel and other nuclear materials are discussed. Generally, analysis of radioactive elements requires enclosing the instrument inside the glove box. Studies were carried out to develop sample preparation method for radioactive samples without making the spectrometer radioactive. This novel approach avoids cumbersome working procedure in glove box. The highlights of the work carried out in this thesis are as follows:

The TXRF spectrometer was calibrated followed by validation of the analytical results using another working standard.

Trace metallic and non-metallic impurities affect the properties and performance of uranium and thorium. Hence, a TXRF analytical method for the determination of trace metallic impurities in thorium and uranium oxide matrix was developed after matrix separation of the major matrix by solvent extraction. Medium and high Z metallic impurities were determined in thorium oxide using ITAL Structures TX-2000 spectrometer in air atmosphere. Among the trace metallic impurities low Z elements such as Na, Mg and Al, were analysed using a Vacuum Chamber TXRF spectrometer, WOBISTRAX. The sample preparation method and instrumental parameters were standardized / optimised for these determinations.

A TXRF methodology was also developed to analyse non-metallic trace impurities such as sulphur and chlorine in nuclear fuel. For the determination of chlorine in nuclear fuel pyrohydrolysis hyphenated TXRF methodology was developed. This methodology involves separation of chlorine from solid nuclear samples followed by its collection in dil NaOH solution and finally its determination in air/ helium atmospheres, without any sample dissolution process. For sulphur determinations, the major matrix was separated by solvent extraction. Chlorine analysis by TXRF in acidic medium leads to its loss during the sample preparation. This is because chlorine gets evaporated as HCl during heating of the samples on quartz sample support, as a part of TXRF sample preparation. Hence, a novel method for chlorine determination in acidic medium using TXRF was developed. This method is based on the addition of excess amount of AgNO₃ in the sample solution containing chlorine for precipitating chlorine as silver chloride followed by TXRF determination of silver in the solution after filtering out the precipitate.

Apart from trace analysis, another feature of TXRF is microanalysis. Micro analysis is the chemical identification and quantitative analysis of very small amounts of analyte or very small surfaces of material. Use of very small sample amount for analysis is an attractive feature

of TXRF for analysis of radioactive samples. This feature was exploited for bulk determination of uranium and thorium solutions in presence of each other. Another method for bulk determination of uranium and thorium in solid samples without any dissolution by TXRF was also developed. This method requires gentle touching of (U, Th)O₂ sample in form of pellets/ microsphere on TXRF sample support followed by their determination with respect to each other.

Determination of uranium in its non-conventional sources such as seawater and phosphate fertilizers, with the aim of their recovery from such sources is gaining attention over the past few decades. Studies on the elemental determination of uranium in seawater and fertilizers samples by TXRF were carried out after standardizing the sample preparation method for separation and selective extraction of uranium by solvent extraction.

An EDXRF methodology was developed for the fast and accurate determination of uranium and thorium requiring very less sample (μg level) for analysis. The developed method has an added advantage that radioactive samples can be sealed properly and analysed without making the instrument radioactive. Application of continuum excitation and filters for the determination of cadmium using EDXRF was studied and a method for trace determination of cadmium in uranium matrix was developed.

1.9. References

1. M. V. Balarama Krishna, J. Arunachalam, Trace element analysis of high purity arsenic through vapour phase dissolution and ICP-QMS, *Talanta*, 59 (2003) 485.
2. Taicheng Duan, Jianzhen Kang, Hangting Chen, Xianjin Zeng, Determination of ultra-trace concentrations of elements in high purity tellurium by inductively coupled plasma mass spectrometry after Fe(OH)₃ co precipitation, *Spectrochim. Acta, Part B*, 58 (2003) 1679.
3. Peter Burba, Paul-G. Willmer, M. Becker, R. Klockenkämper, Determination of trace elements in high purity aluminum by total reflection X-ray fluorescence after their separation on cellulose loaded with hexamethylenedithiocarbamates, *Spectrochim. Acta, Part B*, 44 (1989) 525.
4. Mary Gopalkrishnan, K. Radhakrishnan, P. S. Dhama, V.T. Kulkarni, M. V. Joshi, A. B. Patwardhan, A. Ramanujam, J. N. Mathur, Determination of trace impurities in uranium, thorium and plutonium matrices by solvent extraction and inductively coupled plasma atomic emission spectrometry, *Talanta*, 44 (1997) 169.

5. Francesco Saverio Romolo, Pierre Margot, Identification of gunshot residue: a critical review, *Forensic Sci. Int.*, 119 (2001) 195.
6. H.P. Longenrich, B.J. Fryer, D.F. Strong, Trace analysis of natural alloys by inductively coupled plasma-mass spectrometry (ICP-MS): application to archeological native silver artifacts, *Spectrochim. Acta, Part B*, 42 (1987) 101.
7. K. L. Ramakumar, V. A. Raman, V. L. Sant, V. D. Kavimandan, H. C. Jain, Determination of trace impurities in zircaloy-2 and tellurium by spark source mass spectrometry, *J. Radioanal. Nucl. Chem.*, 125 (1988) 467.
8. S. M. Simabuco, C. Va'zquez, S. Boeykens, R. C. Barroso, Total reflection by synchrotron radiation: trace determination in nuclear materials, *X-Ray Spectrom.*, 31 (2002) 167.
9. K.L. Ramakumar, Analytical challenges in characterization of high purity materials, *Bull. Mater. Sci.*, 28 (2005) 331.
10. Facets of nuclear science and technology, S.K. Aggarwal, D.D. Sood (eds.) (1996).
11. M.C. Freitas, A.M.G. Pacheco, I. Dionísio, S. Sarmiento, M.S. Baptista, M.T.S.D. Vasconcelos, J.P. Cabral, Multianalytical determination of trace elements in atmospheric biomonitors by k_0 -INAA, ICP-MS and AAS, *Nucl. Instrum. Methods Phys. Res., Sect. A*, 564 (2006) 733.
12. M. A. Garwan, M. S. Musazay, G. W. Grime, μ -PIXE trace element analysis of crude oil, *Nucl. Instrum. Methods Phys. Res., Sect. B*, 130 (1997) 649.
13. Madhavi Z. Martin, Nicole Labbé, Nicolas André, Ronny Harris, Michael Ebinger, Stan D. Wullschleger, Arpad A. Vass, High resolution applications of laser-induced breakdown spectroscopy for environmental and forensic applications, *Spectrochim. Acta, Part B*, 62 (2007) 1426.
14. W. Robert Kelly, Robert D. Vocke Jr, John R. Sieber, Thomas E. Gills, Certification of sulfur in SRM 2724 diesel fuel oil by isotope dilution thermal ionization mass spectrometry and X-ray fluorescence, *Fuel*, 72 (1993) 1567.
15. E. Marguá, M. Hidalgo, I. Queralt, Multielemental fast analysis of vegetation samples by wavelength dispersive X-ray fluorescence spectrometry: Possibilities and drawbacks *Spectrochim. Acta, Part B*, 60 (2005) 1363.
16. Christina Strelí, P. Wobrauschek, P. Kregsamer, X-Ray fluorescence spectroscopy applications, *Encyclopedia of Spectroscopy and Spectrometry*, (2009) 3000.

17. Ron Jenkins, X-Ray Fluorescence Spectrometry, 2nd Edition, (1999).
18. E. A. Bertin, Principle and practice of X-Ray spectrometric analysis (2nd edn), Plenum Press, New York, (1984).
19. Reinhold Klockenkämper, A. von Bohlen, Total reflection X-Ray fluorescence moving towards nanoanalysis: a survey, Spectrochim. Acta, Part B, 56 (2001) 2005.
20. M. K. Tiwari, K. J. S. Sawhney, B. Gowri Sankar, V. K. Raghuvanshi, R. V. Nandedkar, A simple and precise Total reflection X-Ray fluorescence spectrometer: construction and its applications, Spectrochim. Acta, Part B, 59 (2004) 1141.
21. P.G. Barbano, L. Rigali, Spectrophotometric determination of uranium in seawater after extraction with ALIQUAT-336, Anal. Chim. Acta, 96 (1978) 199.
22. Dj. Dojozan, M.H. Pournaghi-Azar, J. Toutounchi-Asr, Preconcentration of trace uranium from seawater with solid phase extraction followed by differential pulse polarographic determination in chloroform eluate, Talanta, 46 (1998) 123.
23. Ione Makiko Yamazakia, Luiz Paulo Geraldob, Uranium content in phosphate fertilizers commercially produced in Brazil, Appl. Radiat. Isot., 59 (2003) 133.
24. V. K. Chaturvedi, Nuclear power reactor scenario in India, Characterization and Quality Control of Nuclear Fuels (Eds: C. Ganguli, R. N. Jayaraj), Allied Publishers: New Delhi, (2002) 27.
25. Emerging nuclear fuel Fabrication Activities in India, R N Jayaraj, Energy Procedia, 7 (2011) 120.
26. R.K. Sinha, A. Kakodkar, Design and development of the AHWR—the Indian thorium fuelled innovative nuclear reactor, Nucl. Eng. and Des., 236 (2006) 683.
27. I. V. Dulera, R. K. Sinha, High temperature reactors, J. Nucl. Mater., 383 (2008) 183.
28. Thorium fuel cycle- Potential benefits and challenges, IAEA-TECDOC-1450 (2005).
29. J. Vucina, V. Scepanovic, R. Draskovic, Determination of some trace elements in the industrial process of aluminum production, J. Radioanal. Chem., 44 (1978) 378.
30. C. Degueldre, G. Kuri, M. Martin, A. Froideval, S. Cammelli, A. Orlov, J. Bertsch, M.A. Pouchon, Nuclear material investigations by advanced analytical techniques, Nucl. Instrum. Methods Phys. Res., Sect. B, 268 (2010) 3364.

31. Charles A. Lucy, Lutfiye Gureli, Steve Elchuk, Determination of trace lanthanide impurities in nuclear grade uranium by coupled-column liquid chromatography, *Anal. Chem.*, 65 (1993) 3320.
32. R. B. Yadav, B. Gopalan, Chemical characterization of power reactor fuels at Nuclear fuel complex, *Characterization and Quality Control of Nuclear Fuels* (Eds: C. Ganguli, R. N. Jayaraj), Allied Publishers: New Delhi, (2002) 455.
33. S.V. Godbole, Trace metal assay of nuclear materials, *Chemical characterization of nuclear fuel*, *IANCAS Bulletin*, 7 (2008) 169.
34. R. M. Sawant, M. A. Mahajan, P. Verma, D. Shah, U. K. Thakur, K. L. Ramakumar, V. Venugopal, Fluoride determination in various matrices relevant to nuclear industry: A review, *Radiochim. Acta*, 95 (2007) 585.
35. M. A. Mahajan, M. V. R. Prasad, H. R. Mhatre, R. M. Sawant, R. K. Rastogi, G. H. Rizvi and N. K. Chaudhuri, Modified pyrohydrolysis apparatus for the separation of fluorine and chlorine trace impurities from nuclear fuel samples for quality control analysis, *J. Radioanal. Nucl. Chem.*, 148 (1991) 93.
36. U. Basak, M.R. Nair, R. Ramachandran, S. Majumdar, Fabrication of high density ThO₂, ThO₂-UO₂ and ThO₂-PuO₂ fuel pellets for heavy water reactors, *BARC Newsletter*, Founder's day special issue October-2001 (<http://www.barc.ernet.in/publications/nl/>)
37. S.Rajendran Pillai, S. Anthonysamy, P.K. Prakashan, R. Ranganathan, P.R.Vasudeva Rao, C.K. Mathews, Carburization of stainless steel clad by uranium-plutonium carbide fuel, *J. Nucl. Mater.*, 167 (1989) 105.
38. S. Glasstone and W. H. Jordan, *Nuclear power and its environmental effects standards*, American Nuclear Society, (1990) 167.
39. Toshiaki Hiyama, Toshio Takahashi, Katsuichiro Kamimura, Determination of nitrogen in uranium-plutonium mixed oxide fuel by gas chromatography after fusion in an inert gas atmosphere, *Anal. Chim. Acta*, 345 (1997) 131.
40. Y.A.Sayi, K.L. Ramakumar, V. Venugopal, Determination of non-metallic impurities in nuclear fuels, *Chemical characterization of nuclear fuel*, *IANCAS Bulletin*, 7 (2008) 180.

41. Keshav Chander, S. P. Hasilkar, A. V. Jadhav, H. C. Jain, A titrimetric method for the sequential determination of thorium and uranium, *J. Radioanal. Nucl. Chem.*, 174 (1993) 127.
42. C.E. Johnson, I. Johnson, P.E. Blackburn, C.E. Crouthamel, Effect of oxygen concentration on the properties of fast reactor mixed oxide fuel, *Reactor technology*, 15 (1972) 303.
43. Toshiaki Hiyama, Determination of oxygen-to-metal atomic ratio in mixed oxide fuel by non-dispersive infrared spectrophotometry after fusion in an inert gas atmosphere, *Anal. Chim. Acta.*, 402 (1999) 297.
44. Alexander R. Fox, Suzanne C. Bart, Karsten Meyer, Christopher C. Cummins, Towards uranium catalysts, *Nature* 455 (2008) 341.
45. Masao Tamada, Noriaki Seko, Fumio Yoshii, Application of radiation-graft material for metal adsorbent and crosslinked natural polymer for healthcare product, *Radiat. Phys. Chem.*, 71 (2004) 221.
46. Tetsuya Kiriya, Rokuro Kuroda, Determination of uranium and thorium in phosphate rocks by a combined ion-exchange- Spectrophotometric method, *Mikrochimica Acta [Wien]* III (1985) 369.
47. M.V. Ramaniah, Analytical chemistry of fast reactors fuel-A review, *Pure Appl. Chem.*, 54 (1982) 889.
48. N.L. Misra, K.D. Singh Mudher, V. Venugopal, Determination of uranium in microgram level in different matrices by X-ray fluorescence, *Characterization and Quality Control of Nuclear Fuels* (Eds: C. Ganguli, R. N. Jayaraj), Allied Publishers: New Delhi, (2002) 447.
49. http://www.iaea.org/inis/collection/NCLCollectionStore/_Public/30/050/30050815.pdf

Chapter-2

INSTRUMENTAL TECHNIQUES AND EXPERIMENTAL METHODS

- 2.1. Introduction
- 2.2. X-Ray Fluorescence Spectrometry
- 2.3. Interaction of X-Rays with Matter
 - 2.3.1. Photoelectric absorption
 - 2.3.2. Scattering
 - 2.3.3. Pair production
- 2.4 X-Ray Production
 - 2.4.1. X-ray tube sources
 - 2.4.2. Radioisotopic sources
 - 2.4.3. Synchrotron sources
- 2.5. X-Ray Spectrum
 - 2.5.1. Continuum spectrum
 - 2.5.2. Characteristic line spectrum
- 2.6. X-Ray Detectors
- 2.7. Total Reflection X-Ray Fluorescence (TXRF)
 - 2.7.1. Fundamentals of total reflection of X-rays
 - 2.7.2. Sample carriers
 - 2.7.3. Instrumental parameters
 - 2.7.4. Calibration and quantification
- 2.8. Energy Dispersive X-Ray Fluorescence (EDXRF)
- 2.9. Spectrometers Used in the Present Work
 - 2.9.1. ITAL STRUCTURES TX-2000
 - 2.9.2. WOBISTRAX
 - 2.9.3. Jordan Valley EX-3600 TEC
- 2.10. References

2.1. Introduction

Characterization of any material can be made using several instrumental techniques and hence thorough knowledge of these techniques is required, as no single technique can characterize a material completely. The different techniques used depend on the nature of material and the type of characterization required. Analytical characterization of technologically important materials involve the study of

- (i) Elemental composition of the material for its ultra trace, trace and bulk constituents.
- (ii) Thermodynamic properties.
- (iii) Structural, morphological and speciation studies.
- (iv) Assessment of physical properties like strength, heat and radiation effects, etc.

All these characterizations are equally important and several techniques and methodologies are required for such characterization. In addition, single characterization can be made by several techniques.

Since the discovery of X-rays by Wilhelm Conrad Roentgen in 1895 [1], X-rays have played an important role in the field of material characterization. X-rays are electromagnetic radiations having wavelengths in the range from 10^{-5} to 100 \AA [2]. X-rays show the properties like polarization, diffraction, reflection and refraction. They are also capable of ionizing gases, liberate photoelectrons and blacken photographic plate. Hence similar to light they possess partly corpuscular and partly wave character. X-rays can be produced by two different phenomena. When moving charged particles e.g. electrons, protons, α -particles, etc. are stopped by a target, they lose their energy in steps while passing through the coulomb field of the nucleus of the target. The radiation produced by such interaction is called '*bremsstrahlung*' or '*continuous X-rays*'. This spectrum contains energies from zero to short wavelength limit λ_{\min} , corresponding to the maximum energy of the particles. The continuum generated by stepwise deceleration of electrons has substantial intensity but other particles such as proton, deuteron, α - particles do not produce such intense continuum. In addition to this, if the charged particles have sufficient energy to knock out an inner orbital electron of the target atom, the atom becomes unstable. In order to come to ground state, the atom emits X-rays of specific energies, characteristic to the atom. Apart from charged particles, the characteristic X-rays can also be produced by X-rays of sufficient energies in similar way. The primary sources of X-rays are X-ray tubes, radioisotopes and synchrotrons. The X-rays produced from these sources are used to irradiate the sample for material characterization.

Most of the X-ray methods are based on the scatter, emission and absorption properties of X-rays [2]. The most common of them are X-Ray Diffraction (XRD), X-Ray Fluorescence (XRF) and X-Ray Absorption Spectroscopy (XAS). Table 2.1 gives a brief description of various X-ray techniques and the type of information given by these techniques. These techniques are very strong analytical tools for material characterization [3, 4].

Table 2.1: X-ray techniques and their applications

S. No.	Technique*	Type of information
1.	XRD	Phase identification, Bond type, Crystal structure, Crystal defects, Local structure, Crystallite size, Strain
2.	XRF: EDXRF, TXRF, WDXRF	Elemental concentration, Chemical environment, Oxidation state
3.	XPS	Elemental composition, Chemical state, Electronic state, Density of states
4.	XAS : XANES, EXAFS	Local coordination, Oxidation state, Interatomic distances, Coordination number
5.	XRR	Thickness and density of thin films, Interface roughness and multi-layers
6.	SAXS	Particle sizes, Size distributions, Shape and orientation distributions in liquid, powders and bulk samples

*: Acronyms XRD: X-Ray Diffraction, XRF: X-Ray Fluorescence, XPS: X-Ray photoelectron Spectroscopy, XAS: X-Ray Absorption Spectroscopy, XRR: X-Ray Reflectivity, SAXS: Small Angle X-ray Scattering

XRD, based on wave nature of the X-rays, was established in the year 1912 by Laue, Friedrich and Knipping who showed that X-rays could be diffracted using crystals, which are regular array of atoms and act like 3D grating. Later in 1913, W.H. Bragg and W.L. Bragg put forwarded the law for the diffraction of X-rays. The condition for diffraction is that, when an X-ray radiation of wavelength ‘ λ ’ falls on a crystal having an interplanar spacing of ‘ d ’ at an angle ‘ θ ’ (angle between crystal plane and incident X-ray), the X-rays scattered by parallel planes interfere constructively and gives a maxima intensity if :

$$2d \sin \theta = n\lambda \quad \dots\dots\dots (2.1)$$

where, n is the order of diffraction. This equation is known as “Bragg’s Law” and is frequently used in all XRD calculations. XRD is a versatile technique giving several informations about the materials, as given in the Table 2.1 [5, 6].

X-ray Absorption Spectroscopy (XAS) is another class of well established X-ray techniques which measures the absorption of X-rays by the sample at various energies (especially at the region of its absorption edge) [7, 8]. As X-rays obey the same absorption law as other electromagnetic radiations, the incremental loss of intensity, dI , in passing through a medium of incremental thickness, dX , is proportional to the intensity, I .

$$dI \propto I dX \quad \dots\dots\dots (2.2)$$

The constant of proportionality is given by linear absorption coefficient, μ (cm^{-1}), which gives absorption per unit thickness per unit area and depends on the density of the material. Hence, rewriting the above equation

$$dI/I = \mu dX \quad \dots\dots\dots (2.3)$$

Integrating equation 2.3 over the limits gives

$$I/I_0 = e^{-\mu t} \quad \dots\dots\dots (2.4)$$

Another important useful value in XAS is mass absorption coefficient μ_m which gives absorption per unit mass per unit area. It is an atomic property of each element independent of chemical and physical state

$$\mu_m = \mu/\rho \quad \text{cm}^2/\text{g} \quad \dots\dots\dots (2.5)$$

and rewriting e.q. 2.4

$$I/I_0 = e^{-\mu_m t} \quad \dots\dots\dots (2.6)$$

If the absorption of the X-rays by an element is measured by varying the incident X-ray energies, the mass absorption coefficient increases abruptly when the energy of the incident X-ray becomes just above excitation potential of electron of the absorbing atom. This energy of X-ray giving maxima in the absorption is known as the **absorption edge** of the element. Figure 2.1 shows such absorption edges of Pt L levels. Absorption edge energies are characteristic of the element. Each element has many absorption edges as it has excitation potentials: one K, three L, five M, etc. The absorption edges are labeled as, K_{abs} , L_{Iabs} , L_{IIabs} , L_{IIIabs} , M_{Iabs} , ..., corresponding to the excitation of an electron from the $1s$ ($^2S_{1/2}$), $2s$ ($^2S_{1/2}$), $2p$ ($^2P_{1/2}$), $2p$ ($^2P_{3/2}$), $3s$ ($^2S_{1/2}$), ... orbitals (states), respectively.

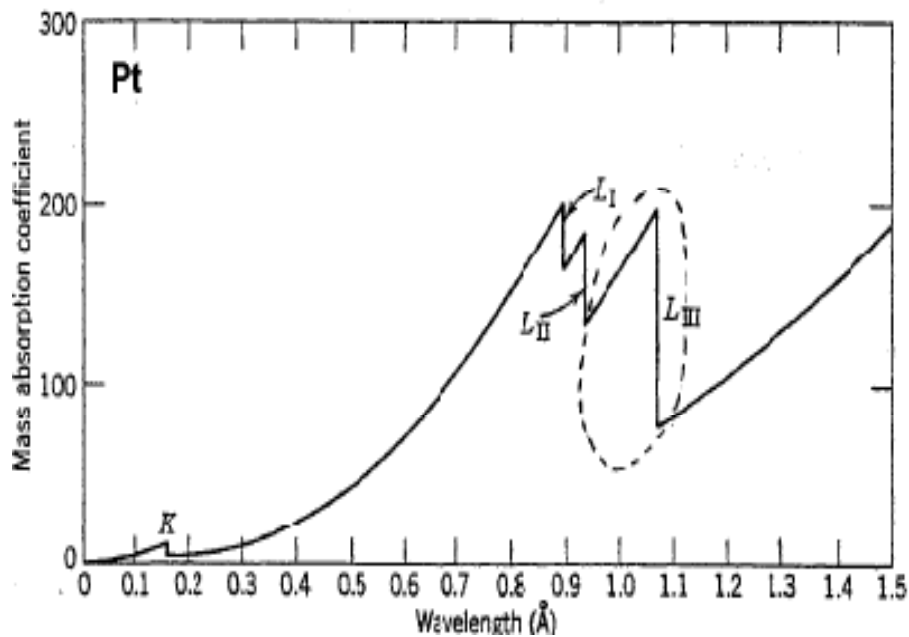


Figure 2.1: X-Ray absorption curve of platinum

An X-ray absorption spectrum is divided into two regimes: XANES (X-ray Absorption Near Edge Spectroscopy) which scans the photon energy range $E = E_0 \pm 50$ eV (E_0 is the absorption edge energy); and EXAFS (Extended X-ray Absorption Fine Structures) which starts approximately from 50 eV before the edge and continues up to 1000 eV above the edge as shown in the Figure 2.2. These two techniques are related, but contain slightly different information. When an atom absorbs radiation, it promotes its core electron out of the atom into the continuum. This ejected electron known as photoelectron interacts with the neighboring atoms in the compound which then act as secondary sources of scattering electron waves. Interference between the photoelectron wave and the back scattered wave gives rise to fine structures in absorption spectrum. The degree of interference depends on local structure, including inter-atomic distances. Figure 2.2 shows a Fe K-edge XAFS spectra of FeO. All these absorption studies are mostly carried out using synchrotron sources.

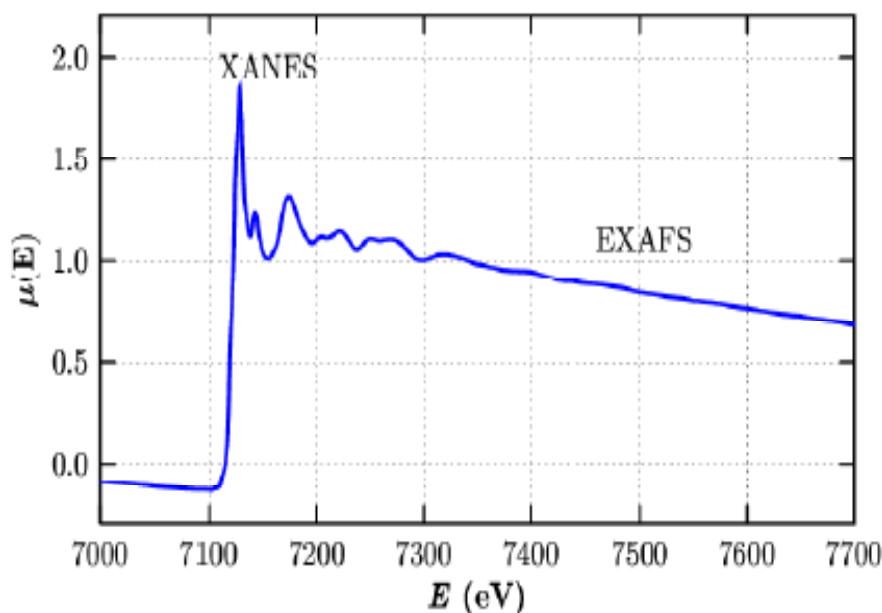


Figure 2.2: XAFS spectra showing Fe K-absorption edge

X-ray Secondary Emission Spectrometry popularly known as X-Ray Fluorescence (XRF) spectrometry is another powerful method of spectrochemical analysis. XRF is mainly used for the compositional characterization of materials. The simplicity, reproducibility, non-

destructive and multi-elemental analysis capability of XRF are the factors which have made it a very popular technique of material characterization among scientific community including metallurgists, chemists, bio-scientists, environmentalists, etc. XRF is classified as EDXRF (Energy Dispersive X-Ray Fluorescence), WDXRF (Wavelength Dispersive X-Ray Fluorescence) and TXRF (Total Reflection X-ray Fluorescence) [9] on the basis of instrumental geometries.

Other X-ray techniques such as XPS (X-ray Photoelectron Spectroscopy), XRR (X-Ray Reflectivity), SAXS (Small Angle X-ray Scattering), etc. are all strong analytical tools providing an insight to the structure of materials at atomic and sub-atomic level [10-14].

In the present thesis, EDXRF and TXRF has been extensively used for the trace and bulk characterization of technologically important materials used in nuclear industry. These techniques are described below.

2.2. X-Ray Fluorescence Spectrometry

The potential use of X-rays for qualitative and quantitative determination of elemental composition was recognized soon after their discovery. In fact, XRF has played a crucial role in the discovery of several elements. Advances in detectors and associated electronics opened up the field of XRF analysis for elemental assay. It is based on the principle of measurement of the energies or wavelengths of the X-ray spectral lines emitted from the sample, which are the characteristic or signature of the elements present in the sample. H.G.J. Mosley in 1913 discovered the relationship of photon energy and element [15] and laid down the basis of XRF. He found that the reciprocal of wavelength ($1/\lambda$) or frequencies (ν) of characteristic X-rays are proportional to the atomic number (Z) of the element emitting the characteristic X-rays. Because X-ray spectra originate from the inner orbitals, which are not affected substantially by the valency of the atom, normally the emitted X-ray lines are independent of the chemical state of the atom. However, in the case of low and medium atomic number elements, the energy of the characteristic X-rays depends on oxidation state. This phenomenon is observed in case of high Z elements also, for the lines originating due to electron transfers from outer orbitals. Moseley's law is represented as,

$$\sqrt{\nu} = \sqrt{\frac{c}{\lambda}} = k_1 (Z - k_2), \quad \dots\dots\dots (2.7)$$

where, c is velocity of light, k_1 and k_2 are constants different for each line and depend on the atomic number. The k_1 values for the individual $K\alpha$ peaks lie between 10-11 eV, for $L\alpha$ peaks between 1.7- 2 eV and $M\alpha$ peaks at about 0.7eV. K_2 is screening constant to correct the effect of orbital electrons in reducing the effective nuclear charge. Figure 2.3 shows the relationship of energy of the X-ray photon with atomic number. As Moseley's law is not very stringent, the exact positions of the characteristic X-rays deviate from this law.

In XRF, the primary beam from an X-ray source (or electrons or charged particles) irradiates the specimen thereby exciting each chemical element. These elements in turn emit secondary X-ray spectral lines having their characteristic energies or wavelengths in the X-ray region of the electromagnetic spectrum. The intensities of these emitted characteristic X-rays are proportional to the corresponding elemental concentrations. Since the X-rays penetrate to about 100 μm depth of the surface of the sample, XRF is near surface characterization technique. This method of elemental analysis is fast and has applications in a variety of fields. This technique has also got sample versatility as sample in the form of solid, liquids, slurry, powder, etc. can be analysed with little or no sample preparation. In most cases, XRF is a non-destructive/non-consumptive technique. All elements having atomic number $Z > 11$ (Na) can be detected and analysed in conventional XRF. But, nowadays, with the advances in the XRF instrumentation, like use of very thin or windowless tubes and

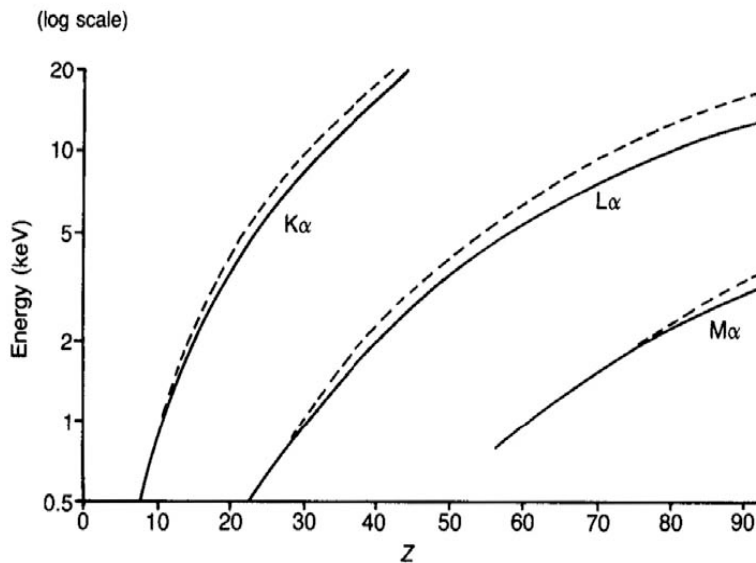


Figure 2.3: Moseley's Law plot of energy versus the atomic number
(----- Dashed line shows the deviation of Moseley –Law at higher atomic number)

detectors, multilayer analyser crystals, reduction in the path length of X-rays (tube - to-sample and sample – to- detector) and application of vacuum or helium atmosphere, elements upto B ($Z=6$) can be detected and quantified [16]. Further, with the development of synchrotron radiation technology, a vast improvement in terms of detection limits has been obtained by tuning of the excitation energies [17]. XRF method has a large dynamic range, sensitive up to microgram per gram level and is considerably precise and accurate. For these reasons, XRF has become a well established method of spectrochemical analysis. It has got a variety of applications in industries of material production, quality control laboratories, scientific research centers, environmental monitoring, medical, geological and forensic laboratories [18-21]. There are two major modes of analysis in X-ray spectrometry: Wavelength Dispersive X-Ray Fluorescence (WDXRF) and Energy Dispersive X-Ray Fluorescence (EDXRF) Spectrometry. The difference in these two modes of analysis lies in the detection component. In EDXRF, the detectors directly measures the energy of the X-rays with the help of multichannel analyzer, whereas in WDXRF, the X-rays emitted from the samples are dispersed spatially using a dispersion crystal and wavelength of the each emitted X-rays is determined by the detector sequentially. The first commercial XRF instrument available was WDXRF, in the year 1940. The basic differences between WDXRF and EDXRF systems as shown in Figure 2.4 are:

- i) In WDXRF, the intensity of X-rays detected are very low in comparison to EDXRF due to the attenuation of X- rays by analyser crystals and a comparatively longer path length (sample- analyzer crystal- detector).
- ii) The crystal is the wavelength dispersive device in WDXRF whereas in EDXRF systems, it is the detector with Multi Channel Analyser (MCA) which acts as the energy dispersive device, though no real dispersion takes place.
- iii) The angular conditions for the collimators and crystals are very severe in WDXRF, no such conditions are required for EDXRF and hence from instrumentation point of view EDXRF is simpler than WDXRF.
- iv) In EDXRF, simultaneous collection of the whole spectrum takes place at a time whereas in WDXRF this measurement is sequential.

The main components of an X-ray spectrometer are: Source, Filters, Secondary targets, Dispersing crystal and Detectors.

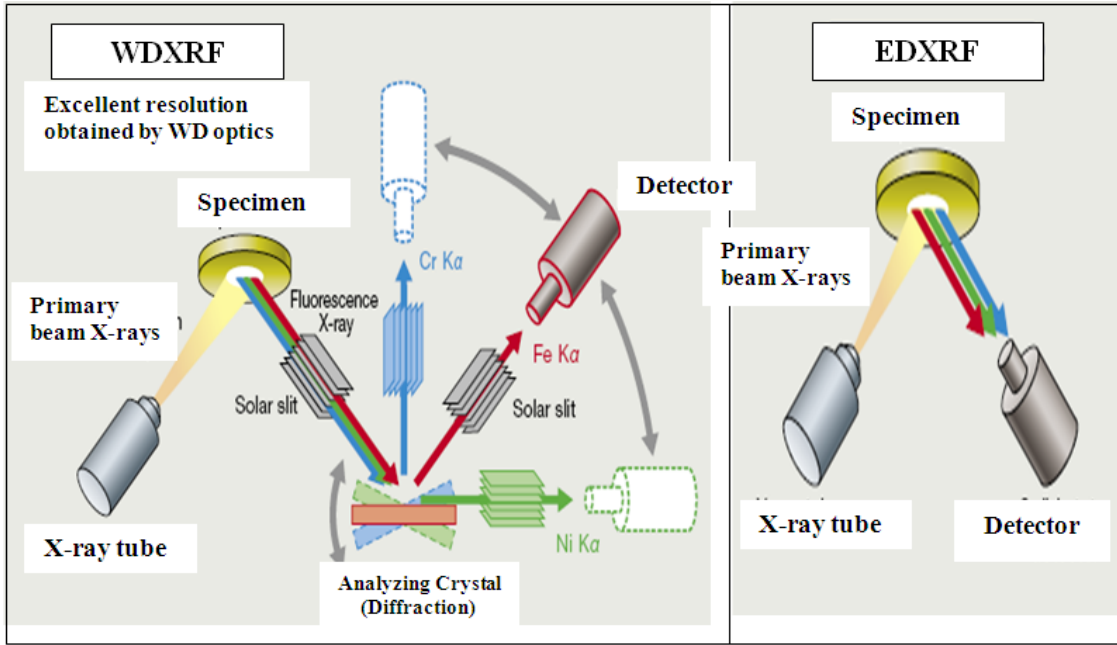


Figure 2.4: Schematic diagram of basic difference between WDXRF and EDXRF

2.3. Interaction of X-rays with Matter

When a beam of photons of intensity $I_0(\lambda_0)$ falls on an absorber having uniform thickness x_a cm and density ρ g/cc, a number of different processes may occur. The most important of these are illustrated in the Figure 2.5. The emergent beam of intensity $I(\lambda_0)$ is given by

$$I(\lambda_0) = I_0 e^{-(\mu_m \rho x_a)} \quad \dots\dots\dots (2.8)$$

where μ_m is the mass absorption coefficient of the absorber at wavelength λ_0 . The number of photons lost in the absorption process corresponds to $(I_0 - I)$. Three phenomena responsible for such photon losses are – photoelectric absorption, scatter and pair production [22]. In the wavelength region of X-ray spectrometry, pair production does not occur and photoelectric absorption is the most predominant.

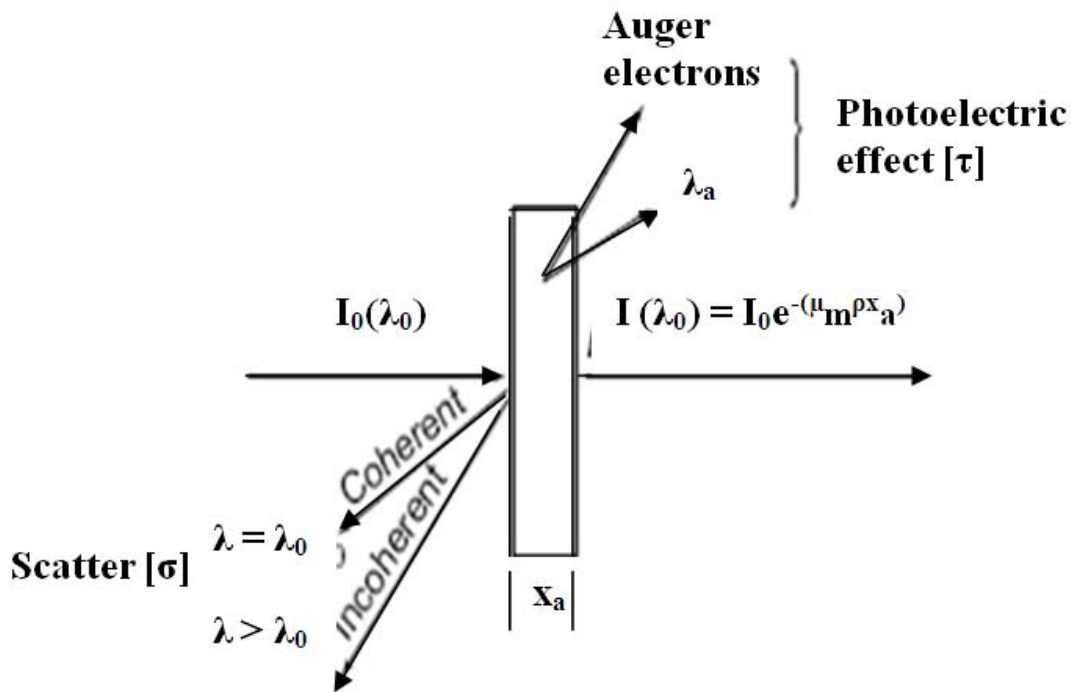


Figure 2.5: Interaction of X-ray photons with matter

2.3.1. Photoelectric absorption

In photoelectric absorption, photons are absorbed completely by losing their total energy in expelling bound orbital electrons and imparting the remaining energy as kinetic energy to the electrons thus expelled. The interaction is with the atom as a whole and cannot take place with free electrons. The kinetic energy of the photoelectron E_e is given by

$$E_e = h\nu - E_b, \quad \dots\dots\dots (2.9)$$

where $h\nu$ is the photon energy and E_b is the binding energy of the electron. When a photoelectron is ejected, it results either in the production of characteristic X-rays or auger electrons. Auger electrons are produced when the X-ray photons produced in an atom are absorbed by another loosely bound electron within the atom itself. Figure 2.6 shows these processes. E_e is the energy of the photoelectron, E_i are the binding energies of the electrons in the i^{th} shell and E_{ae} is the energy of the auger electron. The photoelectric process is mainly the interaction mode of low energy radiation. The photoelectric mass absorption coefficient (τ/ρ)

contribute mainly to the total mass absorption coefficient and depends on atomic mass, atomic number and wavelength of X- ray radiation as given in equation 2.10, known as Bragg- Pierce law

$$\frac{\tau}{\rho} \propto \frac{N}{A} Z^{4.5} \lambda^3 \dots\dots\dots (2.10)$$

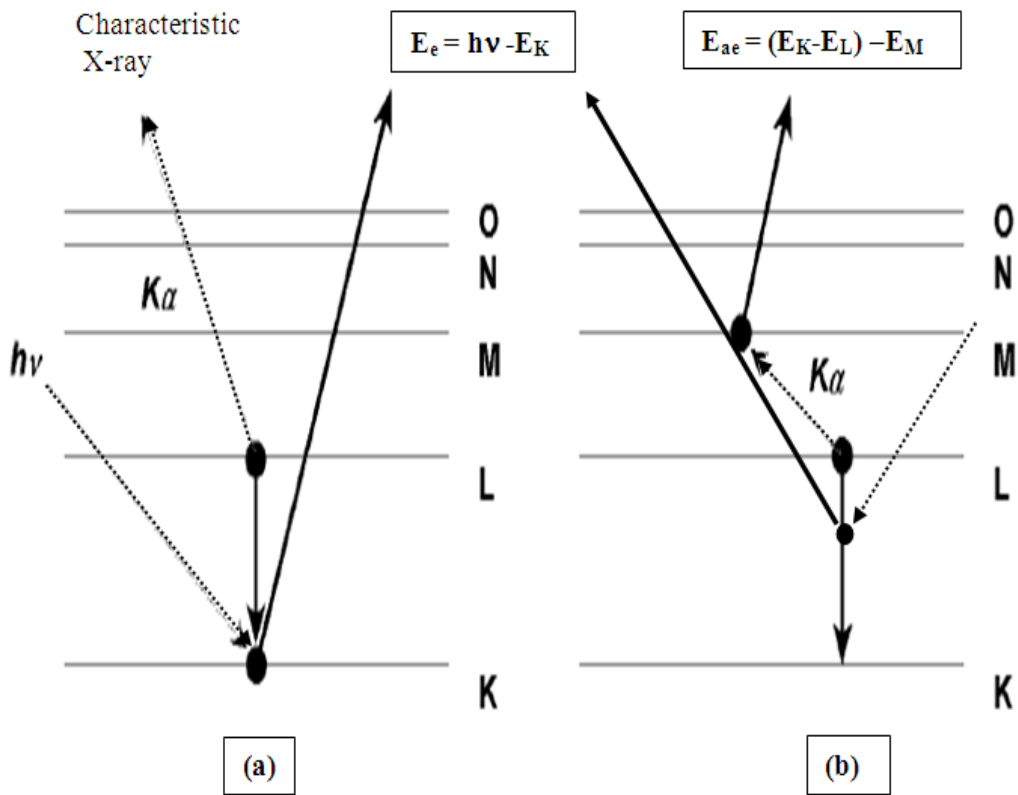


Figure 2.6: Photoelectric effect resulting in (a) Characteristic X-ray emission and (b) Auger electron production

where N is avagadro`s number, A is atomic mass, Z is atomic number and λ is wavelength of the incident beam. Thus this interaction is enhanced for the absorber material with high atomic number and low energy X-rays.

2.3.2. Scattering

The second and the minor component of X-ray attenuation is caused by scattering of X-rays. In this process, photons are not absorbed but are deflected from their linear path due to collision, in effect, disappearing from the emergent beam. Such interactions involve processes which are distinguished as:

- i) The collision of photons with a firmly bound inner electron of an atom leading to change in the direction of the photon without loss of energy. This process is known as Rayleigh or elastic scattering.
- ii) The collision of photons with loosely bound outer electron or free electron, leading to change in direction and loss of energy. This process is known as Compton or inelastic scattering.

The loss of energy suffered by a photon in Compton scattering, results from the conservation of total energy and total momentum during the collision of the photon and the electron. A photon with energy E_γ keeps the part of energy E_γ when it is deflected by an angle θ , while the electron takes off the residual part of energy E_e . Then,

$$E_e = E_\gamma - E_\gamma' \quad \dots\dots\dots(2.11)$$

$$E_e = E_\gamma - \frac{E_\gamma'}{1 + \frac{E_\gamma'}{m_0c^2} (1 - \cos \theta)} \quad \dots\dots\dots(2.12)$$

where m_0c^2 is the rest mass of an electron. E_e depends on the initial energy E_γ but is independent of the scattering substance and the intensity of the scattered radiation depends on initial energy and the deflection angle θ . A minimum intensity is achieved at $\theta = 90-100^\circ$. Rayleigh scattering intensity increases with decreasing photon energy and increasing mean atomic number of the scattering material whereas the Compton scattering increases when the photon energy increases and atomic number decreases.

Scatter is regarded as nuisance in XRF as it increases the background and possibility of spectral line interference. However, there are several advantages of X-ray scattering. Diffraction is a form of coherent scatter and several techniques have been developed for using scattered X-rays to correct the matrix effects.

2.3.3. Pair production

Pair production results in the conversion of a high energy photon (gamma ray), while passing close to atomic nuclei under the influence of strong electromagnetic field, into two charged particles: an electron and positron pair, having energies of E_e and E_p . This process is possible only if the incident photon has energy more than 1.022 MeV. This is mostly in gamma ray region and is of not much importance for X-ray photons.

$$E_\gamma = E_e + E_p + 1.022 \text{ MeV} \quad \dots\dots\dots (2.13)$$

The total absorption coefficients are the result of two phenomena, photoelectric absorption denoted as τ , and scatter coefficient given by σ , each having its own mass absorption coefficients: (τ/ρ) is photoelectric mass absorption coefficient and (σ/ρ) is the absorption coefficient due to scatter which includes both Rayleigh and Compton.

$$\mu_m = \mu/\rho = (\tau/\rho) + (\sigma/\rho) \quad \dots\dots\dots (2.14)$$

2.4. X-Ray Production

The success of any X-ray analytical method is highly dependent on the properties of the sources used to produce X-rays. In spectrochemical analysis like XRF, the characteristic X-rays generated may be classified as primary or secondary depending on whether excitation of the target, used to produce X-rays, is by particles (electrons or ions) or by photons, respectively. In primary excitation, the characteristic line spectrum of the target is superimposed on continuum, which is generated simultaneously, and in secondary excitation, only characteristic X-ray spectra of the target are emitted. The three major sources of X-ray production used in XRF are X-ray tubes, radioisotopes and synchrotron [23-24]. X-ray tubes are the most common source of sample excitation used in laboratories.

2.4.1. X-ray tube sources

The usual source of excitation in XRF is by the primary beam generated in X-ray tubes that irradiates the sample. An X-ray tube consists of a tungsten cathode filament, an anode target, thin beryllium window, focusing cup, a glass envelope that retains the vacuum, high voltage and water connection. W. D. Coolidge in year 1913 introduced the basic design of the modern X-ray tubes [25]. Figure 2.7 shows the X-ray tube of the Coolidge type. The tungsten filament serves as the hot cathode. Electrons emitted from this filament, by thermionic emission, are accelerated by an applied high voltage in the direction of the anode. The high energy electron bombardment of the target produces X-rays that emerge out of this tube through the beryllium window, which is highly transparent to X-rays. However only about 0.1% of the electric power is converted into radiation and most is dissipated as heat. Due to this reason, cooling of the tube target by water is required. The beam emerging from a tube consists of two types of radiation: Continuous and Characteristic.

The intensity of the continuum emitted from the target depends on the excitation parameters and is related as

$$I_{\text{int}} = (1.4 \times 10^{-9}) i Z V^2 \quad \dots\dots\dots (2.15)$$

where I_{int} is the integrated intensity of the continuum, i and V are X-ray tube current and potential, respectively and Z is the atomic number of the X-ray tube target element [26]. Figure 2.8 shows the effect of X-ray tube current, potential and target element on the intensity of continuum X-rays emitted from an X-ray tube.

The characteristic or the principal target line intensity, emitted along with the continuum, for example of K line (I_k), is governed by the equation

$$I_k \propto i (V - V_k)^{-1.7} \quad \dots\dots\dots (2.16)$$

where i is the tube current, V is the applied potential and V_k is K excitation potential [27].

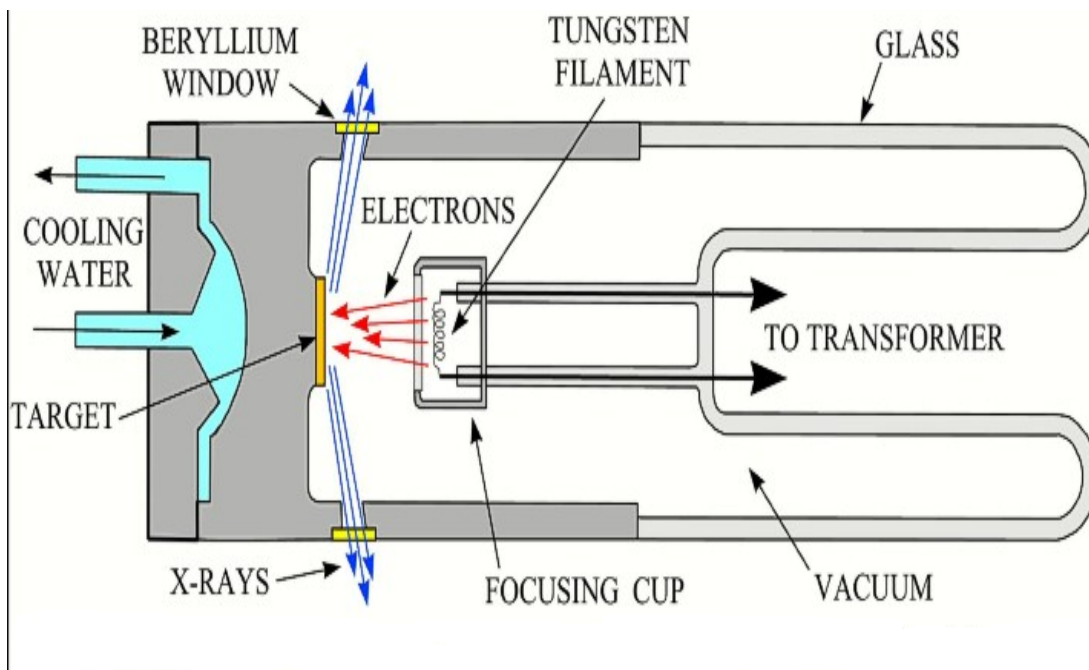


Figure 2.7: Schematic diagram of an X-ray tube of Coolidge type

Figure 2.9 presents the spectrum generated from an X-ray tube showing the high background produced by the continuum and the characteristic peaks of the target superimposed on this background. Tungsten is the most widely used target element. Other used target elements are molybdenum, rhodium and silver. Chromium and aluminum targets are used for the excitation of K lines of low Z elements like magnesium, sodium, etc. For efficient excitation, target element is chosen in such a way that the characteristic X-ray of the target is just above the absorption edge of the analyte in the sample. Also the tube voltage should be 1.5 - 2 times the absorption edge of element of interest. In order to achieve a minimum detection limit, it is often desired to use characteristic spectrum in combination with filters or secondary targets. Depending on the geometry and designs used, X-ray tubes can be classified as: Side - window, End- window and Transmission target. These tubes have maximum permissible power of 2-3 kW.

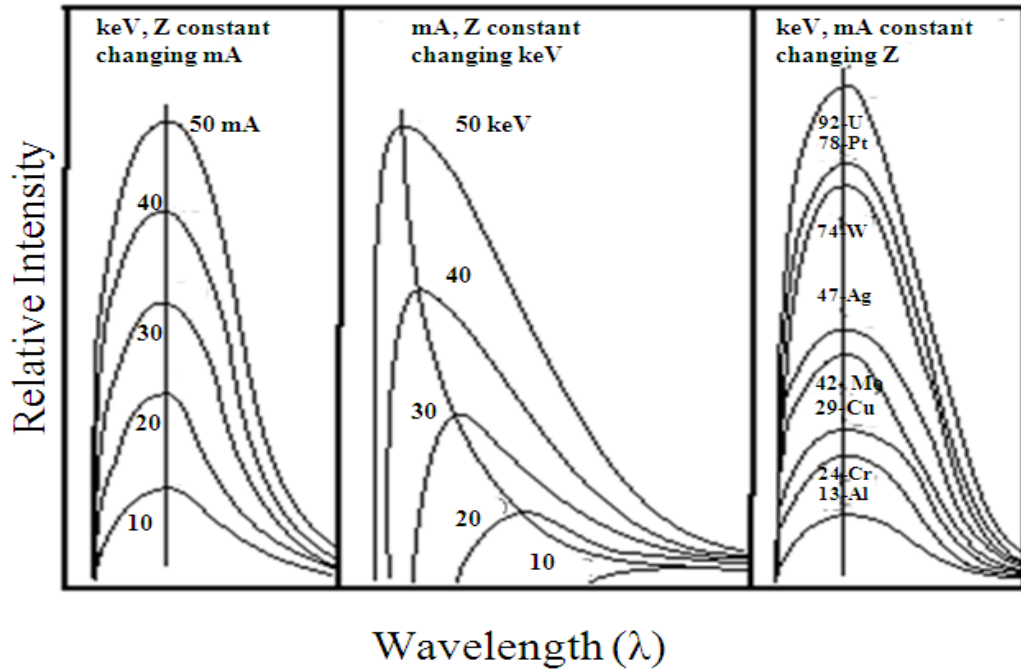


Figure 2.8: Effect of X-ray tube current, potential and target element on the intensity of continuum radiation

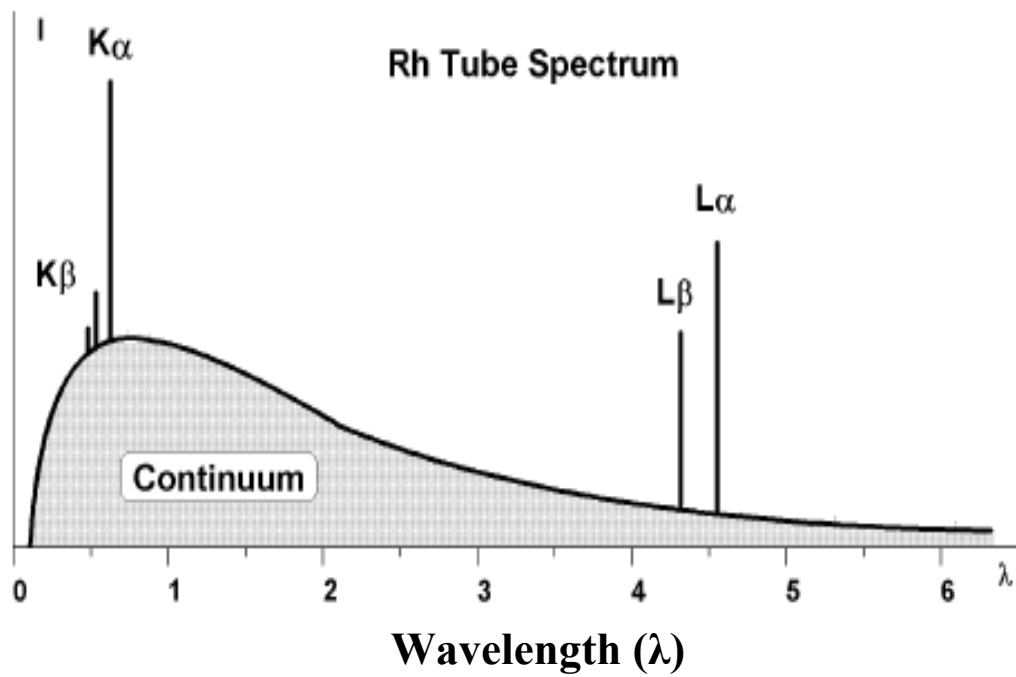
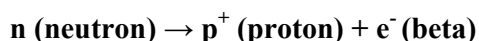


Figure 2.9: Spectrum generated from Rh target X-ray tube

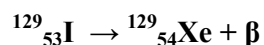
The X-ray tubes described above are typical conventional tubes but other types of X-ray tubes are also manufactured depending on the requirement. Dual target X-ray tube consists of two separate targets. This tube permits excitation using both high and low energy without the inconvenience of changing the tube. Rotating anode X-ray tubes with high permissible power rating of 18kW or more provide X-ray sources of high brilliance. The emergent primary beam intensity is 9 to 15 fold compared to conventional tube. Windowless X-ray tubes are used for the analysis of low Z elements.

2.4.2. Radioisotopic sources

Another commonly used source of X-ray is the radioisotopic source. These sources are used extensively for the XRF analysis of materials especially in portable EDXRF spectrometers. Radioactive isotopes that decay by γ emission may undergo internal conversion during which γ photon is absorbed within the atom and its energy is used to expel an orbital electron. This electron is known as internal-conversion electron. Once the vacancy is created, the electronic rearrangement takes place with the emission of characteristic X-rays. Internal γ conversion is regarded as secondary excitation in which the ionizing photon originates within the atom. The two other modes of decay in radioactive isotopes are β -emission and orbital electron capture. In internal β conversion, the β particle emitted from a radioactive nuclei occurring due to the process,



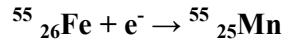
loses a part of its energy in ejecting an orbital electron. The internal conversion results in the emission of X-rays characteristic of the element, Z+1. Thus ^{129}I source emits Xe X-rays.



In orbital electron capture (EC), K or L electron is captured by the nucleus, thereby producing an electron vacancy and a neutron by the process,



decreasing the atomic number to Z-1. Here the characteristic X-rays of the atom having atomic number one lower than the parent atom are emitted.



A Radioisotope source contains a specified amount of a specific radioisotope encapsulated to avoid contamination. These sources are characterized by

- i) Radioactive decay process
- ii) Energy of the emitted radiation
- iii) Activity of the source
- iv) Half- life of radioactive isotope

Table 2.2 lists these properties for some of the commonly used radioisotope sources. These sources are considerably less expensive than other sources of X-rays. Moreover because of their compact size they are very useful for in-field measurements [28]. Apart from being simple, compact, reliable and less expensive, radioisotope excitation is mono energetic but the X-ray photon output is relatively lower than other sources and reduces with time. A

Table 2.2: List of commonly used radioisotope sources for X-ray radiation

Radioisotope source	Decay process	Half life	Useful radiation	Energy (keV)
${}^{129}_{53}\text{I}$	β	60d	Xe K α	29.8
${}^{55}_{26}\text{Fe}$	EC	2.7y	Mn K α	5.9
${}^{57}_{27}\text{Co}$	EC	270d	Fe K α	6.4
${}^{109}_{48}\text{Cd}$	EC	1.3y	Ag K α	22.2
${}^{210}_{82}\text{Pb}$	β	22y	Bi L α	10.8

relatively high activity source (100 mCi) emits 10^9 photons/s, whereas an X-ray tube operating at 100 μ A tube current emits 10^{12} photons/s. Radioisotopic sources reduce to half of its original emission rate after the time equal to its half-life, hence they have to be replaced after one to two half lives. In X-ray tube, the effective wavelength and intensity of the source can be widely varied by changing the applied voltage and current. Thus, X-ray tube sources are much more versatile and flexible but more cumbersome, complex and expensive.

2.4.3. Synchrotron sources

X-ray tubes and radioisotopes are the principal excitation sources of X-rays. During the past 50 years, developments of synchrotron sources have resulted in significant improvements in terms of detection limits in XRF spectrometry. Synchrotron radiations are produced when charged particles travelling at relativistic energies are constrained to follow a curved trajectory under the influence of a magnetic field. The total emitted intensity (I) of the radiation is proportional to

$$I \propto E_p / mc^2 \quad \dots\dots\dots (2.17)$$

where E_p and m are the energy and mass of the particle and c is the velocity of light. The above equation (2.17) shows that for certain energy, the highest intensity will be emitted by the lightest moving particle and hence electrons and positrons will be the most efficient emitters. The schematic presentation of the basic mode of operation of a synchrotron radiation source is shown in Figure 2.10. The emitted radiation has unique properties that make them very much suitable for X-ray analysis applications. They have high photon flux with continuous energy distribution and monoenergetic beams can be tuned over a wide range. This improves the excitation efficiency and detection limits by several orders of magnitude. They have low divergence (natural collimation), high intensity and brightness about 3-4 orders of magnitude greater than those of laboratory sources. The beam is polarized either linearly or circularly, which is extremely important for background reduction. The availability of synchrotron radiation has prompted researchers in the field of X-ray analysis to explore the applicability of such sources in various fields of science [29, 30].

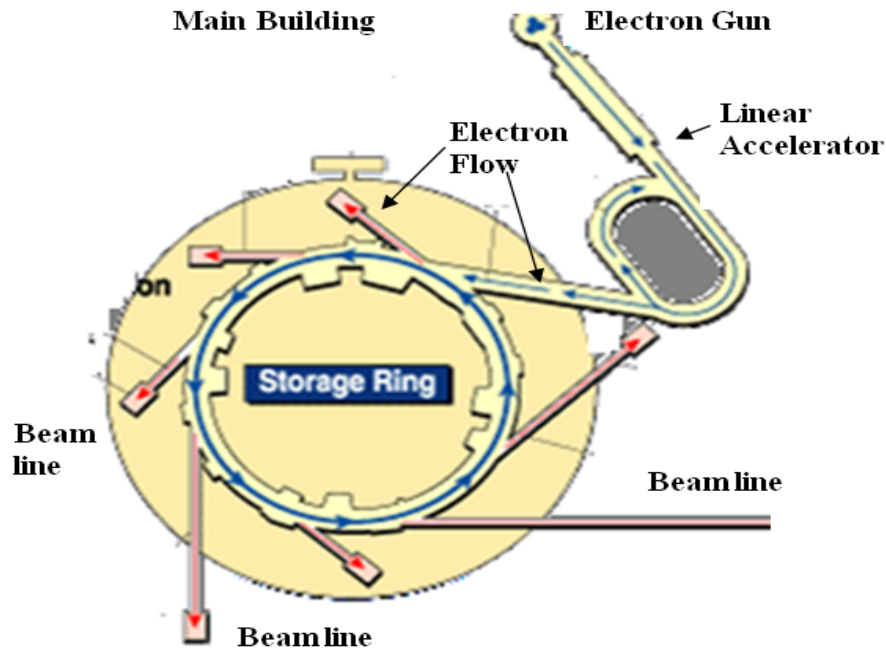


Figure 2.10: Schematic representation of a synchrotron source facility

2.5. X-Ray spectrum

2.5.1. Continuum spectrum

The continuous spectrum of X-rays, also known as bremsstrahlung or white light, is produced when high energy electrons or charged particles undergo stepwise deceleration in the target under the influence of the nucleus of the atom. Figure 2.11 shows a schematic picture of continuum X-ray production. The maximum energy/ minimum wavelength (λ_{\min}) of the X-rays produced when an electron, moving under potential V , is decelerated to zero velocity in a single step is given by

$$\lambda_{\min} = \frac{hc}{eV_0} \quad \dots\dots\dots (2.18)$$

where h is Planks constant, c is the velocity of light, e is the electron charge and V_0 is the potential difference applied to the tube. This relation is known as Duane- Hunt Law [31].

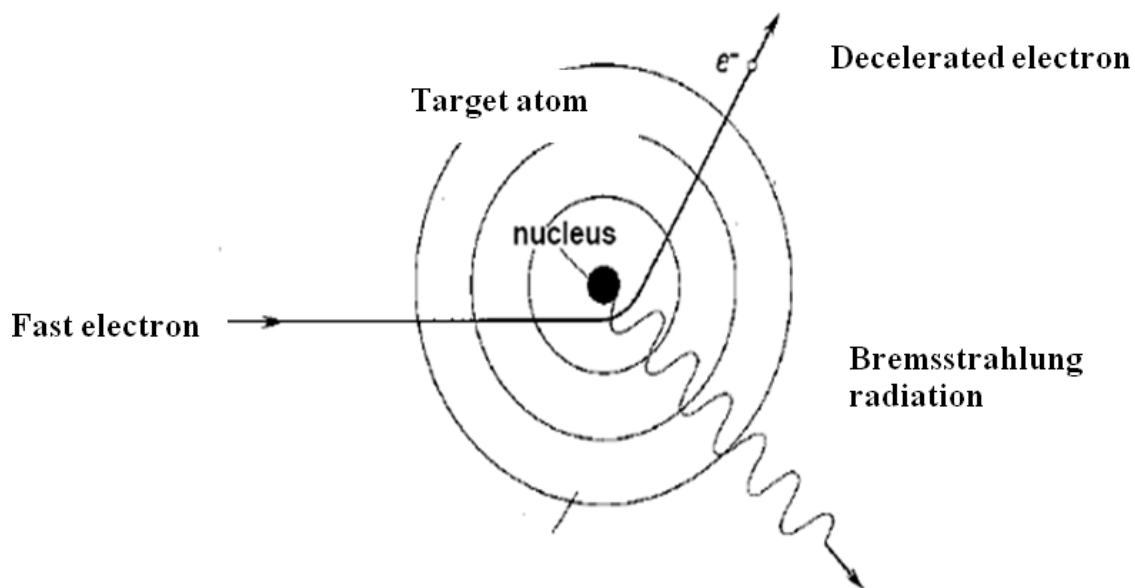


Figure 2.11: Schematic picture of continuum production

This minimum wavelength corresponds to the maximum electron energy and is independent of the target atom. In X-ray spectrochemical analysis, the continuum provides the principal source of sample excitation and is also a source of background.

2.5.2. Characteristic line spectrum

The characteristic line spectrum originates when an atom is destabilized due to knocking out of the inner shell electrons by a high energy radiation or particle. In order to stabilize the atom, electrons from outer levels fall into the vacancies thus created. Each such transition constitutes an energy loss of the destabilized atom. This energy appears as a characteristic X-ray photon. The result of such processes in large number of atoms is the simultaneous generation of K, L, M, N, etc. series of X-ray spectra of that element. Since these electron transitions correspond precisely to the difference in the energy between the two atomic orbitals involved, the emitted X-ray photon has energy characteristic of this difference and thereby the atom. The transitions are substantially instantaneous, occurring within 10^{-12} to 10^{-14} s of the creation of electron vacancy. A very simple representation of the energy levels (K, L, M and N) in an atom is given in Figure 2.12. The transitions from various levels are shown with the commonly used terminology (Siegbahn designation). The theory of X-ray

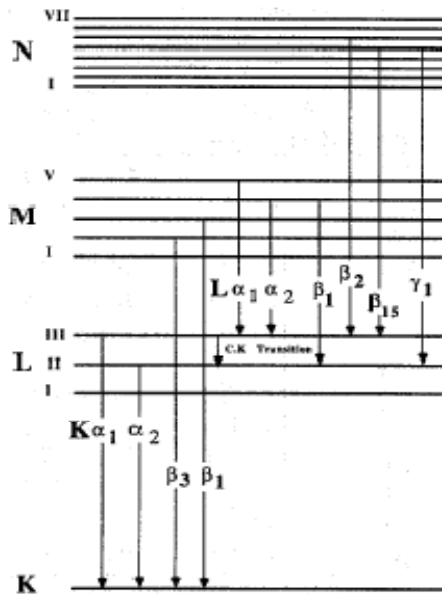


Figure 2.12: Electron transitions producing characteristic X-ray spectrum

spectra reveals the existence of a limited number of allowed transitions, others are forbidden. The allowed transitions are governed by selection rules given in Table 2.3. The relative intensity of the strongest lines in an X-ray series depends on the relative probabilities of expulsion of electrons from the respective shells of the atoms and the probabilities of their respective electron transitions. The intensity of a line series is proportional to the absorption edge jump ratio, r , associated with that series. Absorption edge jump ratio r is given by

$$r_K = \frac{(\mu/\rho)_K + (\mu/\rho)_{L_I} + (\mu/\rho)_{L_{II}} + (\mu/\rho)_{L_{III}} + \dots}{(\mu/\rho)_{L_I} + (\mu/\rho)_{L_{II}} + (\mu/\rho)_{L_{III}} + \dots} \quad \text{..... (2.19)}$$

where $(\mu/\rho)_i$ is the mass absorption coefficients of i^{th} shell.

The actual fraction of the total number of photoionizations that occur, e.g. in K shell is given by

$$1 - (1/r_K) = (r_K - 1) / r_K \quad \text{..... (2.20)}$$

Table 2.3: Selection rules for characteristic X-ray production

Symbol	Name	Allowed values	Selection rules
n	Principal	1, 2, 3,, n K, L, M, N	$\Delta n \neq 0$
l	Azimuthal	0, 1, 2,, (n-1) s, p, d, f,.....	$\Delta l = \pm 1$
m	Magnetic	-l,, 0,, +l	–
s	Spin	$\pm 1/2$	–
j	Inner precession	$l \pm 1/2$, except $j \neq -1/2$	$\Delta j = \pm 1$ or 0

The principal lines of analytical interest and their typical relative intensities are

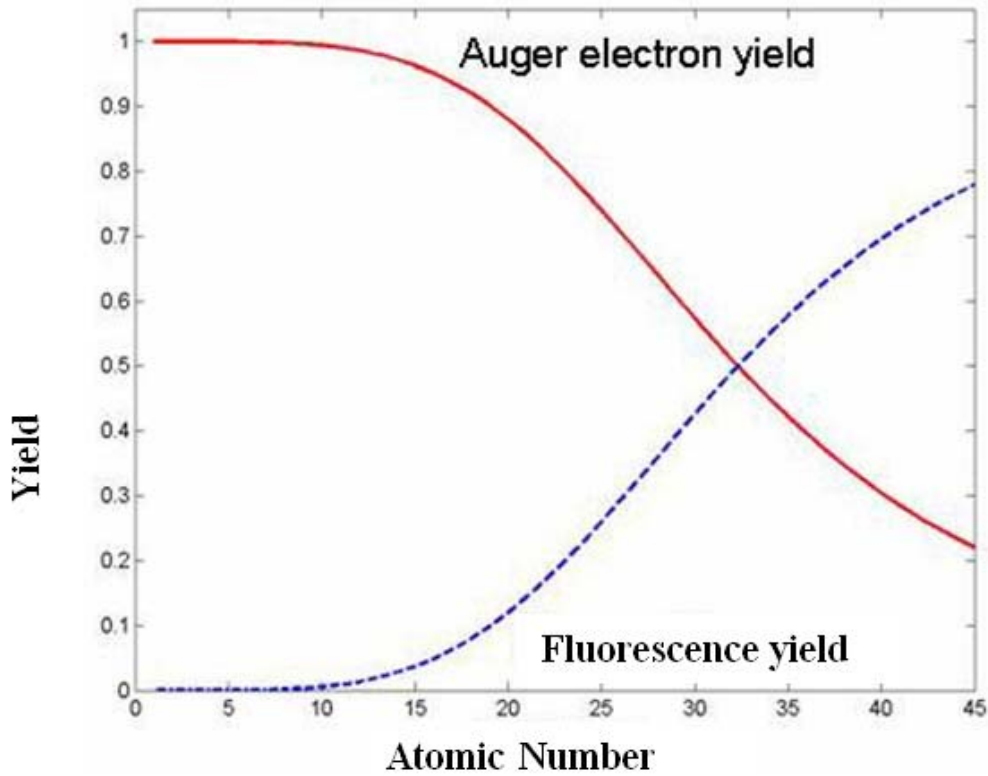
Kα_1	100	Lα_1	100	Mα_1	100
Kα_2	50	Lβ_1	75	Mα_2	100
Kβ_1	15	Lβ_2	30	Mβ_1	50
		Lγ_1	10	Mγ_1	5
		Lι	3		

For the same element, the K, L and M series lines have approximate intensity ratios 100: 10: 1 when excited under same instrumental condition.

The intensity of the total K-, L- and M- series is also a function of the fluorescence yield (ω). Florescence yield is given by the ratio of the number of photons emitted by a particular series (K-, L- or M-) by the number of vacancies formed

$$\omega = \frac{Z^4}{Z^4 + A} \dots\dots\dots (2.21)$$

where Z is the atomic number and A is a constant having values 10^6 and 10^8 for K and L X-rays, respectively. X-ray fluorescence yield is complementary to Auger electron yield. Figure 2.13 shows the plot of X-ray yield versus the Auger electron yield. The X-ray fluorescence yield is low for low atomic number elements and increases with atomic number whereas Auger electron yield follows the reverse trend. The fluorescence yield is the major factor limiting the sensitivity of low atomic number elements.



2.13: Plot of X-ray fluorescence yield versus Auger electron yield

2.6. X-Ray Detectors

An X-ray detector is a transducer for converting X-ray photon energy into voltage pulses. The X-ray photon, entering the detector's active area, interacts through the process of photo-ionization and produces a number of electrons. The current produced by these electrons is converted to digital voltage pulse which corresponds to the energy of X-ray

photon. In XRF, the use of gas filled and scintillation detectors were predominant before the advent of the semiconductor detectors. While gas flow proportional counters are ideal for longer wavelengths, they are insensitive to shorter wavelengths. For shorter wavelengths, scintillation counters are employed. In WDXRF, generally, gas filled proportional and scintillation counters are employed for the detection of X-rays from low Z and high Z elements, respectively but solid state detectors are the heart of the energy dispersive systems [32]. The lithium drifted semiconductor detectors like Si(Li) or Ge(Li) commonly used in EDXRF, basically consist of Si or Ge crystal doped with lithium. In Si(Li) detectors, lithium is added to neutralize the boron impurity which is the most common element present in silicon and modifies silicon to p-type semiconductor. As it is possible to produce high purity germanium, Ge(Li) detectors are replaced by high purity germanium detectors (HPGe). Lithium diffuses into the silicon crystal at elevated temperatures and drifts under the influence of the electric field. In this way, a crystal with high intrinsic resistivity is produced with thin p-type and n-type layer at the end plane and large intrinsic region in between. An inverse DC voltage called reverse bias (p-type layer negative; n-type layer grounded) is applied and the total configuration is termed as p-i-n diode with reverse bias. The detector requires to be cooled to liquid nitrogen temperature (77 K) for two reasons: i) reducing the thermal leakage current and ii) to prevent the reverse diffusion of the Li ions.

The mode of operation of these semiconductor detectors involves interaction of the X-ray photons with the detector crystal and raising the valence band electrons to the conduction band of the crystal lattice thereby creating an electron-hole pair. Because of the applied high voltage, the electron-hole pairs separate and the electrons and holes rapidly drift to the positive and negative electrodes, respectively. A charge pulse is produced for a single photon counting. Since the number of electron-hole pairs is directly proportional to the energy of the detected photon, the magnitude of the charge pulse is proportional to the photon energy. A schematic diagram of the Si(Li) detector crystal is given in Figure 2.14. The different charge pulses produced by the detector are processed by an elaborate electronic system and finally all pulses with certain amplitudes are counted. The efficiency (ϵ) of a semiconductor detector is defined as the percentage of detected photons with respect to the incident photons. A Si(Li) detector, having 3mm thick intrinsic region, has an efficiency of nearly 100% for photon energies between 6 to 11 keV. Semiconductor detectors have better spectral resolution than gas filled proportional and scintillation detectors.

During the past few decades, room temperature operated peltier cooled detectors have become available which offer considerable simplicity and ease of operation since these

detectors no longer require liquid nitrogen cooling [33]. They use peltier cooling instead of liquid nitrogen cooling. Si-PIN photodiode detectors are such detectors which are made of very pure Si, called intrinsic material. Since nothing is doped into them, a simple electrical peltier cooling at approximately -30°C is good enough for reducing the leakage current. Though these electronically cooled detectors have relatively poor energy resolution compared to that of liquid nitrogen cooled detectors, such detectors are widely used nowadays in EDXRF and TXRF spectrometers and are much suited for field applications because of their compact size and no requirement of liquid nitrogen for cooling [34].

Silicon Drift Detectors (SDD) is another type of photodiode detector similar to Si-PIN detectors but having better energy resolution. The resolution of these detectors is comparable to Si(Li). Si-PIN detectors are used where resolution is not critical but detection efficiency is important. SDD detectors are more complicated as well as more expensive [35].

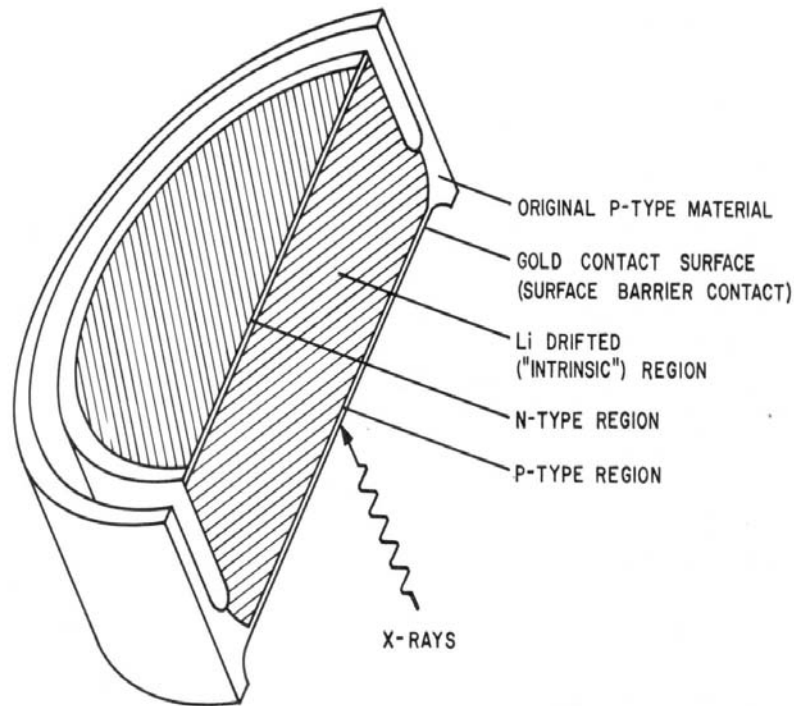


Figure 2.14: Cross sectional view of a Si(Li) detector crystal

2.7. Total Reflection X-Ray Fluorescence (TXRF)

In the past few decades, EDXRF spectrometry has undergone a tremendous progress with the application of total reflection of X-rays on sample reflectors. The phenomenon of total reflection of X-rays, on a sample support surface, was discovered by Compton in 1923. He also found that the reflectivity of a flat polished surface increases strongly below the critical angle [36]. In 1971, two Japanese scientists Yoneda and Horiuchi suggested that the use of total reflection of the exciting beam on optically flat sample support can reduce the background drastically and showed its application for XRF [37] with much improved detection limits. This variant of EDXRF is now considered a separate X-ray spectrometric technique known as Total Reflection X-Ray fluorescence (TXRF) Spectrometry.

In Classical EDXRF, the X-ray beam from an X-ray source falls on the sample at an angle of about 45° and the X-rays emitted from the samples are detected at an angle of 45° . This geometry was known as 45° - 45° geometry. This lead to penetration of X-rays inside the sample to a thickness of about a few 100 microns, thereby resulting in a lot of scattering of the X-rays by the sample and increasing the background drastically. Because of this, EDXRF has relatively poor detection limits and low signal to noise ratio. In TXRF, the exciting beam from the X-ray source falls on the sample support at an angle slightly less than the critical angle of the support so that the beam gets totally reflected. The emitted fluorescence intensity from the sample is detected by the detector mounted at an angle of 90° with respect to the sample support. Hence the geometry in case of TXRF is 0° - 90° . This leads to virtually no interaction of the exciting radiation with the sample support, resulting in a drastic decrease of the scattered radiation and hence negligible background. Moreover since the incident and the totally reflected beam both excite the sample, the fluorescence intensity gets doubled. TXRF, due to very low background and better detection limits, is primarily used for trace and micro elemental analysis. Figure 2.15 shows the geometrical difference between the classical EDXRF and TXRF. A new field of application of TXRF was opened in 1980s for depth profiling of trace elements [38-42].

Another severe drawback in EDXRF is the effect of matrix composition on the analyte line intensity. This is known as matrix inter-element or absorption enhancement effect. Such effect arises due to the following phenomena:

- i) the matrix may have larger or smaller absorption coefficient for the primary X-rays than the analyte,

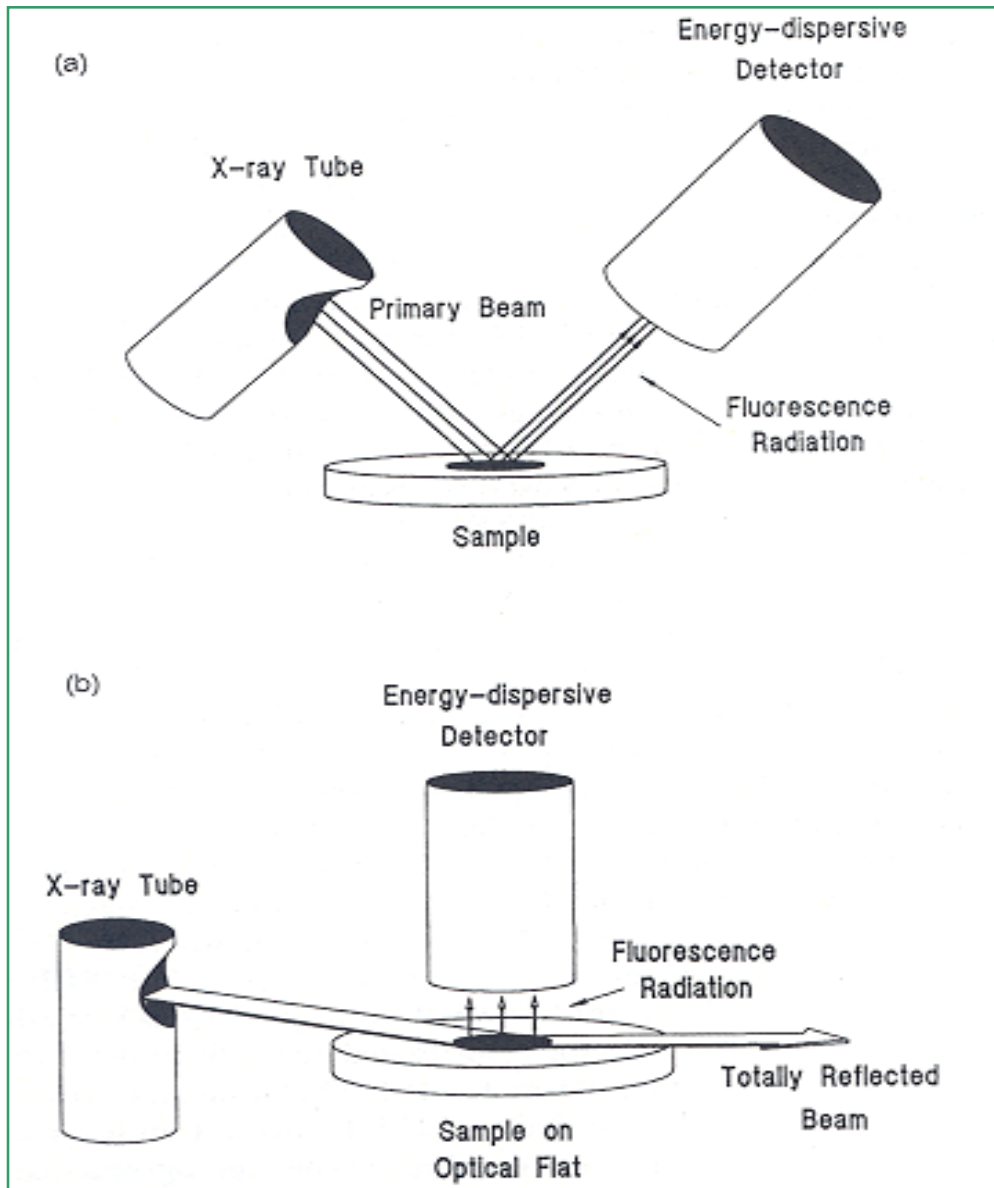


Figure 2.15: Comparison of the geometrical difference between (a) conventional EDXRF and (b) TXRF

- ii) the matrix may absorb the analyte line which will lead to decrease in the analyte intensity than expected and
- iii) the matrix may emit secondary X-rays which may excite the analyte line very efficiently, leading to increase in the analyte line intensity than expected.

As the amount of sample loaded in TXRF analysis is very small and the X-ray penetrates only a few nm, matrix effect is almost absent.

In order to make a meaningful TXRF measurement, the alignment of the instrument is very critical. To ensure the total external reflection, the glancing angle of the incident primary beam must be less than the critical angle of the support used. This angle varies in the order of 0.1° for different sample supports and excitation energies. The primary beam is generated by a X-ray tube and is shaped like a strip of paper realized by an X-ray tube with a line focus. The primary beam filter, consisting of thin metal foils, is placed in the path of the beam to alter the tube spectrum by increasing certain peaks in relation to the spectral continuum. By means of a pair of precisely aligned diaphragms or slits, the beam is shaped like a strip of paper. The primary polychromatic beam consisting of the continuum and the characteristic peaks of the anode material can be altered using simple quartz reflector block acting as low pass filter. It cuts the high energy part of the continuum and the low energy part is used for sample excitation. But sometimes it is required to use a considerably pure spectral line for excitation, which is achieved by using monochromators like natural crystal or multilayers. Both these monochromators work on the principle of Bragg's law with definite energy band selected at a particular angle of reflection. Unlike natural crystals, multilayers consist of stack bilayers, each being isotropic and homogenous. The bilayers are arranged in such a way that, alternately lower and higher refractive indices n_1 and n_2 , respectively are put one above the other. The total thickness (d) is sum of both the layers $d = d_1 + d_2$. The first layer having lower refractive index is called reflector and the other is called spacer. Natural crystals like LiF (200) or graphite have very small energy bandwidth but very poor reflectivity but multilayers have very high reflectivity but energy bandwidth is large.

The sample is deposited on highly polished sample supports. For trace analysis, the support is usually fixed but for depth profiling, positioning and tilting of the support is required. The fluorescence intensity from the sample is recorded by an energy dispersive solid state detectors like Si(Li) which is liquid nitrogen cooled or SDD which is peltier cooled. The detector is mounted perpendicular to the sample support plane to obtain spectra with minimum scattered background and large solid angle. The fluorescence intensity of the sample is registered by MCA, leading to an energy dispersive spectrum. The basic design of

the TXRF instrument is given in Figure 2.16. In TXRF, elements with $Z > 13$ can be analysed in ambient air. Helium purging is used to suppress the argon peak and for analysis of low Z elements below $Z = 13$, vacuum chamber TXRF spectrometer is used.

2.7.1. Fundamentals of total reflection of X-rays

The three important quantities that characterize the total reflection mode of excitation in TXRF are:

- a) Critical angle
- b) Reflectivity
- (c) Penetration depth

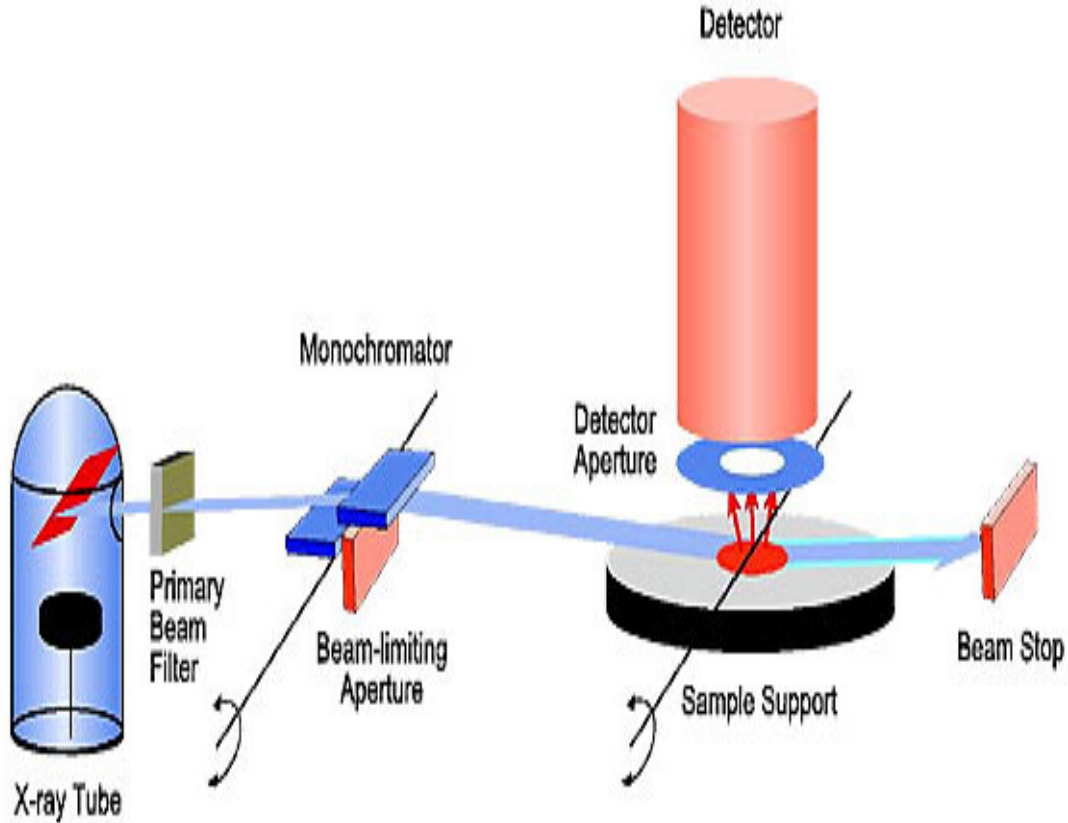


Figure 2.16: Schematic view of the total reflection geometry

When any electromagnetic radiation travels from one medium to another, it gets deflected from its original path. It gets partly reflected into the first medium and partly refracted into the second medium. According to the laws of reflection, the incident angle is equal to the angle of reflection and the incident, normal and reflected rays are coplanar. The glancing angle of the incident and reflected beams are also equal and follow the snell's law which states that

$$n_1 \cos\alpha_1 = n_2 \cos\alpha_2 \quad \dots\dots\dots (2.22)$$

where, n_1 and n_2 are the refractive indices of medium 1 and 2, respectively and α_1 and α_2 are the glancing angles of incident and refracted beam, respectively.

When any electromagnetic radiation travels from an optically rarer medium (n_1) to denser medium (n_2) the refracted beam in the denser medium will be deflected off from the interface boundary. But if the radiation travels from a denser medium to rarer medium, the refracted beam will be deflected towards the interface boundary as shown in the Figure 2.17. For X-rays, any medium is optically thinner than air or vacuum so when it travels from air (optically denser) to solid medium (optically less denser) the refracted beam gets deflected towards the boundary plane (Figure 2.17. (b)). When the glancing angle of the incident beam

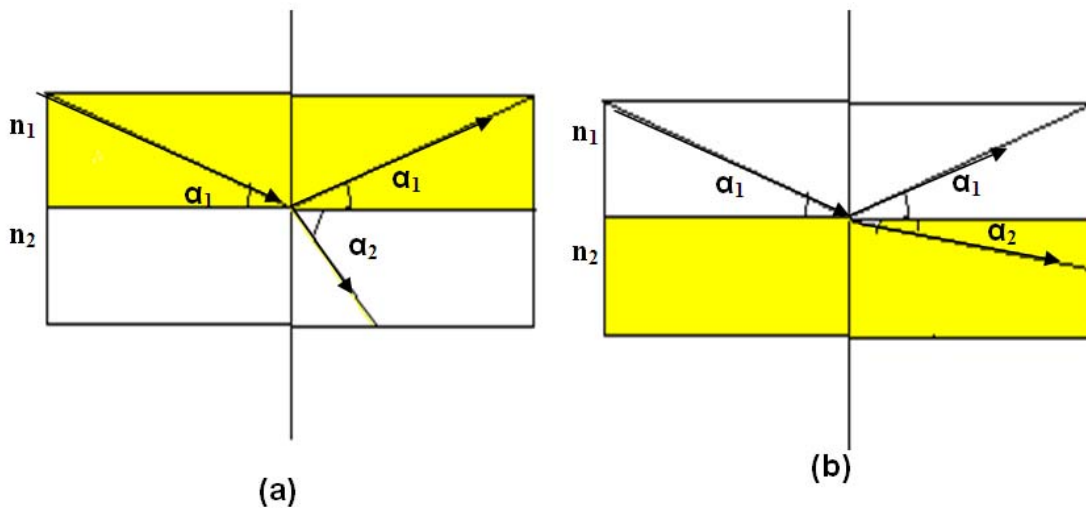


Figure 2.17: The incident, reflected and refracted beam at the interface of two media with refractive indices n_1 and n_2 in (a) $n_1 < n_2$ and (b) $n_2 < n_1$

(α_1) is decreased in steps, at a particular glancing angle α_1 , the corresponding angle α_2 will become zero and the refracted beam will emerge tangentially from the interface boundary. This glancing angle of the incident beam above which refraction is feasible and below which refraction is not feasible, is known as critical angle “ α_{crit} ” and total external reflection of the X-rays takes place at this angle. Accordingly, the equation 2.22 becomes,

$$\cos \alpha_{crit} = n_2 \quad \dots\dots\dots(2.23)$$

For angles α_1 lower than the α_{crit} , the angle of refraction α_2 has no real value as its cosine cannot be greater than one. In that case, no beam enters the lighter medium (solid) and the interface boundary acts as an ideal mirror reflecting the entire incident beam completely back into the denser medium (air). This phenomenon is called *total external reflection*.

The critical angle of a medium (solid) is given by

$$\alpha_{crit} = \frac{1.65}{E} \sqrt{\frac{Z\rho}{A}} \quad \dots\dots\dots (2.24)$$

where E (keV) is the energy of the incident beam, ρ (g/cm³) is the density of the medium and Z and A are the atomic number and atomic mass of the medium material, respectively. This approximation is valid for photon energies above the absorption edges of the medium. The dependence of the path of the incident beam on the glancing angle is shown in the Figure 2.18 and Table 2.4 gives the critical angle values of different media for different incident X-ray energies.

Reflectivity (R) is defined as the intensity ratio of the reflected beam and the incident beam. During total reflection, since the entire beam gets completely reflected back the reflectivity increases to approximately 1. At higher glancing angles the reflectivity is less (less than 0.1%) and increases very steeply to about 100 % when the glancing angle reaches below the critical angle. Figure 2.19 shows the dependence of reflectivity on the glancing angle for Si, Cu and Pt substrates. For trace elemental analysis of granular residue, a sample support with very high reflectivity is required for reflecting the incident beam totally.

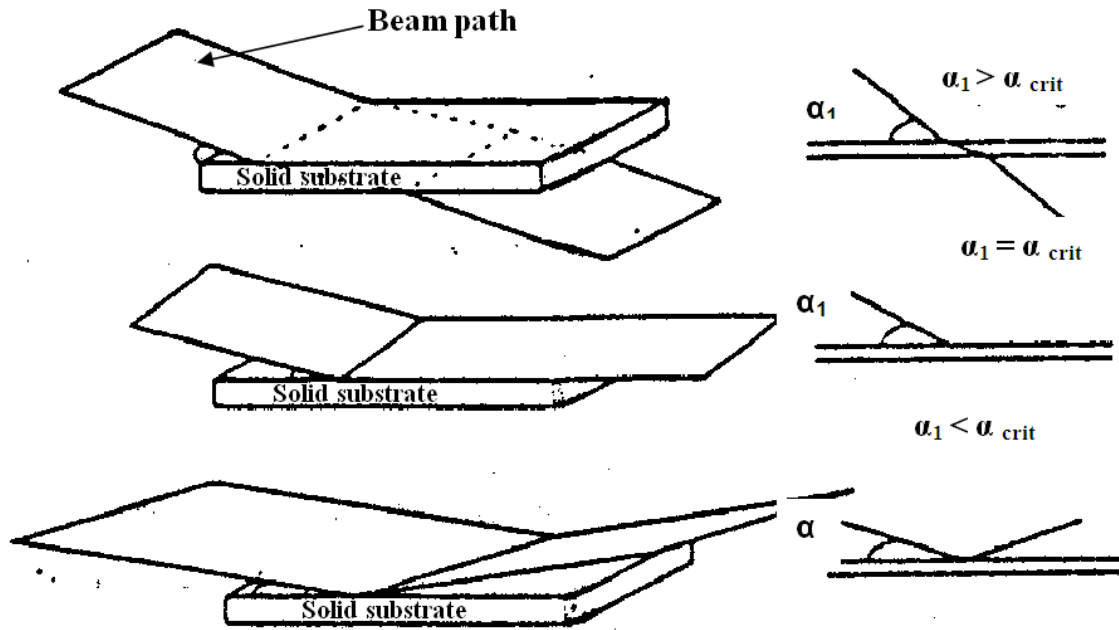


Figure 2.18: Dependence of beam path on the glancing angle α_1

Table 2.4: Critical angle of total reflection for various media and different incident radiation energies

Medium	α_{crit} Values at various photon energies		
	8.4 keV	17.44 keV	35 keV
Pexiglass	0.157	0.076	0.038
Glassy carbon	0.165	0.080	0.040
Boron nitride	0.21	0.10	0.050
Quartz glass	0.21	0.10	0.050
Aluminum	0.22	0.11	0.054
Silicon	0.21	0.10	0.051
Copper	0.40	0.19	0.095
Gallium arsenide	0.30	0.15	0.072
Platinum	0.58	0.28	0.138
Gold	0.55	0.26	0.131

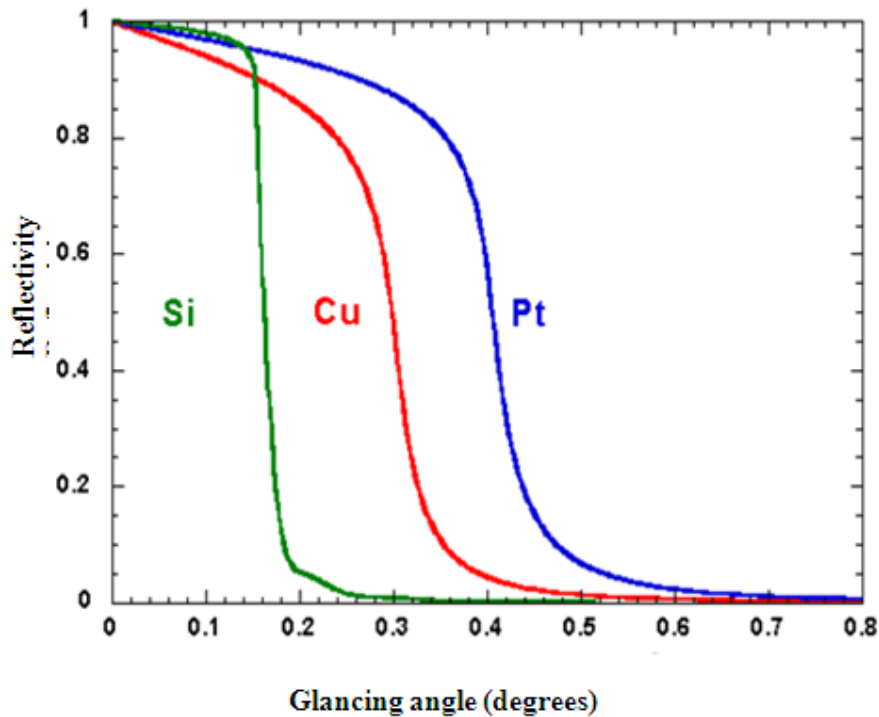


Figure 2.19: Reflectivity versus the glancing angle for quartz, Copper and Platinum

Penetration depth is another critical factor in the total reflection mode of operation. It is defined by that depth of a homogenous medium upto which a beam can penetrate while its intensity is reduced to $1/e$ or 37% of its initial value. The penetration depth at angles greater than the critical angle is of the order of a few micrometers but under total reflection condition, the penetration depth is drastically reduced to a few nanometers. After that it is nearly constant as that of reflectivity curve. The very less penetration at angles less than the critical angle makes this technique inherently sensitive for depth profiling and surface analysis. Penetration depth is a function of glancing angle, Z and photon energies. Figure 2.20 shows the variation in the penetration depth along with the grazing angle for 17.5 keV radiation on Si substrate.

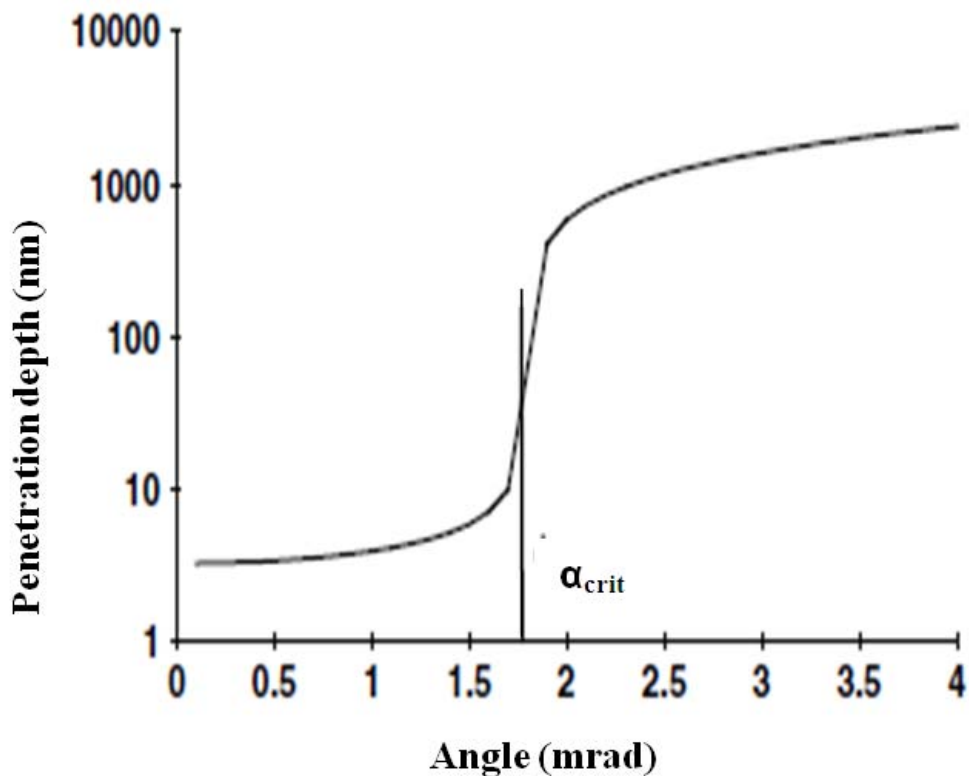


Figure 2.20: Penetration of X-rays depending on the grazing angle for 17.5 keV radiation in silicon

Total reflection X-ray fluorescence offers the following advantages for analysis of materials:

- i) If the glancing angle of the incident beam is adjusted below the critical angle, almost 100% of the incident beam is totally reflected, so this beam scarcely penetrates into the reflector (sample support) and the background contribution from the scattering on the support is drastically reduced.
- ii) The sample is excited by both the direct and the totally reflected beam, which results in the doubling of the fluorescent intensity.
- iii) Due to the geometry, it is possible to position the detector very close to the sample support on which the sample is loaded. This results in a large solid angle for the detection of the fluorescent signal.

All these features make TXRF a very powerful technique for trace and ultra trace analysis with detection limits comparable with the other well established methods of trace analysis.

2.7.2. Sample carriers

TXRF sample carriers are essential part of the TXRF analytical technique. For trace analysis of liquid samples, a carrier is required to serve as sample support as well as reflecting mirror. For such analysis, the mean roughness of the sample carriers should be in the order of a few nm and the overall flatness should be typically $\lambda/20$ ($\lambda = 589$ nm, the mean of visible light wavelength). Many sample carriers have been investigated for their use in TXRF [43-46]. There are some general requirements which the sample carriers must satisfy for their optimal use in TXRF. These include:

- i) A high reflectivity and optically flat surface
- ii) Chemically inert material
- iii) Free from trace impurities
- iv) No fluorescence peak interference from the sample carrier at the region of interest
- v) Easy to clean and economical

As shown in the Figure 2.21 most of the carriers are circular disks of diameter 30 mm and thickness 2-3 mm. Usually, sample solutions with a volume of 2-100 μL are pipetted on the center of the sample carrier and dried under an IR lamp or over a hot plate. On drying, a uniform solid thin film is distributed on the support as shown in the Figure. In Table 2.18, the important characteristics of some commonly available sample supports are given [47]. Quartz gives rise to silicon peak and hence silicon cannot be determined using quartz carrier. Boron nitride is the most resistant material suitable for the analysis of strong acid. Glassy carbon is preferentially used for electrochemical applications and Plexiglas is extremely cheap, once use, sample carrier. In general, quartz and Plexiglas carriers are mostly used for micro and trace analysis.

Cleanliness of the sample supports is very important. After use the carries are immersed in a beaker containing dilute cleansing detergent for a few hours. The carriers are then rinsed with distilled water and put in another beaker containing nitric acid diluted with Milli-Q water. Finally, rinsed with high purity acetone and dried. The cleanliness of such supports is confirmed by recording TXRF spectrum after cleaning. A typical TXRF spectrum of thoroughly cleaned quartz sample support is given in Figure 2.22. The spectrum shows Si $K\alpha$ peak due to the presence of silicon in the sample support made of quartz, Ar $K\alpha$ peak is

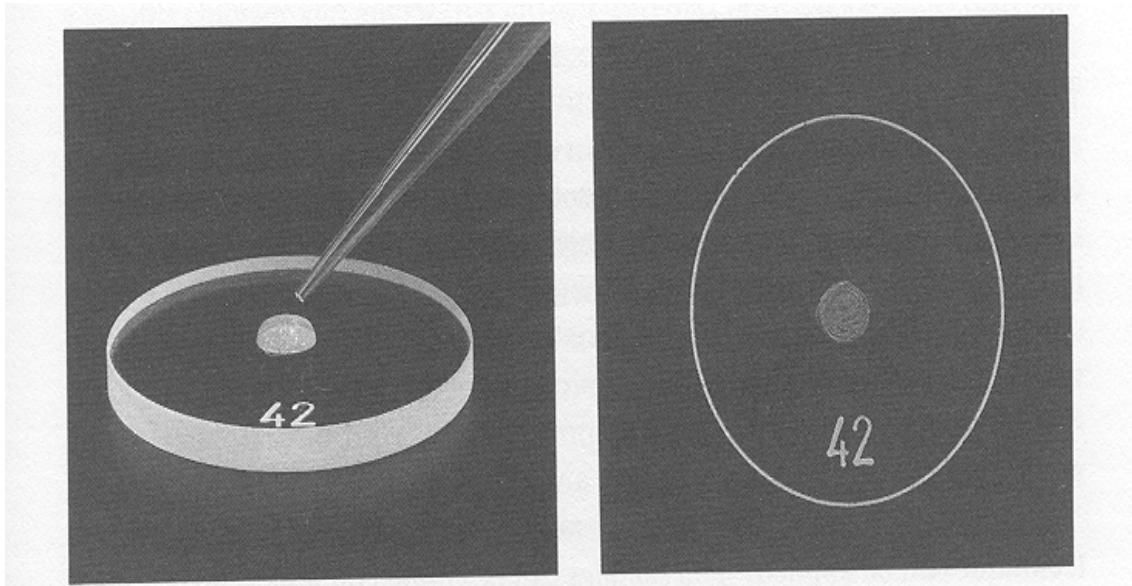


Figure 2.21: Liquid sample pipetted on a clean quartz sample support which leaves a dry residue after evaporation

Table 2.5: Important characteristics of different sample support materials

Features	Quartz	Plexiglass	Glassy carbon	Boron nitride
With Mo Kα excitation				
Reflectivity (R)	0.994	0.998	0.998	0.999
Critical angle (α_{crit})	0.10	0.08	0.08	0.10
Purity	Very Good	Zn	Fe, Cu, Zn	Zn
Surface Quality	Very Good	Good	Satisfactory	Good
Fluorescence Peak	Si	None	None	None
Cleaning	Easy	Impossible	Difficult	Easy
Cost(\$)	30	0.1	30	60

due to its presence in air atmosphere and traces of Ca and Fe are present below ppb level as common impurities.

2.7.3. Instrumental parameters

For multi-elemental analysis, different elements require different conditions for optimum excitation. Consequently, a compromise is generally necessary for such analysis. X-ray tube, multilayer, sample carriers are the components whose parameters can be changed for a particular operation. The X-ray tube position and multilayer/ natural crystal value is adjusted such that the glancing angle is about 70% of the critical angle of total reflection depending on the sample carrier and the incident beam energy. When excitation is performed using X-ray tubes, the continuum as well as the characteristic X-ray radiation of the anode material contributes to the sample excitation with different efficiencies for different elements. As excitation is possible only when the photon energy is greater than that of the absorption edge of the element, choosing the correct anode X-ray tube with proper excitation voltage

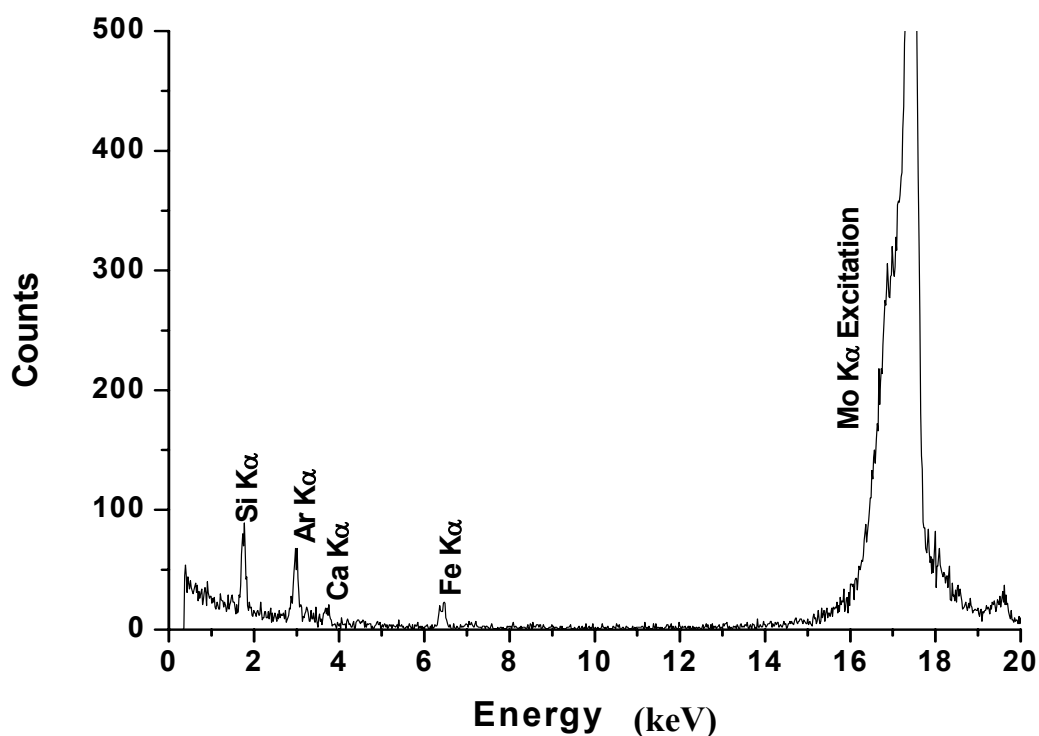


Figure 2.22: TXRF spectrum of a quartz sample carrier after cleaning (measurement time 100 s)

and current is essential. The efficiency for excitation of different elements with various anode target elements (Sc, Cr, Cu, W, Au and Mo) is shown in Figure 2.23. The change in the excitation efficiency of elements when continuum excitation is used can also be seen in the Figure. The continuum is effective for the excitation of wide range of photon energies and maximum efficiency is achieved when the applied voltage is about 1.5-2 times the absorption edge energy. The intensity of the characteristic radiation of the analyte will be high when the peak energy of the tube target is just above the absorption edge of the analyte and the efficiency gradually decreases with decreasing atomic number of the analytes. Excitation with Mo $K\alpha$ can be used for the excitation of almost all the elements from $Z > 13$, but for efficient excitation of low Z elements, W $L\alpha$ or Cr $K\alpha$ are more effective.

For trace and micro analysis of multi-elements, dual target tubes such as W-Mo serve the purpose of efficient excitation of almost all the elements by operating in three different excitation modes achieved by changing the incident glancing angle and multilayer to select a particular energy [48]:

- i) The continuum obtained by a tube operated at 50 kV has intensity maxima at about 30 keV and efficiently excites elements with atomic number $40 < Z < 50$ (K lines).
- ii) Tube operated at 40 kV producing Mo K lines can efficiently excite elements with atomic number $20 < Z < 40$ (K lines) and $55 < Z < 94$ (L lines).
- iii) W Tube operated at 25 kV producing W L lines can efficiently excite elements with atomic number $13 < Z < 20$ (K Lines).

The current value is limited by the dead time of the detector which is generally kept below 30%. Figure 2.24 shows a typical TXRF spectrum of a multi-element standard (MES) having a concentration of $5\mu\text{g/mL}$ of each element recorded in our laboratory TXRF spectrometer. $10\mu\text{L}$ of the standard solution was deposited on a cleaned quartz sample support. The applied voltage and current were 40 kV and 30 mA, respectively. The TXRF spectrometer was aligned and monochromatised beam of Mo $K\alpha$ was used as the excitation source. The measurement time was 1000s.

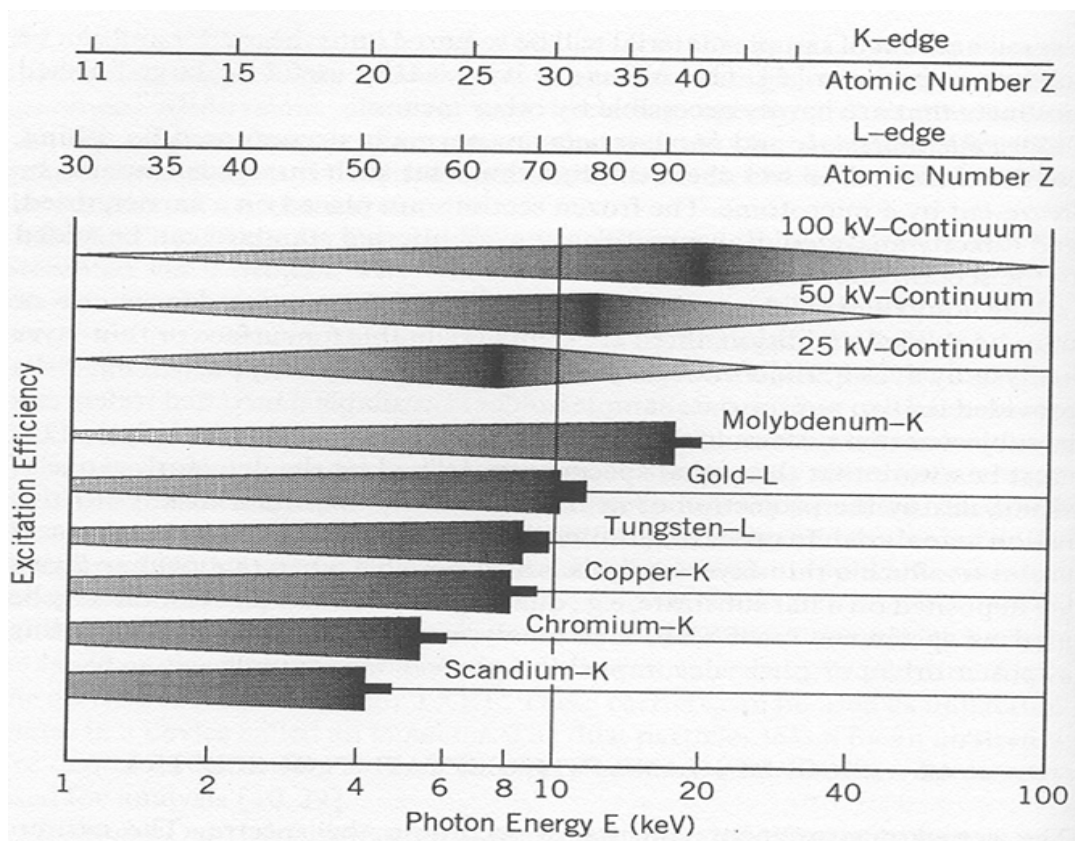


Figure 2.23: Efficiency for the excitation of elements with respect to the excitation source and photon energies

2.7.4. Calibration and quantification

A qualitative analysis is intended to detect elements present in a sample irrespective of their concentration. In TXRF, this can be performed simultaneously using the features of energy dispersive system. It gives information about the elements present in the sample, by means of their characteristic peak energies in the spectrum. Moreover, all these peaks are in accordance with Moseley's Law with regard to their position and intensities of the K-, L- and M- series have fixed ratios. X-ray spectra are quite simple and contain relatively fewer peaks than optical spectra. It enables to design the further analytical strategy required for quantitative analysis.

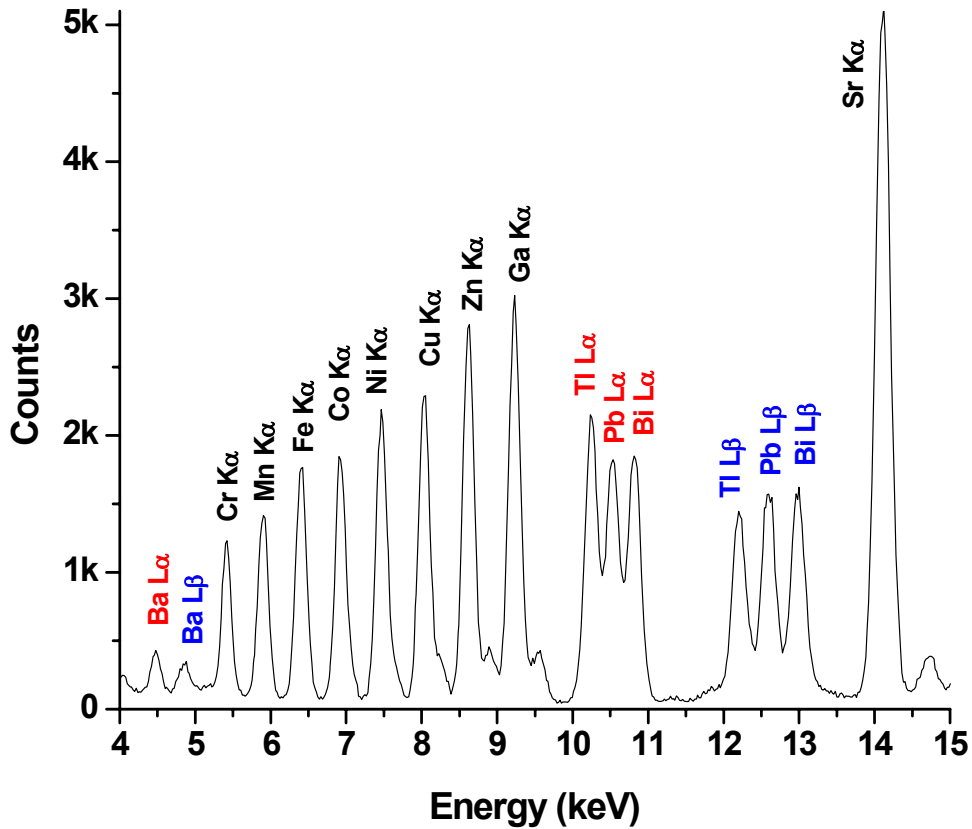


Figure 2.24: A typical TXRF spectrum of multi-element standard solution having a concentration of 5µg/mL

For quantitative analysis, the net intensities of the principal peak (N_x), obtained after correction of the spectral background and the overlapping neighbouring peaks, is determined after recording the spectra. Ideally a linear relationship exists between the X-ray intensity recorded for the analyte x and its concentration in the sample (c_x)

$$N_x = S * c_x, \quad \dots\dots\dots (2.25)$$

where, S is the constant of proportionality called absolute sensitivity. The plot of this equation gives straight line and is known as *calibration plot*. The slope is given by S .

Different elements have different slopes and hence different sensitivities. In classical XRF, this ideal case is seldom obtained and has to be approximated for thin layers or films. The deviation from ideality is due to the matrix effect. In TXRF, only very small residues of sample are subjected to analysis and such samples with tiny mass and thickness meet the condition for the ideal case. Hence, for definite excitation source and instrumental parameter, the calibration is not effected by chemical composition and matrix.

The procedure for elemental quantification is also very simple in TXRF. It is done by adding a single internal standard to the sample. The pre-requisite for the element to be added as internal standard is that, it should not be present in the sample. For quantification, the net intensities of the analytes and internal standard peak need to be determined. Besides this, the relative sensitivity has to be determined for each element. The ratio of the absolute sensitivity of each element to that of the internal standard is called *relative sensitivity*. The mode of excitation along with applied voltage, current, monochromator as well as geometry has to be fixed for fixed set of relative sensitivity values and any alteration requires a new calibration. For determination of relative sensitivities, standard solutions (Merck, Aldrich, etc.) of multi-elements or single elements are chosen. The stock solution, if having a concentration of 1000-500 µg/mL is diluted and internal standard is added to this solution. An aliquot of 2-10 µL is pipette on a clean sample support and dried completely by evaporation. The TXRF spectra recorded for CertiPUR ICP Multi-element standard (ICP-MS) solution-IV having concentration of 1000 µg/mL and diluted to 10 µg/mL looks similar to the one shown in Figure 2.24, when the instrumental parameters are the same as those discussed in section 2.7.3. An aliquot of 10 µL was pipetted on quartz sample support. The exact concentration of all the elements present in this standard is given in Table 2.6. The net intensities of the elements present are determined by peak fitting software available with the spectrometer. The relative sensitivity of each element is calculated by the formula

$$RS_x = \frac{S_x}{S_{IS}} = \frac{N_x * C_{IS}}{N_{IS} * C_x} \dots\dots\dots (2.26)$$

where, RS_x is the relative sensitivity of x^{th} element with respect to the internal standard IS. S_x , N_x and C_x are the sensitivity, net peak area and concentration of element (x) and S_{IS} , N_{IS} and C_{IS} are the corresponding values for internal standard element (IS). The

relative sensitivity values with respect to gallium, determined for different elements, are given in Table 2.6. Figure 2.25 shows the variation of relative sensitivity values with respect to atomic number. The relative sensitivity values of those elements for which standards are not available were obtained by interpolation of the curve. As the relative sensitivity values remain constant for a particular set of instrumental parameters, these values can be used for quantification of elements in samples irrespective of their matrices. Internal standardization based method for TXRF quantification is very simple and reliable. Generally, rare elements which are not usually present as contaminants are chosen as internal standards. Elements with K- lines are preferred as internal standard than elements with L-lines. Moreover, lighter elements are not suitable as internal standards because of their low fluorescence yields.

TXRF is mainly a solution based technique and solid samples need to be digested prior to analysis. Sample preparation and presentation necessitate a clean working table, preferably clean bench of class 100. The different steps of sample preparation and quantification applied for TXRF multi-element analysis are shown in Figure 2.26. To an aliquot of volume (V) of the sample, internal standard of volume (v) is added and thoroughly mixed with a shaker. After homogenization, a small volume (2-10 μ L) of the final solution is pipetted out on a clean sample carrier and dried by evaporation under IR lamp or electric heater. The X-ray spectrum is then recorded using detector which provides the net intensities of the detected elements. Then the concentration is calculated by rearranging the equation 2.26 as

$$c_x = \frac{N_x}{N_{IS} * RS_x} * c_{is} \quad \dots\dots\dots (2.27)$$

where, c_x is the concentration of the x^{th} element present in the sample, N_x and N_{IS} are the net intensities of (x) and (IS) internal standard, RS_x is the relative sensitivity value of (x) with respect to (IS) and c_{is} is the concentration of (IS). For microanalysis of powder, single grain or metallic smears, a few microgram of the sample is deposited on the sample carrier and the quantification is with respect to another element present in the sample such that the sum is set to 100%.

Table 2.6: Concentration and the calculated relative sensitivity values of various elements along with their X-ray energies

Atomic No. (Z)	Element	X-ray energy (keV)	Concentration ($\mu\text{g/mL}$)	Relative sensitivity
K α line				
13	Al	1.486	9.53	0.0154
19	K	3.313	9.47	0.1256
20	Ca	3.691	9.51	0.0981
24	Cr	5.414	9.49	0.2842
25	Mn	5.898	9.49	0.3325
26	Fe	6.403	9.50	0.4380
27	Co	6.929	9.48	0.5090
28	Ni	7.477	9.51	0.6420
29	Cu	8.046	9.40	0.7315
30	Zn	8.637	9.51	0.8679
31	Ga	9.250	9.44	1.0000
38	Sr	14.163	9.80	2.2141
L α line				
56	Ba	4.465	9.55	0.0532
81	Tl	10.267	9.48	0.6610
82	Pb	10.550	9.63	0.6435
83	Bi	10.837	9.56	0.7094
90	Th	12.967	10.0	0.7962
92	U	13.612	10.0	0.8390

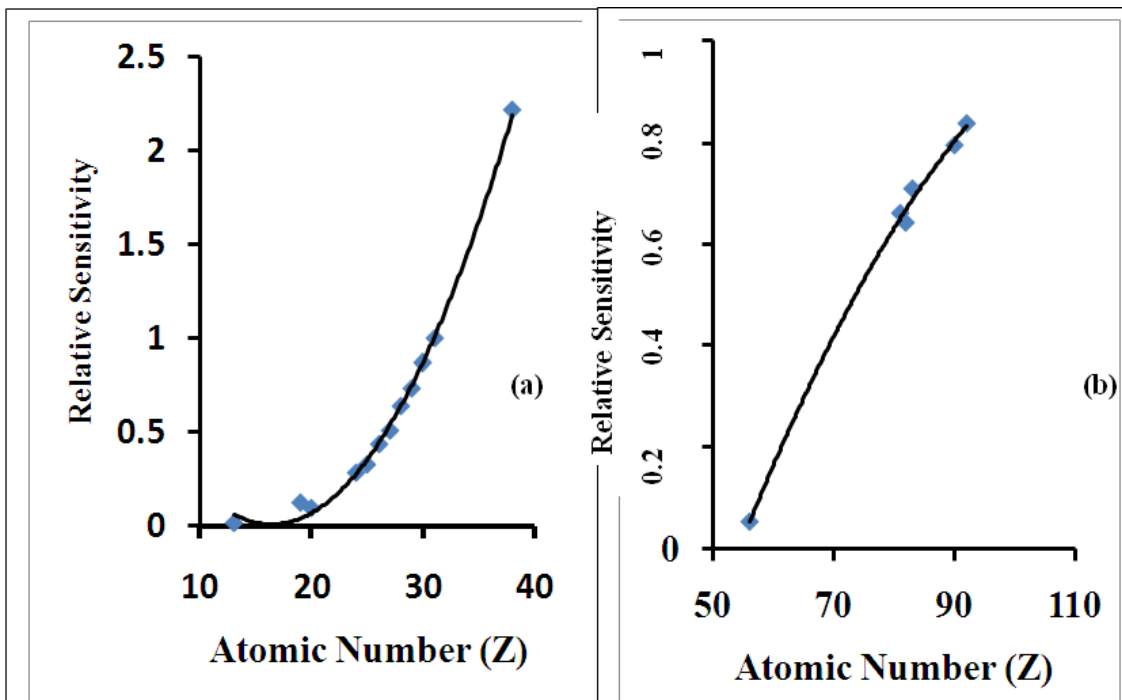


Figure 2.25: Plot of relative sensitivity of different elements versus their atomic number for (a): K lines and (b): L lines

For validation of the method of analysis, in the present study, another multi-elemental standard having a concentration of 900 ng/mL of each element was analysed using the relative sensitivity values given in Table 2.6 and equation 2.27. The analytical results are given in Table 2.7. The detection limits (D_{Li}) of TXRF for each element were calculated using the formula:

$$D_{Li} = \frac{\text{Concentration}}{\text{Peak area}} * 3 * \sqrt{\text{Background}} \quad \dots\dots\dots (2.28)$$

Figure 2.27 shows the variation of TXRF detection limits with respect to the atomic number for the same multi-elemental standard solution. 10 μ L of this standard was pipetted on two clean sample supports and measured for 1000s using Mo $K\alpha$ excitation. The spectrometer was operated at 30mA and 40kV. The detection limits, calculated from equation

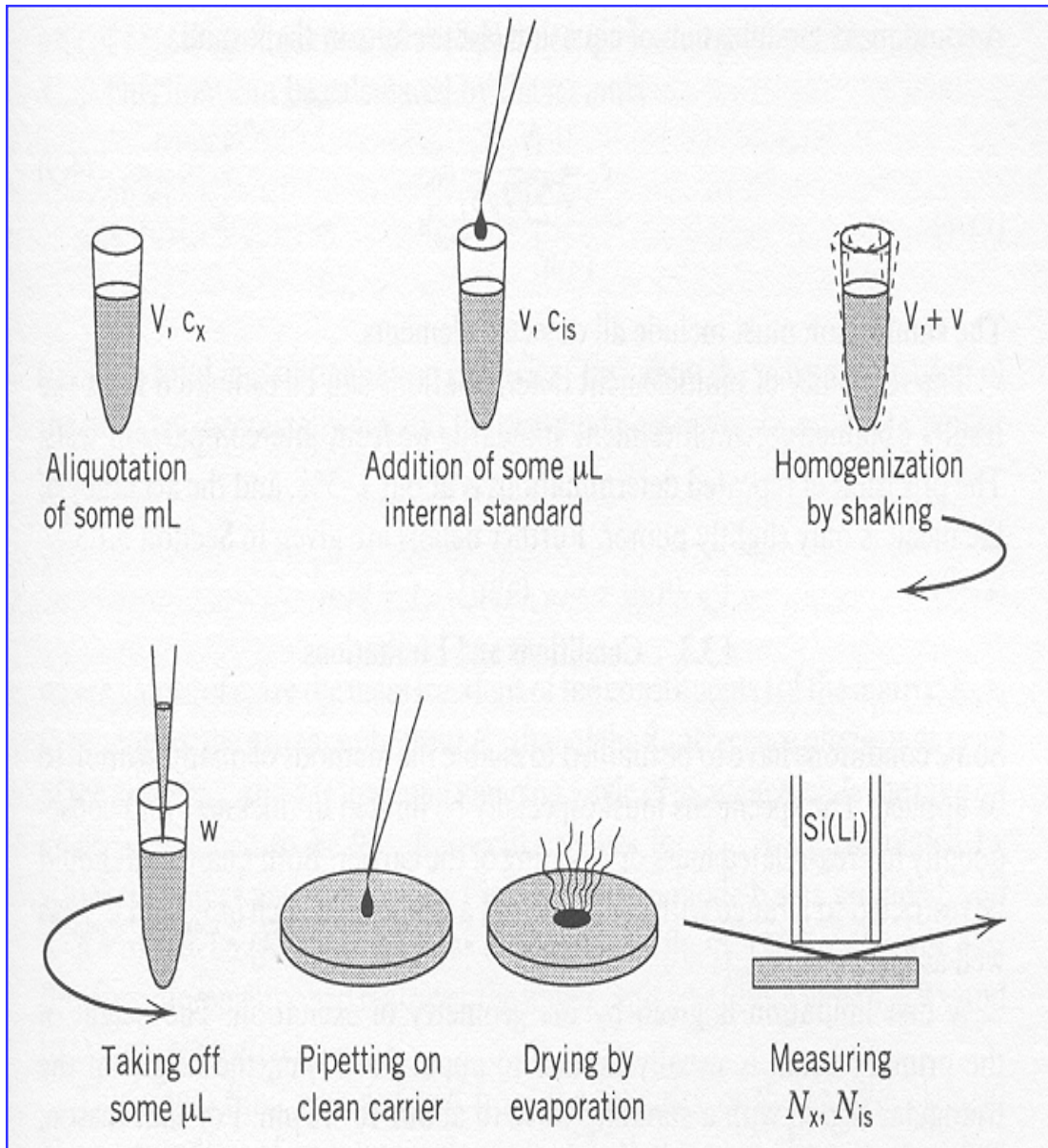


Figure 2.26: The different steps of quantification applied for TXRF analysis

Table 2.7: TXRF analysis results of multi-element standard

Atomic No. (Z)	Element	Concentration (ng/mL)	
		Expected [*]	TXRF [#]
K Lines			
19	K	903	943 ± 143
20	Ca	907	1016 ± 141
24	Cr	906	894 ± 24
25	Mn	906	880 ± 48
26	Fe	906	1072 ± 86
27	Co	905	872 ± 10
28	Ni	907	872 ± 3
29	Cu	896	972 ± 38
30	Zn	904	899 ± 25
38	Sr	934	994 ± 48
L Lines			
56	Ba	911	915 ± 44
81	Tl	904	940 ± 5
82	Pb	918	938 ± 47
83	Bi	912	932 ± 31

^{*}: Calculated on the basis of sample preparation

[#]: TXRF determined values

2.28, were found to improve with increasing atomic number. The detection limit for aluminum was found to be 137 ng/mL and for strontium 1 ng/mL [49]. However, these detection limits depend on the total matrix concentration as well as instrumental parameters. Hence, with respect to the capabilities in terms of analytical features, cost and maintenance, TXRF has far surpassed the conventional XRF and is in competition with the well established methods of trace analysis.

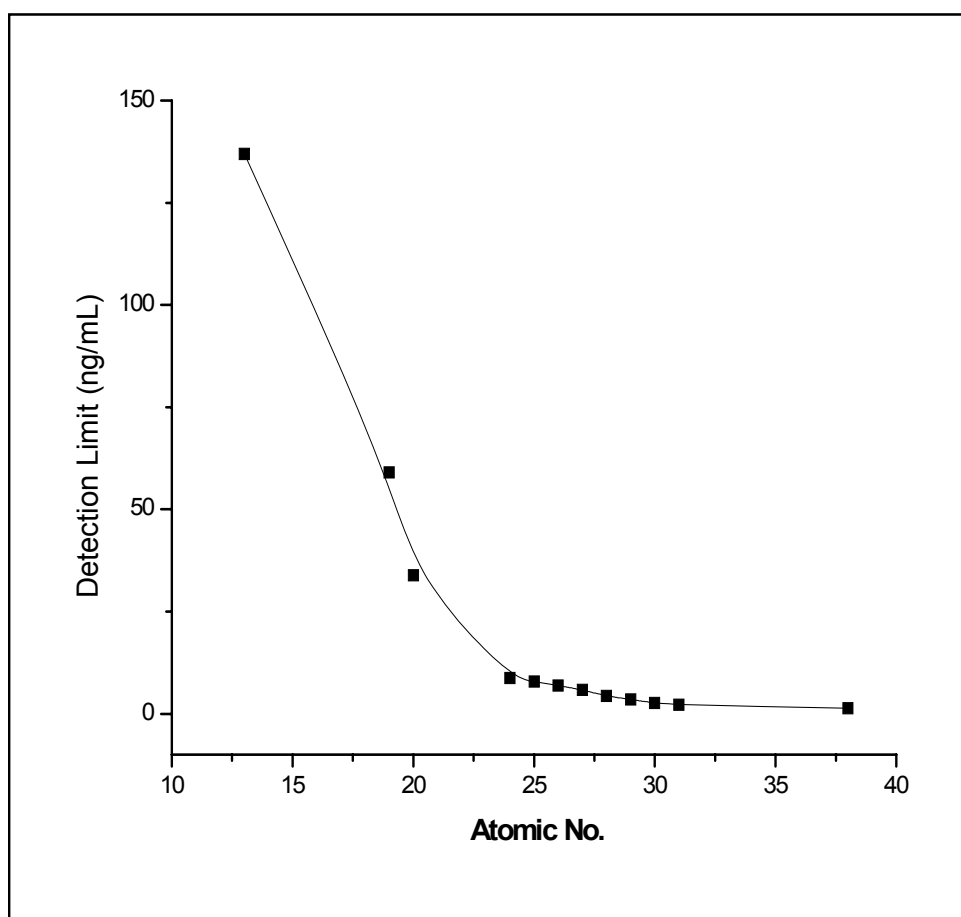


Figure 2.27: Variation of TXRF detection limits with atomic number

2.8. Energy Dispersive X-Ray Fluorescence (EDXRF)

In Energy dispersive X-Ray fluorescence (EDXRF) unlike WDXRF, the wavelengths of all the elements emitted by the specimen are not dispersed spatially prior to detection, but the detector receives the undispersed beam. The detector itself separates the different energies of the beam on the basis of their average pulse heights. Hence the energy dispersive spectrometer consists of only three basic units:

- (a) Excitation source,
- (b) Sample holder unit and
- (c) Detection system, with no wavelength dispersing devices or goniometer.

In XRF spectrometers, X-ray beam emitted from X-ray tube or radioisotope sources is normally used for sample excitation. In tube excited XRF systems, the energy distribution of the spectrum arriving from the sample depends on the tube target element, voltage and current applied. As shown in Figure 2.30, a standard commercial EDXRF spectrometer comprise of the following components: an X-ray tube, sample holder with auto sampler unit, solid state semiconductor detector Si(Li) with liquid nitrogen dewar/ peltier cooled detectors and the spectrometer electronics. Unfiltered direct excitation leads to a combination of both continuum and characteristic peak to fall on the sample. The spectrum shape can be altered by use of various filters and secondary targets present in the filter changer unit. Optimum selection of target, current, voltage and primary beam filter / secondary target are critically important for obtaining the best data from an EDXRF system. The beam filter, made of thin film metal foil and acts as an X-ray absorber, is placed between the source and sample. It is based on the fact that an element absorbs wavelength shorter than its absorption edge strongly. In XRF, primary beam filters are used to eliminate the scattered background drastically and improve the signal to noise ratio at the region of interest (ROI). Apart from this, it also reduces the dead time of the detector significantly [50]. All these features ultimately improve the detection limits. Table 2.9 gives the list of a few filter elements that are generally used in EDXRF spectrometers and the elements that can be analysed using these filters. In Figure 2.31, a clear difference in the signal to noise ratio of gallium can be seen without Fe filter and with Fe filter, using the same tube current and voltage. The drastic reduction in the background can also be seen in the Figure on using Fe filter.

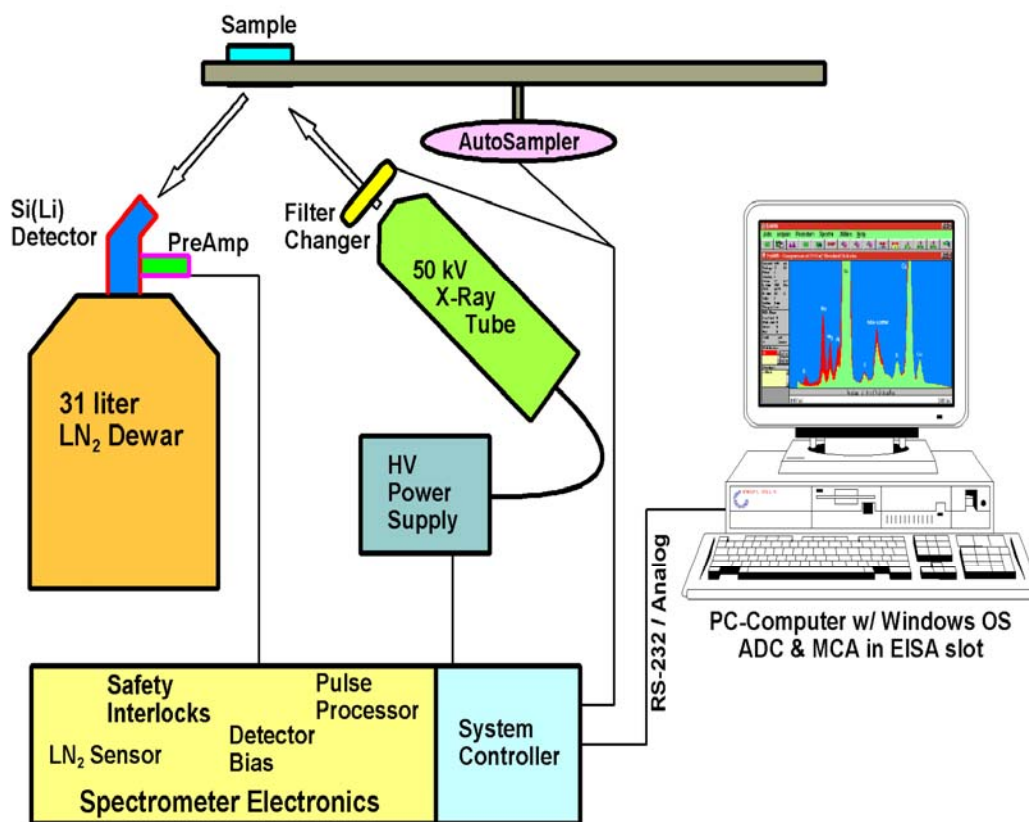


Figure 2.28: Basic layout of EDXRF spectrometers

Another way of improving the detection limits in XRF is by using secondary targets. The X-rays, from the primary X-ray tube target gives a broad spectrum of bremsstrahlung together with the characteristic lines of the anode material. But when this primary beam is made to strike another target known as secondary target, the emitted beam will be quasi monochromatic with reduced background, as the bremsstrahlung radiation will be absent. Moreover, Cartesian geometry of secondary targets also helps in the reduction of the background [51]. However secondary target has a disadvantage of intensity loss. By interchanging the filter and secondary target, the best optimized excitation conditions and improved detection limits can be achieved.

Table 2.8: A few primary beam filters and the elements that can be analysed using those filters

<i>Primary beam filter element</i>	<i>Suitable for analysis of elements</i>
Ti	Cr, Mn, Fe, Co, Ni, Cu, Zn
Fe	Ni, Cu, Zn, Ga, Ge, As, Pb
Cu	Ge, Ar, Se, Pb
Mo	Pd, Ag, Cd, In

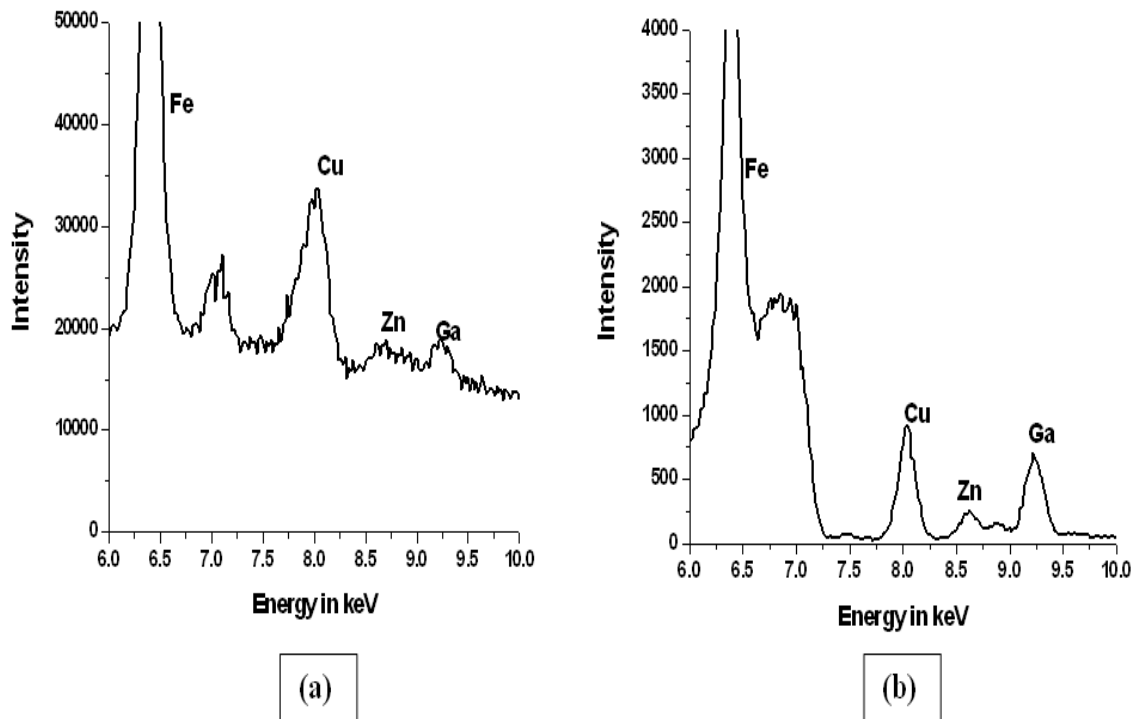


Figure 2.29: EDXRF spectra of Cu and Ga (a) without Fe filter and (b) with Fe filter

Use of high resolution solid state semiconductor detectors was a real breakthrough in this spectrometry. These detection systems directly measure the energies of the X-rays using multichannel analyser (MCA) and semiconductor detectors, with no physical discrimination of the secondary radiation that leaves the sample and enters the detector. This makes EDXRF a simple and fast technique compared to WDXRF. Further in EDXRF, as the detector can be placed very close to the sample, great economy on the intensity of the emitted secondary X-rays from the sample is obtained. This increased sensitivity enables the use of low power X-ray tubes and radioactive isotopes for excitation.

Qualitative analysis in EDXRF is very simple with semiconductor detectors and MCA, where the whole spectrum is accumulated and displayed simultaneously. But qualitative analysis is not as simple as in TXRF due to severe matrix effect. The matrix consists of the entire specimen except the analyte under consideration. The matrix effect also known as absorption-enhancement effect, arises due to preferential absorption or transmission of the primary beam or the emitted secondary beam by the matrix. Sometimes the matrix itself may emit its own characteristic X-rays which may excite the analyte in the matrix. Figure 2.32 shows the mutual absorption-enhancement effects of aluminum and silicon on each other. Ideally, the calibration plot should correspond to the dotted line in the Figure. But this rarely occurs. In a sample containing mixed oxide of aluminum and silicon, $\text{SiK}\alpha$ is strongly absorbed by aluminum. This is because the absorption edge of aluminum (1.569 keV) is just below $\text{SiK}\alpha$ (1.740 keV). Hence the intensity of aluminum will be more and the intensity of silicon will less than the expected intensities. Depending on the matrix (heavy, medium or light), the analyte line intensity varies. Therefore matrix matched calibration standards are must for any EDXRF determination. The intensity data are then converted to analytical concentrations by use of calibration curves and mathematical equations. But availability of matrix matched standards is always not easy. Other X-ray spectrometric analytical methods of absorption-enhancement effect reduction are:

- (i) Standard addition method
- (ii) Thin – film method
- (iii) Matrix dilution method
- (iv) Internal standardization method
- (v) Mathematical correction

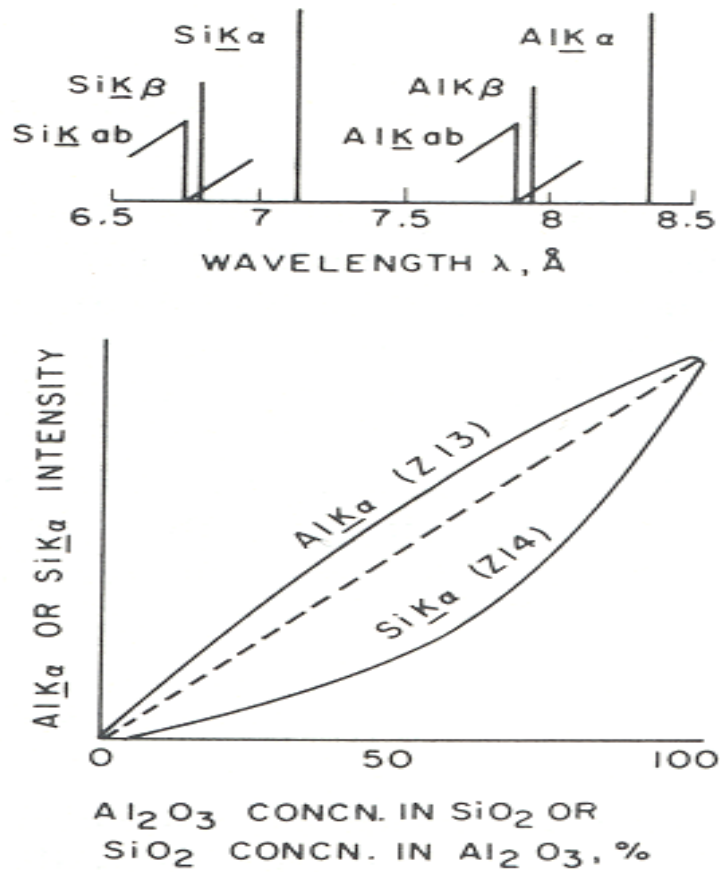


Figure 2.30: Absorption-enhancement effect of aluminum and silicon on each other

In the thin film method, the specimens prepared are so thin that absorption-enhancement effects substantially disappear. In internal standardization method which is a comparative method, an internal standard element is added to all the specimens. This standard is chosen in such a way that absorption-enhancement effects are similar to those of the analyte in the matrix. The calibration plot involves the intensity ratio of the analyte and internal standard X-ray lines. In this way the matrix effect gets nullified on taking the ratio.

2.9. Spectrometers Used in the Present Work

2.9.1. ITAL STRUCTURES TX-2000

In the present studies, an ITAL STRUCTURES TXRF spectrometer TX-2000 was used. This spectrometer can be operated in total reflection as well as conventional XRF i.e. 45°/45° geometry. The spectrometer is equipped to use single or dual target X-ray tubes for excitation. In this spectrometer, Mo-W dual target tube with 3 kW power was used for some experiments. Such dual target tubes can be tuned to allow Mo K α , W L α and W L β beam to fall on sample for excitation without changing the X-ray tube. Mo K α can efficiently excite medium and high atomic number elements K and L lines and W L α/β can excite K lines of low Z elements. These high power X-ray tubes require cooling and hence need a chiller. The primary X-ray spectrum from the X-ray tube consists of the characteristic as well as continuum lines. A W-C multilayer with $2d = 49.4 \text{ \AA}$ is used to monochromatize the incident radiation emitted from the X-ray tube so that a particular energy band can be used for sample excitation. The spectrometer is usually operated at voltage and current of 40 kV and 30 mA, respectively. The sample chamber consists of twelve sample positions. So twelve samples can be loaded simultaneously and measured sequentially. Quartz sample supports of 30 mm diameter and 3 mm thickness were used as sample carriers. The characteristic X-rays emitted from the sample were detected with a Si(Li) detector having a resolution of 139 eV (FWHM) at 5.9 keV (Mn K α). The X-ray spectra were acquired and processed by computer programs TXRFACQ-32 and EDXRF-32, respectively, provided with the instrument. EDXRF32 is an XRF spectra evaluation and quantitative analysis program for both total reflection and traditional XRF geometry. The program EDXRF32 analyses the TXRF spectra by nonlinear least-squares fitting based on the Marquardt algorithm. The position and the intensity of each line required for least squares fitting is read from a database. The elements are determined by means of the total areas of their characteristic X-ray lines and the instrumental calibration by means of standard solutions with known certified elemental concentrations. The ITAL STRUCTURES TX-2000 TXRF spectrometer used in the present studies is shown in Figure 2.28.



(a)



(b)

Figure 2.31: a) ITAL STRUCTURES TX-2000 TXRF spectrometer and b) the inside view of the spectrometer

2.9.2. WOBISTRAX

The determination of low atomic number (Z) elements is important for characterization of technologically important materials. Unfortunately there are not many analytical methods available for rapid and multi-elemental analysis of low Z elements with atomic number <13 (e.g. C, N, O.....Al, etc.) at trace level. In XRF, analysis of low Z elements is difficult because of very low fluorescence yield of these elements, very low characteristic X-ray energies and high attenuation of these X-rays in the spectrometer components as well as by air. Hence one of the suitable methods of determination of low Z elements by XRF is use of vacuum chamber. The measurement under vacuum conditions helps to reduce the air scattering and improves the background conditions. It also reduces the absorption of low energy radiation in air and hence allows the extension of the detectable element range to low Z elements as well as removes the Ar K lines from the spectrum. Table

2.8 gives the characteristic X-ray energies and the fluorescence yields of some low Z elements. The above described ITAL STRUCTURES TX-2000 TXRF spectrometer used in our laboratory is less sensitive for the determination of low atomic number elements below Z=13 at trace levels. A vacuum chamber TXRF spectrometer WOBISTRAX, developed by Atominstytut, Vienna was used for the determination of low Z elements. This spectrometer utilizes chromium X-ray tube for sample excitation. The monochromatic Cr K α X-rays were obtained using a W-C multilayer. The instrument is equipped with a twelve position sample chamber for sequential measurement of the samples. A Peltier cooled, KETEK silicon drift detector of 10 mm² active area, with ultra thin kapton window and electron trap around the window was used for detection and measurement of the X-ray intensities. All the measurements were made under a vacuum of 10⁻² mbar. Also the distance between the source- sample- detector was reduced in this spectrometer to decrease the attenuation of the characteristic X-rays. The TXRF spectra were processed using the AXIL program from IAEA, Vienna. Figure 2.29 shows the view of the WOBISTRAX spectrometer used in the present studies for the determination of low Z elements such as sodium, magnesium and aluminum in uranium matrix.

Table 2.9: Characteristic X-ray energy and the fluorescence yield of low Z elements

Atomic Number	Element	Characteristic X-Ray Energies (keV)	Fluorescence Yield (ω)
6	C	0.283	0.0009
7	N	0.399	0.0015
8	O	0.531	0.0022
10	Ne	0.874	0.0100
11	Na	1.08	0.0200
12	Mg	1.303	0.0300
13	Al	1.599	0.0400



(a)



(b)

Figure 2.32: a) View of WOBISTRAX TXRF spectrometer and b) sample chamber with 12 position sample holder

2.9.3. Jordan Valley EX-3600 TEC

The EDXRF spectrometer used in the present study was Jordan Valley EX-3600TEC. This spectrometer uses sealed low power rhodium target X-ray tube of 50 W and is air cooled. It is usually operated at 40 kV and the current is varied according to the detector dead time which is usually kept below 30%. The excitation beam is collimated to form a spot of about 8 mm in diameter at the center of the specimen area. The sample chamber unit consists of 10 positions to hold the sample supports which moves with the help of motors to reset the sample position. The system is equipped with various primary beam filters (Ti, Fe,

Cu, Mo, W and Rh) and three secondary target elements (Al, Ge and Gd). The spectrometer uses a Peltier cooled ($< -35\text{ }^{\circ}\text{C}$) semiconductor premium Silicon PIN diode detector with a resolution of $(150\pm 10)\text{ eV}$ (FWHM) at 5.9 keV. The data processing is done using the computer program, nEXt, provided with the instrument. Figure 2.33 shows the (a) full picture of the Jordan Valley spectrometer and (b) the sample chamber. The X-ray tube and detector are below the sample holder and the distance between source-sample-detector is very less. This spectrometer is very compact with no chiller for cooling the X-ray tube and no liquid nitrogen for cooling the detector.



(a)



(b)

Figure 2.33: (a) Jordan Valley Ex-3600 TEC EDXRF spectrometer (b) sample chamber

2.10. References

1. W.C. Roentgen, On a new kind of ray, *Ann. Phys.Chem.*, 64 (1898) 1.
2. E.A. Bertin, *Principle and practice of X-Ray spectrometric analysis*, 2nd Edition, Plenum Press, New York, 1984.
3. Ron Jenkins, X-ray techniques: Overview, *Encyclopedia of analytical chemistry* R.A. Meyers (Ed.), John Wiley & Sons Ltd, Chichester, (2000) 13269–13288.
4. *X-ray Characterization of materials*, Eric Lifshin (ed.), Wiley- VCH Verlag GmbH, Federal Republic of Germany, 1999.
5. Åke Kvik, Materials science applications of X-Ray diffraction, *Encyclopedia of Spectroscopy and Spectrometry*, (2009) 1470-1478.
6. B.D. Cullity, *Elements of X-ray diffraction*, Addison-Wesley publishing company, Inc., 1956.
7. *X-Ray adsorption, principles, applications, techniques of EXAFS, SEXAFS and XANES*, D.C. Koningsberger, R. Prins (ed.), Vol. 92 John Wiley and Sons, A Wiley- Interscience publication, 1988.
8. J. B. Metson, S. J. Hay, H. J. Trodahl, B. Ruck, Y. Hu , The use of the X-Ray absorption near edge spectrum in material characterization, *Curr. Appl. Phys.*, 4 (2004) 233.
9. R. E. Van Grieken, A. A. Markowicz, *Handbook of X-Ray spectrometry* (2nd edition) Marcel Dekker Inc., New York (1993).
10. Pedro A.P. Nascente, Material characterization by X-Ray photoelectron spectroscopy, *J. Mol. Catal. A: Chem.*, 228 (2005) 145.
11. B. K. Tanner, D. K. Bowen, *Advanced X-Ray scattering techniques for the characterization of semiconducting materials*, *J. Cryst. Growth*, 126 (1993) 1.
12. N.V. Gelfond, F.V. Tuzikov, I.K. Igumenov, Effect of the deposition temperature on the iridium film microstructure produced by metal-organic chemical vapour deposition: sample characterization using X-ray techniques, *Thin Solid Films*, 227 (1993)144.
13. N. I. Plusnin, Application of AES and EELS for surface/interface characterization, *J. Electron Spectrosc. Relat. Phenom.*, 137 (2004) 161.
14. Y. Travaly, J. Schuhmacher, A. Martin Hoyas, T. Abell, V. Sutcliffe, A.M. Jonas, M. Van Hove, K. Maex, Characterization of atomic layer deposited nanoscale structure on dense dielectric substrates by X-ray reflectivity, *Microelectron. Eng.*, 82 (2005) 639.
15. H.G.J. Moseley, High frequency spectra of elements, *Phil. Mag.*, 26 (1913) 1024.

16. Boron in glass determination using WDXRF, Alexander Seyfarth, JCPDS-International Centre for Diffraction Data 2008 ISSN 1097-0002 269.
17. K. Baur, S. Brennan, B. Burrow, D. Werho, P. Pianetta, Laboratory and synchrotron radiation total-reflection X-ray fluorescence: new perspectives in detection limits and data analysis, *Spectrochim. Acta, Part B*, 56 (2001) 2049.
18. Minemasa Hida, Toshiyuki Mitsui, Yukio Minami, Forensic investigation of counterfeit coins, *Forensic Sci. Int.*, 89 (1997) 21.
19. J.T. Hutton, S.M. Elliott, An accurate XRF method for the analysis of geochemical exploration samples for major and trace elements using one glass disc, *Chem. Geol.*, 29 (1980) 1.
20. Dennis J. Kalnicky, Raj Singhvi, Field portable XRF analysis of environmental samples, *J. Hazard. Mater.*, 83 (2001) 93.
21. S. Canepari, C. Perrino, M.L. Astolfi, M. Catrambone, D. Perret, Determination of soluble ions and elements in ambient air suspended particulate matter: Inter-technique comparison of XRF, IC and ICP for sample-by-sample quality control, *Talanta*, 77 (2009) 1821.
22. Glenn. F. Knoll, *Radiation detection and measurement*, 3rd edition, John Wiley and Sons, Inc., 2000.
23. V. Valkovic, A. Markowicz and N. Haselberger, Review of recent applications of radioisotope excited X-Ray fluorescence, *X-Ray spectrom.*, 22 (1993) 199.
24. A. Iida, K. Sakurai, T. Matsushita, Y. Gohshi, Energy dispersive X-ray fluorescence analysis with synchrotron radiation, *Nucl. Instrum. Methods Phys. Res., Sect. A*, 228 (1985) 556.
25. W. D. Coolidge, A powerful roentgen ray tube with a pure electron discharge, *Phys. Rev.*, 2 (1913) 409.
26. R. T. Beatty, Energy of roentgen rays, *Proc. Soc. (London) A*, 89 (1913) 314.
27. A. Jönsson, Study of intensities of soft X-Rays and their dependence on potential, *Z. Phys.*, 43 (1927) 845.
28. Z. Szökefalvi-Nagy, I. Demeter, A. Kocsonya, I. Kovács, Non-destructive XRF analysis of paintings, *Nucl. Instrum. Methods Phys. Res., Sect. B*, 226 (2004) 53.
29. F. Meirer, A. Singh, P. Pianetta, G. Pepponi, F. Meirer, C. Strelt, T. Homma, Synchrotron radiation-induced total reflection X-Ray fluorescence analysis, *TrAC Trends Anal. Chem.*, 29 (2010) 479.

30. R. J. Cernik, P. Barnes, Industrial aspects of synchrotron X-Ray powder diffraction, *Radiat. Phys. Chem.*, 45 (1995) 445.
31. J. L. Duane, F. L. Hunt, X-Ray wave-lengths, *Phys. Rev.*, 6 (1915) 166.
32. Utz Kramar, X-Ray fluorescence spectrometers, *Encyclopedia of spectroscopy and spectrometry*, (2009) 2989.
33. N. Haselberger, A. Markowicz and V. Valkovic, Comparison of thermoelectrically cooled and conventional Si(Li) X-Ray detectors, *Appl. Radiat. Isot.*, 47 (1996) 455.
34. V.R.K. Murty, K.R.S. Devan, On the suitability of Peltier cooled Si-PIN detectors in transmission experiments, *Radiat. Phys. Chem.*, 61 (2001) 495.
35. C. Strelci, P. Wobrauschek, I. Schraik, Comparison of Si(Li) detector and silicon drift detector for the determination of low Z elements in total reflection X-Ray fluorescence *Spectrochim. Acta, Part B*, 59 (2004) 1211.
36. A.H. Compton, The total reflection of X-Rays, *Philos. Mag.*, [6] 45 (1923) 1121.
37. H. Yoneda, T. Huriuchi, Optical flats for use in X-Ray spectrochemical microanalysis, *Rev. Sci. Instrum.*, 42 (1971) 1069.
38. R. Klockenkämper, Total reflection X-Ray fluorescence analysis, Vol. 140, John Wiley & Sons, New York (1996).
39. N. L. Misra, K. D. Singh Mudher, Total reflection X-Ray fluorescence: A technique for trace element analysis in materials, *Prog. Cryst. Growth Charact. Mater.*, 45 (2002) 65.
40. Reinhold Klockenkämper, A. von Bohlen, Total-reflection X-Ray fluorescence moving towards nanoanalysis: A survey, *Spectrochim. Acta, Part B*, 56 (2001) 2005.
41. Alex von Bohlen, Total reflection X-ray fluorescence and grazing incidence X-Ray spectrometry — Tools for micro- and surface analysis- A review, *Spectrochim. Acta, Part B*, 64 (2009) 821.
42. Yoshihiro Mori, Kenichi Uemura, Kengo Shimano, A depth profile fitting model for a commercial total reflection X-Ray fluorescence spectrometer, *Spectrochim. Acta, Part B*, 52 (1997) 823.
43. J. Knoth, A. Prange, U. Reus, H. Schwenke, A formula for the background in TXRF as a function of the incidence angle and substrate material, *Spectrochim. Acta, Part B*, 54 (1999) 1513.
44. F. Esaka, K. Watanabe, T. Onodera, T. Taguchi, M. Magara, S. Usuda, The use of Si carriers for aerosol particle collection and subsequent elemental analysis by total-reflection X-Ray fluorescence spectrometry, *Spectrochim. Acta, Part B*, 58 (2003) 2145.

45. A. Prange, K. Kramer, U. Reus, Boron nitride sample carriers for total-reflection X-Ray fluorescence, *Spectrochim. Acta, Part B*, 48 (1993) 153.
46. M. Theisen, R. Niessner, Sapphire sample carriers for silicon determination by total-reflection X-Ray fluorescence analysis, *Spectrochim. Acta Part B*, 54 (1999) 1839.
47. A. Prange, H. Schwenke, Trace element analysis using total-reflection X-Ray fluorescence spectrometry, *Adv. X-ray Spectrom.*, 35B (1992) 899.
48. J. Knoth, A. Prange, H. Schwenke, A. Schwenke, Variable X-Ray excitation for total reflection X-ray fluorescence spectrometry using an Mo/W alloy anode and a tunable double multilayer monochromator, *Spectrochim. Acta, Part B*, 52(1997) 907.
49. N.L. Misra, K.D. Singh Mudher, V.C. Adya, B. Rajeswari, V. Venugopal, Determination of trace elements in uranium oxide by total reflection X-Ray fluorescence spectrometry, *Spectrochim. Acta, Part B*, 60 (2005) 834.
50. Liqiang Luo David R. Chettle, Huiling Nie, Fiona E. McNeill, Marija Popovic, The effect of filters and collimators on Compton scatter and Pb K-series peaks in XRF bone lead analysis, *Nucl. Instrum. Methods Phys. Res., Sect. B*, 263 (2007) 258.
51. Hiroyuki Ida, Jun Kawai, An X-Ray fluorescence spectrometer with a pyroelectric X-Ray generator and a secondary target for the determination of Cr in steel, *Spectrochim. Acta, Part B*, 60 (2005) 89.

Chapter-3

ANALYTICAL CHARACTERIZATION OF NUCLEAR MATERIALS BY TXRF: TRACE METALLIC DETERMINATIONS

- 3.1. Introduction
- 3.2. Trace Element Determination in Thorium Oxide Using TXRF
 - 3.2.1. Experimental
 - 3.2.1a. *Sample preparation*
 - 3.2.1b. *Instrumentation*
 - 3.2.2. Results and discussion
- 3.3. Determination of Low Atomic Number Elements at Trace Levels in Uranium Matrix Using Vacuum Chamber TXRF
 - 3.3.1. Experimental
 - 3.3.1a. *Sample preparation*
 - 3.3.1b. *Instrumentation*
 - 3.3.2. Results and discussion
- 3.4. Conclusions
- 3.5. References

3.1. Introduction

Measurements based on analytical chemistry are important to almost every aspect of life. These applications cover an enormous range of concentrations, starting from percentage level to below parts per trillion. Among these, trace and ultra trace analysis plays a key role in many areas of science. In semiconductor industries, the process materials need to be extremely pure to avoid changes in conductivity [1-2]. Presence of trace elements as impurities can affect the chemical and physical properties, economic value and applications, of chemicals and metals of very high purity [3-4]. Similarly, in environmental samples, trace analysis is required for bio-monitoring the level of pollutants in the atmosphere, water and soil [5]. In nuclear industry, determination of trace and ultra trace elements is an important step with respect to quality control and quality assurance of materials having technological importance [6].

Chemical characterization of nuclear materials for the trace constituents is necessary to ensure that the quality of fuel fabricated is in agreement with the chemical specifications for the fuel. Nuclear reactor design incorporates detailed specifications of the impurities in fuel materials which should be satisfied for the smooth and efficient functioning of the reactors. These specifications differ according to the nature of reactor, material used and their applications (research/power). The Indian program of nuclear energy is designed in such a way that, along with utilization of uranium and plutonium as nuclear fuels, a large emphasis is laid on the use of thorium, as India has the largest thorium reserves of the world. The uranium, thorium and plutonium required for such applications have to undergo stringent quality control. Various forms of fuels used in different nuclear reactors are oxides, metals, alloys and advanced fuels like carbides and nitrides. The amount of trace elements, in particular metallic impurities, which get incorporated in nuclear fuel during various fuel fabrication operations like mining, dissolution, separation, pelletization, etc., can affect the working of the reactors adversely. Hence, the concentrations of these trace impurities in nuclear fuel materials must be below the specification limits and these impurities must be determined by suitable analytical methods.

Another important application of analytical characterization of technologically important materials with respect to their trace constituents, is to develop Certified Reference Standards (CRMs) or Standard Reference Materials (SRMs). These materials are very much essential for the calibration and validation of analytical methods as most of the instrumentation methods are comparative. These standards are also required for quality control and quality assurance of

various technologically important materials. Any discrepancy in the reference standard value can lead to poor accuracy of the analytical results. Generally, CRM/SRM are available commercially for materials like food products, cement, oil, drinking water, alloys and metals used in industries [7-9]. They can be easily procured and used. But unfortunately, CRMs for nuclear materials are not commonly available and their procurement is also very difficult. Hence, it is required to develop indigenous standards for nuclear materials. In order to develop any such standards, Inter- Laboratory Comparison Experiment (ILCE), involving participation of large number of laboratories using different analytical methods having different physico-chemical properties, is conducted [10-11]. The analytical results obtained from various laboratories are compiled and certified values are assigned for different elements.

Different analytical techniques are available for the determination of trace metallic impurities in nuclear fuel materials [6,12-13]. Total reflection X-ray fluorescence (TXRF) is a well established technique for determining impurities present at trace and ultra-trace levels in different materials [14-16]. Applicability of TXRF for trace element analysis depends on two features of total reflection of X-rays: High reflectivity and low penetration depth of the primary radiation. These characteristics allow TXRF to be used for both trace and ultra trace elemental analysis as well as for surface analysis. Though many techniques such as ICP-MS, ICP-AES, AAS, NAA, XRF and a variety of electroanalytical methods are available for trace and ultratrace analysis of elements in various matrices, TXRF has quite a few advantages over the other techniques. It has simple instrumentation (in comparison to ICP and NAA), spectral line interferences are minimum (in comparison to AAS and AES), has got a wide specimen versatility (in comparison to ICP and electroanalytical methods which require sample dissolution, samples in the form of suspensions can also be analysed in TXRF), no matrix effect and memory effects (in comparison to classical XRF and ICP techniques), requires a few microgram or microliter amount of sample, can analyse metals and nonmetals alike and can be used for both trace and bulk analysis. All these features of TXRF are well suited for the determination of trace elements in nuclear samples. But only a few such applications of TXRF for nuclear materials have been reported in literature [17-19]. In the last few years, its applicability for trace element determinations in nuclear materials has been demonstrated in uranium matrix using synchrotron radiation induced and laboratory source TXRF [18, 19]. In TXRF, sample preparation is also very simple compared to other techniques. In aqueous

samples, trace elements can be determined directly or by physically pre-concentrating the sample by evaporation depending on the nature of matrix. But if the matrix is such that it contains heavy elements, then matrix separation is mandatory for the following reasons: Firstly, one of the constraints of TXRF analysis is that the thickness of sample deposited should not be more than a few nanogram and the total matrix amount must be less than 10-50 ng (depending on the nature of matrix) in order to avoid matrix effects. In such low amount of matrix, the analyte transferred on the sample support is sometimes below the detection limits of TXRF. Due to this constrain, the major matrix has to be selectively separated from concentrated solution. Secondly, the separation of major matrix, which normally contains uranium, thorium or plutonium in case of nuclear fuel materials, helps in avoiding the absorption of the characteristic X-ray lines of trace analyte by the heavy elements and thirdly, separation of the major matrix reduces the background caused by scattering of the X-rays by the matrix during TXRF measurements. Various matrix separation techniques such as solvent extraction, pyrohydrolysis, chromatographic adsorption, solid phase extraction, etc., are available. The most common procedures employed for the separation of major matrix of uranium, thorium and plutonium after sample dissolution are solvent extraction and ion exchange separations. Solvent extraction for the separation of uranium and thorium using n-tri-butyl phosphate (TBP) as the extractant is a well established method [12].

In this Chapter, development of TXRF method for trace metallic determinations in nuclear fuel materials (thorium and uranium) is described. The sample preparation involves separation of the major element in the matrix by solvent extraction using TBP as the extractant and determination of the trace elements in the aqueous phase by TXRF.

3.2. Trace Element Determination in Thorium Oxide Using TXRF

The Indian Nuclear Energy Program envisages the maximum utilization of thorium because of its limited reserves of uranium and large availability of thorium. Thorium is estimated to be about three to four times more abundant than uranium in the earth crust. Though ^{232}Th is not a fissile material, it is utilized as a breeder to produce ^{233}U , which is an excellent fissile material. Thorium is also used for neutron flux flattening in PHWRs and as a blanket material in fast breeder reactors. It is also proposed to be used as a fuel in the third stage of Indian Nuclear Power Program i.e. AHWRs [20]. Another major application of thorium based fuel is in the

Compact High Temperature Reactors (CHTRs) which shall utilise ^{233}U -Th fuel. Apart from nuclear industry, because of its low work-function and high electron emission, thorium is used to coat tungsten wire used in electronic equipment. Glasses containing thorium oxide have a high refractive index and low dispersion. Consequently, they find applications in high quality lenses for cameras and scientific instruments. Thorium required for such applications as well as for its use in reactor has to undergo stringent quality control. Different analytical techniques such as ICP-AES, GFAAS, MS, etc. are available for trace element determinations in thorium after separation of the major matrix [12, 21-22]. TXRF has good potential for such analysis. But, before TXRF can be used on routine basis for trace element analysis in thorium oxide, the method should be first counter checked for its applicability using certified reference materials.

In the following Section, development of a TXRF method for trace metals analysis in thorium oxide standard after its dissolution in HNO_3/HF mixture followed by separation of thorium by solvent extraction is reported. The analytical results obtained by TXRF have been compared with the certified reference values of the elemental concentrations present in thorium oxide standards. The analytical results of different techniques such as ICP-AES, ICP-MS and AAS have been compared with the TXRF determined values.

3.2.1. Experimental

3.2.1a. Sample preparation

The reagents used e.g. tri butyl phosphate (TBP), tri-n-octyl phosphine oxide (TOPO), carbon tetrachloride (CCl_4) and hydrofluoric acid (HF) were of analytical reagent (AR) grade and HNO_3 was of suprapure grade. Merck single element standard of gallium was used as internal standard. All glasswares used for the sample preparation process were made of quartz. High quality PVC vials were used for sample storage. Milli-Q water was used for sample preparation and cleaning purposes. Four ThO_2 samples namely $\text{ThO}_2\text{-B}$, $\text{ThO}_2\text{-D}$, $\text{ThO}_2\text{-S}$ and $(\text{Th,U})\text{O}_2\text{-MOS}$ prepared by the Department of Atomic Energy, to be developed as certified standard materials, were analyzed for their trace element contents.

Weighed quantities of ThO_2 powder equivalent to 2.5 g of thorium were taken in 100 mL capacity high purity platinum dish. Approximately 10 mL of conc. HNO_3 was added to the ThO_2 taken in the dish and the resultant mixture was boiled gently on a hot plate. In the boiling mixture, 1.5 mL of 0.5% solution of HF was added to get clear solution. This solution was

evaporated to almost dryness. The residue obtained was dissolved in 3 mL of conc. HNO₃ and evaporated to dryness. This process of dissolution and evaporation was repeated four times so that HF was completely removed. After this, the residue was redissolved in 10 mL of 4 M HNO₃. All these dissolution and evaporation operations were carried out inside a hood connected to suction so that corrosive vapours of fluoride are safely collected in an aqueous medium and not left in the atmosphere. The volumes of the solutions obtained after the dissolution of ThO₂ were made up to 15 mL with 4 M HNO₃. For separation of the major matrix thorium, these solutions were equilibrated four times with equal volume of 40% solution of TBP in CCl₄ and later equilibrated two times with 0.2 M TOPO in CCl₄. The major matrix containing thorium was extracted in the organic phase and the aqueous portion containing the trace metallic impurities was carefully separated and made up to 25 mL with Milli-Q water. Aliquots of 1 mL of the above separated solutions were mixed with 100 µL of gallium (19.6 µg/mL) internal standard in pre-cleaned PVC vials. For TXRF measurements, 10 µL aliquot of these solutions were deposited in duplicate on the quartz sample supports and dried under an IR lamp.

3.2.1b. Instrumentation

The TXRF measurements were performed using an ITAL STRUCTURES TXRF spectrometer (TX-2000). Monochromatic Mo K α radiation having energy of 17.44 keV, obtained from a W-Mo dual target tube and a W/C multilayer monochromator, was used for sample excitation. The applied voltage and current were 40 kV and 30 mA, respectively. A live time of 1000 s was used for recording the TXRF spectra of the samples and standards and a live time of 100 s was set to check the cleanliness of the quartz sample supports. All the measurements were carried out in air atmosphere. The characteristic peaks of the trace elements were recorded using a Si(Li) detector having a resolution of 139 eV FWHM at 5.9 keV.

3.2.2. Results and discussion

The TXRF measurements of processed thorium oxide showed that the major matrix thorium was removed almost completely after solvent extraction. A typical TXRF spectrum of the aqueous portion of ThO₂-MOS is shown in Figure 3.1. The thorium oxide samples used in the present study were having different trace elements with varying concentrations, were latter certified by Department of Atomic Energy (DAE) after conducting an ILCE involving a number

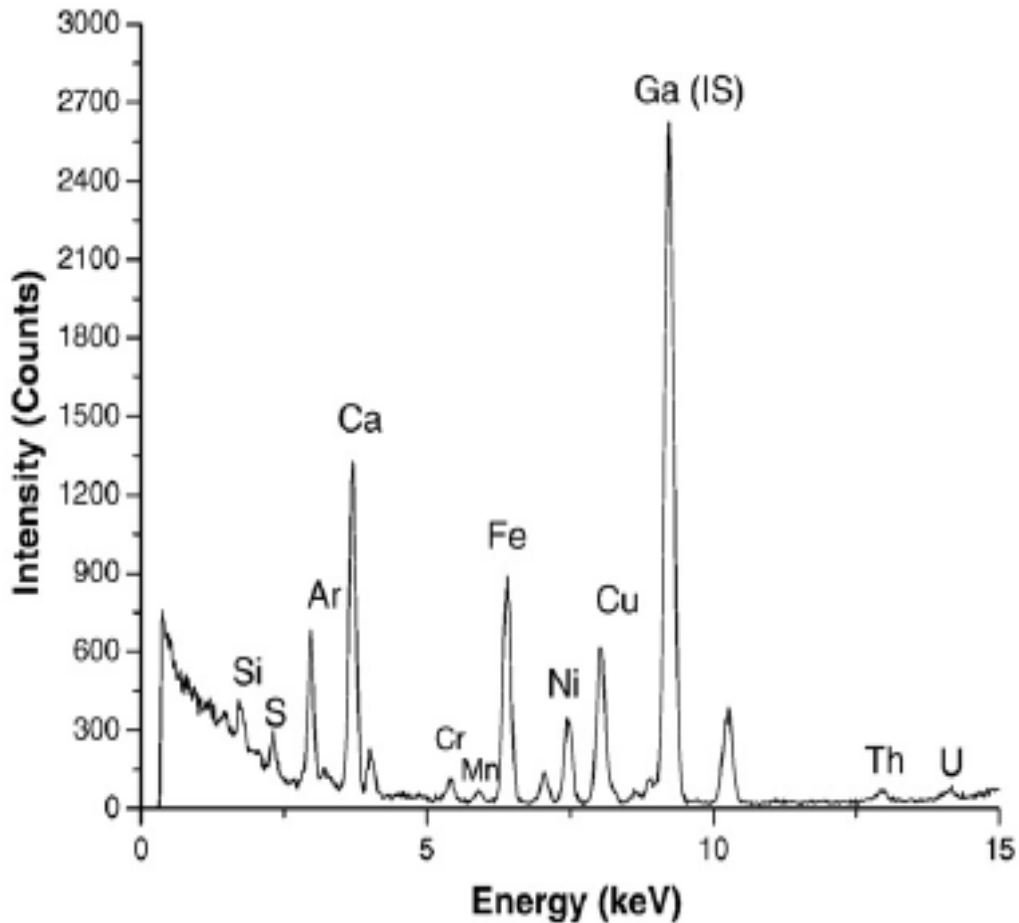


Figure 3.1: A typical TXRF spectrum of a processed thorium oxide (ThO₂-MOS) with gallium internal standard

of laboratories using different techniques. The trace elements certified in these standards were Al, B, Be, Ca, Cd, Ce, Cr, Cu, Dy, Er, Eu, Fe, Gd, Mg, Mn, Mo, Ni, Sb, Sm and V. The certified values were arrived at by considering all the results obtained by different analytical laboratories lying within an uncertainty of 30% (for the elemental concentrations $> 10 \mu\text{g/g}$) and 50% (for the elemental concentrations in the range of $0.1\text{--}10 \mu\text{g/g}$) from the mean of the mean values. Out of the above stated elements, Be and B could not be determined by TXRF because of its limitation for low Z elements. The present TXRF instrumental conditions did not allow the determination of Al and Mg, since $W L\alpha$ excitation source and measurements in vacuum or helium atmosphere would be needed. Although $L\alpha$ lines of Cd, Ce, Dy, Er, Eu, Gd, Mo, Sb and Sm can be detected by TXRF using the present excitation conditions, these elements could not be determined in the present study mainly due to very low concentrations of these elements present in these oxides and relatively lower fluorescence yield of L lines. The rest of the elements Ca, Cr, Cu, Fe, Mn, Ni, and V in ThO_2 were determined by considering the dilution of the matrix and blank corrections. Tables 3.1 and 3.2 give the TXRF determined results of all the four standards and their certified values. The analytical results of the trace elements determined by TXRF differed from the corresponding certified values by $< 20\%$ for most elements where the certified concentration is $> 10 \mu\text{g/g}$ of Th. The average precision of the analytical results were found to be 23%. The TXRF spectrum of the processed samples showed characteristic X-ray lines of some additional elements whose certified concentrations were not available. These additional elements e.g. K, Co, Zn, Sr, Y, Ba and Pb were also determined by TXRF and their analytical results are included in Tables 3.1 and 3.2.

The TXRF determined concentrations of calcium are higher than the certified values in three samples namely $\text{ThO}_2\text{-D}$, $\text{ThO}_2\text{-S}$ and $\text{ThO}_2\text{-MOS}$ (Tables 3.1 and 3.2). This may be due to the presence of calcium in atmospheric aerosol as contaminants. Even a very small contamination of the sample can change the analysis results significantly. In Figure 3.2, a comparison of the TXRF analytical results of calcium in $\text{ThO}_2\text{-S}$ with other laboratories involved is shown. It can be seen that though TXRF determined calcium concentration is higher than the certified calcium concentration, it is within a deviation of 30% from the certified concentration and the average precision is 7% for all the four standards.

Table 3.1: Comparison of TXRF determined elemental concentrations of different elements with the corresponding certified values in thorium oxides ThO₂-B and ThO₂-D

Element	ThO ₂ - B				ThO ₂ - D			
	TX	(σ)	Cer	TX/ Cer	TX	(σ)	Cer	TX/ Cer
Ba	ND	-	NR	-	0.70	1.21	NR	-
Ca	67	7	73	0.92	874	116	586	1.49
Co	0.3	0.4	NR	-	0.6	0.4	NR	-
Cr	4.5	0.6	8.5	0.53	14.6	0.3	13	1.12
Cu	1.9	0.4	3.1	0.61	93	4	110	0.85
Fe	46	8	56	0.82	122	2	134	0.91
K	7.3	0.9	NR	-	2	3	NR	-
Mn	2.4	0.2	3.0	0.80	7	1	7.3	0.96
Ni	7.7	0.6	11	0.70	47	2	57	0.82
Pb	0.5	0.2	NR	-	0.3	0.2	NR	-
Sr	0.28	0.08	NR	-	1.63	0.08	NR	-
V	ND	-	0.2	-	7	2	5.9	1.19
Y	ND	-	NR	-	ND	-	NR	-
Zn	0.7	0.2	NR	-	0.30	0.04	NR	-

σ : Standard deviation (1 s) of TXRF determinations for four measurements.

TX: TXRF determined elemental concentration in $\mu\text{g/g}$ of thorium.

Cer: Certified values of elemental concentration in $\mu\text{g/g}$ of thorium.

ND: Not detected by TXRF.

NR: Not reported in certification.

Table 3.2: Comparison of TXRF determined elemental concentrations of different elements with the corresponding certified values in thorium oxides ThO₂-S and ThO₂-MOS

Element	ThO ₂ - S				ThO ₂ - MOS			
	TX	(σ)	Cer	TX/ Cer	TX	(σ)	Cer	TX/ Cer
Ba	ND	-	NR	-	2.60	4.50	NR	-
Ca	454	8	351	1.29	641	19	479	1.34
Co	1.0	0.4	NR	-	0.3	0.3	NR	-
Cr	6	1	7.3	0.82	14.1	0.8	19.0	0.74
Cu	50	3	63	0.79	50	2	71.0	0.70
Fe	65	6	78	0.83	112.9	1.1	137	0.82
K	ND	-	NR	-	7	3	NR	-
Mn	4.0	0.5	4.3	0.93	4.9	0.2	5.5	0.89
Ni	29	2	32	0.91	25.5	0.9	38	0.67
Pb	ND	-	NR	-	0.3	0.3	NR	-
Sr	0.65	0.05	NR	-	1.4	0.3	NR	-
V	3.1	1.2	3.0	1.03	4.8	0.8	3.3	1.45
Y	ND	-	NR	-	0.3	0.3	NR	-
Zn	1.4	0.1	NR	-	ND	-	NR	-

σ : Standard deviation (1 s) of TXRF determinations for four measurements.

TX: TXRF determined elemental concentration in $\mu\text{g/g}$ of thorium.

Cer: Certified values of elemental concentration in $\mu\text{g/g}$ of thorium.

ND: Not detected by TXRF.

NR: Not reported in certification.

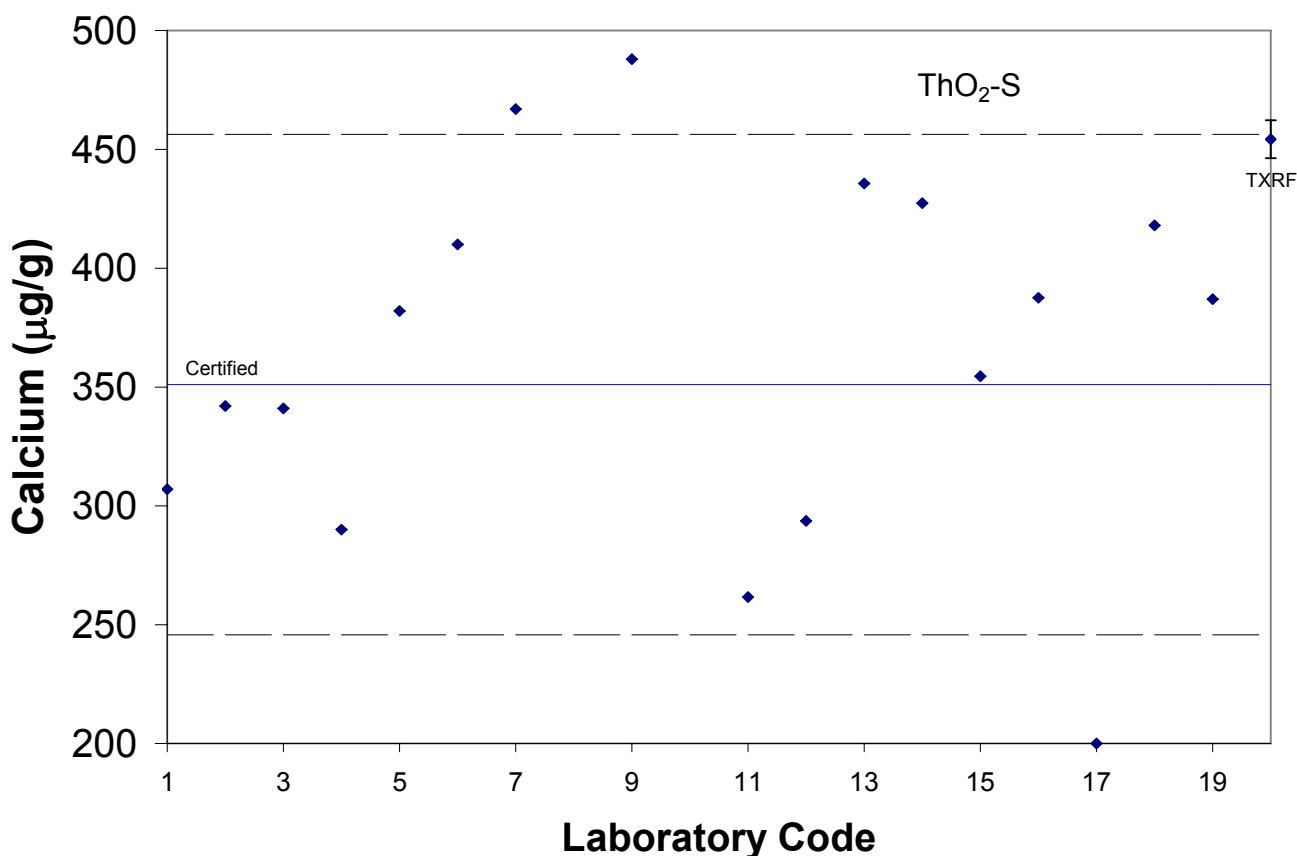


Figure 3.2: A comparison of analytical results of different laboratories with certified and TXRF determined calcium concentration in ThO₂-S

(Error bar represent standard deviation i.e. 1 s obtained in TXRF determinations for four measurements)

The certified concentration of manganese in these samples lies between 3 and 7.3 µg/g. As the concentrations are between 0.1 and 10 µg/g, the requirement for certification of manganese in these samples was that the relative standard deviation (RSD) of different laboratories should be less than 50%. Normally manganese is not present in atmospheric aerosol and hence chances of TXRF samples getting contaminated from the ambient air for manganese are less. A comparison of TXRF determined concentration of manganese in ThO₂-B and that reported by other laboratories is given in Figure 3.3. In this comparison, laboratories 1–16 used Inductively Coupled Plasma-Atomic Emission Spectroscopy (ICP-AES), 17–18 used Inductively Coupled Plasma-Mass Spectrometry (ICP-MS) and 19–21 used Atomic Absorption Spectroscopy (AAS) for trace element determinations. The comparison of TXRF and certified

analytical results for other elements can be seen from Tables 3.1 and 3.2. It can be seen that deviations of TXRF determination results for manganese, in these samples, from the corresponding certified values is 20%. The precision obtained in TXRF determination of manganese is within 15% (1s). These comparisons show the suitability of TXRF for trace elements determinations in thorium oxide. The TXRF method has the prime benefit of requirement of very small amount of sample and multielemental analytical capability. This can be exploited beneficially for the safe and faster analysis of radioactive materials producing smaller waste amounts thereby lesser environmental pollution.

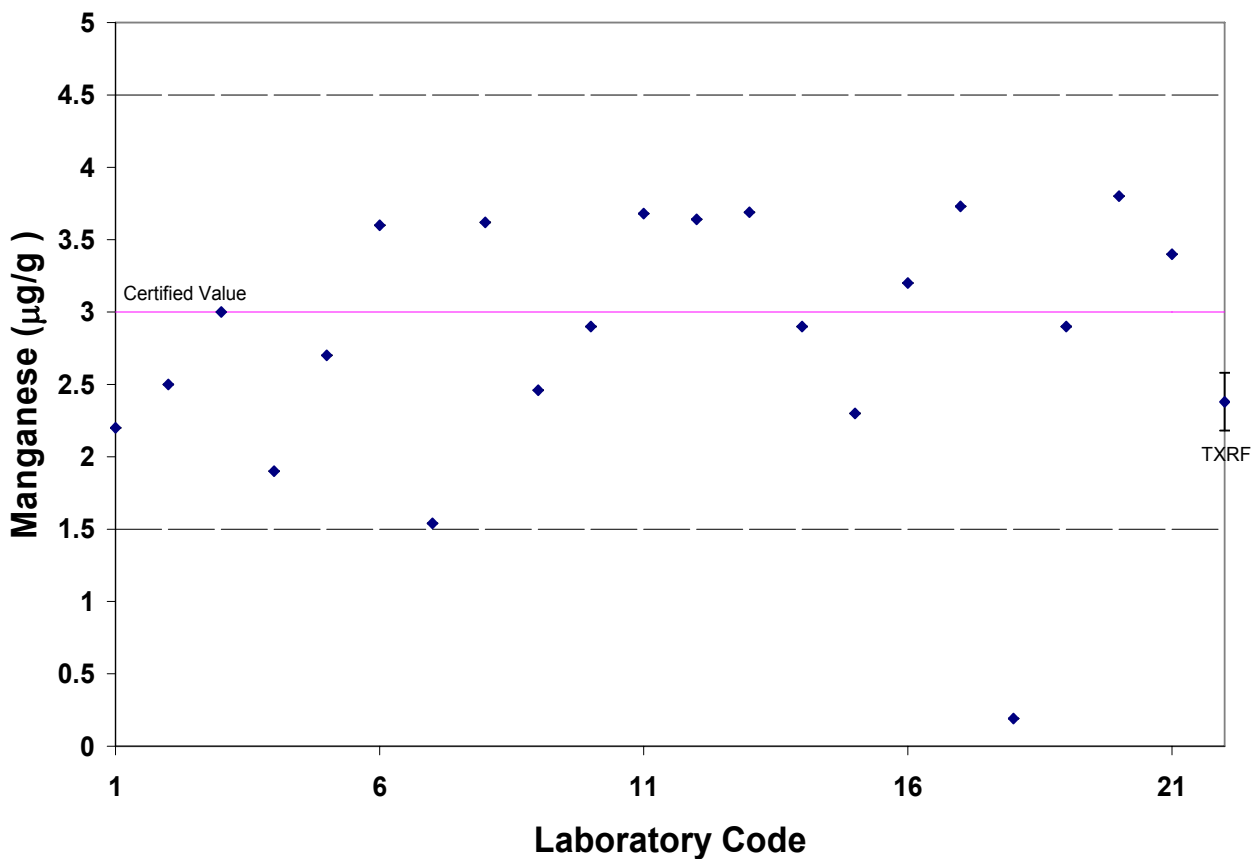


Figure 3.3: A comparison of analytical results of different laboratories with certified and TXRF determined manganese concentration in ThO₂-B

(Error bars represent standard deviation i.e. 1 s obtained in TXRF determinations for four measurements)

3.3. Determination of Low Atomic Number Elements at Trace Levels in Uranium Matrix Using Vacuum Chamber TXRF

The amounts of low atomic number (Z) trace impurities in nuclear fuel should be within specified limits for neutron economy, better fuel density and quality assurance [6, 23-24]. Low Z element boron is a neutron absorber and should not be present in the nuclear fuel as this will absorb neutrons and make the nuclear fission process inefficient [23]. Determination of carbon and nitrogen is important for characterization of advanced carbide and nitride fuels, respectively. Presence of carbon in excess as a trace impurity may cause carburization of cladding materials thereby making them fragile. Oxygen amounts other than the specified values may change the oxygen to metal ratio (O/M) of the oxide fuel leading to changes in thermal conductivity, melting point, diffusion coefficients and vapor pressure [25]. Na, Mg and Al, if present, in uranium oxide fuel in amounts higher than the specified levels, may reduce the relative amount of fissile materials and form appreciable amounts of uranates of these elements having uranium in lower and higher oxidation states in reactor operating and transient conditions. If formation of these uranates is appreciable, it may cause expansion of fuel volume leading to rupture of fuel cladding. Also in accidents involving crack of cladding, uranates with higher valency of uranium may be formed which may lead to fuel expansion, due to their low density, and may propagate further cracking of the clad. Thus determination of low Z elements present at trace and major concentration levels in nuclear fuel is important. A variety of analytical techniques can be employed for the determination of medium and high Z elements but only a few techniques are applicable for the low Z elements ($Z \leq 13$). Trace determination of low Z elements by XRF is challenging because of following reasons [26, 27]:

- i) Low fluorescence yield (ω) and photoelectric mass absorption coefficient (τ/ρ), therefore the emitted intensity from these elements is very low.
- ii) Higher background in the characteristic X-ray energy region and higher absorption of the characteristic X-rays by the spectrometer components and matrix leads to low signal to noise ratio.
- iii) The detector efficiency for detecting low energy X-rays is less. Figure 3.4 shows the plot of efficiency of Si(Li) detector for energies 1-6 keV. The efficiency is low for elements up to Cl (≤ 0.8) and it is almost equal to 1 for Mn [28].

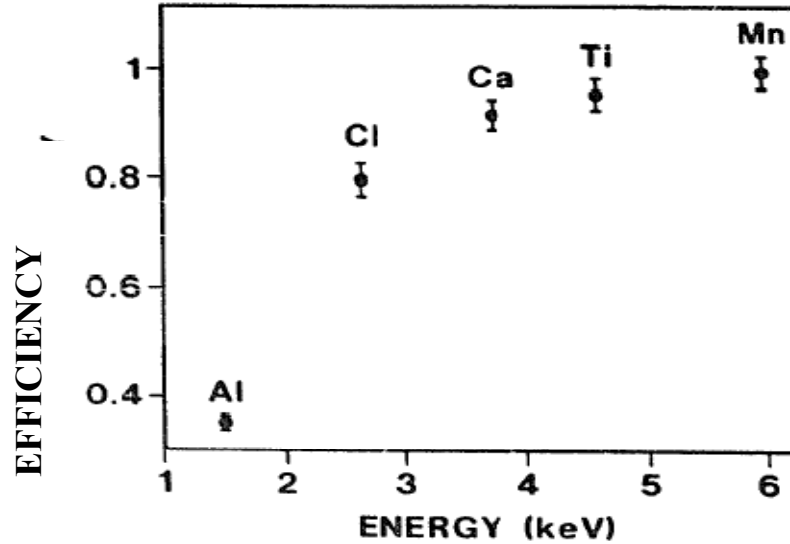


Figure 3.4: Plot of efficiency of a Si(Li) detector versus the X-ray energies of elements ($K\alpha$, in keV)

If efficient excitation sources for low Z elements and the TXRF spectrometer attached with vacuum chamber to minimize the absorption losses, are used then low Z elements at trace levels can be determined by TXRF [29]. The first publication of low Z determination by vacuum chamber TXRF reported the analysis upto oxygen ($Z=8$) [30]. Synchrotron radiation induced TXRF can efficiently excite the low Z characteristic K-line X-rays of elements upto boron and can be used for determination of these elements [31, 32]. However, synchrotron sources are not easily available for routine analysis. The limitations of TXRF spectrometry for low Z elements can be taken care in a special TXRF spectrometer having vacuum chamber and low energy excitation source, though with comparatively higher detection limits than those achievable with synchrotron radiation sources. Since, the specifications of Na, Mg and Al in nuclear fuel materials e.g. UO_2 , ThO_2 , PuO_2 , etc. are comparatively higher than those of other elements and are in $\mu\text{g/g}$ levels, these elements can be determined in such nuclear materials using vacuum chamber TXRF spectrometer. Studies were, therefore, carried out to determine trace levels of Na, Mg and Al in uranium matrix using WOBISTRAX TXRF spectrometer [33, 34] with a Cr target X-ray tube. The major matrix uranium was separated by solvent extraction using TBP prior to the analysis of the trace elements by TXRF.

3.3.1. Experimental

3.3.1a. Sample preparation

The stock solutions of sodium and magnesium were prepared by dissolving high purity NaNO_3 and $\text{MgSO}_4 \cdot 7\text{H}_2\text{O}$ salts of AR grade in 1.5% suprapure HNO_3 in Milli-Q water to get sodium and magnesium concentrations of 375 and 99 $\mu\text{g/mL}$, respectively. Merck single element standard solutions of aluminum and scandium (internal standard) having a concentration of 1000 $\mu\text{g/mL}$ were used after required dilution with 1.5% HNO_3 . These solutions were mixed in different volumes to prepare a calibration solution with Na, Mg, Al and Sc having concentrations of 57, 15, 30 and 13 $\mu\text{g/mL}$, respectively. Ten microliter of this solution was pipetted at the center of three Plexiglas sample supports of 30 mm diameter and 2 mm thickness and left overnight for drying in a class 100 clean bench. After drying, the TXRF spectra of these plexiglas supports were recorded and the relative sensitivities of Na, Mg and Al with respect to Sc were determined using the respective peak areas of $K\alpha$ lines of these elements. Three sample solutions of Na, Mg and Al in uranium matrix were prepared by mixing different volumes of the above stock solutions in nuclear grade uranyl nitrate solution with uranium concentration of 85 mg/mL in such a way that the concentrations of low Z elements Na, Mg and Al were in the range of 100–300 $\mu\text{g/g}$ with respect to uranium and 10–20 $\mu\text{g/mL}$ in the solution as given in Table 3.3. Uranium present in these solutions in major concentration level was separated by solvent extraction using 30% TBP solution in dodecane. The samples were equilibrated thrice with this TBP solution. The organic phase containing uranium obtained after each equilibration was discarded. The aqueous phase containing trace elements obtained after final separation was equilibrated once more with dodecane solution to remove the dissolved TBP and mixed with scandium internal standard as shown in flow chart given in Figure 3.5. Five microliter of each of these solutions obtained from samples-1, 2 and 3 (Table 3.3) was deposited on siliconised Plexiglas sample supports, dried in similar way as the calibration solutions and the TXRF spectra were recorded.

The blanks for different samples were prepared by taking 1.5 % HNO_3 in Milli-Q water instead of Na, Mg and Al solutions in uranyl nitrate solution in the same proportions as used for the preparation of respective sample solutions, processing them in similar manner as the samples, adding scandium internal standard solutions to the aqueous phase obtained after solvent extraction and recording their TXRF spectra.

Table 3.3: Details of preparation of sample solutions for low Z elements

Element	Sample-1			Sample-2			Sample-3		
	Volume taken (μL)	Elemental concentration		Volume taken (μL)	Elemental concentration		Volume taken (μL)	Elemental concentration	
		$\mu\text{g/mL}$	$\mu\text{g / g of uranium}$		$\mu\text{g/mL}$	$\mu\text{g / g of uranium}$		$\mu\text{g/mL}$	$\mu\text{g / g of uranium}$
Na	80	10.3	141	120	14.5	212	180	19.9	318
Mg	300	10.2	140	450	14.3	210	650	19.0	303
Al	30	10.3	141	45	14.4	212	65	19.1	306
U	2500	73024	-	2500	68218	-	2500	62592	-

Concentration of stock solutions used for preparing the samples Na = 375.3 $\mu\text{g/mL}$, Mg = 99 $\mu\text{g/mL}$, Al=1000 $\mu\text{g/mL}$, U=85 mg/mL

3.3.1b. Instrumentation

For TXRF measurements, an Atominsitut Vienna, Austria, vacuum chamber low Z TXRF spectrometer (WOBISTRAX) was used. The spectrometer utilizes Cr $K\alpha$ X-rays for sample excitation. The monochromatic Cr $K\alpha$ X-rays are obtained using a W-C multilayer. A Peltier Cooled, KETEK SDD detector of 10 mm^2 active area, with ultra thin kapton window and electron trap around the window was used for detection and measurement of the X-ray intensities. The TXRF spectra of solution used for calibration of the instrument were recorded for a live time of 1000s whereas those of samples were recorded for a live time of 500s. All the measurements were made under a vacuum of 10^{-2} mbar. The TXRF spectra were processed using the AXIL program from IAEA, Vienna [35].

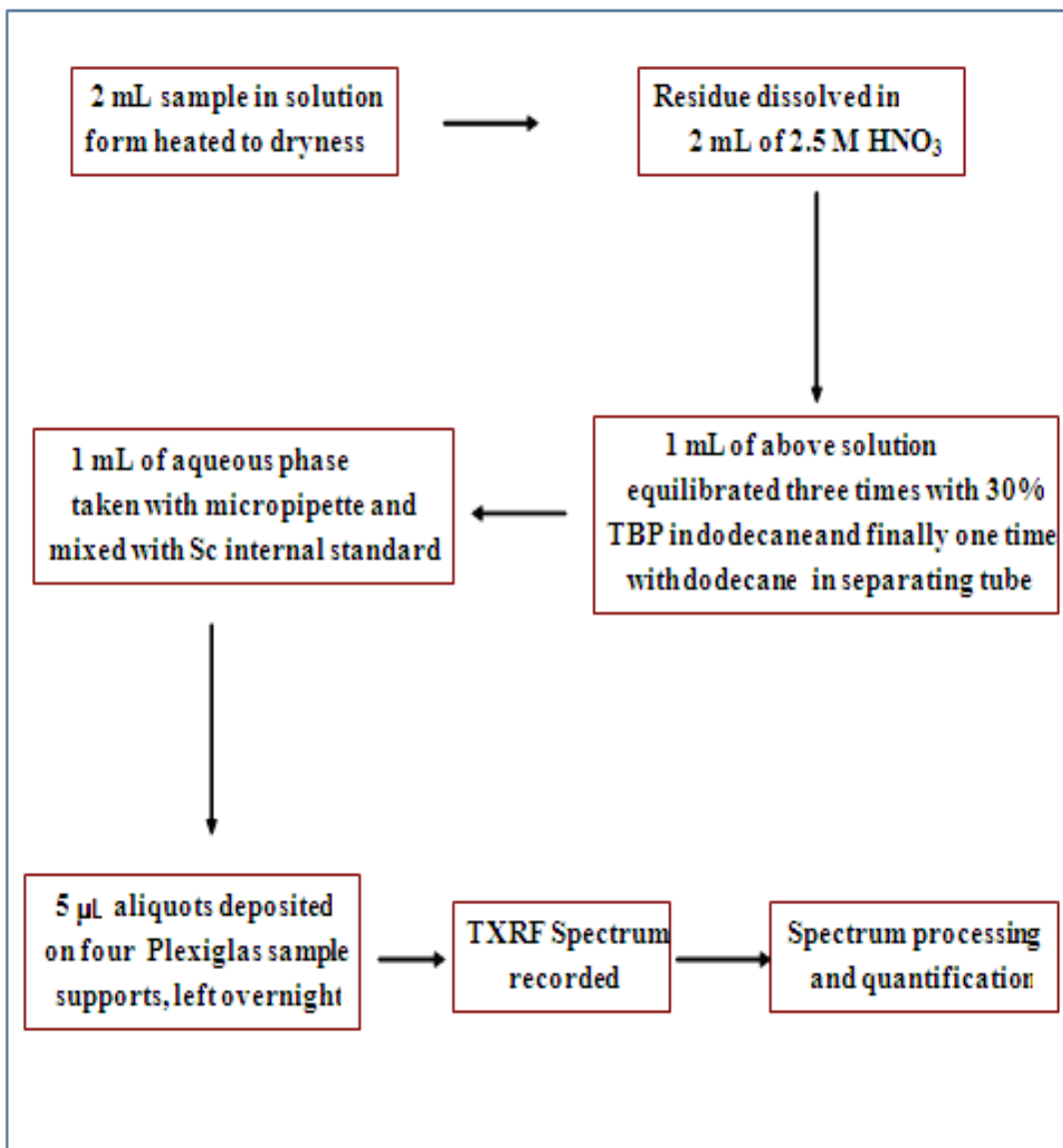


Figure 3.5: Flow chart showing the processing of the sample solutions for the TXRF analysis

3.3.2. Results and discussion

The relative sensitivities of Na, Mg and Al determined with respect to Sc were found to be in increasing order with atomic number showing a trend as shown in Figure 3.6. This increasing trend shows that the TXRF condition is satisfied.

The separation of uranium was accomplished using solvent extraction method optimized for TXRF measurements. In order to avoid any loss of intensity due to thicker and non-uniform samples on plexiglas sample support by heating under IR lamp, especially when the aqueous phase contains a slight amount of organic matter i.e. TBP, because of its partial solubility in nitric acid, the samples were left overnight for self drying on these sample supports in a class 100 clean bench. To keep the background low, only 5 μ L aliquots of the processed samples were deposited on Plexiglas supports. Scandium was used as internal standard as it is not present in samples and can be excited very efficiently (Sc K_{abs} =4.493 keV) with Cr $K\alpha$ (5.414 keV) X-ray source used for sample excitation in the present spectrometer. A representative TXRF spectrum of the aqueous phase of sample-3 mixed with internal standard is shown in Figure 3.7. From this

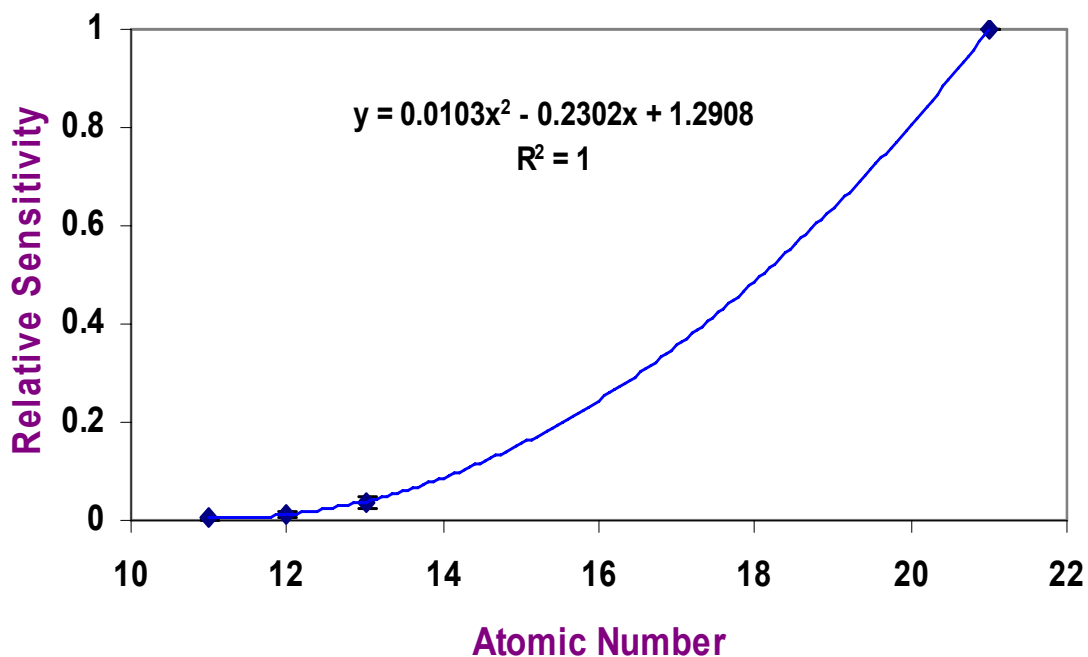


Figure 3.6: Relative sensitivities of sodium, magnesium, aluminum with respect to gallium

spectrum, it can be seen that Na, Mg and Al $K\alpha$ peaks are very clear, though less intense, indicating that the method is promising for TXRF determination of these low Z elements. The intense peaks of $K\alpha$ lines of C (282 eV) and O (523 eV) seen in the spectrum are from TBP and sample supports. A part of the C $K\alpha$ line may be from the detector window also. The peaks of Si $K\alpha$ originating from siliconised plexiglas supports and P $K\alpha$ from TBP are also seen in the spectrum. In addition, the less intense U M lines observed in the spectrum are due to trace amounts of uranium left in the aqueous phase after solvent extraction. Some elements e.g. S from $MgSO_4$, K, etc. are also visible. The $K\alpha$ lines of Na, Mg and Al are visible better in expanded spectrum of the same sample shown in Figure 3.8. For the processing of the spectra, the IAEA

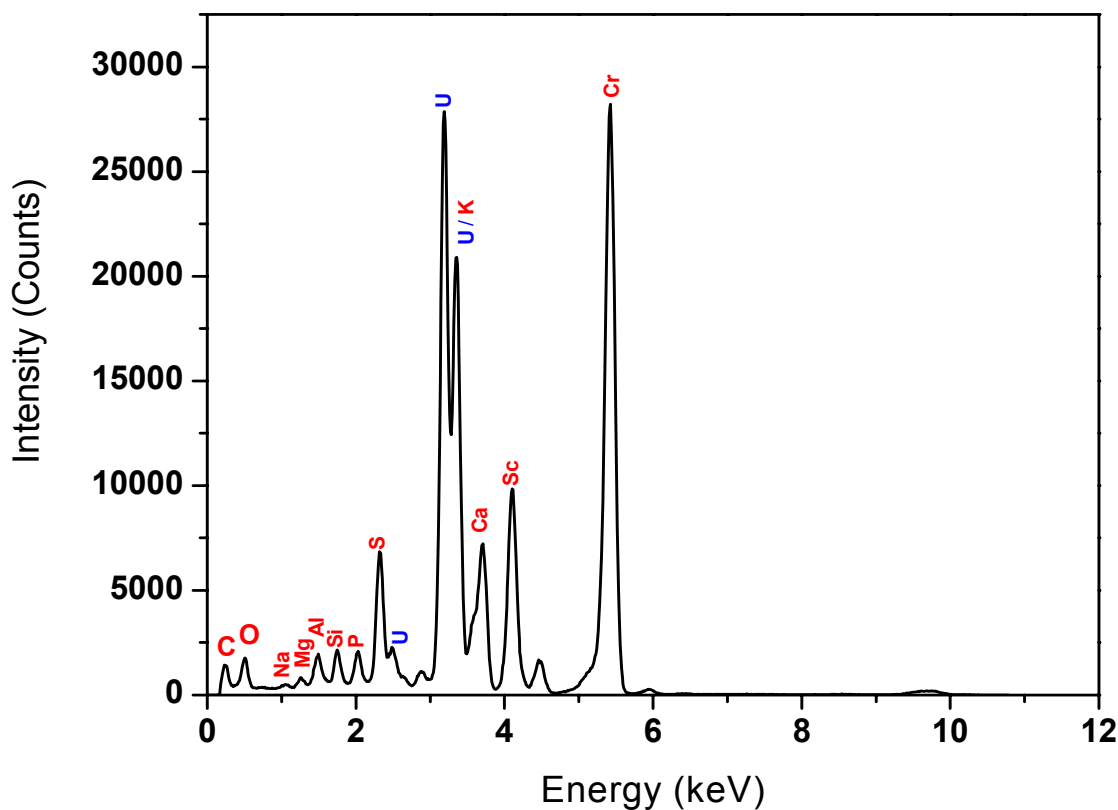


Figure 3.7: TXRF spectrum after selective extraction of uranium and addition of scandium internal standard (Sample-3)

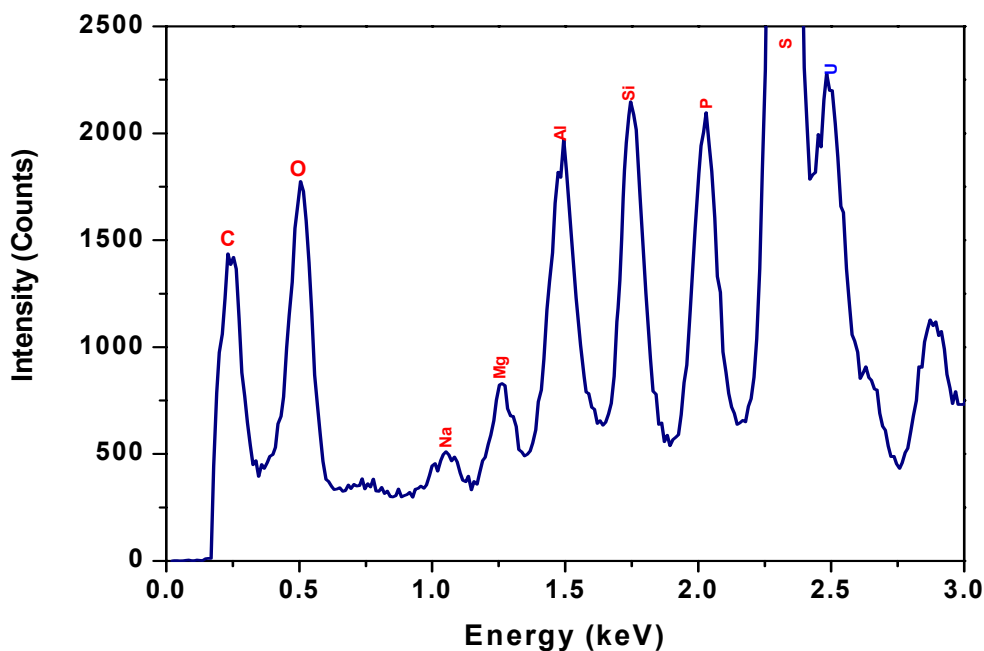


Figure 3.8: Expanded TXRF spectrum after selective extraction of uranium (Sample- 3)

program AXIL was used. In order to assess the area under the analytes peak accurately by profile fitting, the data were processed in two parts. First Na, Mg and Al $K\alpha$ lines were processed together and then Sc $K\alpha$ line was processed separately. The concentrations of Na, Mg and Al were determined by using the net intensities of characteristic $K\alpha$ X-ray peaks of the analytes, internal standard and their relative sensitivity values. The blank values of Na, Mg and Al of each sample were determined and subtracted from the respective values obtained from the TXRF spectra of the samples. The blank corrected TXRF determined concentrations of Na, Mg and Al are given in Table 3.4. It can be seen that the average deviations of the TXRF determined concentrations of Na, Mg and Al from the respective calculated concentrations are within 15, 17 and 9%, respectively. The deviation of TXRF determined Mg values from calculated Mg concentration are quite high in sample-2 and was not included in calculation of the average deviations. The average RSD (1s) of TXRF determined concentrations for the three samples for Na, Mg and Al were found to be 39, 31 and 21%, respectively. The comparison of the calculated

Table 3.4: Results of TXRF determinations of low Z elements in sample solutions

Element	Sample-1		Sample-2		Sample - 3	
	Elemental concentrations ($\mu\text{g/mL}$)					
	Cal [*]	TXRF [#]	Cal [*]	TXRF [#]	Cal [*]	TXRF [#]
Na	10.3	9 \pm 2	14.5	11 \pm 5	19.9	18 \pm 9
Mg	10.2	10 \pm 2	14.3	6 \pm 4	19	13 \pm 1
Al	10.3	10 \pm 2	14.4	15 \pm 4	19.1	23 \pm 4

Cal = Calculated concentrations of the elements on the basis of the preparation of samples
TXRF = TXRF determined concentration of elements \pm 1s (n=4)

and TXRF determined concentrations in three samples is shown in Figure 3.9. It can be seen that the TXRF determined concentrations of all the analytes are in agreement with the calculated concentrations after consideration of the standard error involved. However, the TXRF determined concentration of Mg is very low compared to the calculated Mg concentrations in samples-2 and 3 even after consideration of standard deviation (1s) value.

It can also be seen from Table 3.3 that the minimum amount of low Z elements determined in the present work was 10 $\mu\text{g/mL}$, which is comparatively higher than the amount of trace elements generally determined by TXRF and this amount can be decreased further by dissolving actual uranium fuel samples in smaller amounts of HNO_3 and preconcentrating the aqueous phase obtained after matrix separation. This will lead to lower detection limits required for real uranium sample analysis. These determinations were possible due to use of vacuum chamber, special geometry of the spectrometer and separation of high Z matrix.

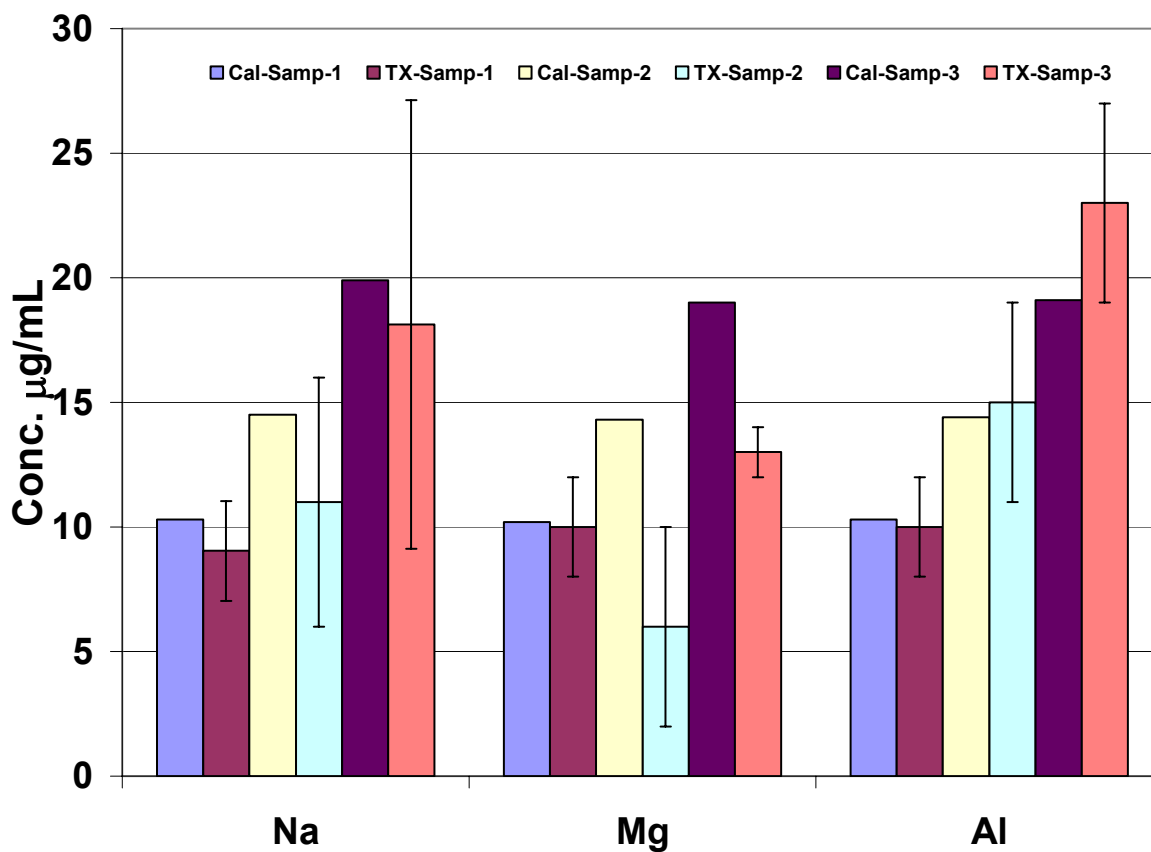


Figure 3.9: Comparison of calculated and TXRF determined concentrations of low Z elements Na, Mg and Al in sample -1, sample-2 and sample-3
 (Cal: Calculated concentrations on the basis of the preparation of the solution, TX: TXRF determined concentrations of low Z elements $\pm 1 \sigma$ (n = 4), Samp: Sample)

3.4. Conclusions

The applicability of TXRF for the determination of trace metallic elements in thorium and uranium was demonstrated.

The TXRF determined analytical results of trace metallic impurities in ThO₂ were in good agreement with the analytical results of different laboratories using different techniques e.g. ICP-AES, ICP-MS, AAS, etc. The precision (1s) and accuracy observed in such TXRF determinations are better than 20%. This method was successfully applied for the development of Certified Reference Materials for trace metallic impurities in ThO₂ standards.

Application of TXRF for determination of low Z elements Na, Mg and Al in nuclear samples was demonstrated for the first time. These elements can be determined by TXRF after dissolving the solid samples and separating the major matrix. The average precision of the TXRF determinations for low Z elements was 31% (RSD 1 σ) and the average deviation of the TXRF determined concentrations of low Z elements from the calculated concentrations was 14%. Though the RSD and deviation of the TXRF determined concentration values from the expected concentrations are slightly higher than the ideal values and will require improvements, these are satisfactory for such nonconventional application of TXRF.

The studies conclude that TXRF is a competitive and complementary technique for the trace element determinations in nuclear materials. In case of analysis of radioactive samples, TXRF has additional benefit of producing less waste and consequently lower radiation hazard risk to the analyst. This technique may be well suited for routine sample analysis of radioactive samples.

3.5. References

1. Kikuo Takeda, Satoru Watanabe, Hideo Naka, Junichi Okuzaki, Taketoshi Fujimoto, Determination of ultra-trace impurities in semiconductor-grade water and chemicals by inductively coupled plasma mass spectrometry following a concentration step by boiling with mannitol, *Anal. Chim. Acta*, 377 (1998) 47.
2. Xie Hualin, Nie Xidu, Tang Yougen, Direct determination of trace elements in high purity gallium by high resolution inductively coupled plasma mass spectrometry, *Chin. J. Anal. Chem.*, 34 (2006) 1570.
3. S.M. Dhavile, S. Thangavel, K. Chandrasekaran, K. Dash, S.V. Rao, S.C. Chaurasia, In situ matrix evaporation by isothermal distillation of high-purity reagents for the determination of trace impurities by ion chromatography, *J. Chromatogr., A*, 1050 (2004) 223.
4. Y.C. Suna, U. C.H. Hsieh, T.S. Linc, J.C. Wenc, Determination of trace impurities in high purity gold by inductively coupled plasma mass spectrometry with prior matrix removal by electrodeposition, *Spectrochim. Acta, Part B*, 55 (2000) 1481.
5. Maurizio Bettinelli, Maurizio Perotti, Sandro Spezia, Claudio Baffi, Gian Maria Beone, Federico Alberici, Sara Bergonzi, Claudio Bettinelli, Paola Cantarini, Laura Mascetti, The

- role of analytical methods for the determination of trace elements in environmental biomonitors, *Microchem. J.*, 73 (2002) 131.
6. M.V. Ramaniah, Analytical chemistry of fast reactor fuels — a review, *Pure Appl. Chem.*, 54 (1982) 889.
 7. Hendrik Emons, Andrea Held, Franz Ulbert, Reference materials as crucial tools for quality assurance and control in food analysis, *Pure Appl. Chem.*, 78 (2006) 135.
 8. A. K. Aggarawal, Certified reference materials of trace elements in water, *Bull. Mater. Sci.*, 28 (2005) 373.
 9. J. Sieber, D. Broton, C. Fales, S. Leigh, B. MacDonald, A. Marlow, S. Nettles, J. Yen, Standard reference materials for cements, *Cem. Concr. Res.*, 32 (2002) 1899.
 10. Ken Sugawara, Interlaboratory comparison of the determination of mercury and cadmium in sea and fresh waters, *Deep-Sea Res.*, 25 (1978) 323.
 11. O.V. Shuvayeva, K.P. Koutzenogii, V.B. Baryshev, V.I. Rezhnikov, A.I. Smirnova, L. D Ivanova, F.V. Sukchorukov, Multi-elemental characterization of the atmospheric aerosols in frames of interlaboratory experiment, *Atmos. Res.*, 46 (1998) 349.
 12. Mary Gopalkrishnan, K. Radhakrishnan, P.S. Dharni, V.T. Kulkarni, M.V. Joshi, A.B. Patwardhan, A. Ramanujam, J.N. Mathur, Determination of trace impurities in uranium, thorium and plutonium matrices by solvent extraction and inductively coupled plasma atomic emission spectrometry, *Talanta*, 44 (1997) 169.
 13. Zlatan Kopajtic, Stefan Rollin, Beat Wernli, Chantal Hochstrasser, Guido Ledergerber, Determination of trace element impurities in nuclear materials by inductively coupled plasma mass spectrometry in a glove-box, *J. Anal. At. Spectrom.*, 10 (1995) 947.
 14. R. Klockenkämper, A. von Bohlen, Total-reflection X-ray fluorescence moving towards nanoanalysis: a survey, *Spectrochim. Acta, Part B*, 56 (2001) 2005.
 15. C. Steen, A. Nutsch, P. Pichler, H. Ryssel, Characterization of impurity profile at the SiO₂/Si interface using a combination of total reflection X-ray fluorescence spectrometry and successive etching of silicon, *Spectrochim. Acta, Part B*, 62 (2007) 481.
 16. János Osán, Szabina Török, Bálint Alföldy, Anita Alseicz, Gerald Falkenberg, Soo Yeun Baik, Rene Van Grieken, Comparison of sediment pollution in the rivers of the Hungarian Upper Tisza region using nondestructive analytical techniques, *Spectrochim. Acta, Part B*, 62 (2007) 123.

17. M. Haarich, A. Knöchel, H. Salow, Einsatz der totalreflexions- röntgenfluoreszenzanalyse in der analytik von nuklearen wiederaufarbeitungsanlagen, *Spectrochim. Acta, Part B*, 44 (1989) 543.
18. S. M. Simabuco, C. Va'zquez, S. Boeykens, R. C. Barroso, Total reflection by synchrotron radiation: trace determination in nuclear materials, *X-ray Spectrom.*, 31 (2002) 167.
19. N.L. Misra, K.D. Singh Mudher, V.C. Adya, B. Rajeshwari, V. Venugopal, Determination of trace elements in uranium oxide by total reflection X-ray fluorescence spectrometry, *Spectrochim. Acta, Part B*, 60 (2005) 834.
20. R.K. Sinha, A. Kakodkar, Design and development of the AHWR—the Indian thorium fuelled innovative nuclear reactor, *Nucl. Eng. Des.*, 236 (2006) 683.
21. B.P. Datta, On the possibility of characterization of thoria by spark source mass spectrometry, *Spectrochim. Acta, Part B*, 52 (1997) 471.
22. Naina Raje, Satish Kayasth, T.P.S. Asari, S. Gangadharan, Preconcentration of trace elements from high-purity thorium and uranium on Chelex- 100 and determination by graphite furnace atomic absorption spectrometry with Zeeman-effect correction, *Anal. Chim. Acta*, 290 (1994) 371.
23. S. Bürger, L.R. Riciputi, D.A. Bostick, Determination of impurities in uranium matrices by time-of-flight ICP-MS using matrix-matched method, *J. Radioanal. Nucl. Chem.*, 274 (2007) 491.
24. Marin, S. Cornejo, C. Jara, N. Duran, Determination of trace impurities in uranium compounds by ICP-AES after organic extraction, *Fresenius' J. Anal. Chem.*, 355 (1996) 680.
25. R. Verma, P.R. Roy, Determination of oxygen to metal ratio of U–Pu mixed oxides by X-ray diffraction, *Bull. Mater. Sci.*, 8 (1986) 479.
26. C. Strelt, H. Aiginger, P. Wobrauschek, Light element analysis with a new spectrometer for total reflection X-ray fluorescence, *Spectrochim. Acta, Part B*, 48 (1993) 163.
27. E.A. Bertin, *Principle and Practice of X-ray Spectrometric Analysis*, Plenum Press, New York, 1984.
28. B. Denecke, G. Grosse, U. Wätjen and W. Bambynek, C. Ballaux, Efficiency calibration of Si(Li) detectors with X-ray reference source at energies between 1 and 5 keV, *Nucl. Instrum. Methods Phys. Res., Sect. A*, 286 (1990) 474.

29. M. Hein, P. Hoffmann, K.H. Lieser, H.M. Ortner, Application of X-ray fluorescence analysis with total-reflection (TXRF) in material science, *Fresenius' J. Anal. Chem.*, 343 (1992) 760.
30. C. Strelı, H. Aiginger, P. Wobrauschek, Total reflection X-ray fluorescence analysis of low Z elements, *Spectrochim. Acta, Part B*, 44 (1989) 491
31. C. Strelı, Light element trace analysis by means of TXRF using synchrotron radiation, *J. Trace Microprobe Tech.*, 13 (1995) 109.
32. Christina Strelı, P. Wobrauschek, V. Bauer, P. Kregsamer, R. Görgl, P. Pianetta, R. Ryon, S. Pahlke, L. Fabry, Total reflection X-ray fluorescence analysis of light elements with synchrotron radiation and special X-ray tubes, *Spectrochim. Acta, Part B*, 52 (1997) 861.
33. C. Strelı, P. Wobrauschek, G. Pepponi, N. Zoeger, A new total reflection X-ray fluorescence vacuum chamber with sample changer analysis using a silicon drift detector for chemical analysis, *Spectrochim. Acta, Part B*, 59 (2004) 1199.
34. P. Wobrauschek, C. Strelı, WOBISTRAX: A Vacuum TXRF Chamber, available online at http://www.ati.ac.at/roelab/wobistrax_info.pdf.
35. International Atomic Energy Agency, Vienna, AXIL Program, available online at <http://www.iaea.org/OurWork/ST/NA/NAAL/pci/ins/xrf/pciXRFdown.php>.

Chapter-4

ANALYTICAL CHARACTERIZATION OF NUCLEAR MATERIALS BY TXRF: TRACE NON-METALLIC DETERMINATIONS

- 4.1. Introduction
- 4.2. Determination of Sulphur in Uranium Matrix by TXRF
 - 4.2.1. Experimental
 - 4.2.1a. *Sample preparation*
 - 4.2.1b. *Instrumentation*
 - 4.2.2. Results and discussion
- 4.3. Chlorine Determination in Nuclear Fuel Samples by TXRF Without Dissolution
 - 4.3.1. Experimental
 - 4.3.1a. *Sample preparation*
 - 4.3.1b. *Instrumentation*
 - 4.3.2. Results and discussion
- 4.4. A Novel Approach for Chlorine Determination in Acidic Medium by TXRF
 - 4.4.1. Experimental
 - 4.4.1a. *Sample preparation*
 - 4.4.1b. *Instrumentation*
 - 4.4.2. Results and discussion
- 4.5. Conclusions
- 4.6. References

4.1. Introduction

Trace determinations of non metallic elements such as H, C, N, O, F, Si, P, S, Cl, etc. in technologically important materials like metals, alloys, fuels and environmental samples is important for their chemical characterization. Non-metallic elements like C, Si, P and S if present in appreciable amounts, have major effect on industrial steels as they influence their mechanical and physical properties [1,2]. Over the last few decades, a large emphasis is laid on the determination of sulphur compounds in the environment as volatile sulphur compounds constitute a significant source of biogenic and anthropogenic atmospheric pollution and can be responsible for environmental damage including acid deposition, rapid acidification of lakes, loss of forests, corrosion of metal structures and historical monuments. Some of the sulphur compounds – though present at trace levels in different waters, foods, beverages and fragrances – are responsible for their taste and odour. Therefore, determination of total organic sulphur, particular classes of sulphur compounds as well as individual components (speciation analysis) is of constant concern in many fields [3]. In petrochemical and other fuel oils, sulphur and chlorine are the main contaminants and even trace levels of these impurities may cause concern because they can poison the catalysts, impart undesirable properties to final products or produce general air pollution when fuel is burned [4]. Chlorine is another non-metallic element which has generated quite a large awareness due to its toxic nature [5].

In nuclear fuels, non-metallics present at both trace and major level play an important role in their performance. In oxide, carbide and nitride based fuels, the O/M, C/M and N/M (M= U, Th and Pu) are important parameters and need be determined very precisely [6, 7]. Other non-metals like H, S, Cl and F also have critical specifications for nuclear materials. Hydrogen in the fuel, if present above 1 ppm can cause embrittlement in the clad. Sulphur causes problem during the sintering of pellets and chlorine and fluorine cause local depassivation and corrosion of the clad, if present above the specified limits.

Different techniques are employed for the determination of non-metals in nuclear samples. For H, O and N determinations, inert gas fusion technique is used [8, 9]. Carbon and sulphur are determined by IR detection method after separation. The method for chlorine and fluorine determinations involves separation of the analyte followed by spectrophotometry. But TXRF is one such technique which can determine both metals and non-metals simultaneously. But one of the disadvantages of XRF is its inability to determine low atomic number elements.

Using XRF it is not possible to determine hydrogen as they do not produce any X-rays, C, O, N and F cannot be determined in air atmosphere. Special instrumentation with vacuum facility are required for their determinations. Even elements like sulphur and chlorine have low characteristic energies and low fluorescence yields. Characteristic peak energy of S K α is 2.307 keV and fluorescence yield (ω) = 0.061 and Cl K α has 2.622 keV energy and ω = 0.078. In addition, the detector efficiency for detecting low energy X-rays is poor. These factor leads to very low X-ray intensities and hence high detection limits.

In this Chapter, studies for the determination of non-metals sulphur and chlorine in nuclear materials by TXRF at trace and major concentration levels are reported. For sulphur determinations in uranium matrix, the major matrix was removed by solvent extraction using TBP followed by its determination in the aqueous phase. The separation of analyte, for the determination of chlorine in various nuclear samples, was carried out using pyrohydrolysis followed by its determination using TXRF. This process does not require any sample dissolution. In order to improve the sensitivity, WL α was used for sample excitation in both the cases. Another novel method of chlorine determination in acidic medium by TXRF is also described in this Chapter. This methodology involves addition of an excess known amount of AgNO₃ in the acidic sample solution to precipitate chlorine as AgCl, filter the solution and determine the unused silver left in the solution. The continuum from the X-ray tube target was used to excite Ag K α .

4.2. Trace Determination of Sulphur in Uranium Matrix by TXRF

Sulphur is widely distributed in the earth. It is used in different forms in industries and is left as a trace element in almost all materials [10]. It occurs in oxidized forms as sulphates, sulphites or in reduced form as sulphides. Thorium, uranium and plutonium are important industrial materials used in different forms as nuclear fuel. Trace amounts of sulphur get incorporated in these materials because of the presence of different forms of sulphur in earth crust and use of sulphuric acid at various stages of the processing of these materials. During fuel fabrication of ThO₂, UO₂ and PuO₂ based fuels, the fuel is taken in the form of pellets and these pellets are sintered at high temperatures (~ 1973 K) in Ar-H₂ atmosphere to get high density pellets. Although, the sulphur impurity in these fuel materials does not affect the fuel sinterability, if it is present below a certain concentration level, sulphur amounts above 400-700

ppm (w/w) have been found to result in the formation of corresponding actinide oxo sulphides and H₂S because of which the fuel pellets, especially ThO₂ pellets, are shattered in powder form during the sintering. Hence, it is desirable to know and control the trace amounts of sulphur in such fuel materials before the fuel is sintered and subsequently put in a nuclear reactor. Also, different actinide sulphates are reported in literature for different applications as well as for academic research [11-13]. Sulphur is present in these compounds as a major element. To know the sulphur content in such compounds is an important step for their characterisation. Thus determination of sulphur in uranium matrix at trace as well as major concentration level is important.

Analytical methods which are employed for determination of sulphur are ion chromatography (IC), isotope dilution mass spectrometry (IDMS), vacuum combustion extraction – quadrupole mass spectrometry (VCE-QMS), gravimetry, titrimetry, spectrophotometry, amperometry, potentiometry, etc. [10-14]. TXRF, due to its various features and the capability to analyse metals and non-metals alike, has a very good potential for trace non-metallic determinations in nuclear samples [15, 16]. But, because of its weak fluorescence yield and the low energy of the emitted fluorescence radiation, absorption effects pose several problems in the determination of sulfur in different matrices [17]. Therefore, before this method can be used for routine analysis, it should be standardised for sulphur determinations in nuclear materials. Keeping this in mind, the present studies were initiated.

4.2.1. Experimental

4.2.1a. Sample Preparation

The HNO₃ used was of suprapure grade and other chemicals e.g. TBP, dodecane, Na₂SO₄, etc. were of AR grade. All the samples and standards were prepared in Milli-Q water. Merck single element standards of scandium and cobalt, after proper dilution, were used as internal standards. Sample preparations were carried out in beakers, separating funnel and separating tubes made of quartz. Since the certified reference materials for sulphur in uranium matrix at trace level were not available commercially, sample solutions were prepared by mixing different volumes of a high purity uranyl nitrate solution having uranium concentration of 14.07 mg/mL and a sulphur standard solution having a concentration of 98.9 µg/mL, prepared by

dissolving Na₂SO₄ in Milli-Q water. These solutions were mixed in different ratios to give different sulphur concentrations with respect to uranium as shown in Table 4.1. Seven such samples were prepared. Two samples out of these namely: S-1 and S-2 did not contain any uranium. The relative sensitivity of S K α with respect to Co K α was determined using another calibration standard solution of sulphur and cobalt having concentrations of 16.48 and 8.25 $\mu\text{g/mL}$, respectively. This solution was prepared by mixing a Na₂SO₄ solution analyzed earlier for SO₄⁻² by ion chromatography and a Merck Single element standard solution of cobalt.

In order to make a thin film of the specimen for TXRF measurement and to avoid the possible absorption of S K α by uranium, especially for those samples where sulphur is present at trace levels, the major matrix was separated. A 30 % TBP solution in dodecane was used for the separation of uranium from those solutions. For such separations, 10 mL volume of each sample was evaporated to dryness under an IR lamp in beakers and the residue was dissolved in 2.5 mL of 2.25 M HNO₃. The resultant solutions were equilibrated with equal amount of 30% TBP solution in dodecane which was pre-equilibrated with 2.25 M HNO₃ in a separating funnel. After each extraction, the organic phase was carefully removed with a micropipette and discarded. Then a fresh TBP solution of same volume was added in its place.

Table 4.1: Details of sample solutions of sulphur in uranium matrix

S.No.	Sample Code	Sulphur with respect to uranium ($\mu\text{g/g}$)	Expected* sulphur concentration ($\mu\text{g/mL}$)
1	S-1	-	12.9
2	S-2	-	16.5
3	SU-1	100,000	50
4	SU-2	2000	1.1
5	SU-3	1058	12.9
6	SU-4	286	1.3
7	SU-5	143	1.0

*: Expected sulphur concentration in sample solutions calculated on the basis of their preparation

Finally, after the third equilibration, the aqueous phase was collected in another beaker and mixed with cobalt internal standard. This solution was evaporated to dryness and then 200 μL of 1.5% suprapure HNO_3 solution in Milli-Q water was added to it so that the residue obtained dissolved completely. Aliquots of 10 μL of each sample solutions were deposited at the center of precleaned quartz sample supports in duplicate and dried under an IR lamp. They were later loaded for TXRF measurements. Each sample support was measured twice. The TXRF determined concentrations and their precision values were calculated by averaging the results obtained from four measurements.

The method developed was further counterchecked for sulphur determinations using $\text{Rb}_2\text{U}(\text{SO}_4)_3$, a standard reference material for uranium developed in our laboratory. This standard has maximum solubility in HNO_3 (285 g/L) [11]. A weighted amount of this standard was dissolved in 1.5% HNO_3 and diluted to different dilutions to give concentrations of sulphur as given in Table 4.2. In the standards RbUS-1 and RbUS-2, the amount of sulphur with respect to uranium was around 40% and, therefore, no separation was carried out. Sulphur was determined as a major constituent in these standards after adding cobalt internal standard. In another set of standards, a known amount of uranium from another uranyl nitrate solution having uranium concentration of 300 mg/mL was added so that in these solutions concentration of sulphur with respect to uranium was in trace levels, as given in Table 4.2. Before determination of sulphur in these solutions, uranium was separated using TBP as described above.

The blank was also processed in a similar way as the samples. For the samples without uranium, the blank value was determined by adding cobalt (IS) in 1.5% HNO_3 in same proportion as was added to the samples. The blank values for the samples containing uranium were determined by taking Milli-Q water of the same amount as the sulfate solutions taken to prepare the samples in uranium and performing all the steps of TXRF determinations in the blank e.g. complete drying of the water and redissolving the residue in 2.5M HNO_3 , separation of major matrix by solvent extraction, drying of the aqueous phase, addition of internal standard in the aqueous phase and determining the sulphur concentration. The blank values for the samples RbUS-1A, RbUS-2A and RbUS-3A, shown in Table 4.2, were determined by adding 1.5% HNO_3 in place of the standard solution of $\text{RbU}(\text{SO}_4)_3$ and determining the sulphur concentration by TXRF in similar way after performing all the steps of uranium separation as done for these samples.

Table 4.2: Details of the standard solutions prepared with $\text{Rb}_2\text{U}(\text{SO}_4)_3$

Sample	Expected * Concentrations ($\mu\text{g/mL}$)		S with respect to U
	Sulphur	Uranium	
S determination as major element			
RbUS-1	586	1453	40.3 %
RbUS-2	293	728	40.3 %
S determination as trace element			
RbUS-1A	117	240000	488 $\mu\text{g/g}$
RbUS-2A	59	240000	244 $\mu\text{g/g}$
RbUS-3A	29	240000	123 $\mu\text{g/g}$

*: Expected sulphur and uranium concentrations in standard solutions calculated on the basis of their preparation

4.2.1b. Instrumentation

For TXRF measurements, ITAL Structures TXRF spectrometer TX 2000 was used. The samples were excited by $\text{W}\text{L}\alpha$ (8.39 keV) radiation obtained from a W–Mo dual target tube operated at 40 kV and 30 mA. The spectrometer was aligned to diffract $\text{W}\text{L}\alpha$ radiation by changing the multilayer and tube shield values accordingly. The TXRF measurements were made in duplicate for each dried aliquot on quartz sample support for a live time of 1000 s. The Si(Li) detector was used to detect the X-rays from the specimens on sample supports.

4.2.2. Results and discussion

As mentioned earlier, sulphur may be present in different materials as sulfate or sulfide. If it is present as sulfate, there is no possibility of loss of sulphur when the sample is heated on a quartz sample support during TXRF sample preparation because most of the sulfates are stable at this temperature ($\sim 100^\circ\text{C}$) in acidic medium. However, if sulphur is present in sulfide form, treatment of samples with acid for dissolution and thereafter drying on quartz sample supports may drive out sulphur in form of H_2S resulting in loss of sulphur at low temperature. During the fabrication and processing of nuclear fuel materials e.g. ThO_2 , UO_2 and PuO_2 , the corresponding precursors like ammonium di-uranates (ADU) or thorium/plutonium oxalates are heated to high temperatures. At such temperatures, all the volatile forms of sulphur, if present, will be driven out and only the sulphur in oxidized form will remain in such materials. This form of sulphur can be conveniently determined by TXRF. Another mode of sulphur loss may be during the selective removal of major matrix uranium. However, TBP is a well established extractant for selective extraction of uranium, hence it was used in the present work.

For TXRF determinations, cobalt was used as an internal standard. Though initially it was proposed to use scandium as the internal standard because the energy of Sc $\text{K}\alpha$ (4.090 keV) is nearer to S $\text{K}\alpha$ (2.308 keV), the escape peak of Sc $\text{K}\alpha$ interferes with S $\text{K}\alpha$. It was observed that the sulphur concentration values determined by TXRF using scandium as an internal standard had poor accuracy probably because of such interference. Due to this reason, cobalt was chosen as an internal standard. The relative sensitivity values of S $\text{K}\alpha$ with respect to Co $\text{K}\alpha$ and Sc $\text{K}\alpha$ along with their characteristic X-ray energies are given in Table 4.3.

The acidity of the sample and standard medium was adjusted to 2.25 M because the extraction efficiency of TBP for uranium is maximum at this pH. The TXRF spectrum of a processed sample SU-2 is shown in the Figure 4.1. Some additional peaks apart from sulphur can be seen in this Figure. The Si $\text{K}\alpha$ is from the quartz sample support used for the measurements, P $\text{K}\alpha$ peak is due to partial solubility of TBP in aqueous phase, Ar $\text{K}\alpha$ peak is from the atmosphere whereas $\text{K}\alpha$ peaks of calcium, manganese and iron are due to the possible contamination. It can be seen that the S $\text{K}\alpha$ peak is clearly separated from other peaks except P $\text{K}\beta$. The program EDXRF32 can take care of such interferences by removing the contribution of P $\text{K}\beta$ on S $\text{K}\alpha$. The selective extraction of uranium from a sulphur-uranium standard solution can be seen

Table 4.3: Elemental characteristic X-ray lines used for TXRF measurements and corresponding absorption edges*

Element	Analytical X-ray line	Relative Sensitivity with respect to		Energy (keV)	K-Absorption Edge* (keV)
		Sc K α	Co K α		
S	S K α	0.109	0.022	2.308	2.471
Sc	Sc K α	1	-	4.090	4.486
Co	Co K α	-	1	6.930	7.712

*: http://www.kavelaby.npl.co.uk/atomic_and_nuclear_physics/4_2/4_2_1.html

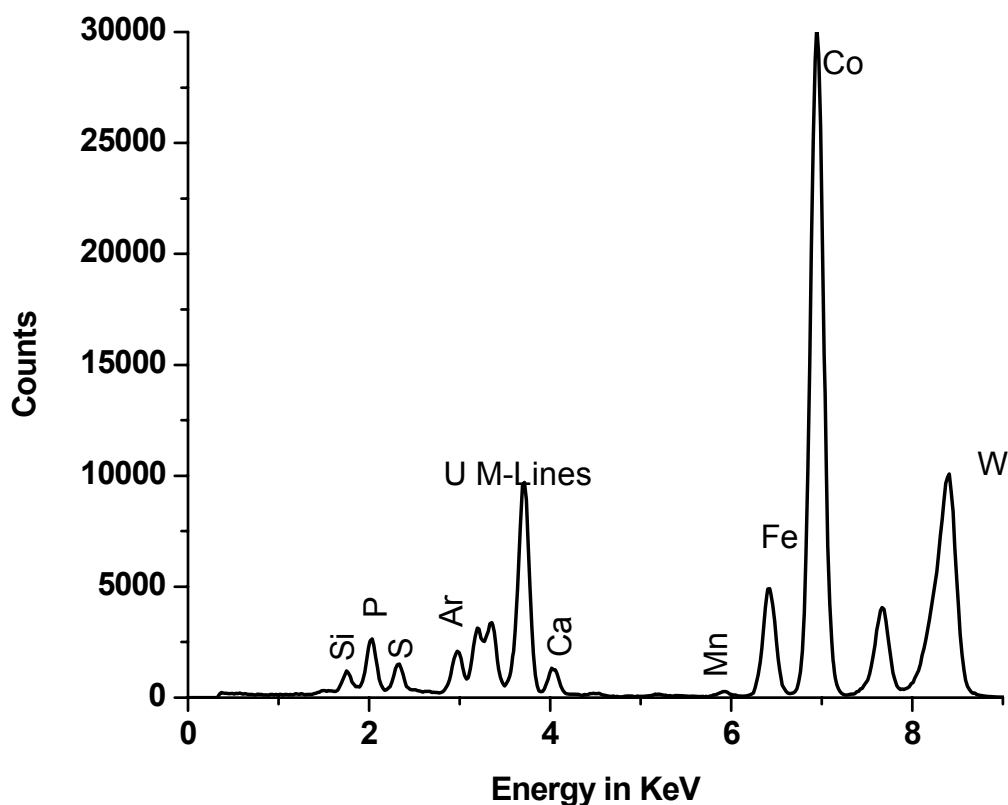


Figure 4.1: The TXRF spectrum of aqueous phase of sample (SU-2) after preconcentration and addition of cobalt internal standard

by comparing the TXRF spectra of the aqueous phases of such standard obtained after one and two equilibrations with TBP. Such TXRF spectra are compared in the Figure 4.2. It can be seen that after each extraction, U $M\alpha$ (3.165 keV) peak intensity decreases showing the selectivity of such extraction process for uranium. Also it can be seen that S $K\alpha$ intensity is very low when uranium is not extracted at all. After first equilibration, the intensity of S $K\alpha$ increases appreciably whereas after second, a very clear peak of S $K\alpha$ can be seen in the spectrum. This

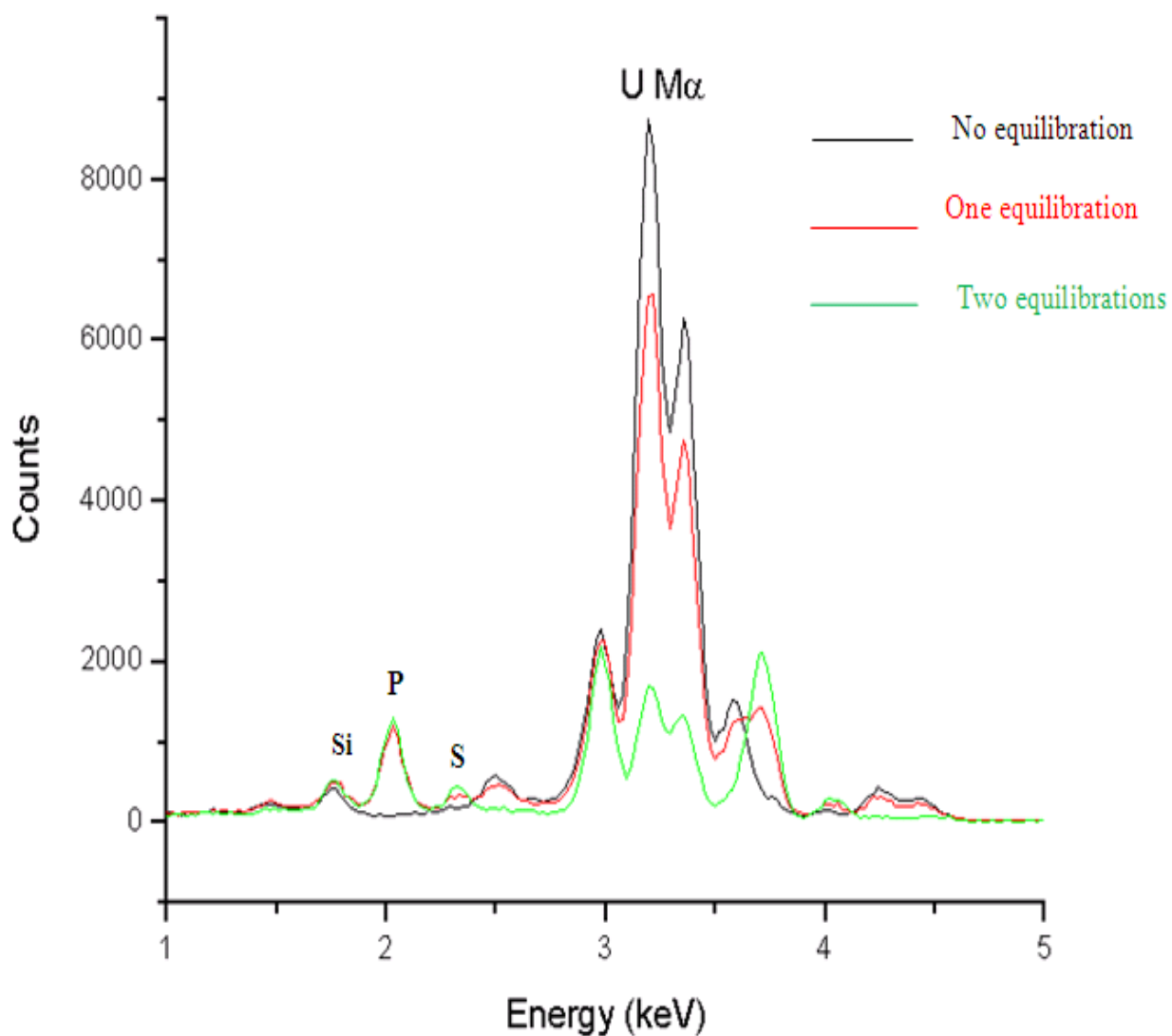


Figure 4.2: A comparison of TXRF spectra of aqueous phase of a standard solution of sulphur obtained after different number of equilibrations with TBP

indicates that three equilibrations with processed TBP will be optimum for determination of sulphur at trace level by TXRF in uranium matrix.

The percent deviation from the expected values and precision of analytical results of sulphur determination in samples (details given in the Table 4.1) is presented in Table 4.4. The blank values for these samples were found to be negligible. But the blank value for the samples containing 300 mg/mL uranium concentration (Table 4.2) was found to be 17 µg/mL. This blank value was subtracted from the TXRF determined concentration of sulphur. The average precision of this method was found to be 8% (1σ) and the average deviation of TXRF determined values from the expected values was 14%. It can be seen that the precision of sulphur determination by TXRF for sample S-1 is poor but the agreement with expected concentration value is good. This would be due to non-uniformity of the thin film formed on the quartz sample support presented for TXRF measurement. The plot of expected and TXRF determined sulphur concentrations is

Table 4.4: Comparison of TXRF determined and expected sulphur concentrations in standard solutions

Sample Code	S Concentration (µg/mL)		RSD % (1 σ)	Deviation (%)
	Expected*	TXRF [#]		
S-1	12.9	12 ± 4	33	- 7
S-2	16.5	15.1 ± 0.4	2.6	- 8.5
SU-1	50	46 ± 4	8.7	- 8
SU-2	1.1	0.97 ± 0.07	7.2	-11.8
SU-3	12.9	9.3 ± 0.7	7.5	-27.9
SU-4	1.3	1.1 ± 0.1	9.1	-15.4
SU-5	1.0	0.82 ± 0.04	4.9	- 18

*: Expected sulphur concentration in sample solutions on the basis of their preparation

[#]: Sulphur concentration in samples as determined by TXRF ± 1 σ (for n=4 determinations)

given in Figure 4.3. The plot indicates good agreement among the TXRF determined and expected sulphur concentrations. These observations establish the suitability of TXRF for sulphur determination in such samples after separation of the major matrix. The applicability of this method was also counterchecked by determining sulphur in $\text{Rb}_2\text{U}(\text{SO}_4)_3$, which is a chemical assay standard for uranium. Table 4.5 shows that the TXRF determined sulphur concentrations in $\text{Rb}_2\text{U}(\text{SO}_4)_3$ solutions of different sulphur concentrations were within 8% of expected values showing reliability of such determinations. The average precision was found to be 12% (1σ). It can be seen that the TXRF determined sulphur concentrations in Table 4.4, have a systematic

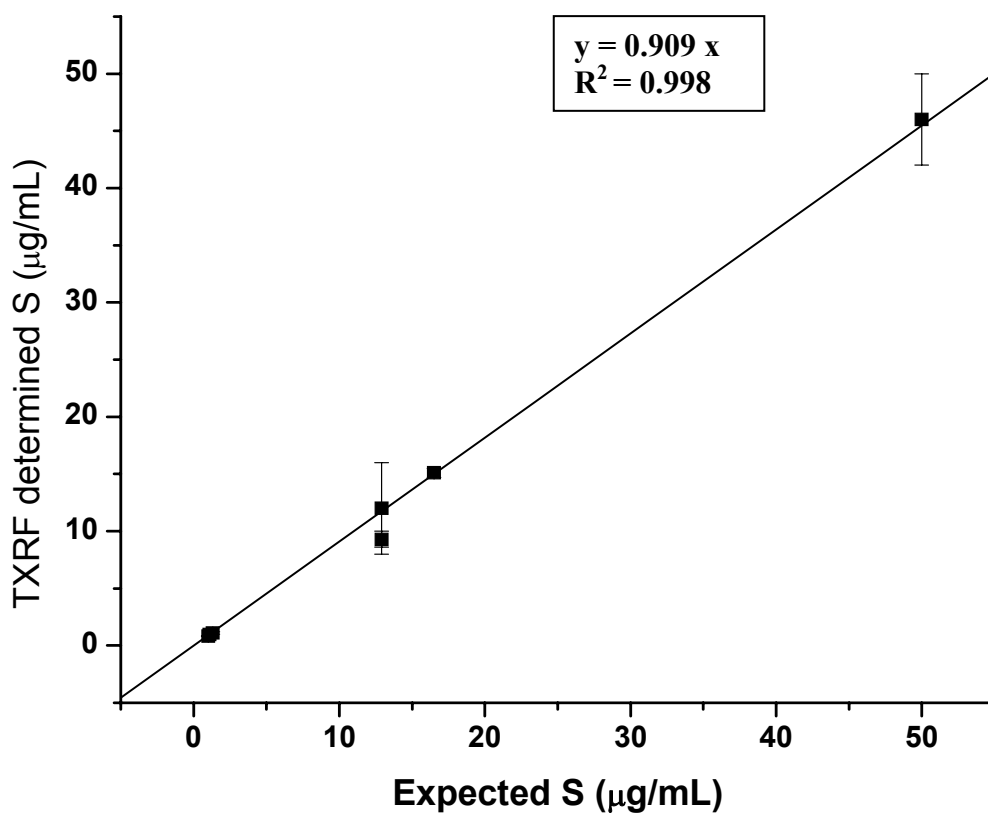


Figure 4.3: Plot between expected and TXRF determined sulphur concentrations in samples
(The error bars represent standard deviation of four TXRF determinations)

negative deviation. One of the reasons for such deviations may be because the samples were prepared by dissolving known quantity of Na₂SO₄ in water, whereas the sensitivity values of sulphur with respect to cobalt were determined using a pre-analyzed Na₂SO₄ solution as mentioned earlier. Due to hygroscopic nature of Na₂SO₄ used for sample preparation, a small amount of absorbed moisture might be giving systematic negative deviation in TXRF determinations of sulphur in such samples as shown in Table 4.4. Since Rb₂U(SO₄)₃ does not have a tendency to absorb moisture, this type of systematic deviation was not seen. From these observations, it can be concluded that TXRF can be used for determination of sulphur in uranium matrix on a routine basis for major as well as trace determinations.

Table 4.5: TXRF determined and expected sulphur concentrations in certified reference material Rb₂U(SO₄)₃

Sample	Sulphur concentration (µg/mL)		TXRF/Expected	Whether uranium was separated
	Expected*	TXRF#		
Sulphur determination as a major element				
RbUS-1	586	595 ± 82	1.01	No
RbUS-2	293	305 ± 40	1.04	No
Sulphur determination as a trace element				
RbUS-1A	117	126 ± 4	1.08	Yes
RbUS-2A	59	70 ± 8	1.21	Yes
RbUS-3A	29	26 ± 5	0.90	Yes

*: Expected sulphur concentration in sample solutions on the basis of their preparation

#: Sulphur concentration in samples as determined by TXRF ± 1 σ (for n=4 determinations)

4.3. Chlorine Determination in Nuclear Fuel Samples by TXRF without Dissolution

Quality control of the nuclear materials for the presence of trace impurities is an important step. The amounts of these trace impurities have to be determined using suitable analytical methods depending upon the nature of sample, sensitivity, precision and accuracy required. Among these trace impurities, chlorine is one of the most important elements to be determined because of its extremely corrosive nature. In nuclear materials, the specification of chlorine ranges from 5 to 50 ppmw as given in Table 4.6. Even at very low concentration of chlorine, it can give rise to depassivation of the oxide film on the surface of the clad thereby

Table 4.6: Typical specification limits for chlorine in nuclear materials

Material	Specification limit (ppmw)	Used as
UO ₂ PHWR and BWR MOX (BWR)	15	Fuel (causes corrosion)
FBTR, PFBR (Cl+F)*	50*	Fuel
ThO ₂	25	Fuel
Zircaloy-2	20	Clad (causes local depassivation of oxide film)
Zircaloy-4	20	Clad
Zr+2.5% Nb	5	Coolant tube (causes oxide depassivation)

* Specification limit for Cl+F. The acronyms PHWR, BWR, MOX, FBTR and PFBR stand for pressurised heavy water reactor, boiling water reactor, mixed oxide, fast breeder test reactor and prototype fast breeder reactor, respectively.

leading to corrosion of the cladding material [18]. Chlorine has low fluorescence yield and low characteristic energy, hence TXRF method of determination requires efficient excitation with low energy X-rays. Use of vacuum or helium purging helps in improving the sensitivity for determination of elements having low energy X-rays. Moreover, samples are required in the form of solution for TXRF analysis. Therefore, dissolution and separation of the matrix for trace determination is mandatory. But sample dissolution is generally a cumbersome procedure and can lead to the possibility of addition of some impurities into the sample. Pyrohydrolysis is a well established method for separation of volatile impurities such as boron, sulphur, chlorine, fluorine, etc. from solid matrix without dissolving the sample [19, 20]. It involves heating of the solid sample to a high temperature (900-1000 °C) in order to break the matrix and release the entrapped volatile impurities. These impurities are carried by a stream of moist argon and collected in a buffer solution. This buffer solution is then analysed for the trace impurity.

In this Section, a new methodology is described which involves separation of chlorine from the nuclear fuel samples by pyrohydrolysis followed by the analysis of the collected condensate by TXRF. This method avoids the cumbersome procedures associated with sample dissolution and the introduction of impurities from the reagents generally used for sample dissolution. The obtained results were also counterchecked with Ion Chromatography (IC) analysis. In order to improve the analytical results and see the effect of helium purging, some TXRF determinations were also carried out in helium gas atmosphere.

4.3.1. Experimental

4.3.1a. Sample preparation

Stock solutions of sodium chloride (NaCl) and sodium hydroxide (NaOH) were prepared by dissolving AR grade powders of the respective salts in Mill-Q water. The sample solutions of chlorine were prepared by dissolving NaCl in NaOH (5 mM) solution, having chlorine concentrations ranging from 125 to 4000 ng/mL. Merck single element certiPUR ICP standard of cobalt mixed with NaOH solution was used as internal standard. One of the solutions, having concentration of 6.25 µg/mL of chlorine, was mixed with cobalt internal standard and used for the calibration of the spectrometer by determining the relative sensitivity of Cl K α with respect to Co K α . The sample solutions were also mixed with cobalt standard solution. An aliquot of 30

μL of each solution and calibration standard was deposited on cleaned quartz sample supports in duplicate and presented for TXRF measurements.

Real solid powder samples of plutonium carbide, oxide and alloy were taken for determination of chlorine in them, after pyrohydrolysis. One sample of U_3O_8 was also analysed for its chlorine content. For pyrohydrolysis, 500 mg of these solid samples were loaded one by one in quartz pyrohydrolysis set up consisting of two concentric tubes as shown in Figure 4.4 [21]. The inner tube holds the sample boat and is connected to the gas outlet through the connector tube. The outer tube has an inlet for flowing of carrier gas (Ar/O_2) along with steam used for pyrohydrolysis. The gas outlet tube is cooled by a water condenser and the condensate collected in polypropylene bottle cooled with water. A furnace is used to heat the sample as

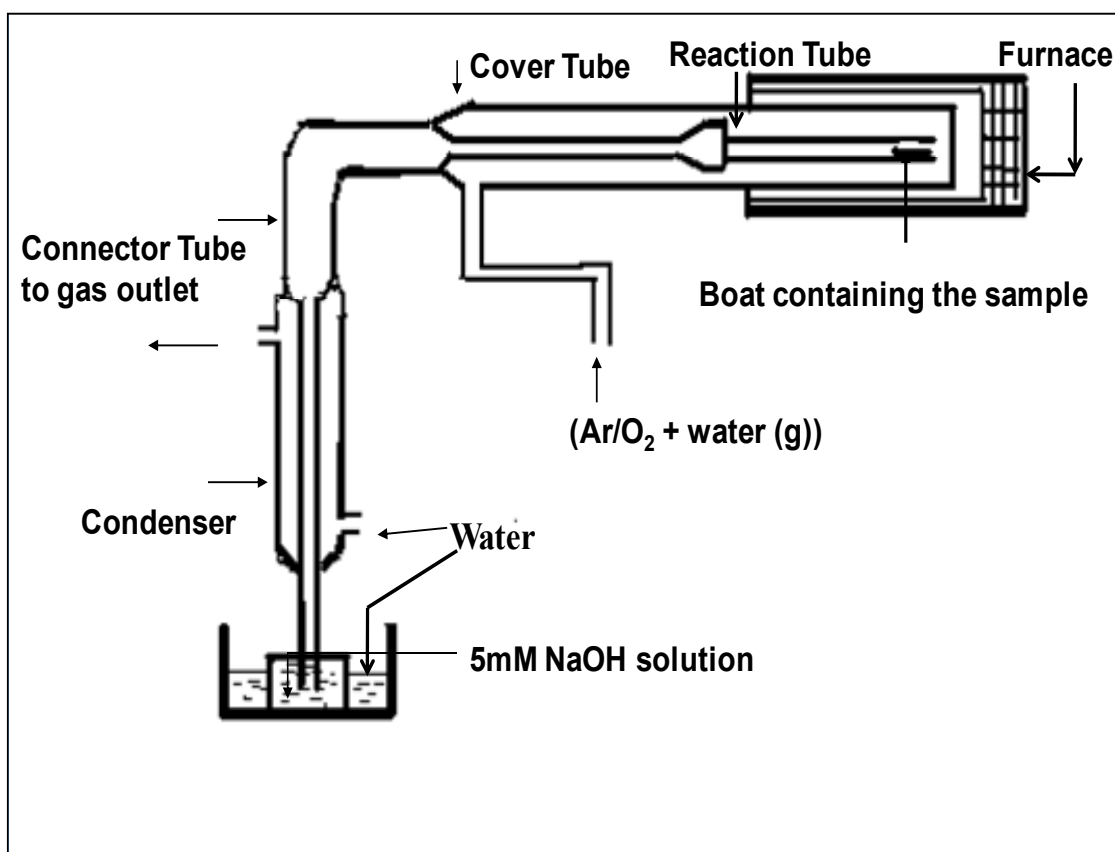


Figure 4.4: Pyrohydrolysis set up for separation of chlorine from nuclear materials

shown in the Figure. The pyrohydrolysis temperature, sample mass, rate of flow of the steam, etc. were optimized earlier [21]. The samples were placed on the quartz boat and heated at 900°C. At this temperature, the sample matrix breaks and the volatile impurities like boron, fluorine and chlorine get liberated. The stream of moist (Ar/O₂) gas passed over the hot sample carries these liberated impurities. The steam was then cooled by a condenser and the liberated chlorine, fluorine, etc. were collected in aqueous solution of NaOH in polypropylene bottles and made up to 25 mL. In one part of this distillate, cobalt internal standard was added and mixed thoroughly. This was taken for TXRF measurement. The other part was analysed by ion chromatography.

4.3.1b. Instrumentation

For TXRF measurements, ITAL STRUCTURES TX-2000 X-ray spectrometer was used. The analytical lines of interest Cl K α (2.622 keV) and the internal standard Co K α (6.930 keV) were excited by W L α (8.396 keV) characteristic X-rays obtained from a W-Mo dual target tube operated at 40 kV and 30 mA. All the samples were prepared in duplicate and counted twice for 2000s. For samples analysed in helium atmosphere, the flow rate of the gas was optimized and set at 800 cc/min using a flow meter.

For IC measurements, a Dionex DX-500 ion chromatography system consisting of an IP-20 isocratic pump, a self regenerator suppressor in external recycle mode and an ED-40 conductivity detector with a conductivity cell and DS-3 stabilizer was used for obtaining the chromatograms. Separation of the anions was achieved with an analytical column (Dionex, Ion Pac, AS 18, 250x4 mm) coupled with a guard column (AGIx8, 50 x4 mm).

4.3.2. Results and discussion

It was observed that when the samples were prepared in slightly acidic medium (1.5 % HNO₃), the chlorine present in the sample was driven out of the solution as HCl while drying the samples on quartz sample carrier and the TXRF measurements did not show any chlorine at all. In order to avoid such losses, the samples were then prepared in Milli-Q water. But even that slight acidity was enough to drive all the chlorine from the samples. Because of this, finally all

the sample solutions were prepared in basic medium (NaOH). After this modification, a clear Cl K α peak was visible in the TXRF spectrum.

Cobalt was used as internal standard as it was not present in the sample and the excitation efficiency of W L α for cobalt is very good. The relative sensitivity of chlorine with respect to cobalt was calculated using the calibration standard and was found to be 0.67 ± 0.02 . This relative sensitivity value was used for the analyses of other samples. A comparison of the expected and TXRF determined concentrations of chlorine, in samples prepared in NaOH medium is shown in Figure. 4.5. The TXRF determined concentrations of chlorine in these

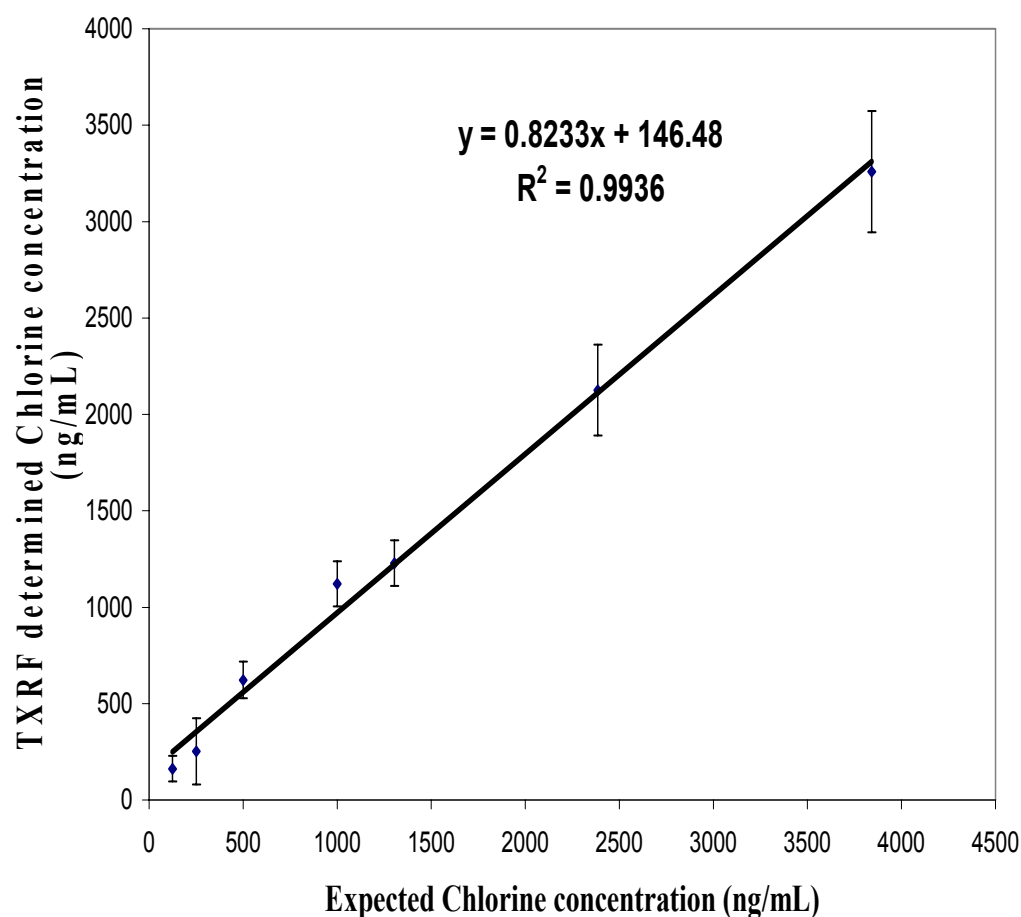


Figure 4.5: Comparison of TXRF determined and expected chlorine concentration in sample solutions

samples were found to be within 15% (average) of the expected concentrations calculated on the basis of sample preparation. The precision was also found to be within 15% (1σ for $n=4$) for chlorine concentration of 500 ng/mL and above. After accessing the applicability of TXRF methodology for the determination of chlorine in NaOH medium, real pyrohydrolysed samples were analysed. The TXRF spectrum of one such NaOH solution containing liberated chlorine from a sample (U,Pu)C-3 and cobalt internal standard is shown in Figure 4.6. These analyses were carried out in the air atmosphere. The analytical results of the samples are given in Table 4.7 and the precision of such determinations was found to be 25 % ($n=4$). The agreement between TXRF and IC determined values for chlorine was within 20%.

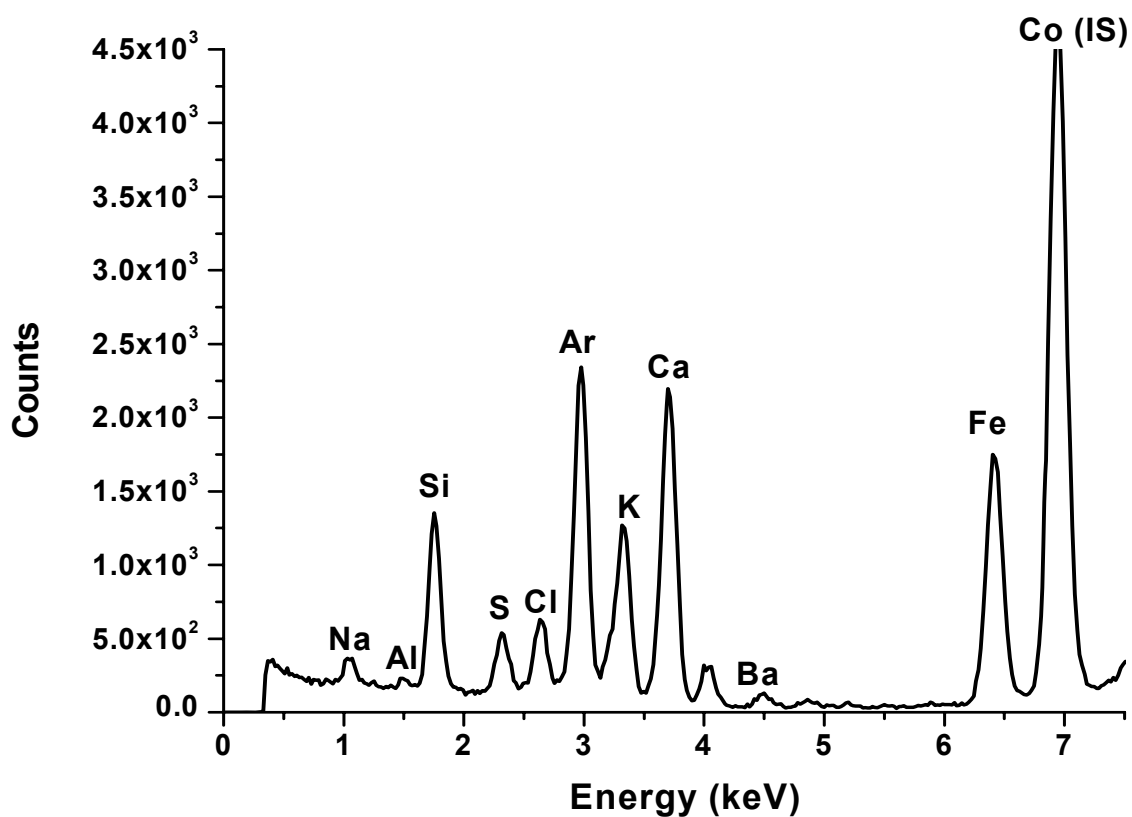


Figure 4.6: TXRF spectrum of pyrohydrolysed (U, Pu)C-3 sample

The effect of TXRF analyses in helium atmosphere was also studied. Purging of the TXRF sample chamber with gas helps in the suppression of the Ar peak (Ar K α 2.957 keV) coming from the atmosphere and thereby avoiding interference or overlap. But there are no reports to the best of our knowledge on gas purged TXRF studies. Hence this is the first report on He gas purged TXRF for chlorine determination. The Ar K α peak is near the Cl K α peak and its removal from the TXRF spectrum helps in better peak profile fitting by the computer software and also reduces the attenuation of the analyte radiation in air. In order to optimize the helium purge flow rate, TXRF spectra were recorded at various helium flow rates from 200-900 cc/ min. From Figure 4.7, it can be seen that flow rate of 600-800 cc/ min was found to be optimum. At this flow rate, Ar K α peak gets completely suppressed. Based on this study, the flow rate of helium purge was fixed at 800 cc/min and TXRF measurements for plutonium oxide and alloy samples after pyrohydrolysis were carried out. The analytical results of TXRF and IC determined chlorine in these matrices are given in Table 4.8. The average precision for chlorine determination was found to be 9% (1 σ) and the agreement between TXRF and IC determined chlorine values was within 15%.

Table 4.7: Comparison of TXRF (in air atmosphere) and Ion Chromatography determination of chlorine in (U,Pu)C samples

Sample	Chlorine concentration ($\mu\text{g/mL}$)		TXRF/IC
	TXRF	IC	
	determined	determined	
U ₃ O ₈	0.89 \pm 0.23	1.232	0.72
(U,Pu)C-1	0.32 \pm 0.07	0.278	1.19
(U,Pu)C-2	0.21 \pm 0.05	0.257	0.82
(U,Pu)C-3	0.41 \pm 0.02	0.333	1.24

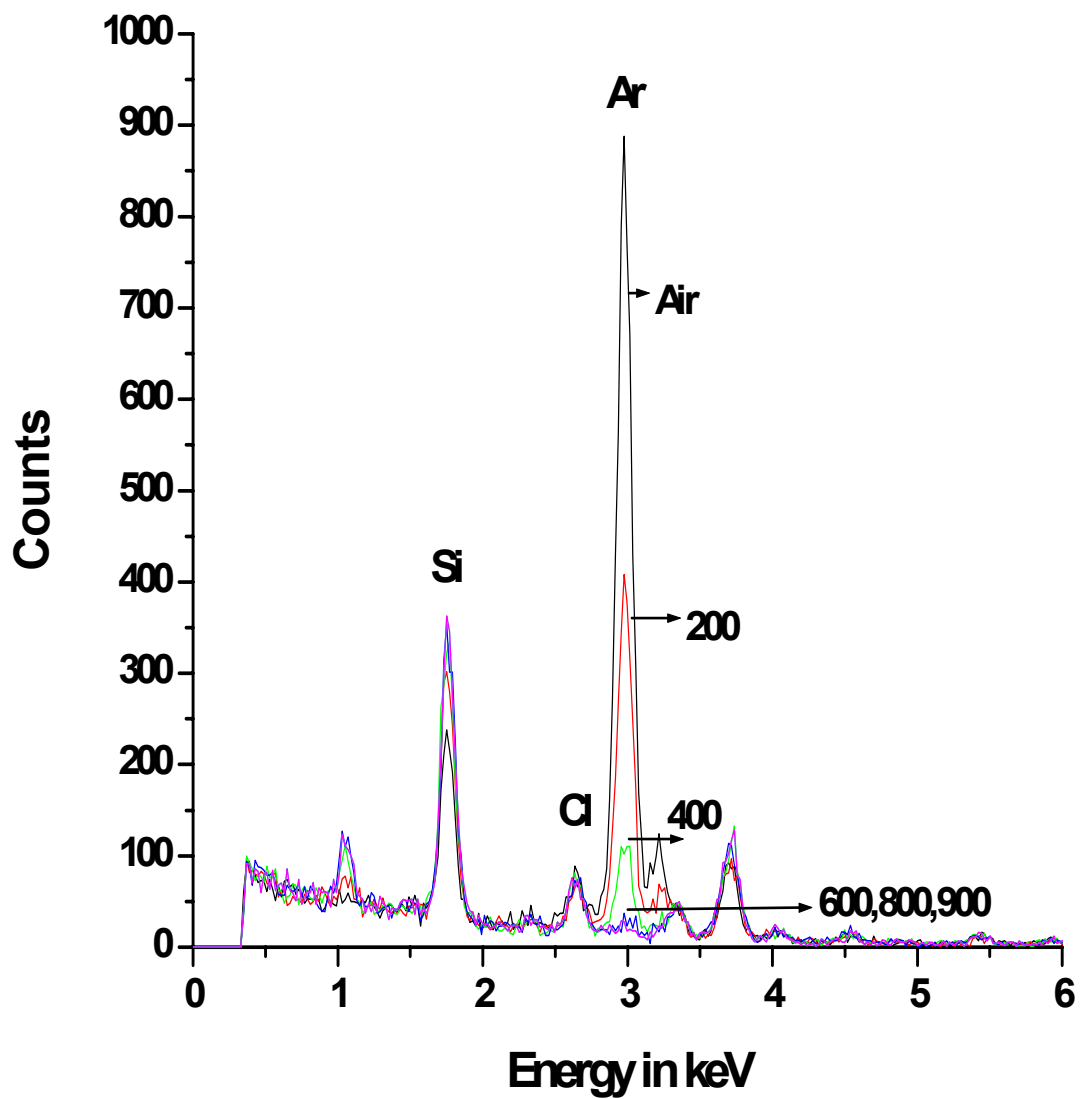


Figure 4.7: Effect of helium gas purging on TXRF spectrum

Table 4.8: Comparison of TXRF (in helium purge) and Ion Chromatography determined chlorine in nuclear material samples

Sample	Cl concentration ($\mu\text{g/mL}$)		TXRF/IC
	TXRF determined	IC determined	
PuO₂ powder			
MDF-24	3.43 \pm 0.08	3.36 \pm 0.02	1.02
MDF-25	12.01 \pm 0.17	10.25 \pm 0.14	1.17
S-63/Cl	2.26 \pm 0.09	2.33 \pm 0.02	0.97
S-63/F	2.47 \pm 0.42	3.01 \pm 0.01	0.82
S-64/Cl	1.81 \pm 0.11	2.12 \pm 0.01	0.86
S-64/F	2.52 \pm 0.61	2.14 \pm 0.01	1.18
T-98/Cl	9.4 \pm 1.1	9.68 \pm 0.28	0.98
T-99/Cl	11 \pm 1	11.59 \pm 0.39	0.95
T-100/Cl	11.37 \pm 0.37	9.75 \pm 0.25	1.17
RVK/Oxide	61.66 \pm 5.57	91.1 \pm 0.51	0.68
Pu alloy			
RVK/Alloy 2A	112 \pm 15	95.64 \pm 0.66	1.17
RVK/Alloy 2B	66.05 \pm 1.16	80.71 \pm 0.35	0.82
MFD/MF/441	3.05 \pm 0.25	4.50 \pm 0.05	0.68
MFD/MF/35	25.82 \pm 4.35	28.09 \pm 0.16	0.92
MFD/MF/440G	1.62 \pm 0.07	1.42 \pm 0.05	1.14

4.4. A Novel Approach for Chlorine Determination in Acidic Medium by TXRF

In addition to nuclear fuels, chlorine is also present at trace levels in different matrices of technological, biological and environmental importance. It is added as a disinfectant in drinking water to kill bacteria and germs and may react with other trace metals present in water to form chlorides [22, 23]. The presence of chlorides above a certain level may cause harmful effects on human health. In view of this, public drinking water standards require chloride levels not to exceed 250 mg/l. Excess chlorine present in water bodies is dangerous to the aquatic life also. For aquatic life protection, chloride levels in water should not exceed 600 mg/l for chronic (long-term) exposure and 1200 mg/l for short-term exposure. Further, the presence of chlorine above a specified limit used in industries can lead to corrosion of the structural materials, e.g. pipes carrying drinking water, boiler sheets of the thermal power plants, etc. [24]. Determination of chlorine in water samples is thus important for human as well as industrial safety.

For trace determination of chlorine in solid samples of industrial materials, it is mandatory to remove the major matrix elements by suitable procedure. For these separations, the solid samples are generally dissolved in acids and the major matrix elements are separated by methods like solvent extraction. If chlorine has to be determined in such dissolved samples, a methodology is required to be developed for its determination in acidic medium.

TXRF has got good potential for determination of chlorine at trace levels, but it is difficult to analyse chlorine in even slightly acid medium as discussed in the previous Section. Thus, a methodology is necessary to determine chlorine in acidic solutions by TXRF. In literature, a report was published which involves addition of silver nitrate as a stabilizer for iodine determination by TXRF [25]. In the present work, an indirect novel method of chlorine determination by TXRF was developed. The method involves addition of a known amount of excess AgNO_3 solution to the sample solution to precipitate all the chloride as AgCl , followed by the determination of the excess (unused) silver in the filtrate by TXRF using cadmium as an internal standard. Then the amount of chlorine is back calculated. This approach avoids the chlorine loss occurring during the direct TXRF determinations.

4.4.1. Experimental

4.4.1a. Sample preparation

Chemicals NaCl and AgNO₃ used for sample preparation were of AR grade. Merck single element cadmium solution was used as an internal standard for TXRF determinations. Stock solutions of NaCl and AgNO₃ in Milli-Q water having Cl⁻ and Ag⁺ concentrations of 1249 µg/mL and 1355 µg/mL, respectively, were prepared. A calibration solution of silver and cadmium having concentrations of 15.9 µg/mL and 25 µg/mL, respectively, was prepared by mixing diluted silver and cadmium solutions. This standard solution was used for experimental determination of sensitivity of silver with respect to cadmium. Five microlitre aliquots of this calibration solution were taken at the centre of pre-cleaned 30 mm diameter quartz sample supports. The solutions on these sample supports were evaporated using a ceramic top hot plate to form a thin film. The dried sample supports were loaded in the TXRF spectrometer for recording their X-ray spectra. Different volumes of NaCl solutions were mixed with 8M HNO₃ and made up by Milli-Q water in such a way that HNO₃ molarity was in the range of 0.4 to 4 M and chlorine concentration was in the range of 1 - 60 µg/mL. The data on the chlorine samples prepared and used in the present work are given in Table 4.9. A slightly excess amount of AgNO₃ solution than that required for stoichiometric precipitation of chlorine as AgCl was added to each solution. The solutions were then shaken and were allowed to settle for about two hours. The resultant precipitate was filtered using a membrane filter paper. The filtrate did not contain any AgCl. To 1 mL of this filtrate, cadmium internal standard solution was added. Ten microlitre aliquots from each of these samples (Table 4.9) were placed at the centre of quartz sample supports and dried in a similar way as described above. The TXRF spectra of each sample thus prepared were recorded in duplicate for a live time of 1500 s. Amount of silver present in filtrate was determined by using Ag K α and Cd K α line intensities, after considering the sensitivity factor. The precision of determinations was calculated from the results of these four measurements. The sample preparations were carried out inside a class 100 clean bench. Experiments to determine the chlorine blank were also done using Milli-Q water in place of sample in HNO₃ and carrying the precipitation with AgCl as described above.

Table 4.9: Details of preparation of sample solutions of chlorine

Sample code	NaCl solution taken		Volume of Milli-Q water added (μL)	Volume of 8M HNO_3 added (μL)	Resultant	
	Volume (μL)	Cl concentration ($\mu\text{g/mL}$)			Cl concentration ($\mu\text{g/mL}$)	HNO_3 molarity (M)
HI-Cl-1	100	1249	1000	1000	59.9	3.8
HI-Cl-2	100	1249	2000	2000	30.5	3.9
HI-Cl-3	100	1249	4000	4000	15.4	4.0
HI-Cl-4	50	1249	4000	4000	7.8	4.0
HI-Cl-5	25	1249	5000	5000	3.1	4.0
HI-Cl-6	400	25	9100	500	1.0	0.4

4.4.1b. Instrumentation

The TXRF spectra were recorded using an ATOMICA EXTRA-II spectrometer with Mo-W target X-ray tube. The spectrometer was operated at 50 kV and 38 mA. Since the useful radiation used for excitation of Ag $K\alpha$ (22.16 keV) and Cd $K\alpha$ (23.17 keV) should be above the absorption edge of Cd $K\alpha$ (26.711 keV), the continuum was used for excitation. The X-rays emitted from the samples were detected using a Si(Li) detector having a resolution of 150 eV (FWHM) at 5.9 keV (Mn $K\alpha$). This instrument is equipped to measure 35 samples sequentially. Each sample was deposited on quartz sample support in duplicate measured for 1500s twice. The precision and average values of TXRF determinations were calculated from these four measurements.

4.4.2. Results and discussion

Direct determination of chlorine by TXRF using Cl K α as the analytical line was discussed earlier. Since it has low X-ray energy and comparatively low fluorescence yield, excitation with WL α and helium purge was used. However, it was not possible to determine chlorine using TXRF in acidic medium samples using these modifications. This problem was circumvented by adding a slight excess amount of AgNO₃ solution in the samples containing chlorine as chlorides for precipitation of chlorine as AgCl. After filtering the solution, the amount of silver remaining in the filtrate was determined by TXRF and the chlorine present in the sample was back calculated. The analytical lines that can be used for TXRF determination of silver are Ag L α (2.984 keV) or Ag K α (22.163 keV). The low energy Ag L α line can be excited by Cr K α or W L α source in an efficient way. However, since it has low fluorescence yield and a strong interference from Ar K α (2.957 keV) which is present in air in appreciable amounts, the measurement must be done in vacuum or helium atmosphere. On the other hand, Ag K α has a high fluorescence yield, does not have any such interference and gives better precision and accuracy due to high intensity of such radiation. Since the instrument offers the possibility of using X-ray tubes with W and Mo targets, it was decided to use W continuum at 50 kV and 38 mA as it is suitable for excitation of Ag K α and Cd K α (internal standard) with K absorption edges 25.514 and 26.711 keV, respectively. The average sensitivity factor of Ag K α with respect to Cd K α was found to be 1.06 ± 0.05 . The TXRF spectrum of the filtrate obtained after chlorine precipitation and mixed with internal standard cadmium is shown in Figure 4.8. It can be seen that Ag K α and Cd K α peaks are well resolved and, therefore, cadmium is a suitable internal standard for such TXRF determinations of silver.

An average blank value of chlorine was found to be 1.5 ± 0.5 $\mu\text{g/mL}$ and was accounted for in the calculations of different samples. A comparison of chlorine concentrations determined by TXRF after blank corrections and expected values in six samples are given in Table 4.10. It was observed that this methodology could be applied to solutions containing more than 7 $\mu\text{g/mL}$ of chlorine with a comparatively better accuracy. The average precision was found to be 11% and the average deviation of TXRF determined values with respect to the expected values was within 10% (chlorine concentration > 7 $\mu\text{g/mL}$). A plot of the expected versus TXRF determined chlorine concentration is shown in Figure 4.9. The regression coefficient value ($R^2=0.995$) and the regression equation confirms that there is a good agreement between the expected and TXRF

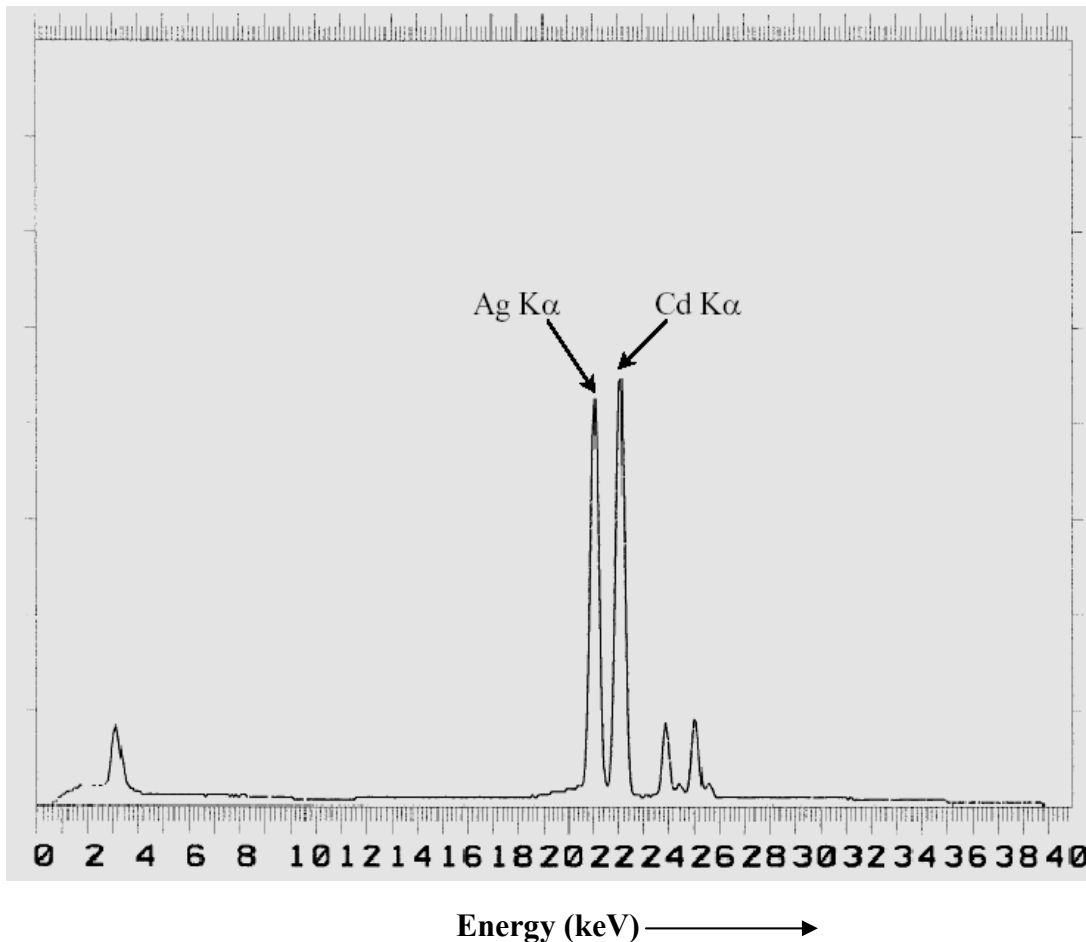


Figure 4.8: A typical TXRF spectrum of the filtrate obtained after addition of cadmium internal standard (Y-axis values are intensity in arbitrary units)

determined chlorine concentrations.

The only limitation of this method is that if other halogens viz. bromine and iodine are also present in the same sample, they also will be precipitated by AgNO_3 and will interfere in chlorine determination. But the presence of these halogens can be confirmed by the TXRF analysis of a small amount of the precipitate.

The TXRF method developed is suitable for determination of chlorine in drinking water, industrial water and acids within its limitations. It is highly promising for determination of

Table 4.10: Comparison of TXRF determined and expected chlorine concentrations

Sample code	Chlorine concentration (µg/mL)		TXRF / Expected ^c
	Expected [*]	TXRF [#]	
HI-Cl-1	59.9	56 ± 4	0.94
HI-Cl-2	30.5	32.6 ± 0.4	1.07
HI-Cl-3	15.4	13 ± 3	0.84
HI-Cl-4	7.8	7 ± 1	0.90
HI-Cl-5	3.1	1.6 ± 0.2	0.50
HI-Cl-6	1.0	2.5 ± 0.2	2.5

* : Expected chlorine concentration calculated on the basis of sample preparation

#:TXRF determined chlorine concentration

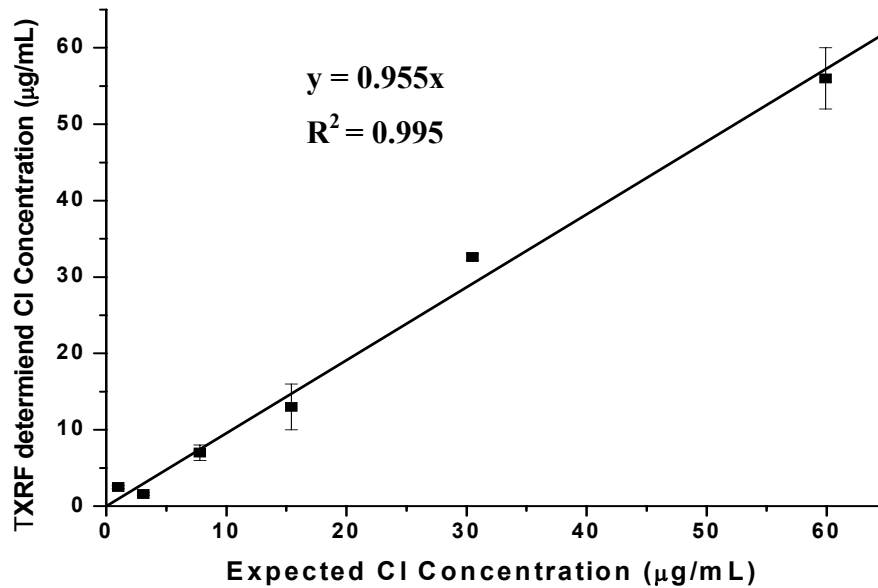


Figure 4.9: A comparison of expected and TXRF determined concentrations of chlorine in samples

chlorine at trace levels in nuclear materials, e.g. uranium, thorium, plutonium, zircaloy etc., after separating the major matrix using solvent extraction from their acidic solutions.

4.5. Conclusions

TXRF can be efficiently applied for the determination of non metals viz. sulphur and chlorine in various nuclear and non-nuclear matrices at trace as well as major concentration levels. The percent deviation and precision for trace element determinations of sulphur were within 15% at a concentration level of 1 $\mu\text{g/mL}$. The accuracy of TXRF method developed was counterchecked with a chemical assay standard $\text{Rb}_2\text{U}(\text{SO}_4)_3$. It was found that the accuracy was within 8% for such determinations. The TXRF methodology developed for chlorine determination in nuclear samples involved separation of the analyte from the matrix by pyrohydrolysis. This method avoids the cumbersome sample dissolution process. The TXRF measurements using helium purge resulted in better precision than the measurements carried out in air atmosphere. Moreover, this methodology helps in the analysis of radioactive samples (plutonium) without putting the spectrometer inside the glove box. A novel TXRF method for trace determination of chlorine in acidic medium samples was developed. The average precision and deviation form expected values, for samples containing chlorine above 7 $\mu\text{g/mL}$, was about 10%. Compared to direct determination of chlorine, it overcomes the problem of loss of chlorine during sample preparation. After suitable modifications, it can be further extended to the determination of chlorine by TXRF in nuclear materials, which require separation of major matrix by solvent extraction leaving behind trace elements in HNO_3 medium.

4.6. References

1. Chiao-Hui Yang, Shih-Jen Jiang, Determination of B, Si, P and sulphur in steels by inductively coupled plasma quadrupole mass spectrometry with dynamic reaction cell, *Spectrochim. Acta, Part B* 59, (2004) 1389.
2. R.A. Nadkarni, B.C. Haldar, Determination of silicon, phosphorus and sulfur in alloy steel by neutron activation analysis, *Anal. Chim. Acta*, 42 (1968) 279.

3. W. Wardencki, Problems with the determination of environmental sulphur compounds by gas chromatography, *J. Chromatogr., A*, 793 (1998) 1.
4. Juliana S.F. Pereira, Paola A. Mello, Diogo P. Moraes, Fábio A. Duarte, Valderi L. Dressler, Guenter Knapp, Érico M.M. Flores, Chlorine and sulfur determination in extra-heavy crude oil by inductively coupled plasma optical emission spectrometry after microwave-induced combustion, *Spectrochim. Acta, Part B*, 64 (2009) 554.
5. Xie Quan, Shuo Chen, Bernhard Platzer, Jingwen Chen, Marion Gfrerer, Simultaneous determination of chlorinated organic compounds from environmental samples using gas chromatography coupled with a micro electron capture detector and micro-plasma atomic emission detector, *Spectrochim. Acta, Part B*, 57 (2002) 189.
6. Travis W Knight, Samim Anghaie, Processing and fabrication of mixed uranium/refractory metal carbide fuels with liquid-phase sintering, *J. Nucl. Mater.*, 306 (2002) 54.
7. Toshiaki Hiyama, Determination of oxygen-to-metal atomic ratio in mixed oxide fuel by non-dispersive infrared spectrophotometry after fusion in an inert gas atmosphere, *Anal. Chim. Acta*, 402 (1999) 297.
8. G. L. Hargrove, R. C. Shepard, Harry Farrar IV, Determination of nitrogen and hydrogen at parts-per-million levels in milligram steel samples, *Anal. Chem.*, 43 (1971) 439.
9. Toshiaki Hiyama, Toshio Takahashi, Katsuichiro Kamimur, Determination of nitrogen in uranium-plutonium mixed oxide fuel by gas chromatography after fusion in an inert gas atmosphere *Anal. Chim. Acta*, 345 (1997) 131.
10. Y.S. Sayi, P.S. Shankaran, C.S. Yadav, G.C. Chhapru, K.L. Ramakumar, V. Venugopal, Determination of total sulphur by vacuum combustion extraction – quadrupole mass spectrometry (VCE-QMS), *Proc. Nat. Acad. Sci. India*, 72 (A) III (2002) 241.
11. K. D. Singh Mudher, K. Krishnan, R. R. Khandekar, M. B. Yadav, N. C. Jayadevan, D. D. Sood, Rubidium uranium trisulphate: A new chemical assay standard for uranium, *J. Radioanal. Nucl. Chem.*, 240 (1999) 183.
12. Valérie Vallet, Ingmar Grenthe, On the structure and relative stability of uranyl (VI) sulphate complexes in solution, *C.R. Chim.*, 10 (2007) 905.
13. D.W. Weater, J. Mulak, R. Banks, W.T. Carnall, The synthesis and characterization of neptunium hydroxy sulfate, $\text{Np}(\text{OH})_2\text{SO}_4$, *J. Solid State Chem.*, 45 (1982) 235.

14. Y.S. Sayi, P.S. Shankaran, C.S. Yadav, G.C. Chhapru, Determination of total sulphur in inorganic compounds – An overview, *Indian J. Chem. Technol.*, 10 (2003) 373.
15. R. Klockenkämper, Total reflection X-ray fluorescence analysis, *Chemical Analysis*, vol. 140, John Wiley & Sons, New York , 1996.
16. M. Mertens, C. Rittmeyer, B.O. Kolbesen, Evaluation of the protein concentration in enzymes via determination of sulfur by total reflection X-ray fluorescence spectrometry - limitations of the method, *Spectrochim. Acta, Part B*, 56 (2001) 2157.
17. S. Steinmeyer, B.O. Kolbesen, Capability and limitations of the determination of sulfur in inorganic and biological matrices by total reflection X-ray fluorescence spectrometry, *Spectrochim. Acta, Part B*, 56 (2001)2165.
18. J.R. Theakar, R. Choubey, G.D. Moan, S.A. Alridge, L. Davis, R.A. Graham, C.E. Colemah, Tenth International Symposium on Zirconium in the Nuclear Industry, ASTM-STP-1245 (1994) 221.
19. S. Jeyakumar, V. V. Raut, K. L. Ramakumar, Simultaneous determination of trace amounts of borate, chloride and fluoride in nuclear fuels employing ion chromatography (IC) after their extraction by pyrohydrolysis, *Talanta*, 76 (2008) 1246.
20. G. E. M. Hall, A. I. MacLaurin, J. Vaive, The analysis of geological materials for fluorine, chlorine and sulphur using pyrohydrolysis and ion chromatography, *J. Geochem. Explor.*, 26 (1986) 177.
21. M. A. Mahajan, M. V. R. Prasad, H. R. Mhatre, R. M. Sawant, R. K. Rastogi, G. H. Rizvi, N. K. Chaudhuri, Modified pyrohydrolysis apparatus for the separation of fluorine and chlorine trace impurities from nuclear fuel samples for quality control analysis, *J. Radioanal. Nucl. Chem.*, 148 (1991) 93.
22. World Health Organization, Guidelines for drinking water quality (2nd edn), vol. 2, World Health Organization: Geneva, 1996.
23. H. M. Murphy, S. J. Payne, G. A. Gagnon, Sequential UV- and chlorine-based disinfectant to mitigate E. coli in drinking water biofilms, *Water Res.*, 42 (2008) 2083.
24. Z. Zhang, E. Stout Janet, L. Yu Victor, R. Vidie, Effect of pipe corrosion scale on chlorine dioxide consumption in drinking water distribution system, *Water Res.*, 42 (2008) 129.
25. I. Varga, Iodine determination in dietary supplement products by TXRF and ICP-AES spectrometry, *Microchem. J.*, 85 (2007) 127.

Chapter-5

ANALYTICAL CHARACTERIZATION OF NUCLEAR MATERIALS BY TXRF: BULK DETERMINATIONS

- 5.1. Introduction
- 5.2. Bulk Determination of Uranium and Thorium in Presence of Each Other by TXRF
 - 5.2.1. Experimental
 - 5.2.1a. *Sample preparation*
 - 5.2.1b. *Instrumentation*
 - 5.2.2. Results and discussion
 - 5.2.2a. *Analytical strategy*
 - 5.2.2b. *Effect of sample amount*
 - 5.2.2c. *Effect of using different internal standards*
- 5.3. Characterization of (U,Th)O₂ Solid Samples by TXRF Without Dissolution
 - 5.3.1. Experimental
 - 5.3.1a. *Sample preparation*
 - 5.3.1b. *Instrumentation*
 - 5.3.2. Results and discussion
- 5.4. Conclusions
- 5.5. References

5.1. Introduction

Apart from the trace determinations in various materials, the composition of the major constituents is also very important for their characterization. The composition of uranium, thorium and plutonium based metallic, oxide, carbide and nitride fuel requires strict quality control by determination of trace as well as major elements present in them. As these materials are very important and precious in nuclear industry and disposal of the waste generated is difficult due to their radioactive nature, it is imperative that sample amount used for such determinations should be as low as possible.

Different analytical methods, both destructive and non-destructive, are used for the determination of the major constituents in different concentration ranges for characterization of nuclear fuel materials [1-3]. Though XRF (WDXRF and EDXRF) methods have the capability of nondestructive analysis and used for major element determination, these methods require different calibration plots for different matrices and composition. Therefore, these techniques are more useful to find out elemental ratios rather than absolute elemental concentrations. TXRF spectrometry, on the contrary, is a destructive but non-consumptive method. It is generally used for trace elements determination but can also be used as a microanalytical technique for determination of major elements after some modifications [4-5]. Micro analysis is chemical identification and quantitative analysis of very small amounts of chemical substances or very small surfaces of material. A conventional XRF technique uses approximately 0.001-10 g of solid sample or 0.1-50 mL solution sample for analysis. In TXRF, depending upon the matrix density, 2-100 μL solution sample and 10 ng-10 μg solid sample is required. The thickness of the specimen is also restricted to a few nanometers. These limitations arise due to the geometry of excitation and counting capability of the detector. In TXRF mode of excitation, the height of the primary beam is usually limited to 20-30 μm . For this reason, the specimen thickness is also restricted to below 10 μm . Moreover if the thickness of the sample is increased, the total reflection condition gets hindered and matrix effect will start to show up. This leads to distinctly poor detection limits just comparable to those of XRF [6].

These two features of TXRF spectrometry namely microanalysis capability and negligible matrix effect are very much beneficial for analysis of nuclear materials. In this Chapter, studies are reported on microanalytical application of TXRF for bulk determination of uranium and thorium in presence of each other in solution form. The absolute amounts of analyte

were determined by adding a single element internal standard. Another novel method of major element determinations in solid samples (pellets, microspheres, etc.) of (U, Th)O₂ by TXRF without sample dissolution was also developed and is described in this Chapter.

5.2. Bulk Determination of Uranium and Thorium in Presence of Each Other by TXRF

Mixed oxides of uranium, thorium and plutonium are the fuels proposed for the third stage of power production by AHWRs. The composition of uranium–thorium oxide fuel to be used should be specific and shall require strict quality control. Most of the methods recommended for major element determination in nuclear fuel elements are wet chemical processes which involve sample dissolution prior to analysis [7-8]. In general, thorium determination is carried out by complexometric titration with ethylene diamine tetra acetic acid (EDTA) [9]. Modified Davies and Gray method and Drummond and Grant method are routinely used for the determination of uranium and plutonium, respectively. These electroanalytical methods give considerably good accuracy and precision (0.2% RSD) for actinide determinations but, require addition of large number of chemicals, strict maintenance of pH and accurate detection of the end point [10]. Interference of other trace impurities present in these samples hinders the analysis by these methods. TXRF can be a very suitable technique, for the applications where a very fast method for verifying the composition of major constituents is required. No further addition of any reagent is required for such determinations, after dissolution is completed. Also presence of common impurities does not affect the TXRF determinations. Using a single internal standard and a single calibration, any element in any matrix can be determined without the requirement of any matrix matched standards.

A few years back Haarich et al. explored the capability of TXRF for analyzing solutions of nuclear reprocessing plants [11]. In this Section, studies on the applicability of TXRF for the bulk determination of uranium and thorium in their mixed matrices in presence of each other in solution are reported. Also the effects of dilution and use of different internal standards on the analytical results were studied.

5.2.1. Experimental

5.2.1a. Sample preparation

Merck uranium standard solution having a concentration of 1000 µg/mL and thorium standard solution having concentration of 891 µg/mL (prepared by dissolving Th(NO₃)₄·5H₂O in suprapure HNO₃ and analysed by complexometric titration using EDTA) were used for the preparation of sample solution mixtures of uranium and thorium. These solutions were mixed after dilution, in different ratios, to obtain mixtures with uranium and thorium contents in the range of 16 to 74% as shown in Table 5.1. Merck single element standard solution of yttrium was used as an internal standard. This standard was mixed in another solution mixture containing known amounts of uranium and thorium for calculating the relative sensitivities of uranium and thorium with respect to yttrium. The composition of the calibration standard used for determining the relative sensitivities of uranium and thorium with respect to yttrium is given in Table 5.2. In the sample solutions of 400 µL each, different volumes of yttrium internal standard were mixed in precleaned PVC bottles and homogenized with the help of an electric shaker. In

Table 5.1: Composition of sample solutions of uranium-thorium mixtures

Sample mixtures	Expected* concentration (µg/mL)		U percent (A/(A+B) *100)	Th percent (B/(A+B) *100)
	Uranium	Thorium		
	A	B		
U-Th-1	0.56	2.79	16.7	83.3
U-Th-2	1.42	2.54	35.9	64.1
U-Th-3	500.0	742.48	40.2	59.8
U-Th-4	3.32	1.97	62.8	37.2
U-Th-5	300.0	133.65	69.2	30.8
U-Th-6	714.24	254.57	73.7	26.3
U-Th-7	142.86	50.91	73.7	26.3
U-Th-8	28.96	9.75	74.8	25.2

*: Expected concentration calculated on the basis of sample preparation

order to see the effect of using different internal standards on the analytical results, Merck single element standard solutions of cobalt and gallium having concentration of 1000 $\mu\text{g/mL}$ were diluted and used as internal standards for analyses of some of the above prepared samples. All dilutions were carried out in 1.5% HNO_3 in Milli-Q water.

5.2.1b. Instrumental conditions

ITAL STRUCTURES TX-2000 TXRF spectrometer was used for measurements. The samples and standard were excited with Mo $K\alpha$ radiation, having energy of 17.6 keV, produced at 40 kV and 30 mA in a dual target X-ray tube having W and Mo targets. The analytical lines of interest were U $L\alpha$, Th $L\alpha$ and internal standards Y $K\alpha$, Co $K\alpha$ and Ga $K\alpha$. For each measurement, 10 μL aliquot of the sample was deposited on the center of quartz sample supports in duplicate and dried under an IR lamp to make a thin film of the sample suitable for TXRF measurements. Each dried specimen was counted twice for a live time of 1000s.

5.2.2. Results and discussion

5.2.2a. Analytical strategy

Determination of the major constituents in U-Th mixed sample solutions was carried out using yttrium internal standard. Yttrium was chosen as internal standard because Y $K\alpha$ (14.956 keV) energy is near to U $L\alpha$ (13.61 keV) and Th $L\alpha$ (12.97 keV) energies and it can be excited by Mo $K\alpha$ (17.44 keV) radiation in an efficient way. TXRF spectrum of one such sample is

Table 5.2: Composition of calibration standard solution used for relative sensitivity determinations of uranium and thorium with respect to yttrium

S.No.	Element	Concentration ($\mu\text{g/mL}$)
1	Uranium	28.57
2	Thorium	10.18
3	Yttrium	0.99

shown in Figure 5.1. Some impurities e.g. Fe, Ca and Zn are present in the sample and can be seen in the TXRF spectrum. The relative sensitivities of uranium and thorium with respect to yttrium were determined to be 0.345 ± 0.006 and 0.306 ± 0.009 , respectively. The analytical results obtained by TXRF analyses were compared with the expected concentrations of uranium and thorium in these solution mixtures and are given in Tables 5.3 and 5.4. It was observed that the precision (n=4) of the TXRF method for uranium determination was better than 1.6% (1 s) whereas for thorium determinations it was better than 2.2% (except U–Th-6) (1 s). The average deviations of uranium and thorium determined by TXRF with respect to the expected values calculated on the basis of sample preparation were 2.3% and 3.1% (except U–Th-5), respectively.

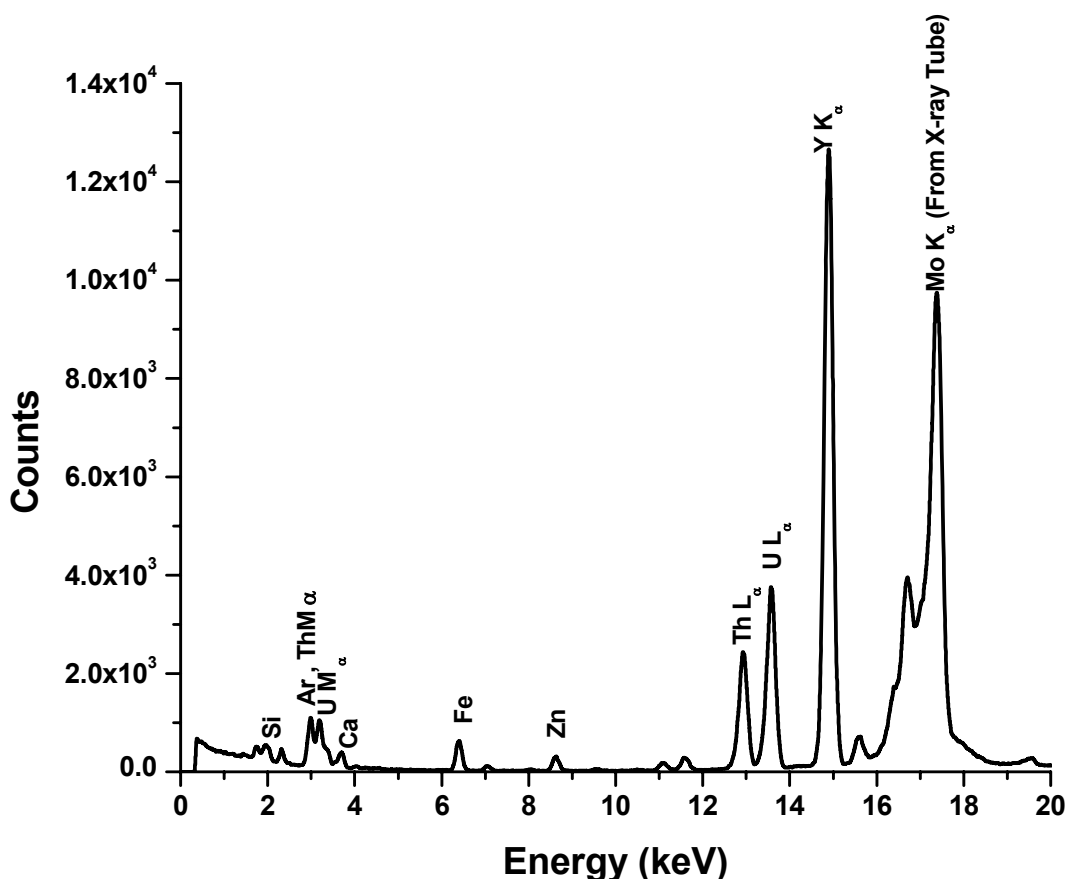


Figure 5.1: TXRF spectrum of a uranium-thorium synthetic sample (U-Th-4) mixed with internal standard

Table 5.3: Comparison of TXRF determined and expected uranium concentrations in sample solutions

S. No.	Sample mixture	Uranium concentration ($\mu\text{g/mL}$)		TXRF ³ (ng)	TXRF/Expected
		Expected ¹	TXRF ²		
1.	U-Th-1	0.56	0.53 ± 0.01	5.3	0.946
2.	U-Th-2	1.42	1.355 ± 0.009	13.55	0.954
3.	U-Th-3	500	523 ± 18	5230	1.046
4.	U-Th-4	3.32	3.29 ± 0.07	32.9	0.991
5.	U-Th-5	300	297 ± 5	2970	0.990
6.	U-Th-6	714.24	727 ± 8	7270	1.018
7.	U-Th-7	142.86	143 ± 2	1430	1.001
8.	U-Th-8	28.96	29.0 ± 0.2	290	1.001

¹: Expected concentration on the basis of dilution of the standard solution.

²: Average of TXRF determined concentrations of four measurements ± 1 s.

³: TXRF determined uranium with $10 \mu\text{L}$ sample size.

Table 5.4: Comparison of TXRF determined and expected thorium concentrations in sample solutions

S. No.	Sample mixtures	Thorium concentration ($\mu\text{g/mL}$)		TXRF ³ (ng)	TXRF/Expected
		Expected ¹	TXRF ²		
1.	U-Th-1	2.79	2.88 ± 0.02	28.8	1.032
2.	U-Th-2	2.54	2.55 ± 0.09	25.5	1.004
3.	U-Th-3	742.48	721 ± 1	7210	0.971
4.	U-Th-4	1.97	1.89 ± 0.06	18.9	0.959
5.	U-Th-5	133.65	152 ± 8	1520	1.137
6.	U-Th-6	254.57	242 ± 40	2420	0.951
7.	U-Th-7	50.91	53.8 ± 0.2	538	1.057
8.	U-Th-8	9.75	9.8 ± 0.2	98	1.005

¹: Expected concentration on the basis of dilution of the standard solution.

²: Average of TXRF determined concentrations of four measurements ± 1 s.

³: TXRF determined thorium with 10 μL sample size.

5.2.2b. Effect of sample amount

In TXRF, the amount of sample loaded for measurement on sample supports affects the analytical results. If the sample amount is too high, then the matrix effect becomes appreciable. In Table 5.3, it can be seen that the average precision and percentage deviation from the expected values of the uranium were 1.35% and 2.21%, respectively, for uranium concentration below 150 $\mu\text{g/mL}$. These values have increased to 2.08 % and 2.46 % for uranium concentrations above 150 $\mu\text{g/mL}$. Similarly from Table 5.4, it can be seen that for thorium the average precision and percentage deviation from the expected values were 1.96% and 2.77%, respectively, for thorium concentrations below 150 $\mu\text{g/mL}$. These values changed to 2.70 % (except U-Th-6) and 3.92 %

(except U-Th-5) for thorium concentrations above 150 $\mu\text{g/mL}$. Hence, it can be concluded that TXRF analytical values become slightly poor when the total matrix amount is above 400 $\mu\text{g/mL}$ including both uranium and thorium. For better precision and accuracy, it will be advisable to dilute the samples of uranium and thorium in this concentration range. For higher range of concentrations, the absorption and enhancement effects contribute to comparatively poor precision and accuracy of the method. The plot of expected uranium calculated on the basis of sample preparation versus TXRF determined concentrations of uranium in the samples gave a regression coefficient 0.999 for a linear fit. This plot is given in Figure 5.2. Similarly the plot of expected thorium versus TXRF determined thorium concentration in U-Th matrix gave a regression coefficient of 0.998. The regression equations of $y = 1.022 * X$ and $y = 0.974 * X$ (Figure 5.2) for uranium and thorium, respectively, shows that there is a good agreement between the expected and TXRF determined concentrations in both these cases and the matrix effects are negligible.

5.2.2c. Effect of using different internal standards

One of the advantages of TXRF technique over EDXRF and WDXRF is that same calibration is valid for different matrices, because TXRF has negligible matrix effects. Therefore, different internal standards can be used for elemental determinations irrespective of their energies and absorption edges. In order to experimentally investigate the effect of using different internal standards on the analytical results of uranium and thorium determinations, cobalt, gallium and yttrium Merck single element standards were mixed in two synthetic samples of uranium and thorium prepared in similar way as described above. The absorption edges and energies of Y K line are 17.01 keV and 17.44 keV (Y $K\alpha$), Ga K line are 10.36 keV and 9.24 keV (Ga $K\alpha$) and Co K line are 7.70 keV and 6.925 keV (Co $K\alpha$), respectively. The three different internal standards were chosen in such a way that their energies and absorption edges are in the different energy regions. The results of these determinations are given in Table 5.5. It can be seen that these results are comparable with one another as well as with the expected uranium and thorium concentrations with respect to precision and accuracy. From these observations, it can be concluded that TXRF method gives a flexibility of using different internal standards.

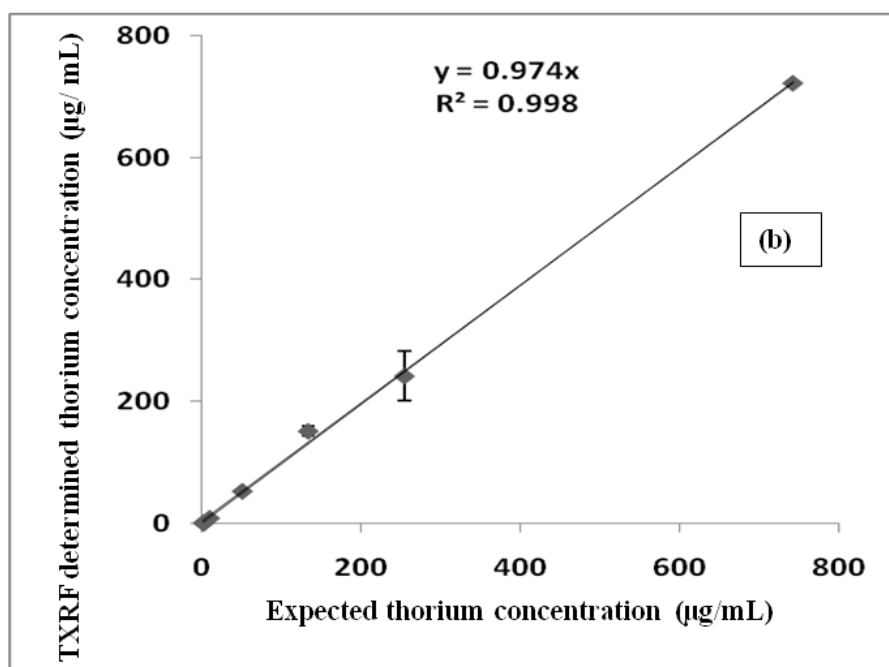
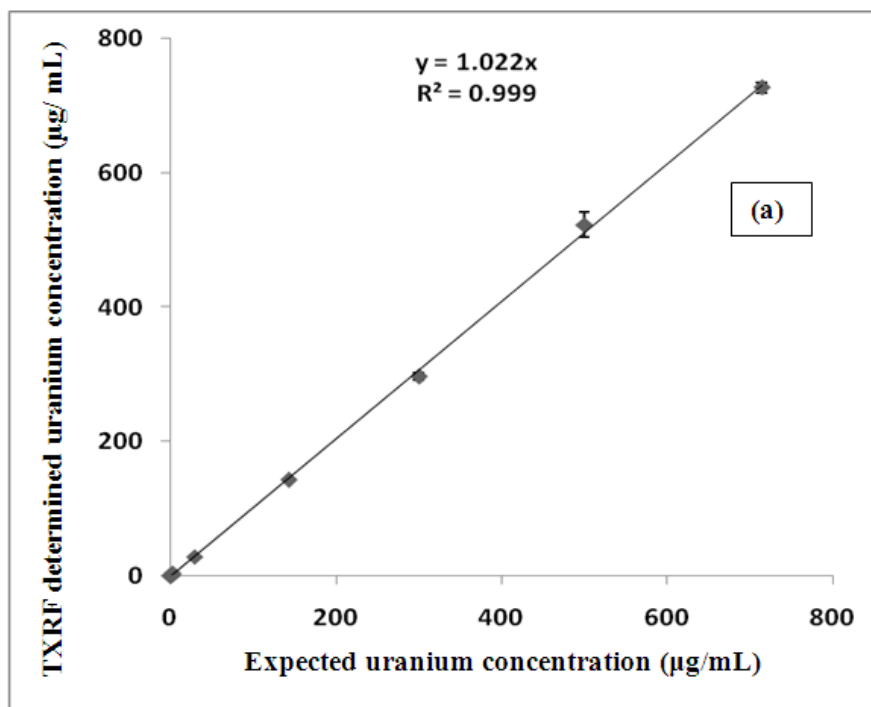


Figure 5.2: Calibration plot of TXRF determined and expected concentration of (a) uranium and (b) thorium in U-Th samples

Table 5.5: TXRF determination of uranium and thorium using Co, Ga and Y as internal standards

Sample	Internal standard	Uranium ($\mu\text{g/mL}$)		
		Expected *	TXRF [#]	TXRF/ Expected
U-Th-IS-1	Co	2.22	2.31 ± 0.06	1.04
	Ga	2.22	2.21 ± 0.04	1.00
	Y	2.22	2.20 ± 0.02	0.99
U-Th-IS-2	Co	1.81	1.81 ± 0.07	1.00
	Ga	1.81	1.78 ± 0.05	0.98
	Y	1.81	1.77 ± 0.04	0.98

Sample	Internal standard	Thorium ($\mu\text{g/mL}$)		
		Expected *	TXRF [#]	TXRF/ Expected
U-Th-IS-1	Co	1.32	1.38 ± 0.05	1.05
	Ga	1.32	1.32 ± 0.03	1.00
	Y	1.32	1.31 ± 0.01	1.00
U-Th-IS-2	Co	1.62	1.59 ± 0.05	0.99
	Ga	1.62	1.57 ± 0.04	0.97
	Y	1.62	1.56 ± 0.02	0.97

*: Expected concentration on the basis of dilution of the standard solution.

[#]: Average of TXRF determined concentration of four measurements \pm standard deviation (1s).

*: Ratio of TXRF determined and expected concentrations.

5.3. Characterization of (U,Th)O₂ Solid Samples by TXRF Without Dissolution

Analytical characterization using non-destructive methods has many advantages over the wet chemical analysis techniques for characterization of nuclear samples. One of most beneficial advantages is elimination of sample dissolution. Any dissolution process is cumbersome and time consuming. It also results in addition of chemical reagents which leads to the incorporation of impurities. These impurities cause discrepancy in the analytical results. Among the various nuclear fuels used in nuclear industry, dissolution of thorium based fuels is very difficult. ThO₂ and ThO₂ based fuels are chemically inert and do not dissolve even in concentrated nitric acid. Similar is the case with plutonium and its compounds [12-14]. Moreover, compared to green pellets, sintered pellets are very difficult to dissolve. Generally, nitric acid is used for sample dissolution, but these materials require addition of HCl or HF. The fluoride ions are used as catalysts for speeding the rate of dissolution. These are very corrosive chemicals which cause problems during dissolution.

TXRF is a promising technique for the analysis of nuclear materials because of its various features. However, it requires samples in the form of liquid for analysis. Dissolution or digestion is necessary for analysis of solid samples. If TXRF can be used directly for solid sample analysis, the analysis time and cumbersome sample preparation process can be reduced to a large extent with minimum sample handling. Solid samples can be presented for TXRF analysis in the form of suspension or slurry for finely powdered materials, as a thin section of organic material, as a thin foil for metals or as polymer [5, 15-16]. The thickness of the film should be restricted to a few nanometers. Then for quantification, a drop of internal standard is added over the deposited sample. Another way of sample preparation for solid samples is gently rubbing the sample on quartz sample support or the sample support is rubbed on a fixed object. In both the cases, a minute quantity of the material will get smeared on the support. When such supports are taken for TXRF analysis, a qualitative idea of the composition of the material is obtained and the relative percentage of elements present can be calculated.

In the present Section, some studies to assess the feasibility of TXRF determination of major elemental composition of different types of (U,Th)O₂ samples in the form of sintered and green pellets, powders and microspheres without dissolution are reported. The results of TXRF

determinations of uranium are compared with the expected uranium amounts as well as cell parameters of these solid solutions determined by X-Ray Diffraction (XRD), as the cell parameter varies with the composition of solid solutions [17].

5.3.1. Experimental

5.3.1a. Sample preparation

Standard solutions of uranium and thorium were prepared by diluting the single element standard solutions of 1000 $\mu\text{g/mL}$ to a concentration of 9.9 $\mu\text{g/mL}$ with 1.5% supra pure HNO_3 . These standards were mixed together and used for determining the relative sensitivity of uranium with respect to thorium. Solid solution samples of $(\text{U,Th})\text{O}_2$ having uranium atom percent varying in the range of 2 to 50% as well as pure UO_2 and ThO_2 samples in the form of pellets, powders and sol-gel microspheres with different sample preparation techniques were used for TXRF analyses. The pellet samples were gently rubbed on the clean quartz sample supports in such a way that very small amount, not visible with naked eyes, was transferred on them. For powder samples, about 10 mg of the sample and one sol-gel microsphere were ground separately in a pestle-mortar for about fifteen minutes, to get powder as finely as possible. A few drops of collodion solution were added in these powders to make a paste. Then with the tip of the pestle, a few μg of the sample was transferred on clean quartz sample supports. These supports were presented for TXRF measurement. Four specimens were prepared for each sample and each specimen was measured twice.

5.3.1b. Instrumentation

An ITAL Structures, TXRF spectrometer, TX-2000 was used for measurements. The Mo K_α radiation produced in an X-ray tube having Mo-W dual targets and operated at 40 kV and 30 mA was used for sample excitation. A live time of 1000s was used for the measurement of standards for determining the relative sensitivity. The solid solution samples supports were measured for 500s each. The precision was calculated for $n=8$.

XRD measurements were made using a STOE X-ray diffractometer with Cu K_α radiation ($\lambda= 1.5406\text{\AA}$) produced at 55 kV and 35 mA, monochromatized with a graphite monochromator.

The XRD patterns were recorded in 2θ range from 25 to 60 degrees. The XRD patterns were indexed using computer program “TREOR”.

5.3.2. Results and discussion

For the analysis of solid samples by TXRF, two main difficulties that should be addressed for better quality results are non-uniformity and bigger particle size. Since TXRF is a microanalytical technique, non-uniformity in the sample will cause a large deviation in the analytical results. Bigger particle size will result in matrix effect and, therefore, particle size should be minimum. Despite best efforts to mix ThO_2 and UO_2 powder in different ratios along with an internal standard Y_2O_3 by grinding for a long time and dispersing a very small amount of this mixture in 10 mL of water with the help of a shaker and ultrasonicator, a wide range of spread in analytical results was obtained. The main reason for this spread was attributed to non-uniform mixing of the analytes and the internal standard. The pellets, powder or microspheres of $(\text{U,Th})\text{O}_2$ solid solutions which are used as fuel have a good compositional uniformity. Such oxides with different ratios of uranium and thorium were used for the analyses. Solid solutions are solid-state solutions in which an atom or ion of one element from the parent structure, directly replaces an atom or ion of similar size and same charge without changing the crystal structure of the parent. Some systems exhibit complete range of solid solution. The criterion for formation of such solid solution is that two end member phases must be isostructural, but vice versa is not true. Both uranium and thorium oxide are cubic system and, therefore, form solid solution in complete range. TXRF can be applied for the direct analyses of such $(\text{U,Th})\text{O}_2$ solid solutions in the form of pellets, powders and microspheres for determination of uranium using thorium as an internal standard.

For TXRF determinations of uranium using thorium as internal standard, the relative sensitivity of uranium with respect to thorium was determined using the standard solutions. The pellet samples, both sintered and green, were rubbed on the center of quartz sample supports gently without scratching the support. The microspheres were very small in size and could not be rubbed on the sample support by holding it. Due to this reason, one microsphere sample was finely ground in pestle mortar with collodion and a very small portion of it was placed on the sample support with the help of the tip of pestle. Powder samples were also deposited on the

sample supports in similar way. The TXRF spectra of the samples thus prepared were recorded for 500 s and uranium was determined using thorium as an internal standard. One such TXRF spectrum of (U,Th)O₂ sample containing 4% uranium is shown in Figure 5.4. Using the relative sensitivity value of uranium with respect to thorium, obtained from measurement of the standard solutions, the uranium atom percent was calculated and the composition of uranium in (U,Th)O₂ solid solutions were determined. The expected and TXRF determined uranium percent in solid solutions are given in Table 5.6. It was seen that the average precision of uranium atom percent determined in the solid solutions was 2% and was comparable with the values obtained from

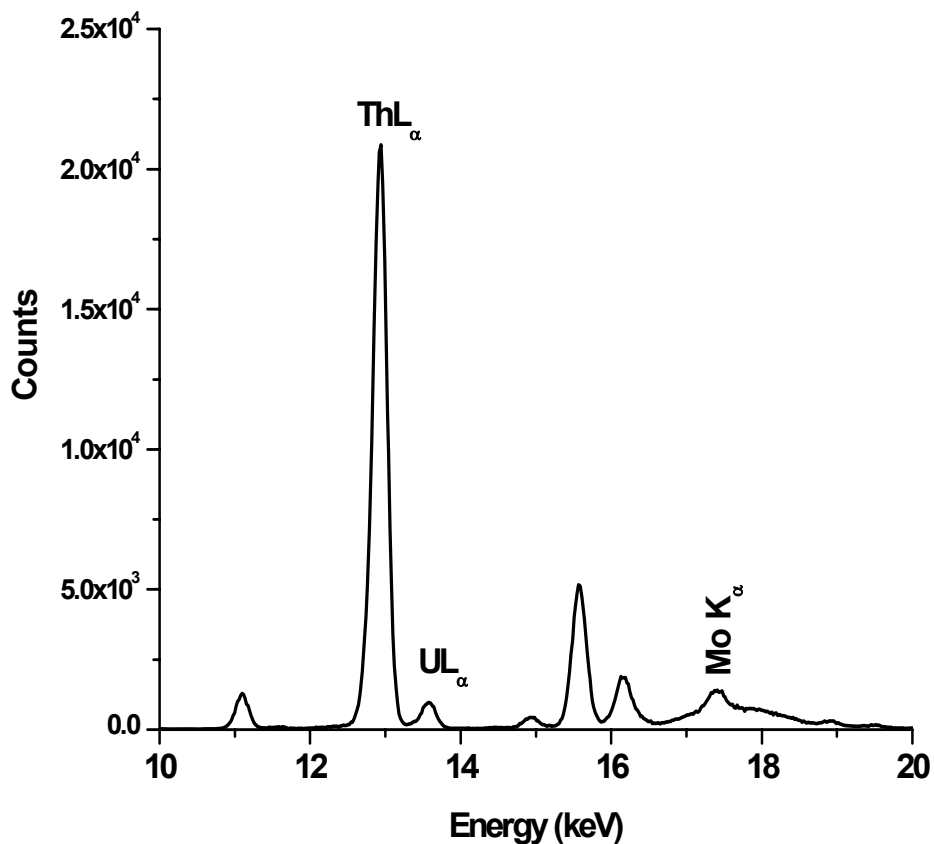


Figure 5.3: TXRF spectrum of (U_{0.04}Th_{0.96})O₂ sample measured after rubbing the pellet on sample support

Table 5.6: Results of TXRF determined composition of solid solutions and their expected values

S. No.	Uranium atom percent		TXRF/ Expected
	Expected *	TXRF determined	
1	0	0.20 ± 0.01	-
2	2	2.18 ± 0.05	1.09
3	4	4.09 ± 0.04	1.02
4	6	6.19 ± 0.13	1.03
5	10	11.17 ± 0.17	1.12
6	30	28.68 ± 0.24	0.94
7	50	49.62 ± 0.34	0.97
8	100	99.57 ± 0.59	0.996

*: Calculated on the basis of sample preparation

samples in form of solution. The average deviation of TXRF determined values of uranium atom percent with the expected values was 4.5%.

A plot of expected and TXRF determined uranium present in solid solutions is given in Figure 5.5. From this graph it can be seen that the agreement between the expected and TXRF determined uranium atom percent is quite satisfactory.

XRD is used to identify the crystal structure and also obtain information about the composition of the solid solution. The unit cell undergoes a small contraction or expansion as the composition varies [18]. In a crystal when a relatively smaller atom is replaced by a larger atom, then the d spacing (cell parameter) increases. So the whole pattern shifts to lower 2θ values. The XRD patterns of the solid solutions analysed by TXRF are shown in Figure 5.6. It can be seen that there is a systematic change in 2θ values with increase in uranium atom percent. The ionic

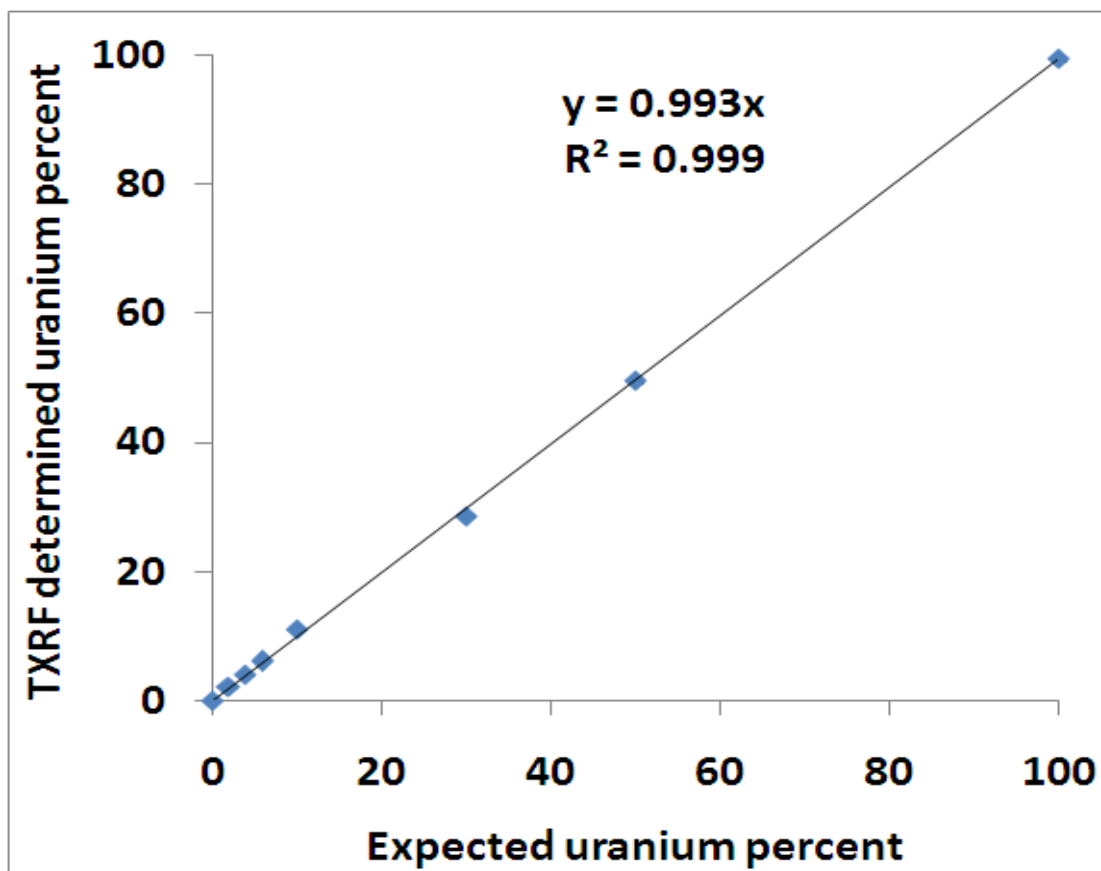


Figure 5.4: Expected and TXRF determined uranium percent in (U,Th)O₂ solid solution samples

radius of uranium (IV) ion is 97 pm and that of thorium (IV) ion is 102 pm. So, when thorium ion is replaced by uranium ion in the parent structure of ThO₂, the lattice parameter of the unit cell decreases and the 2θ value increases as seen in the Figure. The cell parameter of the (U,Th)O₂ solid solutions determined from the indexing of the XRD patterns using TREOR are included in Table 5.7. According to Vegard's law, unit cell parameter should change linearly with composition [19]. Hence the composition of a solid solution may be obtained if the d spacing of the XRD pattern can be determined accurately. It was found that the cell parameter 'a' varied linearly with the expected and TXRF determined uranium percentage in these solid solutions. The plot and equation correlating the expected and TXRF determined uranium atom percent and cell parameters determined by XRD for the solid solution are shown in Figures 5.6 and 5.7, respectively. It can be seen that both the graphs are almost identical in nature further

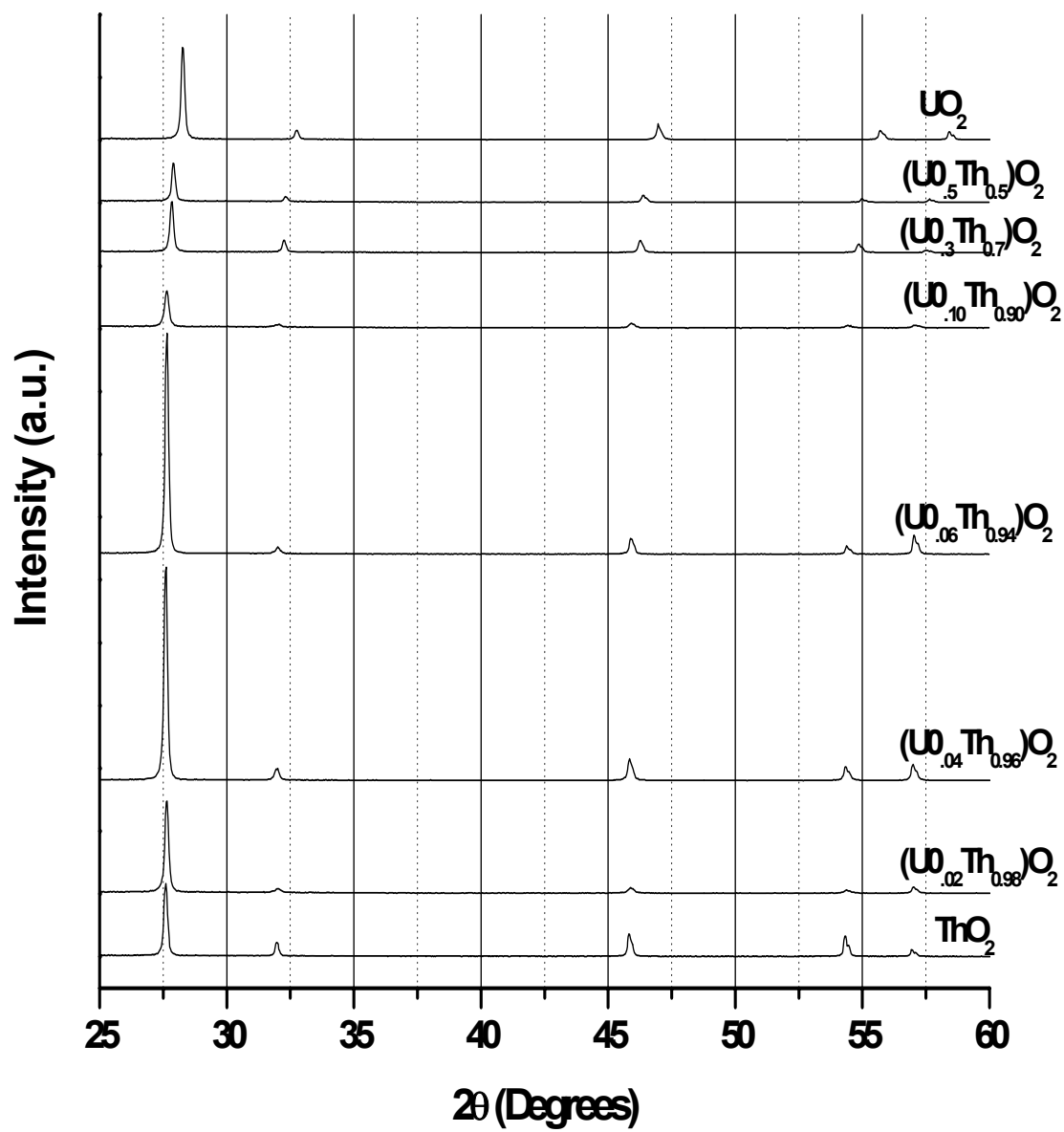


Figure 5.5: XRD patterns of (U,Th)O₂ solid solutions

Table 5.7: Results of TXRF determined composition of solid solutions and their cell parameters

S. No.	Uranium atom percent		Deviation (%)	Cell parameter (Å)
	Expected*	TXRF determined		
1	0	0.20	-	5.5958 (3)
2	2	2.18	9	5.5903 (4)
3	4	4.09	2.25	5.5912 (4)
4	6	6.19	3.17	5.5883 (5)
5	10	11.17	11.7	5.5858 (4)
6	30	28.68	-4.4	5.5455 (3)
7	50	49.62	-0.76	5.5339 (5)
8	100	99.57	-0.43	5.4666 (5)

*: Calculated on the basis of sample preparation

confirming a good agreement between the TXRF determined and expected uranium atom percent values.

A comparison of the plots in Figures 5.4 and 5.7 shows that the determination of uranium percent in solid solutions using Vegard's law is less sensitive and more prone to errors whereas the TXRF method of compositional characterization for solid solutions is very sensitive. Moreover, the TXRF method has an advantage that it can be applied for crystalline as well as amorphous materials and is fast compared to quantitative analysis by Vegard's law. Also in addition to uranium analysis, this method gives information about other elements/impurities present in the (U,Th)O₂ samples. Finally, the study indicates that the TXRF method of bulk characterizations of (U,Th)O₂ can be extended to carbide, oxide and nitride samples used as nuclear fuel. Thus, TXRF method can be applied for the compositional characterization of (U,Th)O₂ samples with very less sample amount and as a routine used analytical technique.

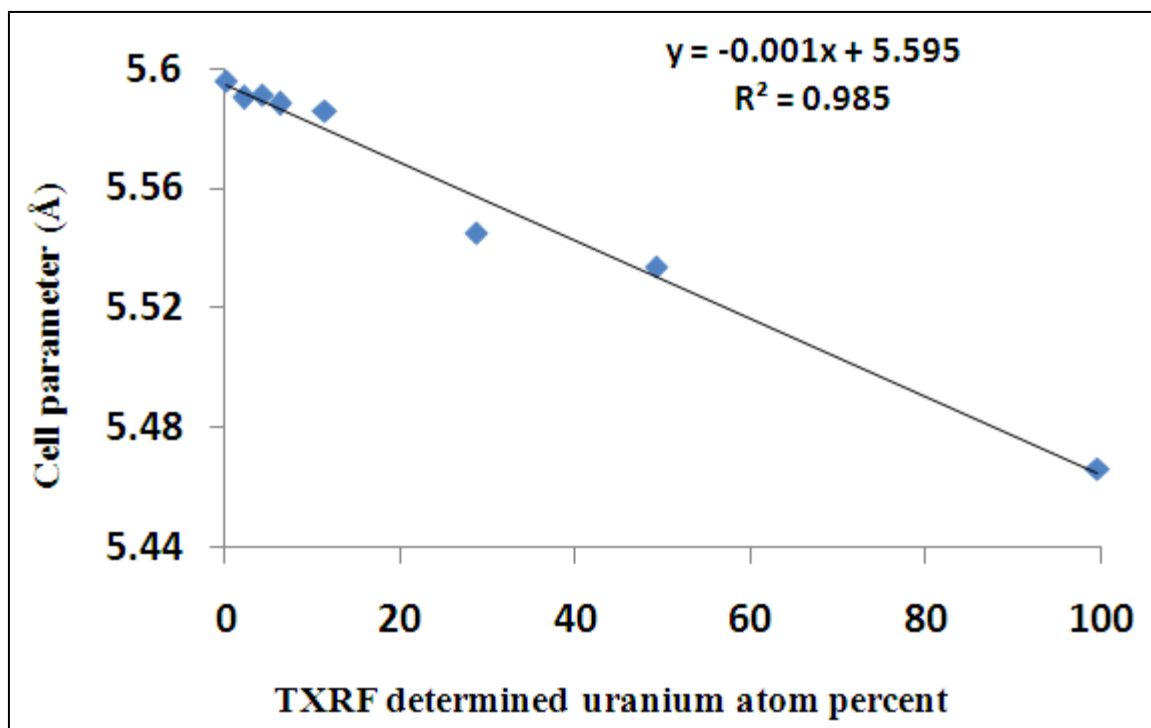


Figure 5.6: Cell parameter versus TXRF determined uranium atom percent

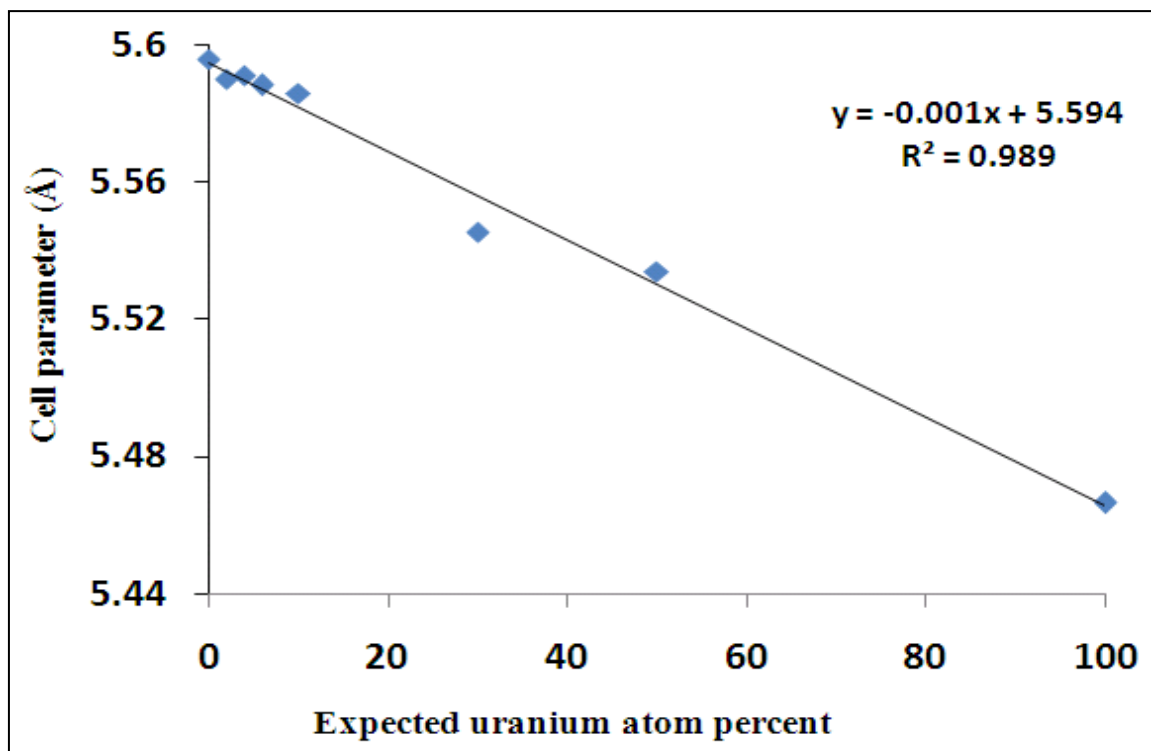


Figure 5.7: Cell parameter versus expected uranium atom percent

5.4. Conclusions

The microanalytical capability of TXRF for characterization of nuclear related materials was assessed. It is concluded that TXRF can be used for the bulk determination of uranium and thorium in presence of each other in solution as well as in solids. The advantages of this method are requirement of very small sample amount (in nanogram range) for analysis. This feature of TXRF will be helpful in minimizing the radioactive waste generated during analysis and the dose imparted to the analyst will also be reduced. The precision obtained was better than 2% in both the solution and the solid samples. The deviation of the TXRF determined values from the expected values for most of the cases was less than 2% (1 s). For solution samples, it was observed that there was not much effect on the analytical results when the sample amount varied from 30 ng to 12 µg (~3 orders of magnitude) including both uranium and thorium. Also the matrix effect was negligible in this range. Hence, this method has the flexibility of using more than one internal standard and the only limitation is that it requires dissolution of the sample. For solid samples, the homogeneity factor is important. If the sample is not homogenous, then accurate analysis cannot be done. This study will initiate a new kind of application of TXRF as a microanalytical technique for the bulk determination of constituents in radioactive samples.

5.5. References

1. Characterization and Quality Control of Nuclear Fuels, C. Ganguli, R.N. Jayaraj (Eds.), Allied Publishers, New Delhi (2002).
2. Iwao Okumura, Sachio Shimada, Kunio Higashi, Spectrophotometric determination of uranium in thorium tetrafluoride, *Anal. Chem.*, 45 (1973)1945.
3. H.A. Woltermann, R.R. Eckstein, P.L. Redding, S.A. Tomes Determination of thorium in plutonium by X-ray spectrometry, *J. Nucl. Mater.*, 54 (1974) 117.
4. Alex von Bohlen, Friedrich Meyer, Microanalysis of old violin varnishes by total-reflection X-ray fluorescence, *Spectromchim. Acta, Part B*, 52 (1997) 1053.
5. Reinhold Klockenkämper, Alex von Bohlen, Survey of sampling techniques for solids suitable for microanalysis by total-reflection X-ray fluorescence spectrometry, *J. Anal. At. Spectrom.*, 14 (1999) 571.

6. A. Prange, Total reflection X-ray Spectrometry: Method and applications, *Spectrochim. Acta, Part B*, 44 (1989) 437.
7. P.A. Pella, A.V. Baeckmann, The x-ray spectrometric determination of uranium and plutonium in solutions of spent nuclear fuels, *Anal. Chim. Acta*, 47 (1969) 431.
8. Omer Cromboom, Lothar Koch, Roger Wellum, The determination of uranium and plutonium in fuel materials by titration and by K-edge absorption, *J. Nucl. Mater.*, 178 (1991) 249.
9. Keshav Chander, S. P. Hasilkar, A. V. Jadhav, H. C. Jain, A titrimetric method for the sequential determination of thorium and uranium, *J. Radioanal. Nucl. Chem.*, 174 (1993) 127.
10. G.C. Goode, J. Herrington, W.T. Johns, High-precision analysis of nuclear materials by constant-current coulometry: Part I Determination of Uranium, *Anal. Chim. Acta*, 37 (1967) 445.
11. M. Haarich, A. Knöchel, H. Salow, Einsatz der totalreflexions – röntgenfluoreszenzanalyse in der analytik von nuklearen wiederaufarbeitungsanlagen, *Spectrochim. Acta, Part B*, 44 (1989) 543.
12. Erich Zimmer and Erich Merz, Dissolution of thorium-uranium mixed oxides in concentrated nitric acid, *J. Nucl. Mater.*, 124 (1984) 64.
13. K. Anantharaman, V. Shivakumar, D. Saha, Utilisation of thorium in reactors, *J Nucl. Mater.*, 383 (2008) 119.
14. Dissolution of plutonium dioxide- A critical review, Jack L.Ryan, Lane A. Bray, Actine separations, ACS symposium Series Vol. 117, ACS publications (1980).
15. R. Fernández-Ruiza, V. Bermúdez, Determination of the Ta and Nb ratio in $\text{LiNb}_{1-x}\text{Ta}_x\text{O}_3$ by total reflection X-ray fluorescence spectrometry, *Spectrochim. Acta, Part B*, 60 (2005) 231.
16. D. von Czarnowski, E. Denkhaus, K. Lemke, Determination of trace element distribution in cancerous and normal human tissues by total reflection X-ray fluorescence analysis, *Spectrochim. Acta, Part B*, 52 (1997) 1047.
17. I.C. Cosentino, R. Muccillo, Lattice parameters of thoria–yttria solid solutions, *Mater. Lett.*, 48 (2001) 253.

Chapter-6

DETERMINATION OF URANIUM BY TXRF IN NON-CONVENTIONAL RESOURCES: SEAWATER AND FERTILIZER

- 6.1. Introduction
- 6.2. Uranium Determination in Seawater by TXRF
 - 6.2.1. Experimental
 - 6.2.1a. *Sample preparation*
 - 6.2.1b. *Instrumentation*
 - 6.2.2. Results and discussion
 - 6.2.2a. *Selective extraction of uranium by diethyl ether*
 - 6.2.2b. *Uranium determination in seawater*
- 6.3. Determination of Uranium in Fertilizer Samples by TXRF
 - 6.3.1. Experimental
 - 6.3.1a. *Sample preparation*
 - 6.3.1b. *Instrumentation*
 - 6.3.2. Results and discussion
- 6.4. Conclusions
- 6.5. References

6.1. Introduction

Uranium is one of the technologically important elements. It has got wide applications in various fields of science and technology. It is the main component in nuclear industry and is used as fuel in nuclear reactors for electricity generation. In addition, it is also used as a catalyst in many organic reactions, in semiconductor industries, etc. [1-3]. Uranium is mined from its ores and with growing demands and limited availability, its exhaustion within 100 years will be apprehensive. The various uranium ores are pitchblende, uraninite, coffinite and carnotite which are present in earth crust. Different scientific groups all over the world are in search of new conventional and non-conventional sources of uranium. In the terrestrial crust, uranium does not occur as a free metal but always exists as compounds of oxide, silicate or potassium. The average concentration of uranium in earth's crust is about 4 $\mu\text{g/g}$ and is more abundant than other heavy metals such as mercury and silver. Its concentration in seawater is around 3 $\mu\text{g/L}$ and is distributed uniformly in all the world's oceans. In surface freshwater (rivers and lakes), the average concentration is as low as 0.5 $\mu\text{g/L}$ and depending on the location and contamination of the water, it can reach concentrations as high as 500 $\mu\text{g/L}$ [4]. Another major unconventional source of uranium is the phosphate rocks. Depending on the location, uranium concentration varies and is considered to be present in the range of 1-600 ppm [5] in these phosphate rocks. Digestion of phosphate rocks in fertilizer production process leads to incorporation of uranium in the resulting phosphate fertilizers. The uranium concentration can be as high as a few hundreds of ppm in phosphate fertilizers. Even phosphoric acid, manufactured using phosphate rocks, is a rich non-conventional source of uranium.

Determination of uranium in seawater as well as phosphate fertilizers is important from the point of view of its recovery as well as environmental concerns. Uranium is present in the environment and water bodies due to leaching of ore deposits and release from various industries. Since it is radioactive and toxic, it has considerable effects on biological organism and the human food chain. The provisional guideline value recommended by WHO (World Health Organization) for uranium in drinking water is 15 $\mu\text{g/L}$ [6]. Only a few techniques such as spectrophotometry, alpha/gamma spectrometry and laser fluorometry are available for the determination of low-level concentrations of uranium in various matrices [4, 7-11]. These techniques require tedious separation and preconcentration steps.

In the present work, studies were carried out to determine uranium in unconventional sources like seawater and fertilizers by TXRF. This involved selective extraction of uranium using solvent extraction thereby pre-concentrating and removing the interfering elements from the analyte matrix.

6.2. Uranium Determination in Seawater by TXRF

Seawater is a treasure of many elements — precious and strategic in nature. The possibility of recovering uranium from seawater has gained importance in last few decades. Uranium is present in seawater in very small concentrations of about 3.3 ng/mL [12,13] as uranyl carbonate anions, but considering the huge amount of seawater in the world, the total amount of uranium in seawater works out to be approximately 1000 times to that in earth crust [12]. Different countries of the world, especially those having a sea coastline, are pursuing studies to explore the feasibility of recovering uranium from seawater in an economic way. India is also actively involved in such studies. Determination of uranium in seawater is an important step in these studies. Though TXRF by Mo $K\alpha$ excitation is a very sensitive method of uranium determination because of better excitation efficiency of Mo $K\alpha$ for U $L\alpha$ X-rays, but direct determination of uranium in seawater by this method becomes difficult due to mainly three reasons:

- i) Large amount of salt matrix
- ii) Very low concentration of uranium in seawater
- iii) Interference of Rb $K\alpha$ (13.40 keV) and Br $K\beta$ (13.29 keV) X-ray lines with U $L\alpha$ (13.62 keV) line, as rubidium and bromine are also present in seawater in appreciable amounts.

Any TXRF analytical method for uranium determination has to address the above problems before it can be applied for routine uranium determinations in seawater. A few methods of uranium determination in seawater using TXRF are reported in the literature but these methods use complex procedures for pre-concentration [14,15].

In the present study, an attempt was made to determine uranium in seawater by selectively extracting it in diethyl ether ($C_2H_5OC_2H_5$) and thus removing the interfering elements from the analyte. This study was pursued with an aim of getting an alternative fast method of uranium determination in seawater with its possible application in uranium recovery technology

from seawater as well as for monitoring of uranium in environment. Also, it will be helpful in establishing TXRF as a routine chemical analysis technique for such determinations.

6.2.1. Experimental

6.2.1a. Sample preparation

The glass wares used in this study e.g. separating funnels, beakers, measuring funnel, etc. were made of high purity quartz. Diethyl ether used was of AR grade, nitric acid was of suprapure grade and water used for cleaning and sample preparation was of Milli-Q grade. The multielement standard used was Merck ICP- standard solution IV. Merck single element standards of uranium and yttrium were used. The glass wares used were cleaned by dipping them in 1.5% solution of suprapure HNO₃ in Milli-Q water for 24 h before use. The cleanliness of the glass wares was ascertained by recording TXRF spectrum of 1.5% suprapure HNO₃ kept in these glass wares for 24 h after cleaning. Four seawater samples, collected in 60 mL cleaned PET wide mouth vials from a site in Arabian Sea near Mumbai City, were processed for the determination of uranium. Diethyl ether was used as an extractant for selective extraction of uranium. Before extracting uranium, diethyl ether was equilibrated thrice with 8M HNO₃. The left over HNO₃ was free of any traces of uranium and, therefore, was used for the sample preparation purpose. However, in this treatment some amount of uranium present in HNO₃ as impurity may get extracted into diethyl ether. To remove such uranium from the treated diethyl ether, it was again equilibrated with equal amount of Milli-Q water. The diethyl ether received after this treatment was equilibrated with treated 8 M HNO₃ to replenish loss of HNO₃ from it. The organic phase (equilibrated diethyl ether) obtained after this treatment was free from any uranium impurity and was used for extraction of uranium from multielement standards and seawater samples.

In order to study the extraction efficiency of uranium by diethyl ether, a working standard having concentration of 4.9 ng/mL was prepared by diluting the ICP multielement standard solution IV with 1.5% HNO₃. As this standard did not contain any uranium, a single element standard of uranium was added to this solution. The elemental concentration of uranium was similar to all the elements in this standard solution. A 50 mL volume of this standard was evaporated to dryness under an IR lamp. The solid mass obtained was first fumed with a few

drops of 8M HNO₃ two to three times on a hot plate and was finally dissolved in 1 mL of 1.5% HNO₃. A known amount of yttrium standard was mixed to this solution as an internal standard. This solution was analyzed for different elements by TXRF. Another 50 mL volume of the same standard was taken in a beaker and was evaporated to dryness under an IR lamp. The solid material received was redissolved in minimum amount of 8M HNO₃ and then made up to 25mL. This solution was equilibrated three times with the equal amount of treated diethyl ether as described earlier. The organic phases received in each equilibration were removed carefully and mixed together. This organic phase was left for evaporation to dryness on a hot plate. The residue obtained was fumed with few drops of equilibrated 8M HNO₃ and then was dissolved in 1 mL of 1.5% solution of HNO₃. This solution was analyzed by TXRF after adding the internal standard. The blank corrections in both these TXRF determinations were made by analyzing 50 mL of 1.5% HNO₃ in Milli-Q water processed in a similar way.

To extract uranium from the actual seawater samples, 50 mL of each seawater sample was filtered through Whatmann filter paper-541 and was collected in separate beakers. These filtrates were evaporated to dryness and the solid residues obtained were dissolved in minimum volume of 8 M HNO₃. For uranium extraction, these solutions were processed in similar way as described earlier. In an earlier study, the solid residue obtained was found to contain high concentrations of bromine and chlorine. Because of Br K β interference with U L α line, it had to be removed from the analyte solution. Bromine was removed from this residue by mixing it with few drops of Conc. HNO₃ and evaporating the resultant solution slowly to dryness over a burner. This process was repeated two to three times for removal of bromine and chlorine. Finally, internal standard yttrium was mixed in the residue and the whole mass was dissolved in 1 mL of 1.5% HNO₃. Two aliquots of 10 μ L of this solution were taken on two quartz TXRF sample supports and dried under an IR lamp.

6.2.1b. Instrumentation

An ITAL STRUCTURES TXRF spectrometer TX-2000 was used for measurements. Mo K α radiation produced from a Mo-W dual target X-ray tube operated at 40 kV, 30 mA and monochromatized by a W-C multilayer was used for sample excitation. A Roentec Si(Li) detector with energy resolution of 139 eV at 5.9 keV (Mn K α) was used for detection of X-rays

produced. For TXRF analysis, 10 μL aliquots of the sample were deposited on clean quartz sample supports and the TXRF spectra were recorded for a live time of 1000 s. Each sample was prepared in duplicate and measured two times. The precision was calculated from the four TXRF determinations.

6.2.2. Results and discussion

6.2.2a. Selective extraction of uranium by diethyl ether

Diethyl ether is known to selectively extract uranium even from very low concentrations [16]. However, it has been now replaced by other extractants for industrial uranium extraction because of its low boiling point and highly inflammable nature. For TXRF analysis of uranium in seawater, its low boiling point was beneficially exploited to remove the organic phase completely, obtained after uranium extraction. The selective extraction of uranium by diethyl ether is maximum from 8 M HNO_3 . However, HNO_3 has some solubility in diethyl ether. If diethyl ether is used without any treatment, it will dissolve some HNO_3 from the feed solution and will change its molarity. This will affect its selective extraction behaviour for uranium. In order to overcome this problem, the diethyl ether was saturated with 8 M HNO_3 before its use by equilibrating in a separating funnel for three minutes. The left over acid was free from any uranium impurity because if there was some uranium, it would have gone into the diethyl ether phase during equilibration. This acid was used for further sample preparations.

The concentrations of different elements in synthetic multielement standard solution having concentration of 4.9 ng/mL was determined by TXRF and their expected concentrations are given in Table 6.1. The ratio of TXRF determined and expected elemental concentrations are also given in this Table. The precision, calculated on the basis of four measurements, for most of the elements was within 8% (1σ). The average difference in expected and TXRF determined values of elemental concentrations of elements for which $K\alpha$ lines were used was 6% after excluding Ca, Fe and Zn data. The large deviation in case of Ca and Fe were because of their presence in environment as aerosol particulate and water contaminants. The precision and accuracy are poor indicating requirement of clean room conditions for the determination of these elements in this concentration range. The accuracy was poorer for the elements for which

Table 6.1: TXRF analysis results of elements present in multi-element standard

Elements	Elemental Concentration (ng/mL)		TXRF/ Expected
	Expected	TXRF determined	
Ca	4.9	17 ± 8	3.46
Cr	4.9	4.7 ± 0.3	0.96
Mn	4.9	5.2 ± 0.4	1.06
Fe	4.9	22.5 ± 0.9	4.59
Co	4.9	5.1 ± 0.3	1.04
Ni	4.9	5.4 ± 0.4	1.10
Cu	4.8	5.1 ± 0.2	1.04
Zn	4.9	1.2 ± 0.3	0.25
Ga	4.9	5.5 ± 0.4	1.12
Sr	5	4.8 ± 0.3	0.96
Tl	4.9	5.1 ± 0.4	1.04
Pb	4.9	5.8 ± 0.6	1.18
Bi	4.9	5.2 ± 0.1	1.06
Ba	4.9	8.5 ± 2.6	1.74
U	4.9	6.2 ± 0.5	1.27

L α lines were used as the analytical lines of interest. The average percentage deviation was found to be within 13% for such elements except Ba, which had a large deviation.

TXRF analysis of the aqueous phase after solvent extraction of the working standard showed that the recovery of uranium in organic the phase was complete. For Ca and Fe, the recovery was significant whereas for other elements e.g. Ni, Cu, Zn, Ga, Sr, Tl and Bi, it was negligible. The significant recovery of Ca and Fe observed may be due to contamination from the atmospheric aerosol but these elements do not interfere with uranium analysis by TXRF and

will not affect its subsequent determination. A comparison of TXRF determined concentrations of the elements present in the standard and those extracted in organic phase of diethyl ether extraction is shown by means of a bar graph in Figure 6.1.

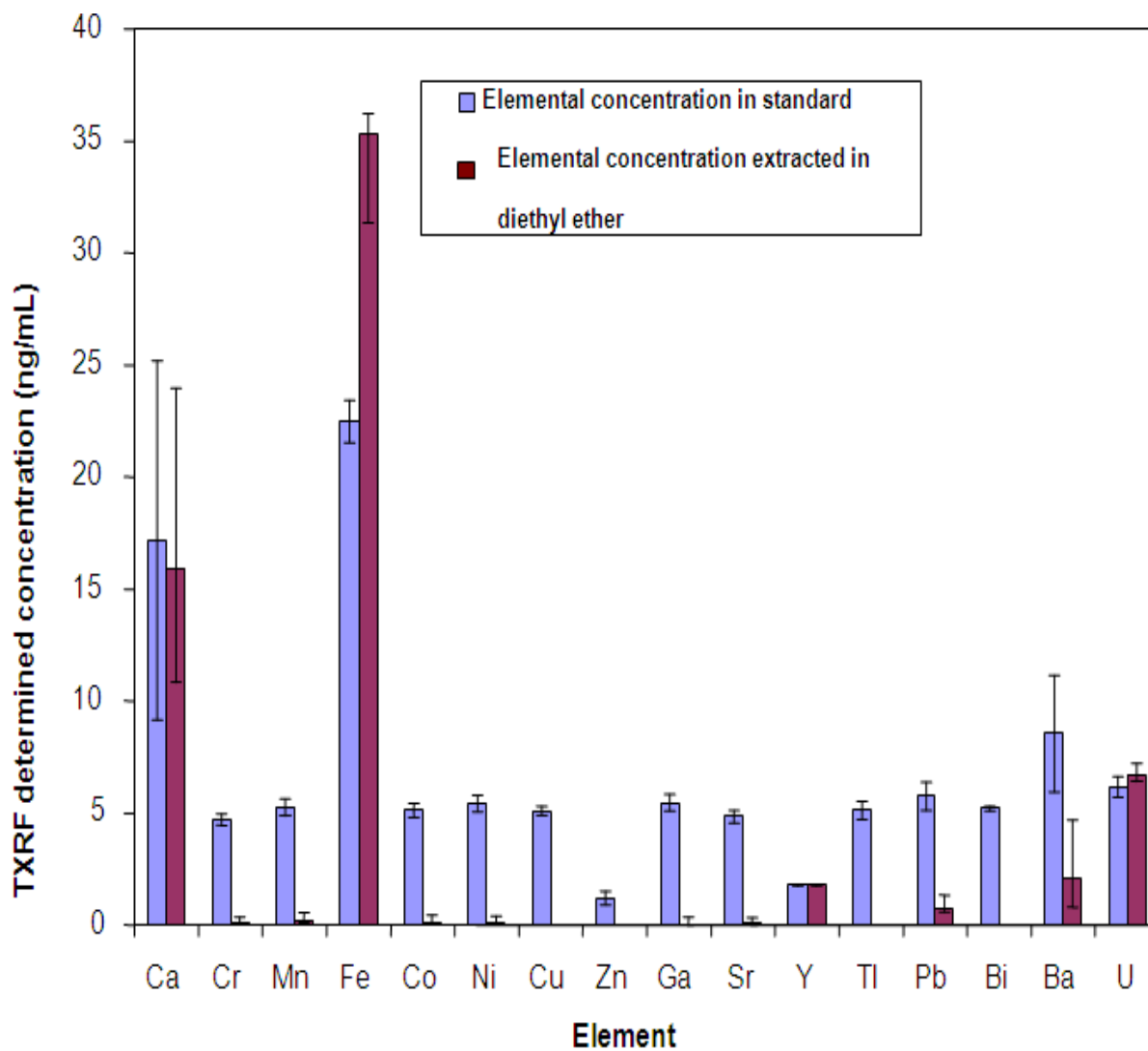


Figure 6.1: A comparison of concentrations of different elements present in standard before and after extraction

6.2.2b. Uranium determination in seawater

Concentration of bromine after treatment with concentrated HNO_3 , as observed in the TXRF spectrum given in Figure 6.2, was reduced to negligible amounts. Absence of Rb $K\alpha$ peak in the spectrum indicates negligible extraction of rubidium by diethyl ether. Hence the two elements, which were interfering with the determination of uranium, were removed successfully.

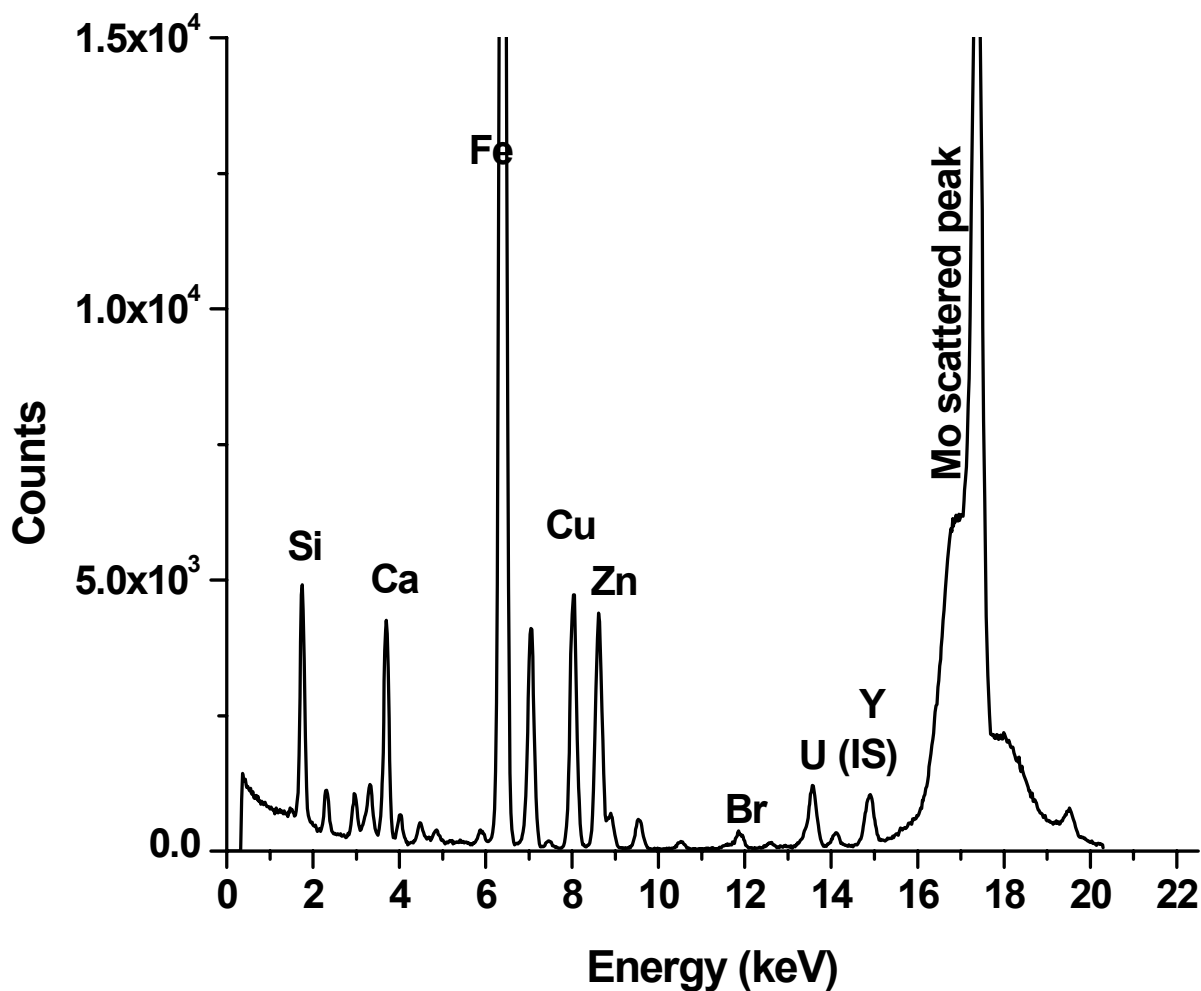


Figure 6.2: TXRF spectrum of organic phase obtained after selective extraction of uranium in diethyl ether

Four samples of processed seawater were analyzed by TXRF and the results obtained for uranium in these seawater samples are given in Table 6.2. The agreement between TXRF determined values with the reported literature value was found to be satisfactory, showing good extraction recovery for uranium by diethyl ether. Uranium is reported to be present in seawater as a dissolved trace metal at a concentration of 3.3 ng/mL [12] and the average TXRF determined uranium concentration was found to be 2.8 ± 0.5 ng/mL. The precision of uranium determinations was better than 17% (1σ). A comparison of TXRF determined uranium concentration values with the expected values of uranium present in seawater, as reported in the literature, is shown as bar graph in Figure 6.3. The deviation of TXRF values from the expected concentration was about 15%. The detection limit of uranium after the preconcentration step of its extraction in diethyl ether reached 67 pg/mL. These observations clearly indicate that TXRF can be used as a routine technique for uranium determination in seawater samples.

Table 6.2: Results of TXRF determined uranium in seawater samples

Sample	TXRF determined uranium concentration (ng/mL)
Sample-1	2.6 ± 0.07
Sample-2	3.4 ± 0.15
Sample-3	2.1 ± 0.08
Sample-4	3.1 ± 0.09

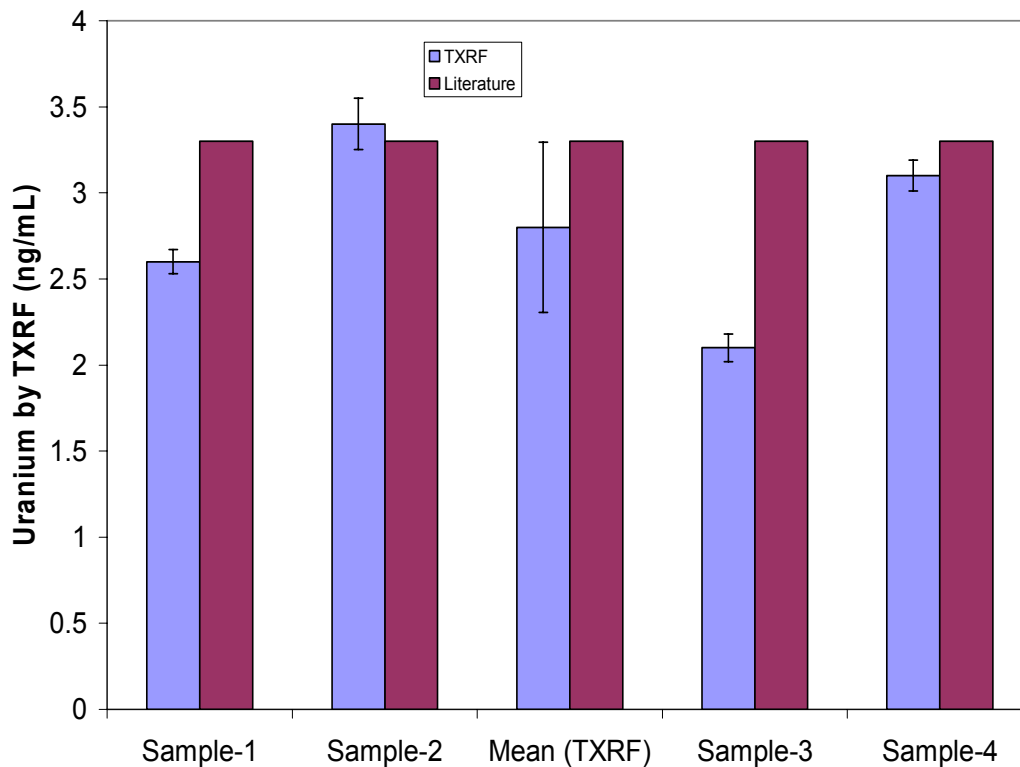


Figure 6.3: Comparison of TXRF determined concentration of uranium in four seawater samples and literature reported concentration

6.3. Determination of Uranium in Fertilizer Samples by TXRF

Fertilizers employed in agriculture usually contain traces of heavy elements and especially phosphate fertilizers are known to contain uranium in high concentration [17]. The high uranium content in these fertilizers is due to occurrence of this element in phosphate rocks which is usually the raw material for the synthesis of these fertilizers. Because of the concern about the exhaustion of uranium resources in the world, phosphate fertilizers are seen as an alternative source of uranium. The project involving recovery of uranium from such unconventional sources, require a suitable method of uranium determination at trace levels in these fertilizers. Also, there is environmental concern regarding the use of these fertilizers routinely due to the addition of uranium in the soil. Solid State Nuclear Track Detector (SSNTD) is an

excellent tool for the determination of low levels of uranium in environmental samples [18-20]. The only limitation of this technique is the requirement of nuclear reactors for irradiation purpose. TXRF can be used for the determination of uranium in fertilizer samples, provided uranium can be selectively separated from the major matrix of the fertilizers.

Studies are reported in this Section about TXRF determination of uranium in four phosphate fertilizers of Hungarian origin. Uranium was selectively extracted from the phosphate fertilizers using the solvent extraction procedure employing TPB as the extractant.

6.3.1. Experimental

6.3.1a. Sample preparation

All the glasswares such as beakers, separating funnel, measuring cylinder were made of high purity quartz. Solvents like tri butyl phosphate (TBP) and dodecane used were of AR grade. Nitric acid used for dissolution and sample preparation was of suprapure grade. Water used for diluting samples / reagents and washing was of Milli-Q grade. Calibration standards of uranium and yttrium internal standard were prepared by diluting and mixing the Merck single element standards of these elements having a concentration of 1000 $\mu\text{g/mL}$.

Accurately weighed fertilizer samples, about 1 g each, were soaked in a minimum amount of concentrated HNO_3 for 3 h. Any remaining supernatant was evaporated under IR lamp and then 5 mL of 2.5 M HNO_3 was added to the residue thus formed and left overnight. The resultant solution was filtered and the solid material left undissolved was washed with 2.5 M HNO_3 . The washings were collected along with filtrate and equilibrated thrice with 30% solution of TBP in dodecane. The organic phase containing extracted uranium was collected carefully after each extraction. Finally, after three equilibrations, the total organic phase collected was equilibrated again with 1.5% HNO_3 . The aqueous phase obtained after this extraction was separated from the organic phase and mixed with the internal standard. This solution was evaporated to dryness and then made up to 2 mL with 1.5% HNO_3 . The flow chart showing the sample preparation steps in detail is given in Figure 6.4. For the blank determinations, the same sample preparation procedure was followed and instead of sample, HNO_3 was used. Aliquots of 10–30 μL of calibration solution and processed fertilizer samples were deposited on float glass sample supports to measure their TXRF spectra.

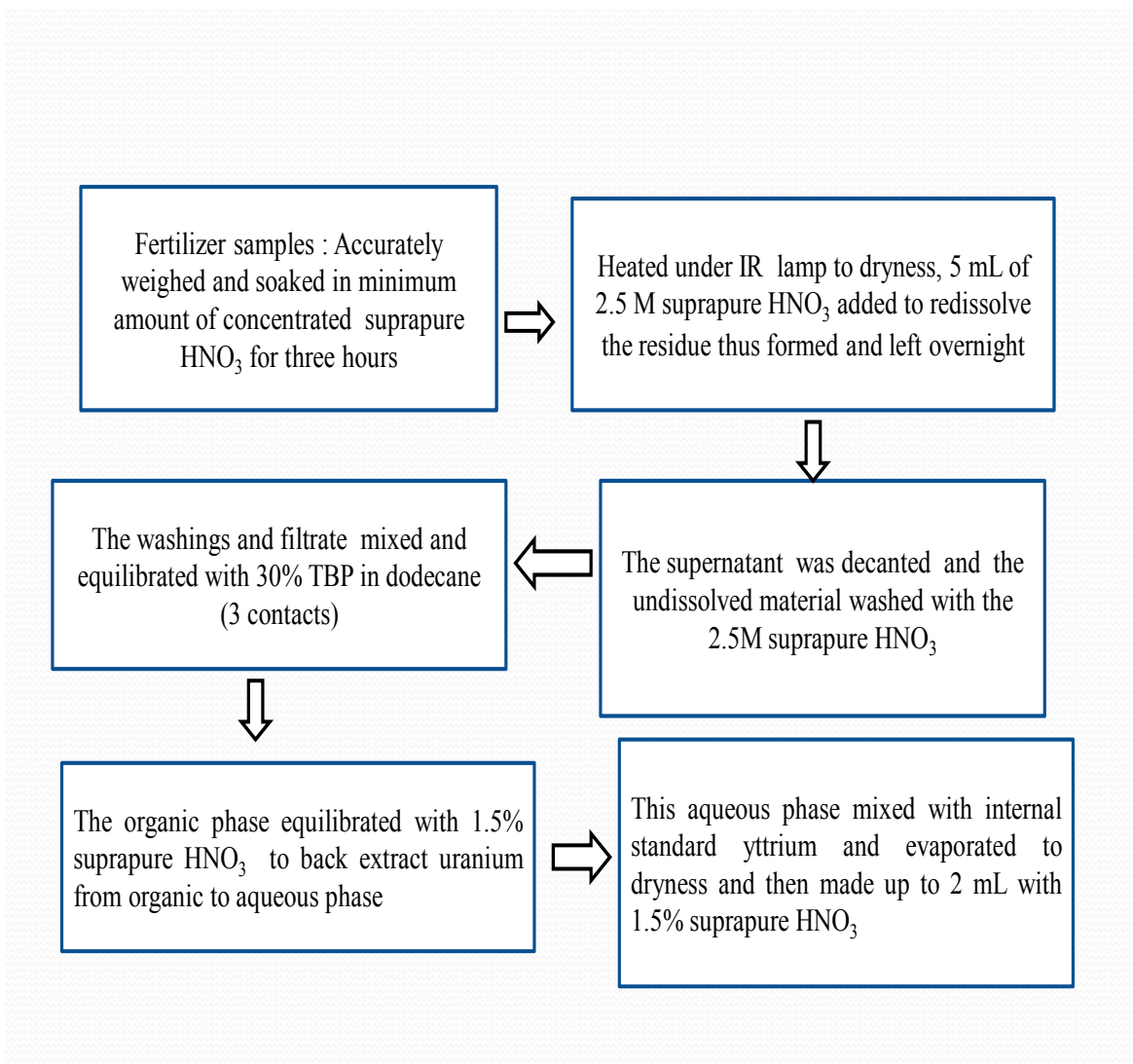


Figure 6.4: Flow chart showing steps involved in the sample preparation methodology for TXRF analysis of uranium in fertilizer samples

6.3.1b. Instrumentation

The TXRF measurements were carried out using the spectrometer assembled at Raja Ramanna Centre of Advanced Technology (RRCAT) Indore, India [21, 22]. A monochromatized Mo K α radiation source obtained from the Mo target tube operated at 30 kV and 20 mA using a W-C multilayer was used for sample excitation. The samples were deposited on float glass supports [23]. The live time used varied from 1000 to 3000 s depending on the intensity of U L α

peak. The quantity of uranium in the fertilizer samples was determined using the net intensities of U $L\alpha$ and Y $K\alpha$ (internal standard) and blank corrections.

6.3.2. Results and discussion

TBP is a well established extractant for selective extraction of uranium from nitric acid medium. 30% TBP in dodecane has maximum extraction efficiency of uranium at 2-4 M HNO_3 . Hence all the samples were prepared with 2.5 M HNO_3 . Direct determination of uranium in organic phase by TXRF is difficult. This is because in TXRF, the samples deposited on the sample supports need to be dried completely before presenting for measurements. TBP/dodecane have boiling points more than 200°C and hence complete evaporation is difficult and time consuming. The other alternative method is to back extract uranium in the aqueous medium. Therefore, the organic phase was equilibrated with dilute HNO_3 to back extract uranium from organic to aqueous phase. The TXRF spectrum of a typical fertilizer sample after complete processing is shown in Figure 6.5 along with uranium and yttrium peaks. A strong peak of strontium is also seen in the Figure. This is because of its presence as a common trace element in water and environmental samples.

To find out the area of U $L\alpha$ and Y $K\alpha$ peaks, profile fitting using the program ORIGIN was used. The sensitivity of the U $L\alpha$ with respect to Y $K\alpha$ was determined using TXRF measurements of four specimens taken from the calibration standard solutions of uranium and yttrium. The amounts of uranium in the fertilizer samples were determined using the above sensitivity values and U $L\alpha$ and Y $K\alpha$ peak intensities. The uranium amount was found to be in the range of 4– 6 $\mu\text{g/g}$ in two samples, whereas other two fertilizer samples did not show any uranium. The TXRF determined values are given in Table 6.3. The precision of the TXRF determination of uranium was found to be better than 8% (1σ). The TXRF spectra of the leftover solid residues were also measured. These spectra did not show any uranium peak. These observations indicate that uranium present in phosphate fertilizers was in TBP extractable form and such trace amounts of uranium present in fertilizer samples can be leached, extracted and then analysed by TXRF as described above.

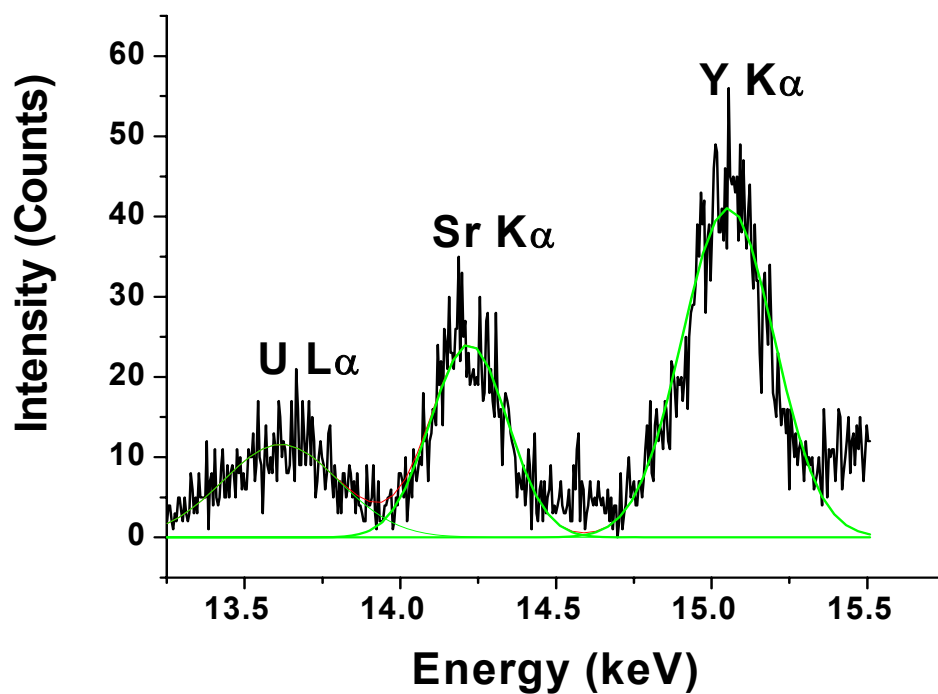


Figure 6.5: Profile fitted TXRF spectrum of a processed fertilizer sample (Sample Code :1845)

Table 6.3: TXRF determined values of uranium in fertilizer samples

Fertilizer Sample Code	Description	TXRF Determined uranium ($\mu\text{g/g}$) $\pm 1s$
1844	N based mainly NH_4NO_3	Not Detected
1845	N-P-K, mainly P_2O_5	4.1 ± 0.3
ANT	P based P_2O_5	6.0 ± 0.1
LAWN	N-P-K Fertilizers	Not Detected

6.4. Conclusions

This study reveals that uranium can be determined in seawater and fertilizer samples by TXRF, after its selective extraction using a suitable solvent. Solvent extraction serves two purposes: (i) matrix separation and (ii) pre-concentration.

Seawater samples collected from the Arabian Sea were analyzed for uranium after extraction with diethyl ether. The results were found to be in good agreement with the uranium content in seawater reported in literature. The precision of the uranium determination was found to be better than 17%.

The technique applied for the trace determination of uranium in fertilizers involved its selective extraction by TBP. As direct determination of uranium in TBP is difficult, back extraction of uranium in dilute acid was carried out as an additional step.

Both the studies suggest that TXRF is one of the suitable techniques for trace determination of uranium in seawater and fertilizer samples on a routine basis.

6.5. References

1. Thomas T. Meek, B. Von Roedern, Semiconductor devices fabricated from actinide oxides, *Vacuum*, 83 (2008) 226.
2. Stuart H Taylor, Catherine S Heneghan, Graham J Hutchings, Ian D Hudson , The activity and mechanism of uranium oxide catalysts for the oxidative destruction of volatile organic compounds, *Catal. Today*, 59 (2000) 249.
3. Frank J. Berry, Andrew Murray, Norman D. Parkyns, Nickel-uranium oxide catalysts: characterization and evaluation for methanation, *Appl. Catal., A*, 100 (1993) 131.
4. Juracir S. Santos, Leonardo S.G. Teixeira, Walter N.L. dos Santos, Valfredo A. Lemos, Jose M. Godoy, Sérgio L.C. Ferreira, Uranium determination using atomic spectrometric techniques: An overview, *Anal. Chim. Acta*, 674 (2010) 143.
5. Abdulla W. Al-Shawi, Roger Dahl, Abdulla W. Al-Shawi, Roger Dahl, Determination of thorium and uranium in nitrophosphate fertilizer solution by ion chromatography, *J. Chromatogr., A*, 706 (1995) 175.
6. http://www.who.int/water_sanitation_health/dwq/chemicals/uraniumsum.pdf

7. Sanjukta A. Kumar, Niyoti S. Shenoy, Shailaja Pandey, Suvarna Sounderajan, G. Venkateswaran, Direct determination of uranium in seawater by laser fluorimetry, *Talanta*, 77 (2008) 422.
8. S. Antoniou, C. Costa, I. Pashalidi, Alpha-radiometry of seawater by liquid scintillation counting, *J. Radioanal. Nucl. Chem.*, 270 (2006) 593.
9. Dj. Dojozan, M.H. Pournaghi-Azar, J. Toutouchi-Asr, Preconcentration of trace uranium from seawater with solid phase extraction followed by differential pulse polarographic determination in chloroform eluate, *Talanta*, 46 (1998) 123.
10. I. Pashalidis, H. Tsertos, Radiometric determination of uranium in natural waters after enrichment and separation by cation-exchange and liquid-liquid extraction, *J. Radioanal. Nucl. Chem.*, 260 (2004) 439.
11. Z. Tosheva, K. Stoyanova, L. Nikolchev, Comparison of different methods for uranium determination in water, *J. Environ. Radioact.*, 72 (2004) 47.
12. M. Tamada, N. Seko, F. Yoshii, Application of radiation-graft material for metal absorbent and crosslinked natural polymer for healthcare product, *Radiat. Phys. Chem.*, 71 (2004) 221.
13. P.G. Barbano, L. Rigali, Spectrophotometric determination of uranium in seawater after extraction with ALIQUAT- 336, *Anal. Chim. Acta*, 96 (1978) 199.
14. Vasilios Hatzistavros, Pavlos Koulouridakis and Nikolaos Kallithrakas-Kontos, Complexing membrane for uranium detection by total reflection X-ray fluorescence, *Anal. Sci.*, 21 (2005) 823.
15. Peter Freimann, Diether Schmidt, Application of total reflection X-ray fluorescence analysis for the determination of trace metals in the North sea, *Spectrochim. Acta, Part B*, 44 (1989) 505.
16. Donald F. Peppard, Liquid – Liquid extraction of the actinides, *Annu. Rev. Nucl. Sci.*, 21 (1971) 365.
17. Ione Makiko Yamazaki, Luiz Paulo Geraldo, Uranium content in phosphate fertilizers commercially produced in Brazil, *Appl. Radiat. Isot.*, 59 (2003) 133.
18. A.F. Saad, T.M. Talaat, S.T. Atwa, G. Espinosa, M. Fujii, Determination of the uranium content of Egyptian phosphate ores by passive and active detectors, *Radiat. Meas.*, 36 (2003) 561.

19. M.A. Misdaq, H. Khajmi, F. Aitnough, S. Berrazzouk, W. Bourzik, A new method for evaluating uranium and thorium contents in different natural material samples by calculating the CR-39 and LR-115 type II SSNTD detection efficiencies for the emitted α -particles, Nucl. Instrum. Methods Phys. Res., Sect. B, 171 (2000) 350.
20. A.S. Paschoa , O.Y. Mafra , D. O. Cardoso, A. C. S. Rocha, Application of SSNTD to the Brazilian phosphate fertilizer industry to determine uranium concentrations, Nucl. Tracks Radiat. Meas., 8 (1984) 469.
21. M.K. Tiwari, K.J.S. Sawhney, B. Gowri Shankar, V.K. Raghuvanshi and R.V. Nandedkar, A simple and precise total reflection X-ray fluorescence spectrometer: construction and its applications, Spectrochim. Acta, Part B, 59 (2004) 1141.
22. M. K. Tiwari, G. S. Lodha, K. J. S. Sawhney, B. Gowrisankar, A. K. Singh, G. M. Bhalerao, A. K. Sinha, Arijeet Das, A. Verma and R. V. Nandedkar, Progress in total reflection X-ray fluorescence spectrometry at Raja Ramanna Centre for Advanced Technology, Curr. Sci., 95 (2008) 603.
23. M.K. Tiwari, M.H. Modi, G.S. Lodha, A.K. Sinha, K.J.S. Sawhney, R.V. Nandedkar, Non-destructive surface characterization of float glass: X-ray reflectivity and grazing incidence X-ray fluorescence analysis, J. Non-Cryst. Solids, 351 (2005) 2341.

Chapter- 7

ANALYTICAL CHARACTERIZATION OF NUCLEAR MATERIALS USING EDXRF : BULK AND TRACE DETERMINATION

- 7.1. Introduction
- 7.2. An EDXRF Method for Determination of Uranium and Thorium in AHWR Fuel After Dissolution
 - 7.2.1. Experimental
 - 7.2.1a. *Sample preparation*
 - 7.2.1b. *Instrumentation*
 - 7.2.2. Results and discussion
 - 7.2.2a. *Uranium determinations*
 - 7.2.2b. *Thorium determinations*
- 7.3. EDXRF Determination of Cadmium in Uranium Matrix Using Cd K α Line Excited by Continuum
 - 7.3.1 Experimental
 - 7.3.1a. *Sample preparation*
 - 7.3.1b. *Instrumentation*
 - 7.3.2. Results and discussion
 - 7.3.2a. *Cadmium determination in absence of uranium*
 - 7.3.2b. *Cadmium determination in presence of uranium*
- 7.4. Conclusions
 - 7.4.1. Bulk determination of uranium and thorium
 - 7.4.2. Trace determination of cadmium in uranium matrix
- 7.5. References

7.1. Introduction

Chemical quality assurance of uranium, thorium and plutonium based fuels requires elemental characterization of trace constituents as well as bulk contents. EDXRF is a fast, easy and simple analytical technique for bulk as well as trace determination in nuclear materials [1]. Bulk determination of nuclear materials generally does not require any separation and direct analysis is possible. Samples in the form of solids, liquids, powder, slurry, etc. can be analysed without any sample preparation for determination of major elements by EDXRF. For trace determinations, matrix separation is generally required depending on the nature of the matrix and the concentration of the analyte.

Apart from geometrical differences between TXRF and EDXRF, EDXRF has two major disadvantages viz. severe matrix effects and poor detection limits. But in view of simplicity in instrumentation and operation, EDXRF is widely used in many industries and research laboratories [2, 3]. In nuclear industry, determination of radioactive samples requires enclosure of the spectrometer inside the glove box. Maintenance and operation of such spectrometers is relatively difficult and time consuming. Due to the simpler instrumentation, the maintenance and operation is easier in EDXRF compared to TXRF. Due to these advantages, development of EDXRF methodologies for determination of trace and bulk elements in nuclear materials is promising. Before the spectrometer is put into the glove box for analyzing radioactive samples, it is desirable to check the feasibility of such analyses by analyzing nonradioactive samples. Moreover, matrix effects also known as absorption-enhancement effects in XRF are systematic, and can be predicted and corrected for [4-7]. Various methods like thin film method, matrix dilution, internal standardization, external standard method and mathematical corrections are applied to account for matrix effects. As EDXRF is a comparative method, accuracy of such determinations depends on the reliability of standards. The detection limits in EDXRF can also be improved by decreasing the source-sample-detector distance and by using suitable filters or secondary targets [8].

In the present studies, applicability of EDXRF for bulk and trace elements determination in nuclear materials was investigated. This spectrometer has very short (approximately 10 mm) source-sample-detector distance and provision of using filters to reduce background.

7.2. An EDXRF Method for Determination of Uranium and Thorium in AHWR Fuel after Dissolution

The Advanced Heavy Water Reactors (AHWRs) are being developed with the specific aim of utilizing thorium for power generation. The proposed fuel compositions for AHWR are: (Th- ^{233}U)O₂ and (Th- ^{239}Pu)O₂ for these reactors [9]. A fast analytical method to verify the composition of fuel is required during fuel fabrication, whereas accurate and precise data are needed for the chemical quality assurance and certification. As thorium is not a fissile, but a fertile element it gets converted to fissile material by neutron absorption. During this process, ^{233}U is generated. The problem associated with thorium based fuel cycle is due to production and handling of ^{233}U which contain ^{232}U in the range of a few ppmw to 500 ppmw, depending on the flux characteristics of the reactor and the duration of irradiation [10]. The two daughter products of ^{232}U decay chain, namely ^{212}Bi and ^{208}Tl produce γ – radiation of 0.7-1.8 MeV and 2.6 MeV, respectively. These products cause personnel exposure problem and hence it is desirable to minimize the amount of sample to be used for determination of fuel composition.

XRF is a well established method for fast and accurate determination of elemental composition of nuclear fuel samples. The samples in the form of pellets or solutions when analysed by XRF, require a few milligrams/ milliliters of the sample [11, 12]. In case of radioactive samples this may give appreciable amount of radiation burden on the instrument as well as to the analyst.

In the present work, an energy dispersive X-ray fluorescence (EDXRF) method was investigated for determination of uranium and thorium in AHWR fuel after dissolution. Natural uranium was used as a surrogate for ^{233}U . The possibility of using minimum sample amount and achieving acceptable precision and accuracy was evaluated and is presented in this Chapter. The matrix effect was corrected by presenting the samples in the form of thin film and adding an internal standard.

7.2.1. Experimental

7.2.1a. Sample preparation

For preparation of calibration standard and sample solution, high-purity uranyl nitrate and

thorium nitrate solutions of known uranium and thorium concentrations were used. Y_2O_3 powder (AR grade) was used for preparing internal standard solution and HNO_3 used for dissolution was of suprapure grade. The internal standard solution was prepared by dissolving Y_2O_3 powder in concentrated HNO_3 , evaporating the solution to near dryness and then redissolving the residue in 1.5% HNO_3 in Milli-Q water (v/v). The final concentration of yttrium in the solution was 45.83 mg/mL. Two sets of calibration and sample solutions were prepared by mixing different volumes of uranium and thorium solutions in clean glass vials. In Set-I, the amount of thorium was kept constant whereas the amount of uranium was varied to cover the uranium percentage (0–5%) in (U + Th), as expected in AHWR fuel. In Set-II, both uranium and thorium amounts were varied, and a fixed amount of internal standard was added to both the sets. The details of the calibration solutions and samples of Set-I and Set-II are given in Tables 7.1 and 7.2, respectively. Each solution was homogenized by shaking using an electric shaker. Aliquots of about 20 μ L were taken from each mixture on 30 mm diameter Whatmann 541 filter papers suspended uniformly over a perspex ring having 25 mm internal diameter, 26 mm outer diameter and 1 cm height in such a way that the solution spreads uniformly in the central area of the filter paper without touching the sides of the ring. The solutions on the filter papers were allowed to dry at ambient temperature and were placed in the XRF sample holders which were mounted in the sample chamber of EDXRF spectrometer. Table 7.3 gives the amounts of thorium, uranium and yttrium present in 20 μ L of the solution taken on the filter paper. Two independent filter papers were used for depositing each calibration standard and sample solution of Set-I and Set-II.

7.2.1b. Instrumentation

A Jordan Valley EX-3600-TEC spectrometer having a Rh target operated at 40 kV and 500 μ A was used. The spectrometer uses a Peltier-cooled semiconductor premium Si PIN diode detector with a resolution of (150 ± 10) eV (FWHM) at 5.9 keV. The data processing was done using the computer program, nEXt, provided with the instrument. U $L\alpha$ and Th $L\alpha$ characteristic lines of analytes and Y $K\alpha$ characteristic line of the internal standard were used for obtaining the calibration plots as well as for the determination of uranium and thorium in the samples. The samples were loaded on EDXRF sample holders and measured sequentially. EDXRF spectrum of each specimen prepared in duplicate for Set-I and Set-II, were measured for 300 s live time in

duplicate. The average mean values and precision were calculated on the basis of all these measurements.

Table 7.1: Details of Set-I calibration and sample solutions

Solution code	Uranium*		Thorium*		% Uranium in (U + Th)	Yttrium*	
	Volume (µL)	Amount (mg)	Volume (µL)	Amount (mg)		Volume (µL)	Amount (mg)
Calibration solutions							
C-1-1	0	0	500	168	0	100	4.58
C-1-2	500	1.65	500	168	0.97	100	4.58
C-1-3	1000	3.30	500	168	1.92	100	4.58
C-1-4	1500	4.96	500	168	2.87	100	4.58
C-1-5	2500	8.26	500	168	4.69	100	4.58
Sample solutions							
S-1-1	750	2.48	500	168	1.45	100	4.58
S-1-2	800	2.64	500	168	1.54	100	4.58
S-1-3	1000	3.30	500	168	1.92	100	4.58
S-1-4	2000	6.61	500	168	3.78	100	4.58

*Concentrations of uranium, thorium and yttrium in the stock solutions were 3.305 mg/mL, 336 mg/mL and 45.83 mg/mL, respectively.

Table 7.2: Details of Set-II calibration and sample solutions

Solution code	Uranium*		Thorium*		% Uranium in (U + Th)	Yttrium*	
	Volume (µL)	Amount (mg)	Volume (µL)	Amount (mg)		Volume (µL)	Amount (mg)
Calibration Solution							
AH-2-1	0	0	100	33.6	0	100	4.58
AH-2-2	400	1.45	500	168.0	0.85	100	4.58
AH-2-5	700	2.53	350	117.6	2.11	100	4.58
AH-2-8	820	2.97	200	67.2	4.23	100	4.58
AH -2-10	1100	3.98	210	70.6	5.34	100	4.58
Sample Solution							
AH -2-3	600	2.17	450	151.2	1.41	100	4.58
AH -2-4	650	2.35	400	134.4	1.72	100	4.58
AH -2-6	800	2.89	300	100.8	2.79	100	4.58
AH -2-7	850	3.07	250	84.0	3.53	100	4.58
AH-2-9	1000	3.62	225	75.6	4.56	100	4.58

*Concentrations of uranium, thorium and yttrium in the stock solutions were 3.616 mg/mL, 336 mg/mL and 45.83 mg/mL, respectively.

Table 7.3: Amounts of analyte and internal standard transferred on filter paper when 20 μL solution was taken for EDXRF analysis

Sample Code	Amount deposited on filter paper*		
	(μg)		
	Th	U	Y
C-1-1	5600	0	152.8
C-1-2	3054	30.0	83.3
C-1-3	2100	41.3	57.3
C-1-4	1600	47.2	43.6
C-1-5	1084	53.3	29.6
S-1-1	2489	36.7	67.9
S-1-2	2400	37.8	65.5
S-1-3	2100	41.3	57.3
S-1-4	1292	50.8	35.3

*: Amounts calculated on the basis of sample preparation

7.2.2. Results and discussion

The energies of the characteristic X-ray lines of Th $L\alpha$, U $L\alpha$ and Y $K\alpha$ are 12.97, 13.61 and 14.96 keV, respectively. The corresponding absorption edges are at 16.3, 17.2 and 17.0 keV, respectively, whereas Rh $K\alpha$ energy is 20.22 keV. Since the energies of Th $L\alpha$, U $L\alpha$ and Y $K\alpha$ are on the pre-edge side of all these three absorption edges, any of these elements can be used as internal standard for the determination of other two. Also, since the Rh $K\alpha$ energy is above the L_3 absorption edges of thorium and uranium as well as the K absorption edge of yttrium, efficient excitation of Th $L\alpha$, U $L\alpha$ and Y $K\alpha$ is possible using this excitation source. In view of these facts, yttrium was chosen as an internal standard and the Rh target X-ray tube was used for sample excitation. A typical EDXRF spectrum of calibration solution C-1-2 (Table 1) is shown in Figure 7.1. It can be seen that Th $L\alpha$, U $L\alpha$ and Y $K\alpha$ peaks are well resolved and have good intensities.

For determination of detection limits, 2 μL aliquot of a calibration solution (AH-2-10) was absorbed on a filter paper and dried as mentioned earlier. The EDXRF spectrum of this sample was measured for 1000 s. After processing the spectrum, the detection limit (D_{Li}) was calculated using the formula:

$$DLi = \frac{\text{Concentration}}{\text{Peak area}} * 3 * \sqrt{(\text{Background})}$$

The detection limits calculated for thorium and uranium, using the above formula, were found to be 70 ng and 60 ng, respectively.

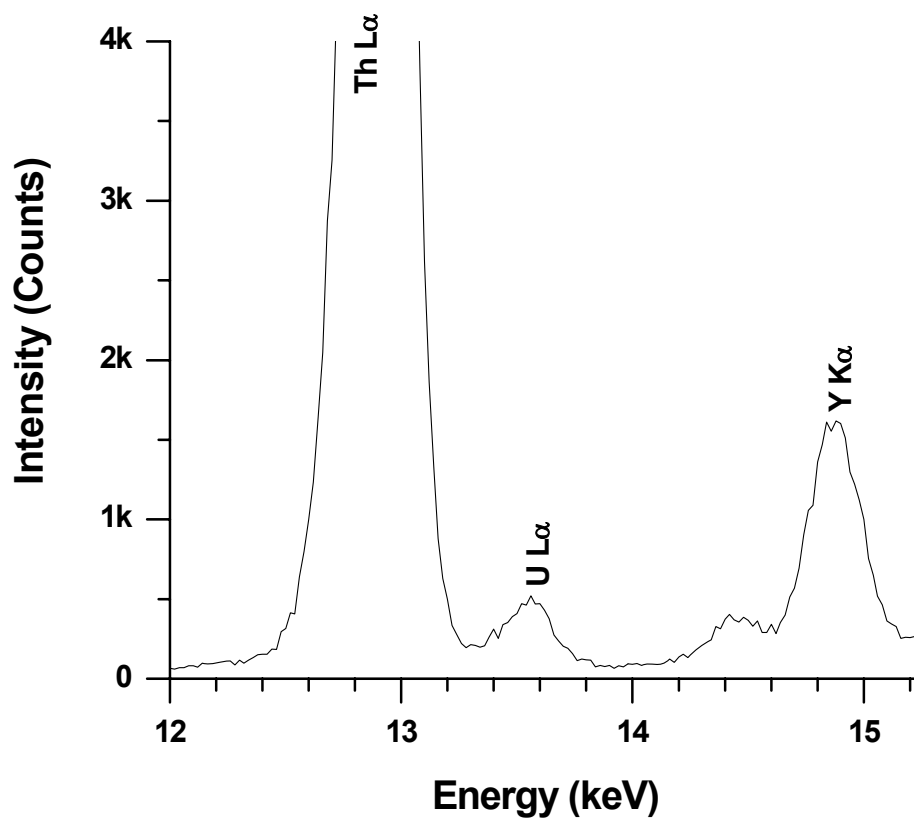


Figure 7.1: An EDXRF spectrum of calibration solution C-1-2

Since pipetting of different volumes of solution for preparing calibration solutions and samples will have different extents of errors, the volume of thorium solution used to prepare calibration and samples solutions of Set-I was kept constant (500 μL), whereas the uranyl nitrate solution volume was changed and in Set-II, both uranium and thorium amounts were varied. The volume of yttrium internal standard solution was maintained constant in both the sets.

Only 20 μL of the dissolved solution containing $<50 \mu\text{g}$ of uranium was used for measuring the EDXRF spectrum by depositing on the center of the filter papers. If this method is extended to actual AHWR fuel, such an aliquot will have ^{232}U at approximately 100 nanogram level and the radiation burden from such a small amount of ^{232}U will be negligibly small. Table 7.4 shows the U $\text{La}/\text{Y K}\alpha$ and Th $\text{La}/\text{Y K}\alpha$ intensity ratios obtained from four independent EDXRF spectra for a typical sample solution (AH-2-9), along with the intensity values of U La ,

Table 7.4: Intensities of U La , Th La and Y $\text{K}\alpha$ and the intensity ratios of U $\text{La} / \text{Y K}\alpha$ and Th $\text{La} / \text{Y K}\alpha$ in AH-2-9 sample from Set-II

Filter paper No.	Intensities			Intensity ratio	
	U La	Th La	Y $\text{K}\alpha$	U $\text{La} / \text{Y K}\alpha$	Th $\text{La} / \text{Y K}\alpha$
1	37963	829736	94542	0.402	8.8
2	27305	585800	67555	0.404	8.7
3	35456	782254	86491	0.410	9.0
4	31289	702400	77940	0.401	9.0
Average $\pm 1\sigma$	33003 \pm 4063	725048 \pm 92378	81632 \pm 10025	0.404 \pm 0.003	8.9 \pm 0.2
RSD (%)	12	13	12	1	2

Th $L\alpha$ and Y $K\alpha$ peaks. This Table also gives the corresponding average intensity values along with standard deviations involved. Though the sample amounts were very less, the intensities are appreciably high. It can be seen that the precision values in the measurement of four different spectra for the intensities of U $L\alpha$, Th $L\alpha$ and Y $K\alpha$ were about 12% whereas the precision in their intensity ratios i.e. U $L\alpha$ / Y $K\alpha$ and Th $L\alpha$ /Y $K\alpha$ are 1% and 2%, respectively. The poor precision in case of individual intensities is due to non uniform spreading of the solution at the center of the filter paper, whereas this non uniformity is taken care during calculation of intensity ratio. This shows the suitability of using only 20 μ L of sample amount on filter paper and addition of yttrium internal standard.

7.2.2a. Uranium determinations

For the determination of uranium in Set-I samples, the calibration plot was obtained by plotting U/Y amount ratios against the average intensity ratios of U $L\alpha$ /Y $K\alpha$ obtained from the EDXRF spectra of the calibration solutions of Set-I as shown in Figure 7.2. It can be seen that the calibration is linear over the entire range of uranium concentration used in the present work. Using this calibration plot, uranium was determined in the samples S-1-1 to S-1-4 of Set-I and the results obtained are given in Table 7.5. A similar calibration plot was drawn for the determination of uranium in Set-II using the calibration solutions of Set-II. This plot is shown in Figure 7.3. Using this calibration plot, uranium was determined as described above. The analytical results are given in Table 7.5. The calibration plots of uranium in Figures 7.2 and 7.3 are similar with negative intercepts and slope ~ 3 . The average precision and deviation from the expected values determined on the basis of sample preparation for uranium (Table 7.5) in Set I and II were 1.8 and 2.6 %, respectively, for samples containing up to 5% uranium with respect to (U+Th).

7.2.2b. Thorium determinations

Since identical amounts of thorium and yttrium were taken in all the solutions of Set-I, amount ratio of (Th/Y) was same for all the calibration solutions and samples. Therefore, it was not possible to obtain a calibration plot between Th $L\alpha$ / Y $K\alpha$ intensity ratios and Th/Y amount ratios for thorium determination, as was done for uranium determination. Hence in order to

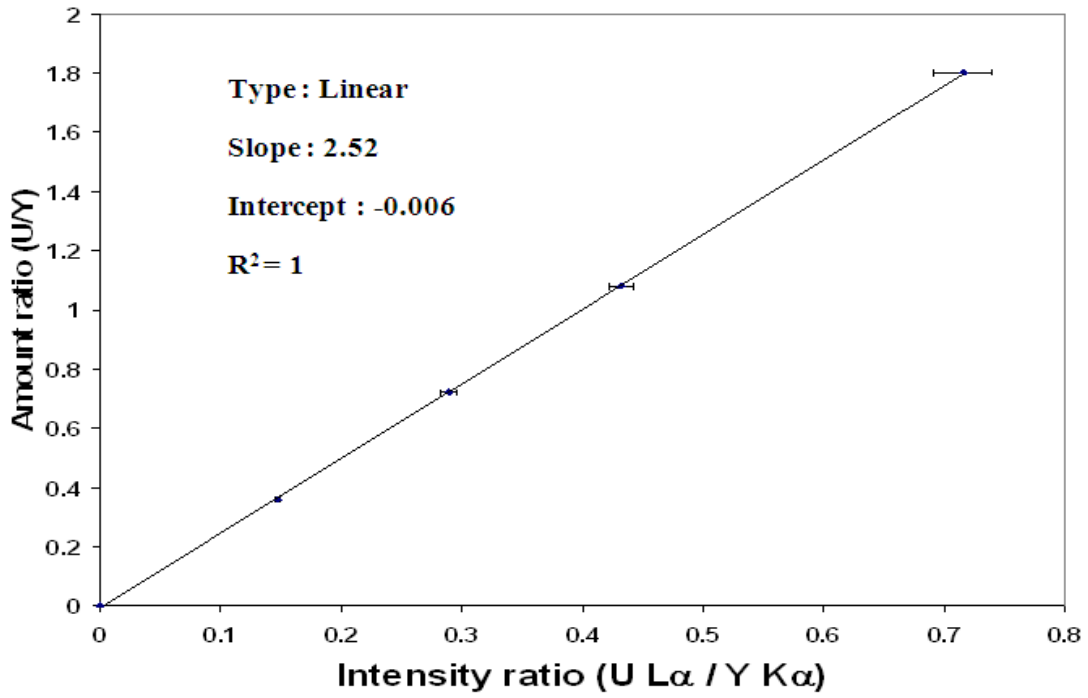


Figure 7.2: Calibration curve for uranium determination of Set -I

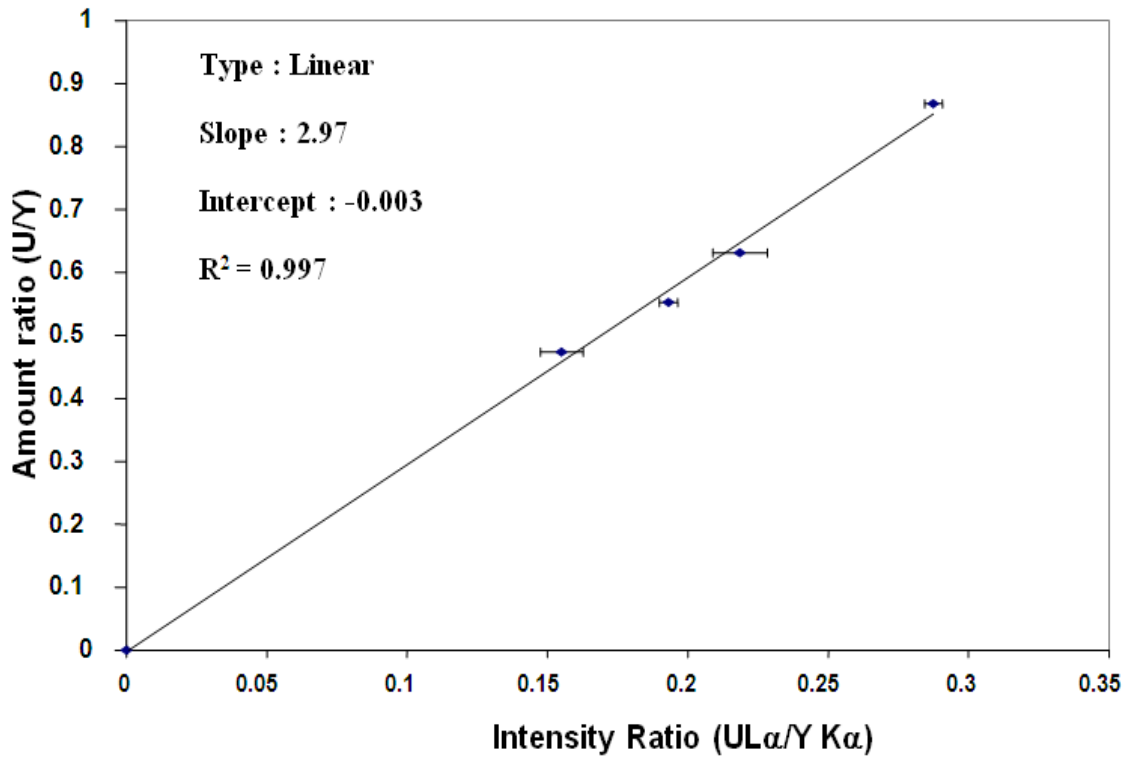


Figure 7.3: Calibration curve for uranium determination of Set -II

determine thorium, a calibration plot as shown in Figure 7.4 was obtained by plotting U $L\alpha$ /Th $L\alpha$ intensity ratios against the corresponding amount ratios.

In order to study the effect of changing the amounts of both uranium and thorium and still maintaining the percentage of uranium in the range of 0–5% with respect to (U + Th), another set of calibration and sample solutions (Set-II) was prepared. Calibration plots for the calibration solutions of Set-II were obtained by plotting intensity ratios of Th $L\alpha$ /Y $K\alpha$ versus corresponding elemental amount ratios for the determination of thorium as shown in Figure 7.5. The amount of thorium in samples of Set-I and II were determined using the respective calibration plots and the analytical results are given in Table 7.6. The average precision for the thorium determinations for Set-I and II was found to be 2% and the deviation of the EDXRF determined values from the expected values calculated on the basis of sample preparation was also 2%.

Table 7.5: Analytical results of uranium determinations in sample solutions of Set-I and II

Sample code	% Uranium in (U +Th)	Uranium amount (mg)		EDXRF/ Expected
		Expected*	EDXRF [#]	
Analytical results of set-I				
S-1-1	1.45	2.48	2.49 ± 0.01	1.004
S-1-2	1.54	2.64	2.75 ± 0.01	1.042
S-1-3	1.92	3.30	3.33 ± 0.06	1.009
S-1-4	3.78	6.61	6.9 ± 0.1	1.044
Analytical results of set-II				
AH-2-3	1.41	2.17	2.04 ± 0.05	0.940
AH-2-4	1.72	2.35	2.3 ± 0.1	0.979
AH-2-6	2.79	2.88	2.95 ± 0.06	1.024
AH-2-7	3.53	3.07	3.1 ± 0.1	1.010
AH-2-9	4.56	3.62	3.71 ± 0.03	1.025

*: Expected uranium amount on the basis of sample preparation

[#]: EDXRF determined uranium amount

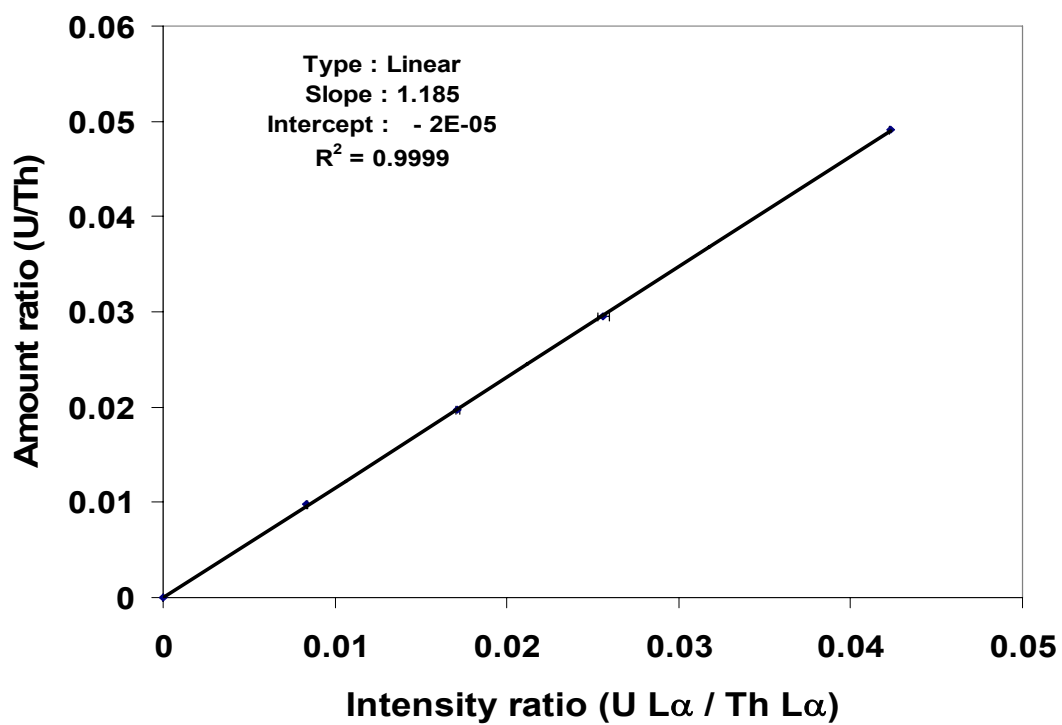


Figure 7.4: Calibration curve for thorium determination of Set -I

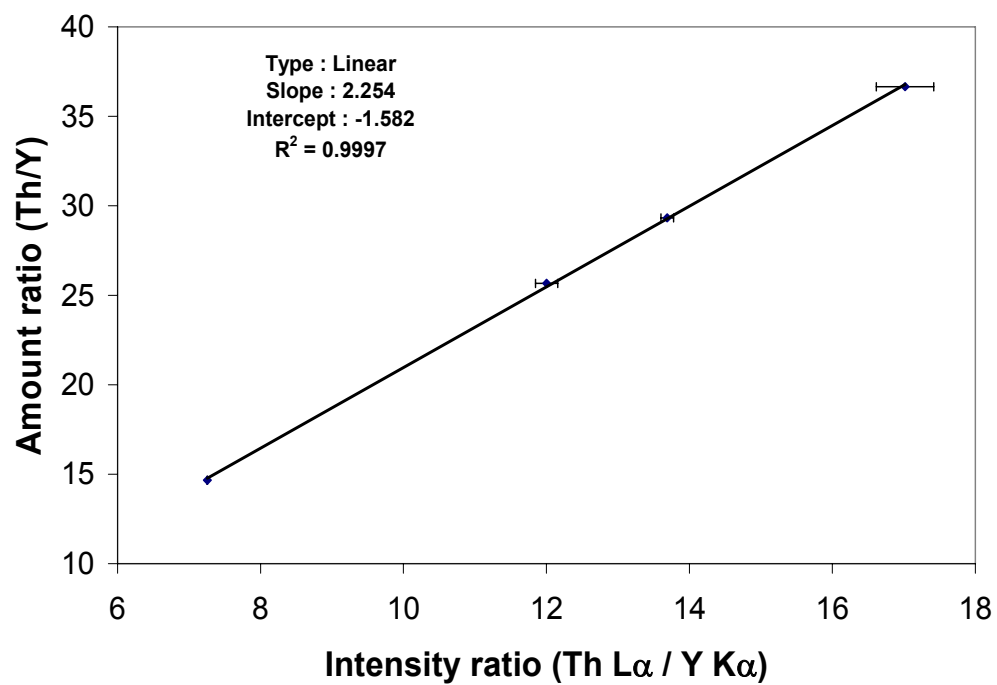


Figure 7.5: Calibration curve for thorium determination of Set -II

Table 7.6: Analytical results of thorium determinations in sample solutions of Set-I and II

Sample code	% Thorium in (U + Th)	Thorium amount (mg)		EDXRF/ Expected
		Expected*	EDXRF#	
Analytical results of set-I				
S-1-1	98.55	168	176 ± 3	1.048
S-1-2	98.46	168	176 ± 1	1.048
S-1-3	98.08	168	170 ± 4	1.012
S-1-4	96.22	168	175 ± 3	1.042
Analytical results of set-II				
AH-2-3	98.59	151.2	148 ± 6	0.979
AH-2-4	98.28	134.4	134 ± 5	0.997
AH-2-6	97.21	100.8	101 ± 3	1.002
AH-2-7	96.47	84	85 ± 3	1.012
AH-2-9	95.44	75.6	77±1	1.019

* : Expected thorium amount on the basis of sample preparation

: EDXRF determined thorium amount

Based on the amounts of thorium and uranium determined in samples of Set-I and Set-II, the percentage of uranium and thorium in (U+Th) matrix was determined. Table 7.7 shows a comparison of the experimentally obtained data and the expected percentage of uranium and thorium. It can be seen that the EDXRF determined percentage of uranium and thorium were in good agreement with the expected values. The agreement in case of uranium was 2% and for thorium was 0.03%. The poor agreement in case uranium was attributed to its low concentration compared to thorium.

Table 7.7: Comparison of EDXRF determined percent uranium and thorium with the expected values in samples of Set –I and II

Sample	% uranium in (U+Th)		EDXRF/ Expected	% thorium in (U+Th)		EDXRF/ Expected
	Expected	EDXRF		Expected	EDXRF	
Set-I						
S-1-1	1.45	1.40	0.959	98.55	98.60	1.0006
S-1-2	1.55	1.54	0.994	98.45	98.46	1.0001
S-1-3	1.93	1.92	0.997	98.07	98.08	0.0001
S-1-4	3.79	3.79	1.002	96.21	96.21	0.9999
Set-II						
AH-2-3	1.41	1.36	0.961	98.59	98.64	1.0006
AH-2-4	1.72	1.69	0.982	98.28	98.31	1.0003
AH-2-7	2.78	2.84	1.022	97.22	97.16	0.9994
AH-2-8	3.53	3.52	0.998	96.47	96.48	1.0001
AH-2-9	4.57	4.60	1.006	95.43	95.40	0.9997

The major advantage of this method was that the total amount of analyte transferred on filter paper was low ($< 60 \mu\text{g}$ of uranium as shown in Table 7.3). The absorption of solution on the filter paper occurs over a circular area of 1.5 cm diameter whereas the X-ray beam has an approximate diameter of 8 mm. Hence, the volume of sample transferred on the filter paper can be further reduced if desired. It can be seen that the precision of uranium and thorium determinations is better than 2% (1σ), and the results deviated from the expected values within the statistical uncertainty of the experimental results. Since the amount of uranium on the filter paper is in microgram level, the radiation hazards due to radioactivity associated with ^{232}U and their daughter products will be minimal. However, this approach requires dissolution of fuel samples, but does not involve any additional work as the sample solutions required can be taken from the solutions prepared for trace element determinations of these fuel samples by

conventional trace elemental analytical techniques, e.g. ICP-OES, ICP-MS, etc. The results obtained in the present work will be useful to evaluate the data on precision and accuracy using solid samples, in future.

7.3. EDXRF Determination of Cadmium in Uranium Matrix using Cd K α Line Excited by Continuum

Quality assurance of uranium is very important in nuclear fuel fabrication and processing for efficient energy generation in reactors. Uranium, to be used as nuclear fuel, is not acceptable if the impurities present exceed certain specification limits. Among the trace impurities present in nuclear fuel, determination of neutron poisons viz. boron (B), cadmium (Cd) and rare-earths e.g. gadolinium (Gd) is important for thermal reactors from point of view of neutron economy as well as for certifying the total impurities as a part of the chemical quality assurance of fuels. Cadmium has a high absorption cross-section for thermal neutrons, hence its presence in amounts > 1 ppm is not acceptable in nuclear materials [13-15]. Further, cadmium being one of the heavy toxic elements, its presence has to be monitored in water, food and environment periodically to avoid its adverse health effects on humans and animals [16, 17]. Because of the above reasons, determination of cadmium at trace and major levels, in presence and in absence of uranium, is of importance.

Many techniques such as Neutron Activation Analysis (NAA), Atomic Absorption Spectrometry (AAS), Inductive Coupled Plasma-Atomic Emission Spectrometry (ICP-AES), Inductive Coupled Plasma- Mass Spectrometry (ICP-MS), Voltammetry, Differential Pulse Anodic Stripping Voltammetry (DPASV), X-ray fluorescence (XRF), etc. have been reported for the determination of trace levels of cadmium in nuclear and environmental samples [13 - 21]. XRF is a simple, fast and accurate technique having potential applications for the determination of different elements in various matrices. For the determination of cadmium by XRF, normally Cd L α line is used though it has certain disadvantages e.g. low fluorescence yield and lying in low energy region having high background etc. [17]. In the presence of uranium, the situation becomes further complicated as there is strong interference of U M α line (3.171 keV) with Cd L α line (3.133 keV). There are some reports in literature on the use of Cd K α line for the determination of cadmium in percentage levels in uranium matrix using wavelength dispersive

X-ray fluorescence (WDXRF) [20]. It is very difficult to resolve Cd $L\alpha$ line and U $M\alpha$ while using energy dispersive X-ray fluorescence (EDXRF). If cadmium is determined by XRF using Cd $K\alpha$ (23.172 keV) as analytical line, these problems can be counterchecked to a large extent provided a suitable excitation source is available for Cd $K\alpha$ excitation. The commonly available X-ray tubes for XRF analysis have Mo, Ag or Rh targets and use mainly Mo $K\alpha$, Ag $K\alpha$ and Rh $K\alpha$ lines for sample excitation. None of these lines can excite Cd $K\alpha$. Radioisotopic and synchrotron sources can give high energy X-rays and can excite Cd $K\alpha$ line but these sources have their own problems e.g. low diminishing intensity with time and non-availability for routine sample analysis, respectively. The continuum part of X-ray tube spectra can be used for the determination of cadmium using Cd $K\alpha$ as an analytical line for routine sample analysis. Another major problem in determination of cadmium in uranium matrix is that U L_1 and L_2 absorption edges are at 21.757 and 20.948 keV, respectively and Cd $K\alpha$ line will be strongly absorbed in uranium. In order to overcome this problem, uranium must be separated from the samples before XRF determination of cadmium.

In the present work, the possibility of employing EDXRF for the determination of cadmium in uranium using the continuum produced by the Rh target to excite the Cd $K\alpha$ lines was investigated. In order to improve the detection limits as well as to minimize the matrix effect, uranium was separated by solvent extraction from the calibration and sample solutions. Though continuum sources are of lesser intensity compared to characteristic X-rays, these can be suitably tuned for experimental requirements by suitable choice of instrumental parameters.

7.3.1. Experimental

7.3.1a. Sample preparation

Standard solution of cadmium (100 $\mu\text{g/mL}$) was prepared by diluting Merck cadmium single element standard solution having a concentration of 1000 $\mu\text{g/mL}$. The HNO_3 used was of suprapure grade. All dilutions and sample preparations were carried out in 1.5% HNO_3 in Milli-Q water. Two uranyl nitrate standard solutions having uranium concentration of 85 and 500 mg/mL were prepared by dissolving high purity nuclear grade U_3O_8 powder in HNO_3 . Calibration and sample solutions of cadmium in presence of uranium and without uranium were prepared.

For solutions of cadmium without uranium, different volumes of the standard solutions of cadmium were mixed in 1.5% HNO₃ and the composition of these calibration solutions and samples are given in Table 7.8. The concentration of cadmium varied from 6 to 38 µg/mL in these solutions.

Two sets (Set-I and Set-II) of calibration and sample solutions of cadmium with uranium were prepared by mixing different volumes of standard solutions of cadmium and uranyl nitrate. Concentration of cadmium in these calibration and sample solutions was in the range of 9 to 90 µg/mL. The cadmium concentration with respect to uranium was in the range of 90 to 500 µg/g.

Table 7.8: Details of calibration and sample solutions of cadmium without uranium

Solution Code	Volume (µL)		Concentration of cadmium (µg/mL)
	Cadmium standard solution	1.5 % nitric acid	
Calibration Solution			
STD-Cd-1	100	1500	6.25
STD-Cd-2	300	1500	16.67
STD-Cd-3	500	1500	25.00
STD-Cd-4	700	1500	31.82
STD-Cd-5	900	1500	37.50
Sample Solution			
Samp-Cd-1	200	1500	11.76
Samp-Cd-2	400	1500	21.05
Samp-Cd-3	600	1500	28.57
Samp-Cd-4	800	1500	34.78

The details of preparation of cadmium calibration solutions in presence of uranium of Set-I and II are given in Table 7.9. The EDXRF determination of cadmium in samples of Set-I and II was done after separation of the major matrix uranium by solvent extraction. For selective extraction of uranium from the calibration as well as sample solutions, a 30% TBP solution in dodecane after pre-equilibration with 2.5 M HNO₃ was used and the solutions were equilibrated with TBP three times as described in the flowchart given in Figure 7.6.

Table 7.9: Details of calibration solutions of cadmium in presence uranium in Set-I and II

Calibration Solution	Concentration of		Concentration of cadmium (µg/g of uranium)
	Cadmium (µg/mL)	Uranium (mg/mL)	
Calibration Solution Set-I			
STD-U1-Cd-1	9.12	98.28	92.8
STD- U1-Cd-2	12.89	94.16	136.9
STD- U1-Cd-3	21.58	84.76	254.6
STD- U1-Cd-4	32.28	77.28	417.7
STD- U1-Cd-5	37.92	70.84	535.3
STD- U1-Cd-6	42.70	65.39	653.0
Calibration Solution Set-II			
STD-U2-Cd-1	50	500	100
STD- U2-Cd-2	65	500	130
STD- U2-Cd-3	80	500	160
STD- U2-Cd-4	90	500	180

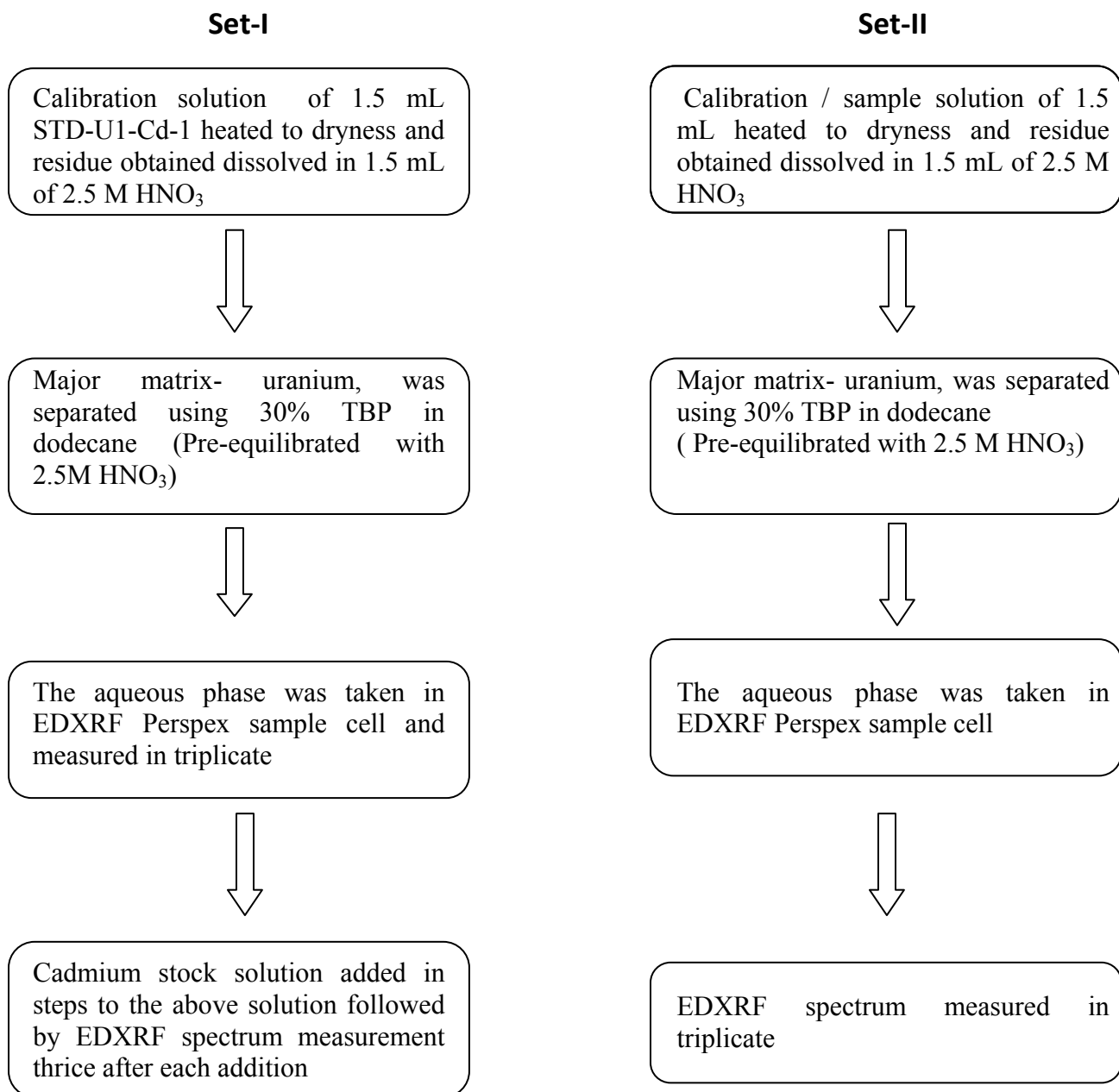


Figure 7.6: Flow chart showing processing of calibration solutions of Set-I and II, the samples of both the Sets were processed using the procedure of Set-II.

In Set-I, the calibration solutions were prepared by solvent extraction of uranium in one solution (STD-U1-Cd-1) and subsequent addition of cadmium standard solution in steps to this processed solution after each EDXRF measurements. All the calibration solutions and samples of Set-II and only samples of Set-I were processed in a similar way.

7.3.1b. Instrumentation

A Jordan Valley EX-3600TEC EDXRF spectrometer having rhodium target was used for the EDXRF measurements. The low power tube was operated at 50 kV and 750 μ A and a molybdenum filter was used for background reduction. The analytical line of interest was Cd K α having energy of 23.17 keV. As the absorption edge of the analyte is at energy higher than that of Rh K α (20.22 keV), the analyte line is mainly excited by the relevant part of continuum produced at this voltage and current, having maxima at around 30 keV.

A specially designed in-house fabricated sample cell of highly pure perspex was used for the EDXRF measurements. This sample cell has an outer diameter of 40 mm and an inner diameter of 20 mm and can be tightly closed with perspex lid. The height of the sample cell after closing the lid was 30 mm and it was sitting properly in the sample holder seat of the EDXRF spectrometer. The base thickness of the cell was about 1 mm to allow for the penetration of X-rays of Cd K α . 1.5 mL of the aqueous phase of calibration solutions and samples were taken in these sample cells and loaded in spectrometer for measurements. The EDXRF spectrum of each calibration solution and sample was measured thrice for a live time of 500 s.

7.3.2. Results and discussion

For determination of cadmium using Cd K α excited by continuum, the disadvantage is the loss of intensity. This is because the characteristic excitation has higher intensity compared to the continuum. But if the geometry of the XRF system is improved and the signal to noise ratio in Cd K α energy region can be increased by suitable filter, a better detection limit can be achieved. In the Jordan Valley EDXRF spectrometer used in the present work, the distance between detector and sample is very less (approximately 10 mm) and due to this, the intensity loss of the X-rays from source to sample and samples to detector will also be less. Moreover, the use of molybdenum filter improved the signal to noise ratio significantly. The Mo K_{abs} edge is at

19.97 keV and hence a Mo filter was used for reducing the background in the energy region of approximately 20–24 keV. As the Cd K α energy lies in this region, peak to background ratio appreciably increased with the use of this filter when placed between the sample and X-ray tube. This feature was beneficially exploited to reduce the background in the energy region of Cd K α . In addition, the Mo filter reduced the intensity of Rh K β to a negligible level and this avoided the undesirable effects of interference of Rh K β with Cd K α on the analytical results of cadmium determination by EDXRF. These effects can be seen in Figure 7. 7, where a comparison of tube spectra obtained after passing through molybdenum and rhodium filters is shown. The reduction in background in Cd K α energy region while using Mo filter is clearly visible. Both these features were beneficially used for improving the detection limit, precision and accuracy of EDXRF determinations of cadmium using Cd K α analytical line by continuum excitation.

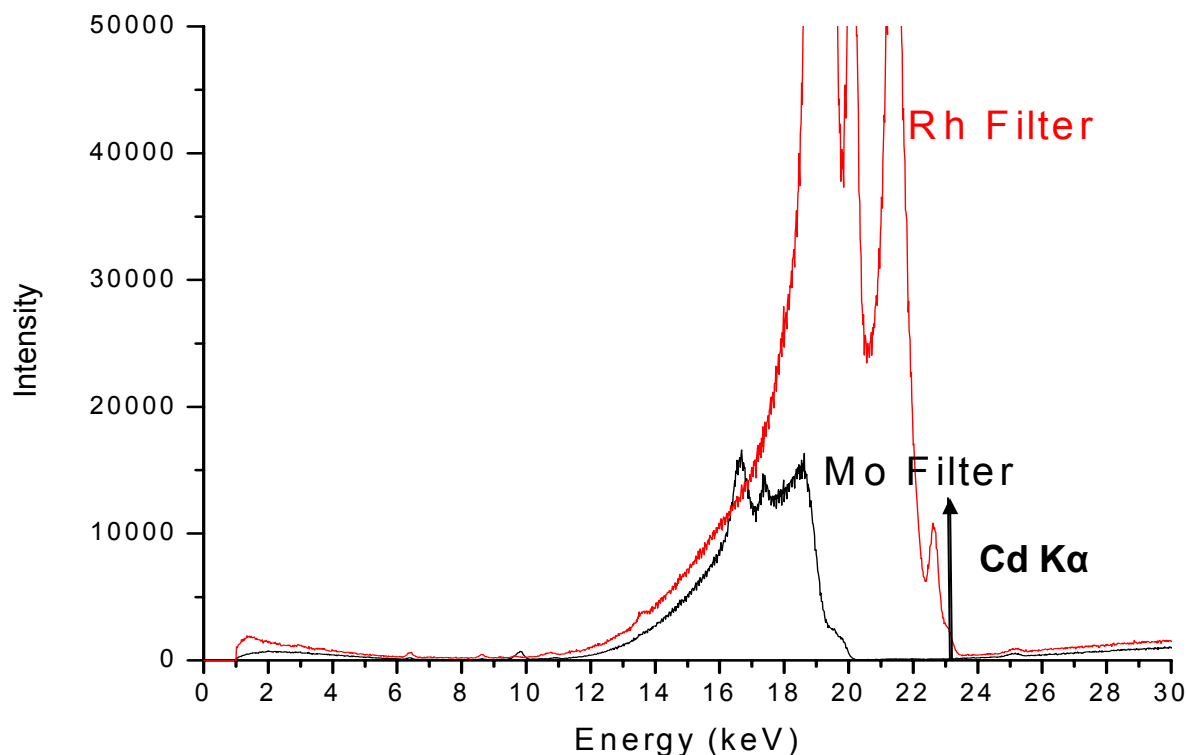


Figure 7.7: Effect of Mo and Rh filters on the tube spectrum in Cd K α energy region

7.3.2a. Cadmium determination in absence of uranium

For the determination of cadmium in samples containing no uranium, 1.5 mL of the calibration solutions (Table 1) was taken in perspex sample cell, EDXRF spectrum was measured and a calibration curve was made by plotting cadmium concentration against average net intensity obtained in three measurements as shown in Figure 7.8. The error bars of X-ray intensities were much larger compared to the expected statistical variations. This was probably due to non uniformity in base thickness of in-house built Perspex cells. Based on this calibration curve, the samples were analyzed and the results are shown in Table 7.10. The cadmium concentration $< 6 \mu\text{g/mL}$ could not be detected. The average precision and deviation from the expected values calculated on the basis of sample preparation for cadmium determinations were 5 and 16 %, respectively.

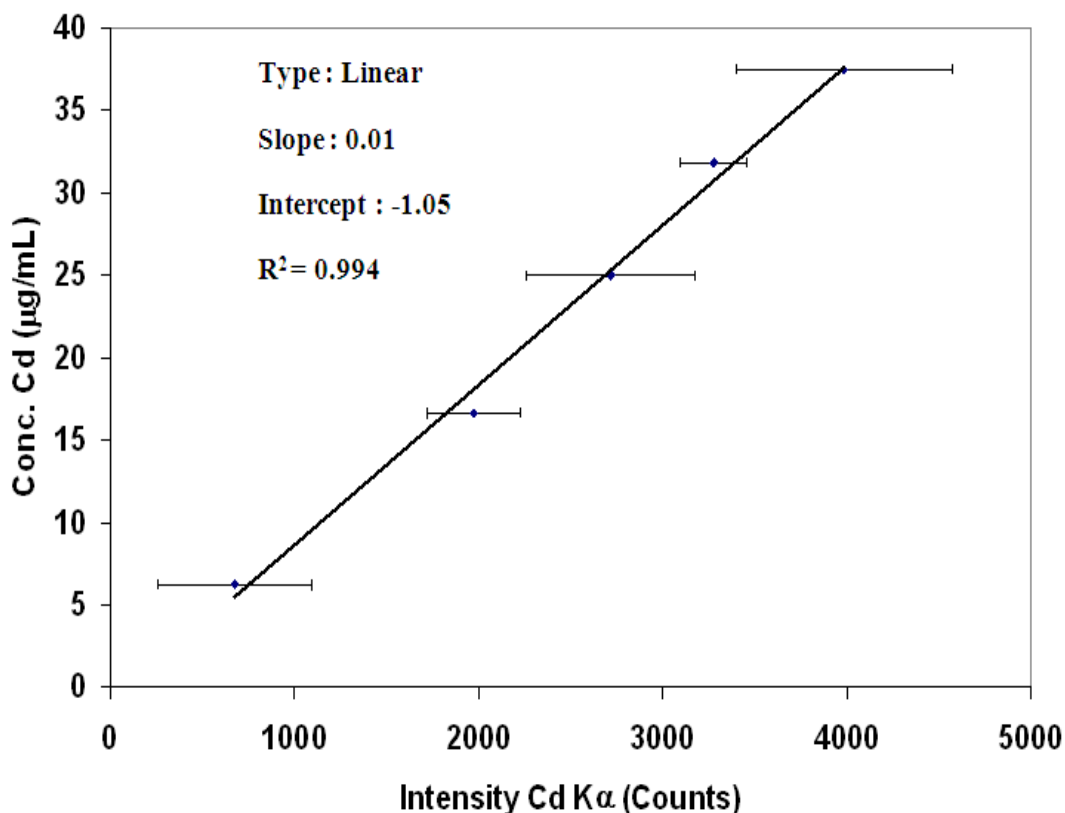


Figure 7.8: Calibration plot for cadmium determination in samples without uranium (Error bars represent the standard deviation of intensity measurements, n=3)

Table 7.10: Analytical results of EDXRF determination of cadmium in samples without uranium

Sample Solution	Concentration in $\mu\text{g/mL}$		EDXRF/ Expected
	Expected*	EDXRF [#]	
Samp-Cd-1	11.76	7.9 ± 0.3	0.67
Samp-Cd-2	21.05	17.7 ± 0.6	0.84
Samp-Cd-3	28.57	26 ± 2	0.93
Samp-Cd-4	34.78	38 ± 2	1.09

*: Expected cadmium concentration on the basis of the preparation of samples

[#]: EDXRF determined cadmium concentration $\pm 1 \sigma$ (n=3)

7.3.2b. Cadmium determination in presence of uranium

When cadmium needs to be determined at trace level in the presence of a heavy element like uranium, the improvements in detection limit obtained by the above instrumental features will be nullified by absorption of Cd $K\alpha$ line by uranium. For such determinations, uranium matrix should be separated from the calibration/sample solutions and this was achieved by using well established method of solvent extraction with TBP in dodecane. The effect of such separation on Cd $K\alpha$ intensity in EDXRF spectrum of a calibration solution is shown in Figure 7.9. The Cd $K\alpha$ peak which was not visible before separation of uranium, is clearly visible after separation. It can also be seen that the less intense lines of uranium U $L\gamma_3$ and $L\gamma_4$ are visible at approximately 20.70 and 21.5 keV, respectively, in the EDXRF spectrum of the sample measured before extraction because of the high uranium concentration. These lines disappeared in the EDXRF spectrum measured after uranium extraction.

Radioactive materials cannot be handled in open atmosphere and the instrument should be put in a glove box. This makes handling of sample as well as instrument maintenance very difficult. In order to avoid such difficulty, leak proof Perspex sample cells, as described above, were fabricated so that these samples can be sealed properly and analysed without making the spectrometer active. Since the Cd $K\alpha$ energy (23.174 eV) is quite high, it can penetrate the perspex sample cell and thus cadmium can be determined using such sample cells.

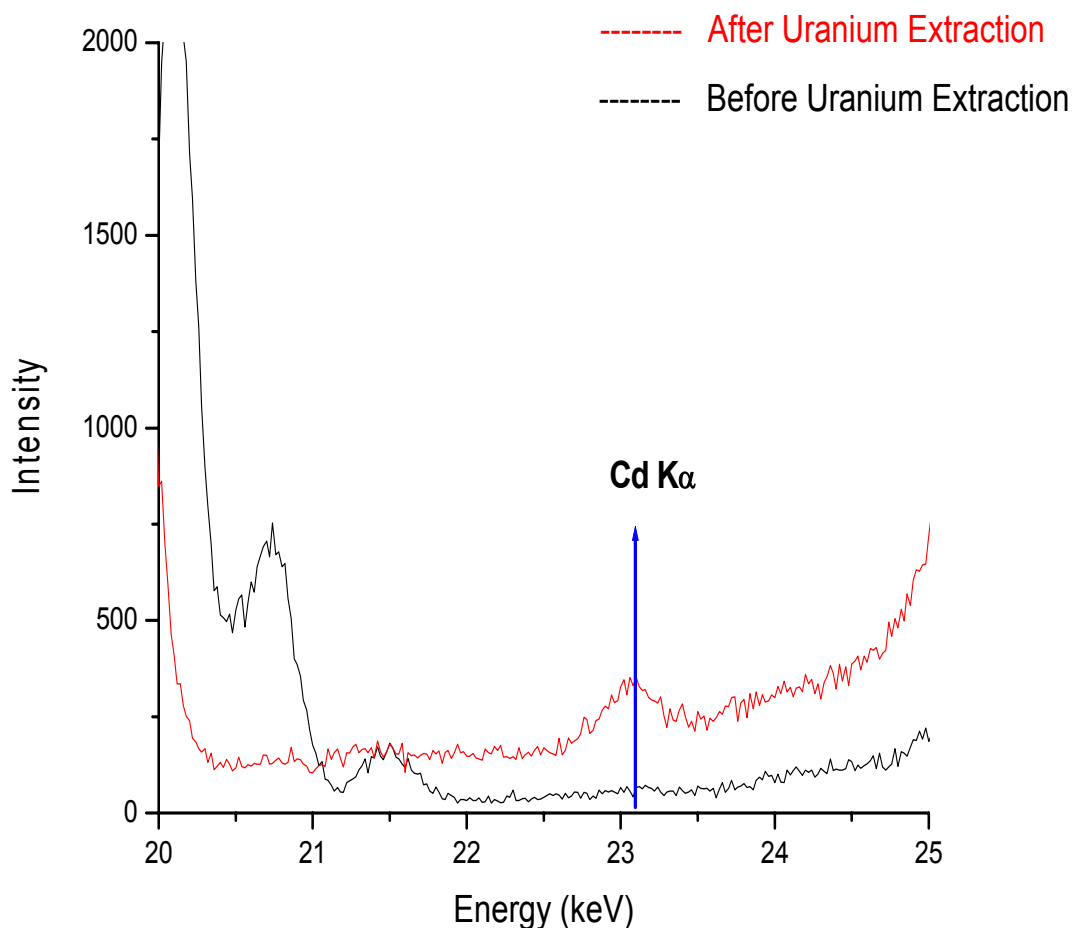


Figure 7.9: Effect of extraction of uranium on the intensity of Cd K α

For accurate determination of any analyte by XRF, the concentration of the analyte in the standards used for calibration should be accurately known. In order to fulfill both the conditions i.e. removal of uranium matrix and maintaining concentration of cadmium in these aqueous calibration solutions accurately, uranium present in the calibration solution STD-U1-Cd-1 of Table 7.9 was selectively removed and EDXRF spectrum of the aqueous phase was measured as described in the flowchart (Figure 7.6 (Set-I)). The spectrum did not show any peak of Cd K α even after selective removal of uranium by solvent extraction. Cadmium amount in the sample cell was increased in steps to get other calibration solutions having cadmium concentration as shown in Table 7.9. After each addition of cadmium, the sample was well shaken and the

EDXRF spectra were measured. The Cd K α peak started appearing from calibration solution STD-U1-Cd-3. Finally a calibration graph was made by plotting the average Cd K α net intensity against the cadmium concentration as shown in Figure 7.10. This calibration plot was used to analyze cadmium in the samples of Set-I after selective extraction of uranium from each sample. As the fabricated Perspex cell did not have uniform base thickness, a single cell was used for all the EDXRF measurements. Table 7.11 gives the analytical results of cadmium in this Set. The average precision and deviation from the expected cadmium concentration were 2 and 10%, respectively. The standard deviation on the intensities of Cd K α was reduced to quite a large extent. It can be seen from Table 7.11 that the EDXRF determined cadmium values are

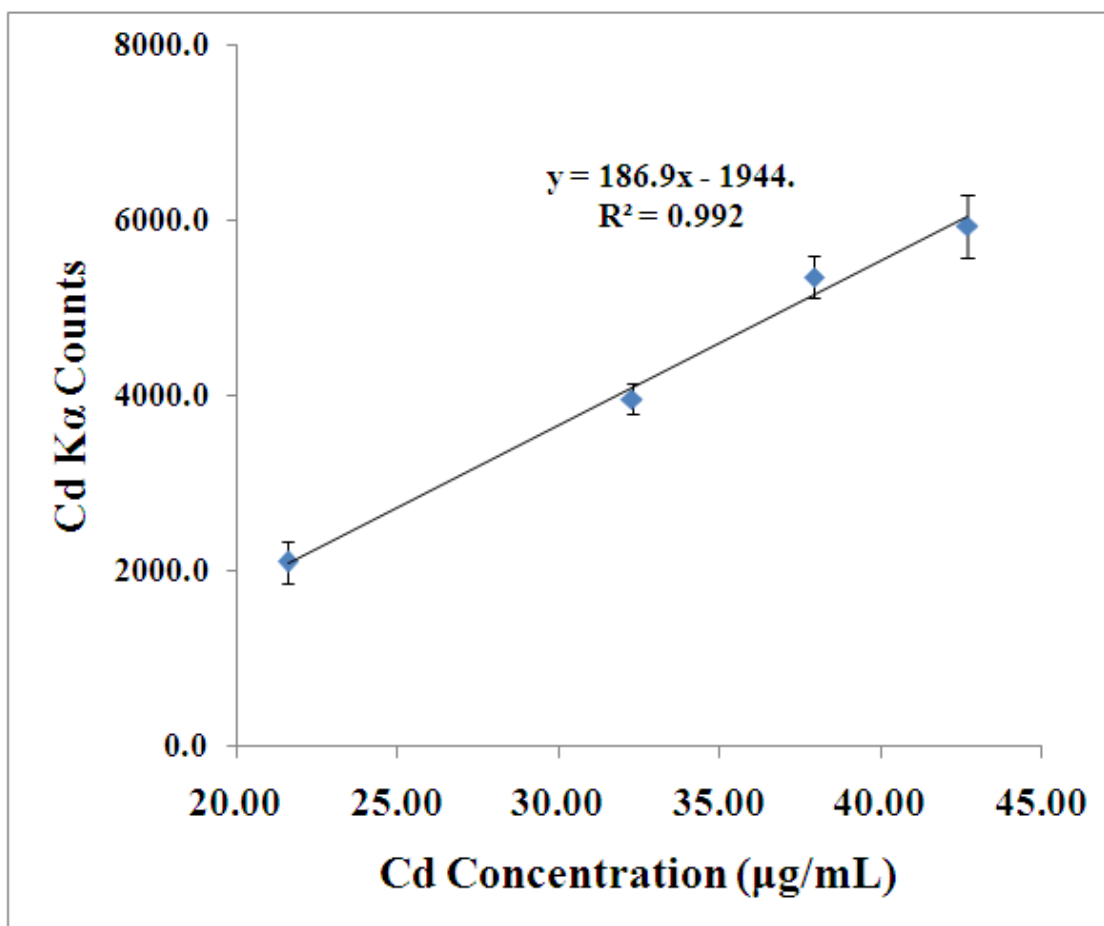


Figure 7.10: Calibration plot for cadmium determination in samples of Set-I (Error bars represent the standard deviation of intensity measurements, n=3)

Table 7.11: Analytical results of EDXRF determination of cadmium in samples of Set-I

Sample code	Cd concentration ($\mu\text{g/mL}$)		EDXRF / Expected
	Expected [*]	EDXRF [#]	
Samp - U1-Cd-1	25	24.57 ± 0.36	0.98
Samp - U1-Cd-2	30	29.17 ± 0.21	0.97
Samp - U1-Cd-3	35	30 ± 2	0.86
Samp - U1-Cd-4	40	31.02 ± 0.03	0.78

^{*}: Expected cadmium concentration on the basis of the preparation of samples

[#]: EDXRF determined cadmium concentration $\pm 1 \sigma$ (n=3)

systematically lower than the expected values. This negative deviation may be due to two reasons arising due to different sample preparation methodology adopted for calibration and sample solutions: Firstly, small losses of cadmium during extraction process during the preparation of samples and secondly, presence of comparatively smaller amounts of uranium in calibration solutions (due to the dilution of trace amounts of un-extracted uranium, occurring after each addition of cadmium in aqueous phase of STD-U1-Cd-1) compared to those of sample solutions. Therefore, absorption of Cd $K\alpha$ line by uranium in calibration solution is less compared to that of sample solutions.

In order to confirm these assumptions, another set of calibration solutions Set-II was prepared and each calibration solution was equilibrated with processed TBP. A calibration curve was made by plotting the concentration of cadmium in calibration solutions against Cd $K\alpha$ intensity values. The samples of Set-II, prepared in similar way as the calibration solutions, were analyzed using this calibration plot. The analytical results are given in Table 7.12. No negative bias was observed in the EDXRF determined concentration of cadmium. This indicates that the sample and calibration solution should be processed in a similar way for better analytical results. The average precision observed was 2% (1σ) and the average deviation from the expected values was 3%. The Y-intercept obtained in calibration plot shown in Figure 7.10 indicates that the method is insensitive to cadmium concentration of lower than $10 \mu\text{g/mL}$. The present EDXRF

Table 7.12: Analytical results of EDXRF determination of cadmium in samples of Set-II

Sample	Cd concentration ($\mu\text{g/mL}$)		EDXRF / Expected
	Expected*	EDXRF [#]	
Samp - U2-Cd-1	60	64 ± 1	1.07
Samp – U2-Cd-2	70	67.73 ± 0.56	0.97
Samp – U2-Cd-3	75	73 ± 3	0.97
Samp – U2-Cd-4	85	86 ± 2	1.01

*: Expected cadmium concentration on the basis of the preparation of samples

[#]: EDXRF determined cadmium concentration $\pm 1 \sigma$ (n=3)

methodology appears to be complicated but similar sample preparation procedures involving dissolution and separations are adopted in ICP-MS and ICP-AES determinations. These sample preparation steps help in improving the detection limits of EDXRF determinations to match with other well established trace element analytical techniques. The EDXRF method, especially in the presence of uranium, is prone to less interference compared to ICP-AES. The method of determination of cadmium in samples without uranium will find applications in environmental samples e.g. water, soil, etc. In the present study, the uranium bearing samples having cadmium concentrations $> 21.58 \mu\text{g/mL}$ ($254.56 \mu\text{g Cd/g of U}$) only showed the Cd $K\alpha$ peak even after uranium extraction. For the samples containing no uranium, Cd $K\alpha$ peak could be observed in samples having Cd $> 6.25 \mu\text{g/mL}$. In real sample analysis, this limit can be improved by dissolving uranium in smaller amount of nitric acid, taking the calibration samples and standards for recording EDXRF spectra in sample cells of thinner base and concentrating the aqueous phase by evaporation before recording the spectra. Perspex sample cells were used because of their transparency to X-rays, desired mechanical strength, easy machining to desired shape and are free of any cadmium. Also 2.5 M nitric acid can be handled in these cells several times without any chemical attack. In addition, the leak proof perspex sample containers can be sealed in very thin alkathene sheets inside a fume hood and can be loaded in EDXRF sample chamber.

This will be very much helpful in analyzing radioactive materials as the cumbersome operation/maintenance of instrument inside the glove box can be avoided.

7.4. Conclusions

The present studies indicate the successful applications of EDXRF for bulk as well as trace analysis of nuclear materials. Radioactive samples can be sealed properly and then analysed without making the spectrometer active.

7.4.1. Bulk determination of uranium and thorium

The present EDXRF method for bulk determinations of uranium and thorium is well suited for routine sample analysis of AHWR fuel as it requires small amounts of the sample after dissolution. The actinide elements can be recovered by ashing of the filter paper used for sample loading. Compared to solid sample analysis on pellets prepared using binder, this method requires little sample preparation. The precision observed was better than 2% (1σ) and the results deviated from the expected uranium and thorium concentrations within the statistical uncertainties. The method of depositing solution samples on thin filter papers avoids matrix effect.

7.4.2. Trace determination of cadmium in uranium matrix

An EDXRF method was developed for cadmium determination at trace levels in uranium matrix by using its $K\alpha$ as the analytical line and exciting by continuum. Molybdenum filter was used for the background reduction in the EDXRF tube spectra and the samples were loaded in the spectrometer after selective separation of uranium and taking the samples in perspex cell. Treatment of calibration solutions and samples for selective extraction of uranium in similar way gives better results. In the present condition, the method is applicable to uranium samples having cadmium concentration $> 22 \mu\text{g/mL}$ in aqueous phase obtained after extraction of uranium. The extension of the method to cadmium determinations in real samples of uranium will require concentration of the aqueous phase by evaporation and taking the samples in cells of thinner base. Use of W/Au $K\alpha$ excitation using rotating anode and TXRF geometry will improve the

detection limits appreciably. The average precision observed in present the conditions was 2% (1σ) and results deviated from the expected values by 3%. The method will also find application in determination of cadmium in environmental samples.

7.5. References

1. E.A. Bertin, Principle and practice of X-Ray spectrometric analysis, 2nd Edition, Plenum Press, New York, 1984.
2. R. Polat, A. Gürol, G. Budak, A. Karabulut, M. Ertuğrul, Elemental composition of cement Kiln dust, raw material and cement from a coal-fired cement factory using energy dispersive X-ray fluorescence spectroscopy, *J. Quant. Spectrosc. Radiat. Transfer*, 83 (2004) 377.
3. N. Ekinçi, R. Ekinçi, R. Polat, G. Budak, Analysis of trace elements in medicinal plants with energy dispersive X-ray fluorescence, *J. Radioanal. Nucl. Chem.*, 260 (2004) 127.
4. Kirk K. Nielson, Matrix Corrections for Energy Dispersive X-ray Fluorescence Analysis of Environmental Samples with Coherent/Incoherent Scattered X-rays, *Anal. Chem.*, 49 (1977) 641.
5. N. S. Mahapatra, An Approach to the Solution of Matrix Problems in the XRF Analysis of Lead-Zinc Ore by the Use of an Internal Standard and Mathematical Corrections, *X-ray spectrum.*, 16 (1987) 171.
6. Rafał Sitko, Quantitative X-ray fluorescence analysis of samples of less than ‘infinite thickness’: Difficulties and possibilities, *Spectrochim. Acta, Part B*, 64 (2009) 1161.
7. R. Al-Merey, J. Karajou, H. Issa, X-ray fluorescence analysis of geological samples: exploring the effect of sample thickness on the accuracy of results, *Appl. Radiat. Isot.*, 62 (2005) 501.
8. O. Gonzalez-Fernandez, I. Queralt, M.L. Carvalho, G. Garcia, Elemental analysis of mining wastes by energy dispersive X-ray fluorescence (EDXRF), *Nucl. Instrum. Methods Phys. Res., Sect. B*, 262 (2007) 81.
9. R.K. Sinha, A. Kakodkar, Design and development of the AHWR—the Indian thorium fuelled innovative nuclear reactor, *Nucl. Eng. Des.*, 236 (2006) 683.

10. K. Anantharaman, V. Shivakumar, D. Saha, Utilisation of thorium in reactors, *J. Nucl. Mater.*, 383 (2008) 119.
11. M. E. A. Robertson, C. E. Feather, Determination of gold, platinum and uranium in South African ores by high energy XRF spectrometry, *X-Ray Spectrom.*, 33 (2004) 164.
12. S. Assad, Al-Ammar, F. H. Ali, Determination of impurities in nuclear- grade uranium compounds by X-ray fluorescence spectrometry, *X-Ray Spectrom.*, 21 (1992) 211.
13. B. Li, M. Luo, J. Li, W. Liu, Y. Sun, G. Guo, Determination of cadmium and lead in high purity uranium compounds by flame atomic absorption spectrometry with on-line micro-column preconcentration by CL-7301 resin, *J. Radioanal. Nucl. Chem.*, 278 (2008) 3.
14. L.S. Jing, R.M. Barnes, Determination of cadmium in pure zirconium by inductively coupled plasma-atomic emission spectroscopy, *Appl. Spectrosc.*, 38 (1984) 284.
15. S.K. Thulasidas, M.J. Kulkarni, N.K. Porwal, A.G. Page, M.D. Sastry, Direct determination of beryllium, cadmium, lithium, lead and silver in thorium nitrate solution by electrothermal atomization atomic absorption spectrometry, *Anal. Lett.*, 21 (1988) 265.
16. H. Matusiewicz, M. Koprak, R.E. Sturgeon, Determination of cadmium in environmental samples by hydride generation with in situ concentration and atomic absorption detection, *Analyst*, 122 (1997) 331.
17. C. Fondàs, E. Marguí, M. Hidalgo, I. Queralt, Improvement approaches for the determination of Cr(VI), Cd(II), Pd(II) and Pt(IV) contained in aqueous samples by conventional XRF instrumentation, *X-ray Spectrom.*, 38 (2009) 9.
18. R.J. Rosenberg, R. Zilliacus, Determination of impurities in nuclear fuel element components by neutron activation analysis, *J. Radioanal. Nucl. Chem.*, 169 (1993) 113.
19. B. Pihlar, C.J. Choi, Direct voltammetric determination of some heavy metals in uranium, *Analyst*, 112 (1987) 1583.
20. R. Qadeer, J. Hanif, M. Khan, XRF estimation of Cd, Hf, Hg, and Gd in uranium solution, *J. Radioanal. Nucl. Chem.*, 172 (1993) 137.
21. S. Bürger, L.R. Riciputi, D.A. Bostick, Determination of impurities in uranium matrix by time-of-flight ICP-MS using matrix matched method, *J. Radioanal. Nucl. Chem.*, 274 (2007) 491.

SUMMARY

Analytical characterization of technologically important materials involves study of elemental composition with respect to major, minor, trace and ultra-trace constituents, thermodynamic properties, structural and morphological properties, assessment of strength, heat and radiation effects, etc. All these characterizations are equally important and require the application of several techniques and methodologies. Characterization of elemental composition is essential, in order to assess the quality of any material and decide its subsequent applications, as the quality is greatly influenced by impurities present in them and its composition. Hence, analytical characterization is a step of immense importance for quality assessment and development of technologically important materials.

The nuclear fuel, which consists of uranium, thorium, plutonium and their compounds, is technologically the most important component of a nuclear reactor. Other technologically important materials in nuclear industry are: coolants, moderators, structural materials, control rod, etc. For the efficient as well as safe operation of the reactors, chemical quality assessment and characterization with respect to their trace impurities and bulk composition of starting material, process intermediates and final product is mandatory. Before putting the fuel in the reactor, the fuel matrix should be as pure as possible. But this is seldom possible. In due course of fuel fabrication and processing a number of trace impurities get incorporated into the fuel matrix. These impurities cause detrimental effect on the fuel properties and performance under reactor operating conditions.

As no single technique can analyze all the elements, different techniques and instrumental conditions are required for the complete characterization of a material. X-Ray Fluorescence (XRF) is a well established analytical technique for qualitative as well as quantitative determination of elemental composition in a sample, independent of their chemical and physical form. Unfortunately, the classical XRF spectrometers have relatively poor detection limits and hence cannot compete with the well established methods for trace and ultra trace determinations. Moreover, XRF has severe matrix effect due to the penetration of X-rays inside the sample to a few microns depth. This leads to errors during quantitative analysis. Thus matrix effect and high spectral background are the two main drawbacks of XRF which limit its

application and detection limits to comparatively high values (in the range of a few ppm in the most suitable condition). In the year 1971 two Japanese scientists, Yoenda and Horiuchi, put forward the possible application of Total reflection X-Ray Fluorescence (TXRF), an advanced variant of EDXRF (Energy Dispersive X-ray Fluorescence), which utilizes the property of total external reflection of X-rays for trace elemental determinations. TXRF, a comparatively new technique, has detection limits several orders of magnitude lower than the conventional XRF instruments. It is also a micro analytical technique which requires only few microgram or microliters of the sample for analysis. TXRF has negligible matrix effect and very low background compared to the conventional XRF. These features of TXRF make this technique very attractive for application in nuclear industries, as most of these materials are radioactive / toxic and it is desirable to have very small sample amount for analysis so that the analyst as well as the instrument is exposed to minimum radiation dose. Such methodology will also generate less radioactive waste. Another problem in the analysis of radioactive samples is the non availability of matrix matched standards for quantification. In TXRF, quantification is also very simple as it requires a single internal standard addition to the sample and the quantification is done with respect to the standard. Hence, no matrix matched standards nor cumbersome calibration curves, are required. In spite of all these advantages only a few literature reports on applicability of TXRF in the field of nuclear industries are reported.

The objective of the present thesis was to develop TXRF and EDXRF methodologies for analytical characterization of nuclear materials. TXRF methods for the determination of metallic and non-metallic trace impurities in various nuclear material matrices and bulk characterization of uranium and thorium in nuclear fuel was developed. In addition, studies have been carried out for trace and bulk characterization of nuclear materials by EDXRF.

The important highlights of the thesis are:

1. Calibration and validation of the TXRF spectrometer was done using an MERCK ICP multi-elemental standard solution. The relative sensitivities and detection limit values were determined at trace and ultra-trace levels. **The detection limits for strontium was found to be 1 ng/mL and for aluminum 137 ng/mL, which is comparable with other well established trace elemental analysis techniques.**

2. A TXRF analytical method for the determination of trace metallic impurities in thorium oxide matrix was developed. **This method was successfully applied for the development of Certified Reference Materials for trace metallic impurities in ThO₂ standards.**
3. Sample preparation method and instrumental parameters were standardized / optimised for the determination of low Z elements viz. sodium, magnesium and aluminum in uranium matrix, using a vacuum chamber TXRF spectrometer (WOBISTRAX), as the conventional TXRF spectrometer cannot be used for the quantitative determination of low Z elements. **The method developed was successfully applied for real samples for the first time.**
4. As XRF has potential to analyse both metal and non-metal alike, TXRF methodology for the determination of sulphur in uranium matrix was developed after the separation of major matrix by solvent extraction. **The method developed was counterchecked for sulphur determinations using a chemical assay standard for uranium Rb₂U(SO₄)₃ and was found to be satisfactory.**
5. A pyrohydrolysis hyphenated TXRF method was developed for the chlorine determination in nuclear fuel matrix of radioactive samples for the first time and **was successfully applied to nuclear fuel and other samples e.g. U₃O₈, (U,Pu)C and alloy samples without any sample dissolution.**
6. Another novel method for chlorine determination in acidic medium using TXRF was developed. **This method involves indirect determination of chlorine after precipitating it as silver chloride and determining the excess silver in the solution.**
7. A micro-analytical TXRF method for bulk determination of uranium and thorium in solutions as well as soils was developed. For solid samples, containing solid solution in form of pellets/microspheres, the method developed requires gentle touching the samples on TXRF sample support followed by their determination with respect to each other without any sample dissolution process. **The advantages of this method are requirement of very small sample amount (in nanogram range) for analysis. This feature will be helpful in**

minimizing the radioactive waste generated during analysis and the dose imparted to the analyst will also be reduced. The precision obtained was comparable in both the solution and the solid samples.

8. TXRF methodologies for determination of uranium in seawater and fertilizers were developed after selective extraction of uranium using organic solvents. **The method was successfully applied for such determinations of uranium in the above non-conventional sources.**
9. An EDXRF methodology was developed for the fast and accurate determination of uranium and thorium. This method requires very less sample amount (μg level) for analysis. **The developed method has an advantage that radioactive samples can be sealed properly and analysed without making the instrument radioactive.**
10. EDXRF method for the trace determination of cadmium in uranium matrix was developed. **Application of Cd Ka as analytical line excited by continuum and use Mo filter helped for getting better detection limit.**

List of publications (Journals)

1. *Uanium determination in seawater by total reflection X-ray, fluorescence spectrometry, N.L. Misra , S. Dhara, K.D. Singh Mudher, Spectrochimica Acta Part B, 61 (2006) 1166–1169.
2. *Bulk determination of uranium and thorium in presence of each other by Total Reflection X-ray Fluorescence spectrometry, Sangita Dhara, Nand Lal Misra, Khush Dev Singh Mudher, Suresh Kumar Aggarwal, Spectrochimica Acta Part B, 62 (2007) 82–85.
3. *Trace element determination in thorium oxide using total reflection X-ray fluorescence spectrometry , N.L. Misra , Sangita Dhara, V.C. Adya , S.V. Godbole, K.D. Singh Mudhera, S.K. Aggarwal Spectrochimica Acta Part B, 63 (2008) 81–85.
4. *Determination of sulphur in uranium matrix by total reflection X-ray fluorescence spectrometry, Sangita Dhara, N.L. Misra and S.K. Aggarwal, Spectrochimica Acta Part B, 63 (2008) 1395-1398.
5. *An EDXRF method for determination of uranium and thorium in AHWR fuel after dissolution, Sangita Dhara, S. Sanjay Kumar, N.L. Misra and Suresh K. Aggarwal, X-ray Spectrometry, 38 (2009) 112-116.
6. *A novel approach for chlorine determination in acidic medium by total reflection X-ray fluorescence, N.L. Misra, Imre Varga, Sangita Dhara and S.K. Aggarwal, X-ray Spectrometry, 38 (2009) 182-185.
7. Forensic application of total reflection X-ray fluorescence spectrometry for elemental characterization of ink samples, Sangita Dhara, N.L. Misra, S.D. Maind, Sanjukta A. Kumar, N. Chattopadhyay, S.K. Aggarwal, Spectrochimica Acta Part B, 65 (2010) 167–170.
8. *Determination of low atomic number elements at trace levels in uranium matrix using vacuum chamber total reflection X-ray fluorescence, N.L. Misra, Sangita Dhara, M. Óvári, Gy. Zárny, S.K. Aggarwal, Imre Varga, Spectrochimica Acta Part B, 65 (2010) 457–460.

9. *Energy dispersive X-ray fluorescence determination of cadmium in uranium matrix using Cd K α line excited by continuum, *Sangita Dhara*, N.L. Misra, S.K. Aggarwal, V.Venugopal, Spectrochimica Acta Part B, 65 (2010) 461-465.
10. Energy Dispersive X-Ray Fluorescence Determination of Thorium in Phosphoric Acid Solutions, N.N. Mirashi, *Sangita Dhara*, S. Sanjay Kumar, Satyajeet Chaudhury, N.L.Misra, and S.K. Aggarwal, Spectrochimica Acta Part B, 65(2010) 461-465.
11. *Trace Determination of Uranium in Fertilizer Samples by TXRF, N.L. Misra, *Sangita Dhara*, Arijeet Das, G.S. Lodha, S.K. Aggarwal, and I. Varga, PRAMANA- Journal of Physics 76(2011) 357-360.
12. Application of Total Reflection X-ray Fluorescence Spectrometry for Interlaboratory Study for Development of Rainwater Standard, *Sangita Dhara* and *N.L. Misra*, PRAMANA- Journal of Physics 76(2011) 361-366.

Conferences Total (25)

National Conference (15)

International Conference (10)

*** Results from these publications are included in this thesis**